LF 47b

UNIVERSITY OF LEICESTER

Author STONEHOUSE, A. H.

Title Expression of the inwardly rectifying Potassium ion channel, Kir2.2, and its

Degree Ph.D. Date 1999

DECLARATION TO BE SIGNED BY EACH READER CONSULTING THIS THESIS

NAME AND ADDRESS (BLOCK LETTERS PLEASE) SIGNATURE DATE

EXPRESSION OF THE INWARDLY RECTIFYING POTASSIUM ION CHANNEL, Kir2.2, AND ITS MODULATING RECEPTOR, NK-1 R, IN RAT BRAIN

Thesis submitted for the degree of

Doctor of Philosophy

at the University of Leicester

by

Anthony Harold Stonehouse BSc (Sussex), MSc (Leicester)

Department of Biochemistry

University of Leicester

September 1999

ProQuest LLC
789 East Eisenhower Parkway
P.O. Box 1346
Ann Arbor, MI 48106-1346

Expression of the Inwardly Rectifying Potassium Ion Channel, Kir2.2, and its Modulating Receptor, NK-1 R, in Rat Brain.

By Anthony Harold Stonehouse

Abstract

Potassium current flowing through channels of the Kir2.0 subfamily of inward rectifier channels contributes to resting membrane potential in many cell types. Suppression of inward rectifier (Kir) activity by neurokinin neurotransmitters increases neuronal excitability. Despite functional studies reporting modulation of whole-cell Kir current in the locus coeruleus (LC) of the medulla, little information is available describing the specific molecules involved.

Isoform specific polyclonal antibodies were raised, characterised and utilised, revealing differential distribution patterns. (a) Kir2.2 protein was observed in the cerebellum and medulla: a similar distribution was obtained by *in situ* hybridisation with Kir2.2 riboprobes. (b) Kir2.1, Kir2.2 and Kir2.3 were expressed in the hippocampus. Detailed observations of tissue sections revealed immunostaining patterns in macroglia, endothelia, ependyma and vascular smooth muscle cells for Kir2.1 and Kir2.2.

The NK-1 receptor was localised to plasma membranes of neurons, neuronal processes and oligodendroglia. Kir2.0 channels appeared to be distributed on plasma membranes and within the nucleus. This intracellular distribution was mimicked in transiently transfected Chinese hamster ovary cells expressing Kir2.0 isoforms.

Channel and receptor co-localisation supported the hypothesis that neuronal excitability in locus coeruleus is controlled by substance P-initiated suppression of Kir2.0 channel activity via protein phosphorylation. Tyrosine phosphorylation of Kir2.2 was investigated after administration of SP, in SN56 cell cultures. This produced a 62 kDa band, detectable by anti-Kir2.2 and anti-phosphotyrosine antibodies indicating that Kir2.2 protein could be phosphorylated via events initiated by SP. In addition, *in vitro* translated [^{35}S]-Methionine-labelled Kir2.2 protein was phosphorylated *in vitro* by PKA and PKC isoforms.

In conclusion, Kir2.2 and NK-1 receptor proteins have been co-localised in locus coeruleus neurons. Some evidence has been presented consistent with Kir2.2 *in vivo* tyrosine phosphorylation in response to NK-1 receptor activation. In addition, *in vitro* phosphorylation of *in vitro* translated Kir2.2 protein by PKA and PKC has been demonstrated.

Table of Contents

Table of Figures

Acknowledgements

I would like to thank my supervisors: Professor Bill Brammar for all his understanding, help and support over the last three years: he has been truly invaluable; Dr Ed Conley for supporting my early efforts with molecular biology. Further, I would like to acknowledge the generous support of an MRC PhD studentship which allowed me to undertake this work.

I would also like to recognise the efforts of Dr Howard Pringle and Dr Bob Norman for their guidance with molecular biology and protein biochemistry techniques. I was fortunate in having the opportunity to work in the Biochemistry (Hodgkin Building, Ion Channel Gene Expression Group), Medicine and Pathology departments. I would therefore like to thank everyone in these departments for their time, tolerance and support. Finally, I would like to mention Professor Peter Stanfield for his advice and insights into neurobiology and ion channels.

Abbreviations

A	-	Astrocyte
ABC-AP	-	Biotin/Streptavidin Complex-Alkaline Phosphatase Detection System
AKAP(79)	-	A-Kinase Anchoring Protein (79)
AMV-RT	-	Avian Myeloblastosis Virus-Reverse Transcriptase
ATP	-	Adenosine Triphosphate
BCIP	-	5-Bromo-4-Chloro-3-Indolyl-Phosphate
bp	-	Base Pair
BSA	-	Bovine Serum Albumin
CA1 Neurons	-	CA1 Field Pyramidal Neurons
CA3 Neurons	-	CA3 Field Pyramidal Neurons
cAMP	-	Cyclic Adenosine 3', 5' Monophosphate
cA-PK	-	Cyclic AMP-Dependent Protein Kinase Catalytic Subunit
CAT	-	Chloramphenicol Acetyltransferase
cDNA(s)	-	Complementary Deoxyribonucleic Acid(s)
CE	-	Capillary Endothelia
CHO Cells	-	Chinese Hamster Ovary Cells
CIAP	-	Calf Intestinal Alkaline Phosphatase
CMFPBS	-	Calcium/Magnesium Free-Phosphate Buffered Saline
CNS	-	Central Nervous System
COS7 Cells	-	African Green Monkey Kidney Cells
CTP	-	Cytidine Triphosphate
DAG	-	Diacylglycerol

dATP	-	Deoxyadenosine Triphosphate
dCTP	-	Deoxycytidine Triphosphate
DEPC	-	Diethylpyrocarbonate
dGTP	-	Deoxyguanosine Triphosphate
DIG	-	Digoxigenin
DIG-11-dUTP	-	Digoxigenin-11-Deoxyuridine Triphosphate
DIG-UMP	-	Digoxigenin-Uridine Monophosphate
DIG-UTP	-	Digoxigenin-Uridine Triphosphate
DNA	-	Deoxyribonucleic Acid
DOG	-	1,2-sn-Dioctanoylglycerol
DTT	-	Dithiothreitol
dTTP	-	Thymidine Triphosphate
dUTP	-	Deoxyuridine Triphosphate
EC	-	Ependymal Cells
EDHF	-	Endothelial Derived Hyperpolarising Factor
EEG	-	Electroencephalogram
EGF(R)	-	Epidermal Growth Factor (Receptor)
E_K	-	Potassium Equilibrium Potential
E_m	-	Membrane Potential
ER	-	Endoplasmic Reticulum
ERK	-	Extracellular-Signal-Regulated-Kinase
FCS	-	Foetal Calf Serum
G	-	Oligodendroglia And Astrocytes
GAP	-	Ras.GTPase activating protein
GC(L)	-	Granule Cell (Layer)
G-Protein	-	Guanine-Nucleotide-Binding Protein
Gα Subunit	-	G-Protein-α Subunit

$G\alpha_{i2}$ Subunit	-	G-Protein-α_{i2} Subunit
$G\alpha_{i3}$ Subunit	-	G-Protein-α_{i3} Subunit
$G\alpha_{o}$ Subunit	-	G-Protein-α_{o} Subunit
$G\alpha_{q/11}$ Subunit	-	G-Protein-$\alpha_{q/11}$ Subunit
$G\alpha_{s}$ Subunit	-	G-Protein-α_{s} Subunit
$G\beta\gamma$ Subunit	-	G-Protein-$\beta\gamma$ Subunits
GRK(2/3)	-	G-Protein-Coupled Receptor Kinase (2/3)
GTP	-	Guanosine Triphosphate
H5	-	Potassium Channel Pore Region
HEK 293 Cells	-	Human Embryonic Kidney Cells
IgG	-	Immunoglobulin G (Heavy and Light Chains)
I_k	-	Potassium Current
I_{KACh} Receptor	-	Atrial m2 Muscarinic Receptor Gated Potassium Channel
IPTG	-	Isopropyl-β-D-thiogalactoside
IVth V	-	IVth Ventricle
K_{ATP} Channel	-	ATP-Sensitive Potassium Channel
kb	-	Kilo Base
K_{Ca} Channel	-	Calcium-Activated Potassium Channel
GFP	-	Green Fluorescent Protein
Kir(s)	-	Potassium Inwardly Rectifying Ion Channel(s)
Kv Channel	-	Voltage-Gated Potassium Channel
Kvα Subunit	-	Voltage-Gated Potassium α Subunit
Kvβ Subunit	-	Voltage-Gated Potassium β Subunit
LB	-	Luria Broth
LC	-	Locus Coeruleus
M1 and M2	-	Kir Channel Transmembrane Domains 1 and 2

MAP Kinase	-	Mitogen-Activated Protein Kinase
MC(L)	-	Molecular Cell (Layer)
MCTrks	-	Anti-Nerve Growth Factor Receptor Antibody
MEL Cells	-	Murine Erythroleukaemia Cells
Me5N	-	Mesencephalic Trigeminal Nucleus
mRNA	-	Messenger RNA
N	-	Nucleus
N(NN)	-	Noradrenergic Neuron with Nuclear Localisation
NBM	-	Nucleus Basalis of Meynert
NBT	-	Nitroblue Tetrazolium
NGF(R)	-	Nerve Growth Factor (Receptor)
NIH 3T3 Cells	-	National Institutes of Health 3T3 Cells
NK-1 Receptor (R)	-	Neurokinin-1 Receptor
NMDA Channel(s)	-	N-Methyl-D-Aspartate Channel(s)
NN	-	Noradrenergic Neuron
NTP's	-	Nucleoside Triphosphates
OA	-	Okadaic Acid
OG	-	Oligodendroglia
[α^{32}P]	-	[α^{32} Phosphorus]
[γ^{32}P]	-	[γ^{32} Phosphorus]
PBS	-	Phosphate Buffered Saline
PC(L)	-	Purkinje Cell (Layer)
PCR	-	Polymerase Chain Reaction
PDZ Domain	-	[PSD-95, Discs Large, Zonula Occludentes] Domain
Pfu	-	*Pfu* Proof-Reading Polymerase
PIP_2	-	Phosphotidylinositol 4,5-Bisphosphate

PKA	-	Protein Kinase A
PKC(γ)	-	Protein Kinase C (γ)
PLC(β1)	-	Phospholipase C (β1)
PM	-	Plasma Membrane
PSD-95	-	Post-Synaptic Density Protein-95
RT-PCR	-	Reverse Transcription-Polymerase Chain Reaction
PY99	-	Anti-Phosphotyrosine Antibody
RGS(7/8)	-	Regulator of G-Protein Signalling (7/8)
RNA	-	Ribonucleic Acid
[^{35}S]	-	^{35}Sulphur
S1-S6	-	Kv Channel Transmembrane Domains 1-6
SDS	-	Sodium Dodecyl Sulphate
SH2 Domain	-	Src-Homology 2 Domain
SH3 Domain	-	Src-Homology 3 Domain
SP	-	Substance P
SSC	-	Standard Saline Citrate
SUR1	-	Sulphonylurea Receptor 1
T1	-	Kv Channel N-terminal and S1 Transmembrane Domain
Taq	-	*Taq* Polymerase
TBS	-	Tris Buffered Saline
T_m	-	Melt Temperature
TNT	-	Transcription and Translation
Tris	-	Trizma Base (Tris[Hydroxymethyl]aminomethane)
UF	-	Uncinate Fasciculus

UTP	-	Uridine Triphosphate
X-gal	-	5-Bromo-4-Chloro-3-Indolyl-β-D-Galactoside

Chapter 1: General Introduction

The control of neuronal excitation is vital to the efficient functioning of the central nervous system (CNS). Inwardly rectifying potassium ion (Kir) channel proteins are expressed in neurons, where they contribute to the control of neuronal excitation by setting the electrical threshold required for the generation of an action potential (Hille, 1992). Peptide neurotransmitters such as substance P (SP) cause neuronal excitation, in part, by the suppression (closure) of Kir channels (Stanfield *et al.,* 1985). Previous studies involving the locus coeruleus (LC), the main noradrenergic centre in the CNS, have identified SP as causing neuronal excitation via suppression of a Kir channel and the activation of mixed cation channels (Shen & North, 1992 and Koyano *et al.,* 1993). The Kir channel isoform(s) involved in this process, together with the second messenger pathways linking the NK-1 receptor (SP receptor) and the Kir channel isoform(s), have not been identified. The intention of this study is to identify Kir isoform(s) expressed in the LC and to seek evidence for a receptor-channel interaction.

1.1 Inwardly Rectifying Potassium Ion Channel Function

Inwardly rectifying potassium ion channels are present in excitable and non-excitable cells (Reimann & Ashcroft, 1999) and are responsible for setting the resting membrane potential of the cell close to the potassium equilibrium potential (E_K) (Hille, 1992). Kir channels contribute to the control of membrane potential (E_m) in neurons by their ability to conduct ions in the inward direction at negative membrane potentials and allow a slight outward conductance at E_ms that are positive to the E_K (Hille, 1992).

The patch clamp technique with whole-cell recording allows voltage clamp to be used to investigate ion channel activity. This allows the membrane voltage of the patched cell to be clamped at potentials that are both depolarised and hyperpolarised with respect to E_K. At each of these voltage commands, membrane currents are measured and plotted to produce a current-voltage relationship as shown in Figure 1-1:

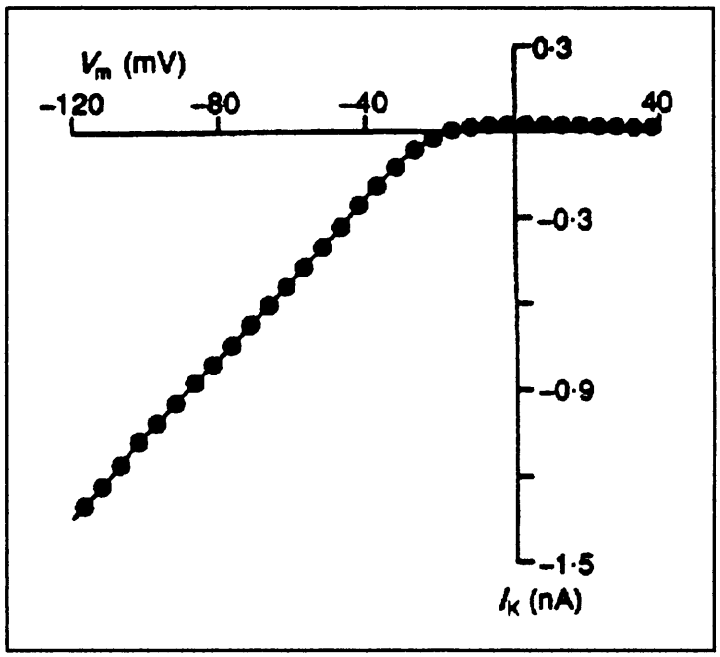

Figure 1-1. Kir2.1 current-voltage relationship. This figure and part of the legend is taken from Stanfield *et al.*, 1994a and describes a current-voltage relationship for Kir2.1 in stably transfected murine erythroleukaemia (MEL) cells. Membrane currents were obtained with an external potassium concentration of 70 mM, under depolarisations in 5 mV steps up to 70 mV from E_K, and under hyperpolarisations in 5 mV steps down to 60 mV from E_K. The ability of Kir channels to allow inward flow of ions at negative membrane potentials is demonstrated here between -120 mV and -20 mV. A slight outward conductance is also shown at positive membrane potentials above -20 mV. mV, membrane potential ; I_k, potassium current.

This inward rectifying ability has been compared by Hille to the latch on a cabinet door (Hille, 1992). Under normal physiological conditions Kir channels allow conduction of a slight outward current that maintains the voltage range of the cell membrane positive to E_K (the door is latched). When the Kirs are suppressed (closed), E_m may change (the latch is removed). Under these conditions the membrane conductance is lowered, resistance raised and the cell moves towards the threshold of excitability. However, suppression of Kir channel activity alone does not cause depolarisation or an action potential to be generated. This also requires the opening of mixed conductance cation (calcium and sodium) channels, shown to occur in response to the application of excitatory neurotransmitters such as substance P (Shen & North, 1992 and Inoue *et al.,* 1995).

The ability to conduct potassium into the cell at the high levels of extracellular potassium found associated with neuronal activity has the effect of provoking a strong inward conduction of potassium ions into glial cells, mediating the potassium buffering effect (Brew *et al.,* 1986). In addition to expression in the CNS, Kir channels are also widely distributed in smooth muscle, where they may potentially provide a glial-type buffering of extracellular potassium, thereby controlling smooth muscle membrane potential and physical functions such as arterial diameter (reviewed by Quayle *et al.,* 1997).

1.2 Inwardly Rectifying Potassium Ion Channel Structure

A number of Kir genes and cDNAs have been cloned and functionally expressed (Reimann & Ashcroft, 1999). The monomer Kir proteins exhibit cytoplasmic N- and C-termini, two transmembrane domains (M1 and M2)

flanking a single pore region (H5) with sequence similarity to the pore region of voltage-gated potassium channels (Ho *et al.,* 1993, Kubo *et al.,* 1993a and 1993b). The Kirs thus constitute a large family of proteins, containing ATP-regulated potassium channels (e.g., Kir1.1a (Ho *et al.,* 1993)) and the strong inward rectifiers (e.g., Kir2.1 (Kubo *et al.,* 1993a, Morishige *et al.,* 1993 and Bond *et al.,* 1994), Kir2.2 (Koyama *et al.,* 1994 and Takahashi *et al.,* 1994), Kir2.3 (Morishige *et al.,* 1994 and Falk *et al.,* 1995) and Kir2.4 (Topert *et al.,* 1998 and Kumar *et al.,* 1999)). There is also a group of G-protein-activated channels containing five members (e.g., Kir3.1 (Dascal *et al.,* 1993a, Dascal *et al.,* 1993b and Kubo *et al.,* 1993b), Kir3.2 (Lesage *et al.,* 1994, Kobayashi *et al.,* 1995, Krapivinsky *et al.,* 1995 and Patil *et al.,* 1995), Kir3.3 (Lesage *et al.,* 1994 and Kobayashi *et al.,* 1995), Kir3.4 (Spauschus *et al.,* 1996) and Kir3.5 (Luchian & Schreibmayer, 1998)). Kir4.1 is a channel expressed predominantly in glial cells of the cerebellum and fore-brain (Takumi *et al.,* 1995). It is also expressed during rat embryonic brain development, suggesting a role in cell proliferation, migration and differentiation in the CNS (Ma *et al.,* 1998). Kir5.1 (Bond *et al.,* 1994), a channel of unknown function cloned from rat brain tissue, was found to be widely distributed in both central and peripheral nervous systems. The classical 'ATP-sensitive potassium channels' (K_{ATP}) also contain subunits of the inward rectifier family (e.g., Kir6.1 (Inagaki *et al.,* 1995) and Kir6.2 (Bond *et al.,* 1994)). Kir7.1 has recently been cloned from a human foetal brain λcDNA library (Krapivinsky *et al.,* 1998a). This gene is expressed in cerebellar Purkinje cells and pyramidal neurons of the hippocampus, in addition to other tissues such as intestine and kidney (Krapivinsky *et al.,* 1998a).

1.3 Voltage-Gated Potassium Ion Channel Structure and Function

Voltage-gated potassium (Kv) channel and Kir channel structures are analogous, in that four subunits are arranged into a tetrameric structure in order to form a functional channel (Li *et al.,* 1992). The M1 and M2 transmembrane domains, together with the H5 pore region of Kir channel subunits are analogous to the Kv channel subunit S5 and S6 transmembrane domains and pore region respectively (Kubo *et al.,* 1993a). Kv channel subunits contain four additional transmembrane domains (S1, S2, S3 and S4) and cytoplasmic N- and C-terminal domains. The Kvα subunits belong to four subfamilies, whose subunits can assemble into heteromultimers within each subfamily. However, heteromultimerisation between different Kvα subfamilies is not seen. Heteromultimerisation is determined by the cytoplasmic region between the cytoplasmic N-terminal and the S1 transmembrane domain (known as T1) (Li *et al.,* 1992).

The S4 transmembrane domain contains positively charged arginine or lysine residues at every third position. The S4 domain is likely to be sensitive to changes in membrane potential, leading to protein conformational changes upon depolarisation (Bezanilla & Stefani, 1994). The intrinsic voltage sensitivity of Kv channels is vital for their role of producing a sustained increase in potassium efflux from cells upon depolarisation (Hodgkin & Huxley, 1952).

Kv channel N-type inactivation is linked to the activity of the cytoplasmic N-terminal blocking particle, which plugs the intracellular mouth of the pore after a prolonged depolarisation (Armstrong & Bezanilla, 1977). Some Kvα

subunits are unable to undergo this type of inactivation, in which case the presence of Kvβ accessory subunits allows N-type inactivation to occur (Rettig *et al.,* 1994). C-type inactivation can occur alone (Grissmer & Cahalan, 1989) or in conjunction with N-type inactivation (Choi *et al.,* 1991). C-type inactivation is associated with a closure of the external pore mouth by pore residues from the channel subunits. Further, C-type inactivation is associated with residues in the S5, pore and S6 domains (Yellen *et al.,* 1994). Additional Kv channel regulation is provided by protein phosphorylation in response to the activities of cellular receptors, a topic discussed in section 6.5.

1.4 Inwardly Rectifying Potassium Ion Channel Pore Structure and Rectification

Kir channels have been characterised electrophysiologically under voltage clamp conditions by their intrinsic gating, which is dependent upon voltage and extracellular potassium concentration; cation selectivity; susceptibility to block by magnesium and polyamines at depolarised membrane potentials, therefore inducing inward rectification; caesium and barium block; open channel probability and single channel conductance characteristics (reviewed by Doupnik *et al.,* 1995 and Nichols & Lopatin, 1997).

Expression of the cloned murine Kir2.1 channel gene in MEL cells, demonstrated that removal of intracellular magnesium from large inside-out membrane patches resulted in brief outward currents at depolarised membrane potentials (Stanfield *et al.,* 1994a). This observation indicated the importance of intracellular magnesium to Kir channel inward rectification

(Stanfield *et al.*, 1994a). Studies utilising mutagenesis and electrophysiology have identified amino acid residues involved in Kir channel gating. For example, a charged aspartate (residue 172) found in the M2 region of the mouse Kir2.1 channel is responsible for potassium- and voltage-dependent gating in the region of E_K (Stanfield *et al.*, 1994b). Substitution of the charged aspartate (residue 172) with uncharged but polar amino acids such as glutamine or asparagine resulted in weaker inward rectification, implying that normal intrinsic gating around E_K was due to a charged amino acid at residue 172 (Stanfield *et al.*, 1994b). In addition, substitution of aspartate by glutamine (D172Q) reduced intracellular magnesium block by fivefold, implying that aspartate residue 172 was involved in both intrinsic gating and magnesium block (Stanfield *et al.*, 1994b). Further, wild type Kir2.1 channels were found to be sensitive to voltage-dependent rubidium and caesium block (Abrams *et al.*, 1996). This block was abolished by mutation of aspartate residue 172 to asparagine (D172N), but not by mutation to glutamine (D172Q) (Abrams *et al.*, 1996). These data indicated that the Kir2.1 channel aspartate residue 172 was important in determining pore size and charge, resulting in either ion blockade or permeation (Abrams *et al.*, 1996). Interestingly, the weaker inward rectifiers such as Kir1.1 do not possess the aspartate residue 172 (Ho *et al.*, 1993). Substitution of asparagine by aspartate in the corresponding position in M2 of the Kir1.1 channel increases strength of rectification (Lopatin *et al.*, 1994). Intrinsic gating of Kir channels at physiological pH is also caused by protonated organic polycations, known as polyamines (reviewed by Williams, 1997).

The H5 pore region amino acid sequence is crucial as demonstrated by the *weaver* mouse mutant, produced by a single mutation resulting in change of

a glycine to a serine residue (G156S) in the Kir3.2 protein. The *weaver* mouse exhibits degeneration of cerebellar granule cells and dopaminergic neurons in the substantia nigra, leading to an ataxic phenotype associated with a reduction in Kir3.2 currents (Surmeier *et al.,* 1996). Premigratory mouse cerebellar granule cells in the *weaver* mouse lacked the Kir3.2 type current, resulting in a failure to migrate and in consequent cell degeneration (Rossi *et al.,* 1998).

Recently, a three-dimensional structure of the *Streptomyces lividans* KcsA channel has been reported with structural homology to both mammalian Kir and Kv channels (Reimann & Ashcroft, 1999). The production of the KcsA channel structure utilised x-ray crystallographic analysis to provide models of the closed (Doyle *et al.,* 1998) and open (Perozo *et al.,* 1999) channel conformations. The KcsA channel is a tetramer, with each subunit being composed of two transmembrane α-helical domains and an extracellular loop, which forms the pore and ion-selectivity filter. The channel subunits are arranged such that their transmembrane domains form an 'inverted teepee' structure. The ion-selectivity filter is formed on the extracellular side of the channel where it removes the potassium ion hydration shell. This dehydration is caused by interaction of the potassium ions with the carbonyl groups of two glycine residues in a glycine-tyrosine-glycine structure provided by each of the channel subunits. The tyrosine residues of the channel ion-selectivity filter interact with the adjacent transmembrane domains, thus maintaining the glycine carbonyl oxygen atoms in the ion-selectivity filter at the optimum distance apart and allowing the passage of dehydrated potassium ions into the channel pore (Doyle *et al.,* 1998 and Perozo *et al.,* 1999).

An additional investigation by Jan and colleagues utilised a yeast genetic screen to analyse mutant Kir2.1 channels (Minor *et al.,* 1999). Mutations within the transmembrane domains indicated that the M1 lipid-facing outer α-helix surrounds the M2 pore-lining inner α-helix. Although the Kir2.1 and previously described KcsA channels have the same structural topology, there appears to be a difference in the transmembrane domain packing, possibly associated with the low sequence homology between the two channels (Minor *et al.,* 1999).

The tetrameric nature of Kir channels is well established (Kofuji *et al.,* 1995, Yang *et al.,* 1995, Pessia *et al.,* 1996 and Tinker *et al.,* 1996). The constitutively active Kir2.0 channels can exist as homomultimers, e.g., Kir2.2 subunits (Raab-Graham & Vandenberg, 1998), or heteromultimers, e.g., Kir2.1 and Kir2.3 subunits (Cohen *et al.,* 1996b). The constitutively inactive Kir3.0 subfamily exist as heteromultimers, an example of which is the I_{KACh} channel, composed of Kir3.1 and Kir3.4 subunits (Krapivinsky *et al.,* 1995). Unlike their counterparts in the voltage-gated potassium channels, the N-terminal sequences of Kirs do not play a role in the assembly of channel tetramers. The proximal C-terminal and M2 regions of Kir2.0 channels determine homomultimerisation (Tinker *et al.,* 1996). The regions determining the heteromultimer structure of Kir3.0 channels are still unclear. However, conserved glutamate and arginine residues in the H5 pore region of Kir channels form salt bridges in the tetrameric channel: mutation of either of these residues results in changes in the selectivity and permeation properties of the channel (Yang *et al.,* 1997).

The distal C-terminal sequences of several Kir proteins are able to bind PDZ domain proteins such as PSD-95 (Cohen *et al.,* 1996a). These PDZ domain proteins may mediate channel clustering and possible cytoskeletal connections (Cohen *et al.,* 1996a).

1.5 NK-1 Receptor and Substance P

Substance P (SP) is a member of the neurokinin group of small peptide neurotransmitters. There are two other members of this group, substance K and neuromedin K. All three neurokinins are encoded by the preprotachykinin gene and arise as a result of differential RNA splicing and post-translational modification (Helke *et al.,* 1990). Neurokinins are distributed widely in the peripheral and central nervous systems, and there is often a pattern of mutually exclusive expression between the neurotransmitter and cognate receptor proteins as demonstrated in the CNS (Nakaya *et al.,* 1994). Immunohistochemistry has been carried out with polyclonal antibodies raised against C-terminal peptides of the NK-1 receptor (Vigna *et al.,* 1994).

The sequence encoding the seven transmembrane domain G-protein-linked NK-1 receptor has been cloned from a rat brain cDNA library (Yokota *et al.,* 1989). Binding of the undecapeptide SP to its receptor induces several physiological processes including inflammation and pain transmission (Helke *et al.,* 1990, Nakanishi, 1991 and Otsuka & Yoshioka, 1993). A viable substance P gene 'knock-out' mouse, with reduced sensitivity to moderate and intense pain stimulation (nociception) has recently been bred (Cao *et al.,* 1998). In addition, protein kinase Cγ (PKCγ) 'knock-out' mice are found to be viable, capable of responding to intense pain stimuli, but do not suffer from

the neuropathic pain syndrome caused by nerve injury (Malmberg *et al.,* 1997). This allows a link to a potential signal pathway intermediate, functionally linking NK-1 receptors with suppression of Kir channels and activation of mixed cation channels to generate a neuronal depolarisation (Stanfield *et al.,* 1985, Yamaguchi *et al.,* 1990, Shen & North, 1992, Koyano *et al.,* 1993 and Inoue *et al.,* 1995).

The NK-1 receptor gene has also been 'knocked-out' in mice, producing animals that are unable to undergo the phenomenon of 'wind up' or amplification of nociceptive reflexes (De Felipe *et al.,* 1998). SP also induces slow neuronal excitation of cholinergic neurons of the nucleus basalis of Meynert (NBM) in the brain (Stanfield *et al.,* 1985, Yamaguchi *et al.,* 1990, Takano *et al.,* 1995 and 1996). Noradrenergic neurons of the locus coeruleus (LC) also undergo this slow neuronal excitation by the SP-mediated suppression of an unidentified Kir channel (Shen & North, 1992, Koyano *et al.,* 1993 and Velimirovic *et al.,* 1995). The administration of SP into the rat hippocampus, after a sub-critical exposure to perforant path stimulation, triggers the condition of self-sustaining status epilepticus, resulting in hippocampal damage similar to that found in epileptic humans (Liu *et al.,* 1999). Self-sustaining status epilepticus has the effect of inducing transcription of the preprotachykinin gene (and thus elevating SP, prolonging the maintenance of status epilepticus) in CA1 and CA3 pyramidal neurons and dentate gyrus granule cells (Liu *et al.,* 1999). There is also an increased release of the excitatory amino acid glutamate from the hippocampus. The enhanced expression of SP during self-sustaining status epilepticus may cause an increase in hippocampal excitability, potentially contributing to the maintenance of self-sustaining status epilepticus (Liu *et al.,* 1999). NK-1

receptor/SP containing neurons have been found in the dorsal raphe nucleus and substantia nigra pars reticulata of the dorsal pontine brain stem (Gerfen 1991, Sutin & Jacobowitz, 1991, reviewed by Otsuka & Yoshioka, 1993 and Futami *et al.,* 1998) and the LC itself (Aston-Jones *et al.,* 1991).

1.6 Locus Coeruleus

The LC is a sexually dimorphic structure (Tseng *et al.,* 1997) located on both sides of the floor in the IVth ventricle of the medulla. It is a histologically homogenous structure, ideal for electrophysiological investigation, with each LC containing about 1700 neurons in the rat (Tseng *et al.,* 1997). A diagram of rat brain LC projections is shown in Figure 1-2:

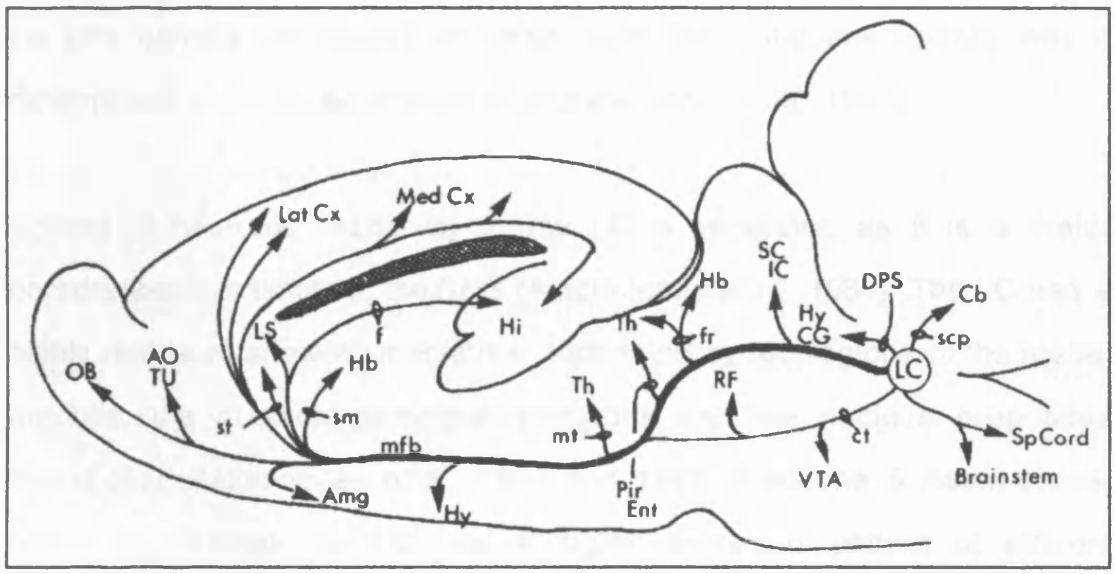

Figure 1-2. Schematic representation of the projections of the locus coeruleus in a rat brain sagittal section. This figure and part of the legend is taken from Loughlin & Fallon, 1985 and describes the efferent projections of the LC. Amg, amygdala; AO, anterior olfactory nucleus; Cb, cerebellum; CG, central grey; ct, central tegmental tract; cx, cortex; DPS, dorsal periventricular system; Ent, entorhinal cortex; f, fornix; fr,

fasciculus retroflexus; Hb, habenula; Hi, hippocampus; Hy, Hypothalamus; IC, inferior colliculus; LS, lateral septum; mbf, median fore-brain bundle; mt, mammillothalamic tract; OB, olfactory bulb; Pir, piriform cortex; RF, reticular formation; SC, superior colliculus; scp, superior cerebellar peduncle; sm, stria medullaris; Th, thalamus; Tu olfactory tubercle; VTA, ventral tegmental area.

The importance of the LC and other noradrenergic structures is highlighted by the 'knock-out' of the *Phox2a* homeobox transcription factor gene (Morin *et al,.* 1997). This resulted in the birth of mutant mice of normal appearance and size. However, these mice were unable to feed and died on the day of birth. Immunohistochemistry on dissected brain tissue sections indicated that Phox2a protein was absent from the brain. Histological examination of the peripheral and central nervous systems indicated that the LC, some sympathetic and parasympathetic ganglia and the VIIth, IXth and Xth cranial sensory ganglia are absent in these mice, indicating that Phox2a was a determinant of the noradrenergic phenotype (Morin *et al,.* 1997).

Control of neuronal excitability in the LC is important, as it is a major noradrenergic structure in the CNS (Aston-Jones *et al.,* 1986). The LC has a highly restricted afferent innervation, dominated by two regions of the rostral medulla; the nucleus paragigantocellularis and the nucleus prepositus hypoglossi (Aston-Jones *et al.,* 1986 and 1991, Pieribone & Aston-Jones, 1991). In contrast, the LC has a highly dispersed pattern of efferent connections as described in Figure 1-2. These include the following areas of the brain stem;

1). When active the noradrenergic neurons in the LC cause a characteristic alert EEG activity in the fore-brain (Foote *et al.,* 1991).

2). During the waking state, noradrenergic neurons of the LC fire regularly at a high level and emit short phasic bursts of firing when triggered by environmental stimuli. During sleep, LC noradrenergic neurons fire regularly at a very low level (Cirelli *et al.,* 1996), causing a characteristic activity in cholinergic neurons, linked with paradoxical sleep (Sakai, 1991).

3). Noradrenalin activity in the LC inhibits noxious evoked neuronal activity in the dorsal horn of the spinal cord. This is possibly mediated by SP, as NK-1 receptors are expressed in deep dorsal horn neurons (King *et al.,* 1997) resulting in the perception of pain (Jones, 1991).

4). The μ opioid receptor and the inwardly rectifying potassium ion channel, Kir3.1 have been co-localised in LC neurons by immunohistochemistry (Bausch *et al.,* 1995). Opiates acutely inhibit electrical excitability in LC neurons by activating Kir channels, suppressing an inward sodium current and inhibiting adenylyl cyclase by the action of $G\alpha_{i/o}$ subunits. However, chronic exposure to opiates results in an increase in the activity of adenylyl cyclase and a rise in cellular levels of cyclic adenosine 3', 5' monophosphate (cAMP) and protein kinase A (PKA). This results in up-regulation of the inward sodium current and potentially, suppression of the Kir channel, leading to an increase in neuronal electrical excitability. In addition, the rise in PKA leads to an enhancement in the cellular level of phosphorylated cyclic AMP response-element binding protein and consequently changes in gene expression associated with long-term opiate addiction. Withdrawal of opiates similarly leads to increasing electrical excitability of the LC, resulting in the condition of 'cold turkey' (reviewed by Nestler, 1996).

5). Noradrenalin originating from the LC has the effect of promoting both short- and long-term enhancement of perforant path responses to complex sensory inputs, in the dentate gyrus synapse of the fore-brain (Harley, 1991). This indicates a role for the LC in memory and attention processes (reviewed by Harley, 1991). SP has also been linked to an increase in NMDA channel openings in dentate gyrus granule cells. SP has, thus, been linked to the control of the excitatory glutaminergic inputs to the dentate gyrus (Lieberman & Mody, 1998).

6). The LC is believed to be a site of carbon dioxide or pH-dependent chemoreception and is part of the brainstem respiratory network in the neonatal rat (Oyamada *et al.,* 1998). Increasing concentrations of carbon dioxide have the effect of increasing LC depolarisation and discharge frequency (as measured by whole-cell recordings on the C4 and C5 phrenic nerve roots) (Oyamada *et al.,* 1998). The resulting changes in respiration yield a shortening of expiration duration and reduce respiratory inhibition. Excitatory amino acid pathways have been implicated in both excitatory and inhibitory effects on the activity of the LC (Oyamada *et al.,* 1998).

1.7 Localisation of Kir channel Isoforms and the NK-1 Receptor in Locus Coeruleus Neurons

The use of *in situ* hybridisation to assess expression of the Kir2.0 and Kir3.0 subfamilies of genes in the adult rat brain (Karschin *et al.,* 1994 and 1996) has indicated that Kir2.2 (low expression), Kir3.1 and Kir3.2 (moderate expression) and Kir3.3 (abundant expression) are expressed in the LC. These observations have been repeated in mouse brain for Kir3.1, Kir3.2 and

Kir3.3 (Kobayashi *et al.,* 1995) and for Kir2.2 (Horio *et al.,* 1996). However, immunohistochemical investigations using Kir3.1 and Kir3.2 splice variant-specific polyclonal antibodies failed to detect these isoforms in the LC, casting doubt upon the earlier *in situ* hybridisation observations indicating the presence of Kir3.1 and Kir3.2 isoforms in the LC (Inanobe *et al.,* 1999). The expression of Kir2.0 and Kir3.0 isoforms has also been assessed during rat ontogenic development by *in situ* hybridisation (Karschin *et al.,* 1997). These studies have assessed the expression patterns of Kir2.0 and Kir3.0 channel isoforms in the rat CNS in general, and the LC in particular. However, there may be expression of other Kir channel subfamilies, whose distributions have yet to be investigated. The NK-1 receptor has been found to be expressed in the LC, using *in situ* hybridisation (Maeno *et al.,* 1993) and immunohistochemistry (Nakaya *et al.,* 1994).

1.8 NK-1 Receptor Modulation of Kir Channels

The second messenger pathways linking hormones and neurotransmitters such as somatostatin, SP and acetylcholine to Kir channels have been investigated over the last decade or so. The neurotransmitter, somatostatin, was shown by the whole-cell tight-seal patch clamp technique to activate Kir channels and hyperpolarise cultured LC noradrenergic neurons (Inoue *et al.,* 1988). Treatment of the cells with pertussis toxin abolished the somatostatin induced hyperpolarisation, but did not affect the resting hyperpolarising current. This indicated a possible Gα pertussis toxin-sensitive subunit modulating a Kir channel, either directly or via a cascade of cytoplasmic factors (Inoue *et al.,* 1988). In contrast, LC neurons from rat brain slices depolarised when stimulated with SP (Shen & North, 1992). Whole-cell

recordings indicated that this was caused by a simultaneous increase in calcium and sodium and decrease in potassium conductances (Shen & North, 1992). Similarly, SP suppressed Kir channel activity in cultured NBM cholinergic neurons, depolarising these cells with a time-independent channel inactivation (Yamaguchi *et al.,* 1990).

1.8.1 Direct G-Protein Modulation of Kir Channels

The experimental evidence supporting the modulation of Kir channel activity by Gβγ subunits is described in the following section. Investigation of acetylcholine activation of the I_{KACh} channel in the heart indicated that the m2 muscarinic receptor was linked to a pertussis-sensitive G-protein, the dissociation of which yielded Gα and Gβγ subunits (Huang *et al.,* 1995). The latter were found to bind to the N- and C-terminal domains of the Kir3.1 protein (Huang *et al.,* 1995 and Kunkel & Peralta, 1995), causing channel activation and cellular hyperpolarisation via a pathway that did not involve water-soluble cytoplasmic factors (Huang *et al.,* 1995 and Kunkel & Peralta, 1995). At present, it appears likely that at least one Gβγ subunit must bind to a channel tetramer protein for activation to occur, but for maximal activation more than one Gβγ subunit is required. Recently, Krapivinsky and colleagues have investigated activation via the Kir3.4 subunit in the I_{KACh} channel by using identical peptides to channel amino acid residues: 209-225 and 226-245 and a C216T mutation. These peptides blocked binding of Gβγ subunits to the Kir3.4 subunit and, thus, prevented activation of the I_{KACh} channel. Similarly, Gβγ subunit-stimulated activation of the Kir3.1/Kir3.4 (C216T) mutant I_{KACh} channel was greatly reduced (Krapivinsky *et al.,* 1998b). The Kir3.0 channel/Gβγ subunit binding sites were investigated by mutagenesis

of Kir3.1 and Kir3.4 (L333E and L339E mutations, respectively) expressed in a heterologous oocyte system. These mutations rendered the channels insensitive to agonist-induced activation and reduced channel/Gβγ subunit binding (He *et al.,* 1999). In addition, the agonist-independent dissociation of Gβγ subunits was observed to contribute to a basal level of Kir3.0 channel activity by binding to other site(s) on the channel proteins. Therefore, at least in a heterologous system, Kir3.0 channels seem able to make a contribution to the resting membrane potential set by Kir2.0 channels (He *et al.,* 1999).

The hydrolysis of phosphotidylinositol 4,5-bisphosphate (PIP_2) by water-soluble cytoplasmic factors involved with Kir2.0 channel modulation was also able to stabilise the binding of Gβγ to the C-terminal of Kir3.0 channels (Huang *et al.,* 1998). In addition, Gβγ subunits have been shown to suppress Kir2.3 channel activity, probably by direct binding to the N-terminal of the protein (Cohen *et al.,* 1996b). These observations indicate that the water-soluble cytoplasmic factors associated with the modulation of Kir2.0 channels, can also affect the activity of Kir3.0 channels. Similarly, the Gβγ subunits associated with the modulation of Kir3.0 channel activity can also bind to and affect the activity of some Kir2.0 channels.

Additional factors that appear to be involved in the regulation of Kir3.0 channels include RGS8 (regulator of G-protein signalling 8). This protein was found in neural tissue where it accelerated both activation and deactivation of Kir3.1/Kir3.2 heteromultimeric, G-protein-activated channels, making rapid regulation of neuronal excitability possible (Saitoh *et al.,* 1997). In addition, the subsequently cloned RGS7 was similarly found to accelerate channel activation, but the rate of deactivation was found to be slower than with RGS8

(Saitoh *et al.,* 1999). These regulatory factors may be associated with the fine control of Kir3.0 channel activity, by affecting the binding of Gβγ subunits to Kir3.0 channel regulatory sites.

1.8.2 Gα Subunit Modulation of Kir Channels by Second Messengers

The experimental evidence supporting the modulation of Kir channel activity by Gα subunits is described in the following section. In cultured LC noradrenergic neurons, Gα pertussis toxin-insensitive subunits activated by SP suppressed, and somatostatin-induced Gα pertussis toxin-sensitive subunits activated the same Kir channel, with suppression being the stronger of the two effects (Velimirovic *et al.,* 1995). In support of these observations, it was shown with cultured NBM cholinergic neurons that SP caused Kir suppression via Gα pertussis toxin-insensitive subunits (Takano *et al.,* 1995). The use of protein kinase C (PKC) inhibitors and a diacylglycerol (DAG) mimic, 1,2-sn-dioctanoylglycerol (DOG) showed that SP suppressed a Kir channel via a PKC-induced phosphorylation and that Kir channels were irreversibly suppressed when SP was administered to neurons treated with okadaic acid (OA), a specific protein phosphatase 1 and 2A inhibitor (Takano *et al.,* 1995). These data indicated that Kir channel suppression involved a diffusible second messenger-mediated signal transduction pathway involving phosphorylation by PKC and that reversal of its effect involved dephosphorylation by protein phosphatase 1 or 2A. Further studies into the second messenger pathways between the NK-1 receptor and Kir channels (Takano *et al.,* 1996) with cultured NBM cholinergic neurons indicated that Kir channel suppression was mediated via a Gα subunit. The isoform and effector involved were shown to be $G\alpha_{q/11}$ and PLC-β1 by inhibition of SP-

induced Kir channel suppression by specific antibodies (Takano *et al.,* 1996). A further study using antisense oligonucleotides and antibodies specific to G α subunit isoforms, indicated that somatostatin-induced Kir activation was mediated by $G\alpha_{i2}$ subunits in LC neural and $G\alpha_{i3}$ subunits in AtT-20 endocrine cells (Takano *et al.,* 1997). These observations, therefore, suggest a tissue specificity for the receptor-channel signalling pathway (Takano *et al.,* 1997).

When a human NK-1 receptor was overexpressed in Sf9-insect cells, an [α^{32}P]-azidoanilido GTP photoaffinity label activated $G\alpha_o$, $G\alpha_s$ and $G\alpha_{q/11}$ subunits, as detected by immunoprecipitation with specific Gα antibodies (Nishimura *et al.,* 1998a). A similar investigation using stably transfected Chinese hamster ovary (CHO) cells demonstrated that activation of NK-1 receptors lead to the activation of $G\alpha_o$ and $G\alpha_s$ subunits in a mammalian cell system (Roush & Kwatra, 1998). Further observations indicated that the activation of NK-1 receptor leads to cAMP formation in stably transfected CHO cells (Nakajima *et al.,* 1992). The discovery (Nishimura *et al.*, 1998a) that $G\alpha_s$ subunits are activated by stimulation of the NK-1 receptor, could explain this cAMP formation and the potential activation of cyclic-nucleotide-gated cation channels, leading to depolarisation and an increase in cell excitability (Nishimura *et al.*, 1998a).

Recently, investigations into the subcellular localisation of channel effector proteins and water-soluble cytoplasmic factors have identified a class of A-kinase anchoring proteins (AKAPs). These proteins contain two functional domains, a PKA regulatory subunit binding domain and a targeting domain which directs the AKAP/PKA complex to a specific channel protein target. In

addition, AKAPs are also capable of binding to other water-soluble cytoplasmic factors such as PKC and protein phosphatases. These complexes potentially allow regulation of channel activity in response to intracellular signalling (reviewed by Fraser & Scott, 1999). Hebert and colleagues investigated the potential roles of AKAPs in the regulation of Kir1.1 channel activity in *Xenopus* oocytes (Ali *et al.,* 1998). Activation of Kir1.1 channels by PKA and PKC was found to be dependent upon the co-expression of AKAP79 with the Kir1.1 channel, implying that AKAP expression was necessary for the regulation of Kir1.1 channel activity (Ali *et al.,* 1998). The evidence presented in this section indicates that activation of the NK-1 receptor results in the release of Gα subunit isoforms, resulting in the production or activation of water-soluble cytoplasmic factors, including PKA and PKC.

1.8.3 Modulation of Kir Channels by Tyrosine Phosphorylation

Although there is considerable evidence pointing to a phosphorylation event mediated by PKC leading to Kir channel suppression, there are other potential pathways that could result in channel phosphorylation and suppression. Co-expression of nerve growth factor (NGF) receptor and Kir2.1 channel in the tsA-201 human kidney cell line resulted in channel suppression in response to the application of nerve growth factor (Wischmeyer *et al.,* 1998), analogous to the effect of SP on the NK-1 receptor. A C-terminal tyrosine residue (Y242) in Kir2.1 (also present in other members of the Kir2.0 subfamily) was shown to be the key target for tyrosine kinases producing the channel suppression. This phosphorylation was sustained by administration of perorthovanadate (protein tyrosine

phosphatase inhibitor) and, thus, led to the retention of a suppressed channel state. Administration of genistein (tyrosine kinase inhibitor) abolished this suppression. Finally, mutation of the tyrosine residue to phenylalanine (Y242F) yielded a fully active channel which could not be suppressed by perorthovanadate (Wischmeyer *et al.*, 1998).

1.8.4 Regulation of NK-1 Receptor Activity

Desensitisation of the NK-1 receptor after agonist binding has important implications on the regulation of Kir channel activity. Rapid desensitisation of the receptor could potentially lead to reversal of Kir channel suppression. The agonist-induced phosphorylation of the NK-1 receptor by the G-protein-coupled receptor kinase: GRK2, leading to the desensitisation of the receptor, has been characterised (Nishimura *et al.*, 1998b). In addition, receptor desensitisation may also be due to internalisation of receptor-ligand complexes, producing vesicles in which the receptor-ligand complexes can be hydrolysed, or eventually returned to the plasma membrane as observed in the dorsal horn of the rat spinal cord (Abbadie *et al.*, 1997, McConalogue *et al.*, 1998 and Barak *et al.*, 1999).

1.9 Summary of Signal Transduction Pathways Potentially Involved in Kir Channel Modulation

The preceding literature review indicates that two classes of Kir operate in LC and NBM neurons to determine neuronal excitability. There appears to be a background potassium inward rectifier that is open at rest, possibly a Kir2.0 channel, setting the resting membrane potential of the neuron. At the same

time there appears to be a second family of Kir channels, possibly Kir3.0, that require G-protein activation. Somatostatin activates the Kir3.0 channel via a direct binding of Gβγ subunits. These somatostatin stimulated Gβγ subunits also maintain Kir2.0 channel activation, possibly by binding to PLC-β isoforms (Conklin *et al.,* 1993, Smrcka & Sternweis 1993, Neer, 1995, Rens-Domiano & Hamm, 1995 and Gudermann *et al.,* 1996). SP suppression overrides the activating effect of somatostatin via Gα pertussis toxin-insensitive subunits, probably $G\alpha_{q/11}$. Activation of PLC-β1 leads to second messenger activation of PKC and thus phosphorylation and suppression of the Kir2.0 channel. The Kir2.0 channel can be dephosphorylated and therefore reactivated by protein phosphatase 1 or 2A. The Kir3.0 channel is normally in the inactive state. However the activated state caused by somatostatin can be reversed (Velimirovic *et al.,* 1995) by the removal of PIP_2, causing destabilisation of Gβγ binding to Kir3.0 channel subunits.

An alternative mechanism of modulating Kir2.0 channel activity may be tyrosine phosphorylation stimulated by the NK-1 receptor with consequent suppression of channels, as described for the NGF receptor and Kir2.1 (Wischmeyer *et al.,* 1998). The channel modulation pathways potentially used by somatostatin and SP are summarised in Table 1-1.

Table 1-1. Channel Modulation Pathways Potentially Utilised by Somatostatin and Substance P

Effector	G-Protein Involved	References
Somatostatin-activates Kirs	1). Gβγ direct binding to and activation of Kir3.0. 2). Gβγ activation of PLC-β isoform and activation of Kir2.0. 3). $G\alpha_i$ pertussis toxin sensitive subunits activate Kir2.0.	Inoue *et al.*, 1988; Smrcka & Sternweis, 1993; Huang *et al.*, 1995; Velimirovic *et al.*, 1995 and Takano *et al.*, 1997.
Substance P-suppresses Kirs	1). Withdrawal of somatostatin resulted in reduced PIP_2 leading to destabilisation of Gβγ/Kir3.0 channel interaction and subsequent Kir3.0 channel inactivation. 2). $G\alpha_{q/11}$ (pertussis toxin insensitive subunits) activate PLC-β1/PKC, leading to phosphorylation and suppression of Kir2.0. 3). Phosphorylation of tyrosine residues in Kir2.0 C-terminus by tyrosine kinase activated through the NK-1 receptor?	Stanfield *et al.*, 1985; Yamaguchi *et al.*, 1990; Takano *et al.*, 1995; Takano *et al.*, 1996; Huang *et al.*, 1998 and Wischmeyer *et al.*, 1998.

In summary, somatostatin hyperpolarises neurons by maintaining both Kir2.0 and Kir3.0 channels in the activated conformation and allowing potassium ion flow. These conditions are overridden by SP, causing slow increases in neuronal excitability, by suppressing Kir2.0 and Kir3.0 channel activities.

1.10 Aims

Although previous electrophysiological studies have identified a slow increase in LC neuronal excitability, due to the suppression of Kir ion channels in response to the administration of substance P, the Kir isoform(s) involved in this suppression have not been identified, either in cultured cholinergic neurons (Stanfield *et al.,* 1985 and Yamaguchi *et al.,* 1990), cultured noradrenergic neurons (Koyano *et al.,* 1993) or dissected brain tissue sections containing noradrenergic neurons (Shen & North, 1992).

The project aims were: 1). To expand existing *in situ* hybridisation data produced using radiolabelled-oligonucleotide probes in the rat CNS. Therefore, high sensitivity digoxigenin-labelled Kir2.2 riboprobes were produced.

2). To raise, characterise and utilise rabbit anti-rat Kir2.1, anti-rat Kir2.2 and anti-rat Kir2.3 antibodies in the rat CNS for the first time.

3). To confirm earlier *in situ* hybridisation data, suggesting the co-localisation of the Kir2.2 channel isoform and the NK-1 receptor in the locus coeruleus of the rat medulla by immunohistochemistry. As the project progressed, additional aims were developed that fitted the overall subject.

4). To identify Kir2.0 non-neuronal sites of expression within the rat CNS, therefore providing evidence for the roles of Kir2.0 channel isoforms in macroglia and vascular smooth muscle by immunohistochemistry.

5). To provide evidence for a functional link between the co-localised NK-1 receptor and the Kir2.2 channel proteins in the rat locus coeruleus by examining second messenger pathways. (i) Initially, to provide evidence that Kir2.2 is a potential substrate for serine/threonine phosphorylation by *in vitro* phosphorylation of *in vitro* translated Kir2.2 channel protein. (ii) The SN56 cholinergic neuronal cell line was found to co-express both receptor and channel proteins. It was therefore used as a model in which tyrosine phosphorylation of the channel protein was assessed in response to stimulation by substance P.

Chapter 2: Materials and Methods

2.1 Generation of Probes for *In Situ* Hybridisation

Murine β-actin and Kir2.2 cDNAs were cloned into the pLITMUS 28 RNA expression vector (New England Biolabs, Hitchin, Herts). These sequences were confirmed to be unique using the BLAST2.0 software (Altschul *et al.*, 1997). A 199 bp mouse brain β-actin cDNA (accession number: X03672) was amplified from mouse brain total RNA by RT-PCR (Promega, Access RT-PCR, Southampton, Hants). The amplification included the fourth and fifth exons and was carried out using the upstream primer 5'-ATCATCCACACA GAGTACTTGCGC-3' and the downstream primer 5'-ATCCCATGAAACTACA TTCAATTCCAT-3'. The cDNA was ligated in reverse orientation into the pLITMUS vector using the SureClone blunt-end ligation kit (Pharmacia, St. Albans, Herts). Sequences encoding 120 amino acid N- and C-terminal regions of mouse Kir2.2 (accession number: X80417) were amplified by PCR from cloned template in pCDNA3 vector (Invitrogen, Leek, The Netherlands). The cDNA fragments were amplified using primers containing *Xho* I (forward primer) or *Xba* I (reverse primer) restriction sites: the N-terminal upstream and downstream primers were 5'-GATCCTCGAGACCCCGGGATGACCGCAGCC-3' and 5'-AGCTTCTAGACCC TCGGCTGGCTCCAGGTCCCCGTGGGCGACAGCAATGAC-3' respectively. The C-terminal upstream and downstream primers were 5'-GATCCTCGAGAGGCTCGCAGTTCCTACCTGGTCAACGAGATCCTGTG-3' and 5'-AGCTTCTAGAGGGCATTCAAATCTCCGACT-3' respectively. PCR products were ligated separately into the p-GEM-T vector (Promega). *Xho* I and *Xba* I (New England Biolabs) restriction digestions of successful transformant

plasmid DNA yielded fragments that were retrieved and subcloned into the pLITMUS vector on a *Xho* I-*Xba* I fragment using sites incorporated in the primers. Cloned cDNAs in pLITMUS were prepared by caesium chloride gradient equilibrium centrifugation (Sambrook *et al.,* 1989) and sequenced using the M13 reverse primer (5'-CAGGAAACAGCTATGACC-3'), with the Prism Sequenase dye terminator kit on an automatic sequencer (Perkin-Elmer, Seer Green, Bucks). All sequencing was carried out by the Protein and Nucleic Acid Chemistry Laboratory, Hodgkin Building, University of Leicester. Caesium chloride gradient equilibrium centrifugation (Sambrook *et al.,* 1989) was also used to purify plasmid DNA template suitable for transcript 'run-offs' (DIG RNA labelling kit (SP6/T7), Boehringer Mannheim, Lewes, East Sussex). The pLITMUS RNA expression vector contains unique restriction sites on the T7 RNA polymerase promoter regions flanking the insert DNA. Linearisation with either *Afl* II or *Spe* I (New England Biolabs) restriction endonucleases produced template DNA that allowed transcription of either antisense or sense riboprobes. Transcription incorporated digoxigenin (DIG)-labelled UTP's to produce labelled antisense and sense riboprobes. Transcription efficiency was assessed by titration of riboprobe onto positively charged nylon membranes (Boehringer Mannheim) and UV cross-linking using a UV Stratalinker 2400 set to auto cross-link, releasing 120 mjoules of energy (Stratagene, Amsterdam Zuidoost, The Netherlands). Colourimetric detection was then carried out using a sheep anti-DIG IgG antibody conjugated with alkaline phosphatase and NBT/BCIP substrate for 16 hours in darkness at room temperature (Boehringer Mannheim).

2.1.1 Small Scale Preparation of Plasmid DNA

Small scale preparation of plasmid DNA was achieved using the Wizard® *Plus* SV miniprep system (Promega). A single bacterial colony was inoculated into 10 ml LB containing 100 μg/ml ampicillin and cultured for 16 hours with aeration. Three millilitres of cells were pelleted by pulsing an MSE Micro Centaur microcentrifuge to 14,000 g for 15 seconds. The cells were resuspended in 250 μl of resuspension buffer (50 mM Tris-HCl pH 7.5/10 mM EDTA/100 μg/ml RNase A) and then lysed by the addition of 250 μl of cell lysis buffer (0.2 M NaOH/1% SDS). The lysate was mixed 4 times by inversion, producing a cloudy precipitate which cleared after 5 minutes. Ten microlitres of alkaline protease was added and incubated for 5 minutes at room temperature. The alkaline lysate was neutralised by the addition of 350 μl neutralisation buffer (4.09 M guanidine hydrochloride/0.759 M potassium acetate/2.12 M glacial acetic acid). The lysate was mixed by inversion, producing a heavy white precipitate which was pelleted by centrifugation at 14,000 g for 10 minutes. The supernatant was transferred to a spin column contained within a 1.5 ml Eppendorf tube and centrifuged at 14,000 g for 1 minute. Contaminants were removed by the addition of 750 μl wash solution (60% ethanol/60 mM potassium acetate/10 mM Tris-HCl pH 7.5) to the spin column, which was centrifuged at 14,000 g for 1 minute. A further wash was carried out with 250 μl washing solution, followed by centrifugation at 14,000 g for 2 minutes. The spin column was placed into a fresh tube and 100 μl of nuclease-free water added. The plasmid DNA was eluted from the spin column by centrifugation at 14,000 g for 1 minute.

2.1.2 Purification of DNA from Agarose Gel

The Genomed JETSORB system (Hybaid, Ashford, Middlesex) was used to extract DNA from agarose gel. The gel containing the desired DNA was excised, placed in an Eppendorf tube and weighed. For each 100 mg of gel, 300 μl of buffer A1 (sodium perchlorate/TBE-solubiliser/sodium acetate) and 10 μl JETSORB suspension (anion exchange resin) were added to the tube. The tube was then vortexed and heated to 50°C for 15 minutes. The JETSORB pellet was resuspended in 300 μl of buffer A1, followed by centrifugation in an MSE Micro Centaur microcentrifuge at 14,000 g for 25 seconds. The supernatant was removed and the JETSORB pellet resuspended in 300 μl of buffer A2 (ethanol/Tris-HCl/EDTA/NaCl), the tube was centrifuged as before. The supernatant was removed and the JETSORB pellet was allowed to dry at room temperature for 10 minutes. The DNA was extracted from the JETSORB pellet by the addition of 20 μl TE buffer (10 mM Tris-HCl pH 8.0/1 mM EDTA) with a 5 minute incubation at 50°C. The tube was centrifuged at 14,000 g for 1 minute in order to pellet the JETSORB material. The DNA was released into the supernatant for recovery. (Precise details of the composition of these buffers, except TE, was not made available by the manufacturer).

2.1.3 Cloning the Mouse Brain β-Actin cDNA Fragment

RT-PCR was carried out using the Promega Access kit. This used AMV-RT (avian myeloblastosis virus-reverse transcriptase) to produce first strand DNA; second strand synthesis then utilised *Taq* polymerase. Appropriate control reactions with control CAT (chloramphenicol acetyltransferase) RNA

and primers were performed, producing a single 323 bp control cDNA band on a 1% (w/v) agarose gel. The reactions contained the following: 1 x AMV-RT/*Taq* reaction buffer, 0.05 mM dATP, 0.05 mM dCTP, 0.05 mM dGTP, 0.05 mM dTTP, 125 nM β-actin forward primer, 125 nM β-actin reverse primer, 2 mM $MgSO_4$, 5.0 μg mouse brain total RNA, 200 units AMV-RT and 5 units *Taq* in a total reaction volume of 50 μl.

The RT-PCR cycling reactions were run on a Biometra TRIO-Thermoblock as follows: 1). First strand synthesis: 48°C for 45 minutes. 2). Denature AMV-RT: 94°C for 2 minutes. 3). Denaturing step: 94°C for 30 seconds. 4). Annealing step: 60°C for 1 minute. 5). Extension step: 68°C for 2 minutes. PCR steps 3-5 were cycled 40 times.

The β-actin cDNA fragment was further amplified by a PCR protocol containing: 1 x Boehringer Mannheim *Taq* reaction buffer, 0.05 mM dATP, 0.05 mM dCTP, 0.05 mM dGTP, 0.05 mM dTTP, 16 nM β-actin forward primer, 16 nM β-actin reverse primer, 2 mM $MgCl_2$, 5 ng β-actin fragment and 2 units Boehringer Mannheim *Taq* in a total volume of 100 μl.

The PCR cycling reactions were run on a Biometra TRIO-Thermoblock as follows: 1). Hot start: 94°C for 3 minutes. 2). Denaturing step: 94°C for 30 seconds. 3). Annealing step: 55°C for 1 minute. 4). Extension step: 72°C for 45 seconds. 5). Finishing extension step: 72°C for 7 minutes. PCR steps 2-4 were cycled 30 times.

The purified pLITMUS vector and β-actin insert were ligated using the SureClone blunt-ending kit. This involved 2 separate protocols, firstly a

blunting/kinasing reaction followed by a ligation reaction. The β-Actin and control blunting/kinasing reactions contained the following components: 1 x buffer, 1 μg β-Actin or control PCR product, 1 unit of polynucleotide kinase and 1 unit of Klenow in a total reaction volume of 20 μl. The reaction was incubated at 37°C for 30 minutes.

The PCR products were separated from nucleotides using Pharmacia S-300 microspin columns. The ligation reaction required an equimolar ratio of insert to vector ends. The following ligation reactions were prepared using the column eluents containing the inserts: 0.1 x ligation buffer, 700 ng β-Actin column eluent or 280 ng control column eluent, 50 ng pLITMUS or control pUC18 vector, 10 mM dithiothreitol (DTT) and 8 units T4 DNA ligase in a total reaction volume of 20 μl. The ligation reactions were incubated at 16°C for 2 hours. Ligation products were transformed into *E. coli* TOP10F' cells (prepared in house) using the chemical transformation protocol (Materials and Methods section 2.2).

2.1.4 Cloning the Mouse Kir2.2 N- and C-Terminal cDNA Fragments

Boehringer Mannheim *Taq* was used to amplify PCR products with 3' overhanging adenines in the following reaction: 1 x Boehringer Mannheim *Taq* reaction buffer, 0.1 mM dATP, 0.1 mM dCTP, 0.1 mM dGTP, 0.1 mM dTTP, 16 nM mKir2.2 N- or C-terminal forward primer, 16 nM mKir2.2 N- or C-terminal reverse primer, 1.5 mM $MgCl_2$, 5 ng mKir2.2 cDNA, accession number: X80417 and 1 unit Boehringer Mannheim *Taq* in a total reaction volume of 100 μl.

The PCR cycling reactions were run on a Biometra TRIO-Thermoblock as follows: 1). Hot start: 94^{o}C for 4 minutes. 2). Denaturing step: 94^{o}C for 1 minute. 3). Annealing step: 55^{o}C for 1 minute. 4). Extension step: 72^{o}C for 1 minute. 5). Finishing extension step: 72^{o}C for 5 minutes. PCR steps 2-4 were cycled 35 times.

2.1.5 Production of the Kir2.2 (Y243F) Mutant

The Stratagene QuikChange site directed mutagenesis kit was used to substitute Kir2.2 tyrosine residue 243 with a phenylalanine residue by a PCR approach. The PCR protocol contained the following components: 1 x Stratagene *Pfu* reaction buffer, 0.05 mM dATP, 0.05 mM dCTP, 0.05 mM dGTP, 0.05 mM dTTP, 64 nM Kir2.2 Y243F mutagenic forward primer, 64 nM Kir2.2 Y243F mutagenic reverse primer, 50 ng Kir2.2 cDNA, accession number: X80417 and 1 unit Stratagene *Pfu* in a total volume of 50 μl.

Mutagenic forward primer: 5'-GGAGGGTGAG**TTC**ATCCCACTGG-3'
Mutagenic reverse primer: 5'-CCAGTGGGAT**GAA**CTCACCCTCC-3'
Bases in bold indicate the mutagenic phenylalanine codon (5'-TTC is the sense strand).

A positive control reaction for the mutagenesis was carried out using pWhitescript with mutagenic primers. pWhitescript vector is a version of pBluescript where the glutamine codon (CAA) at residue 9 of the β-galactosidase gene has been mutated to a stop codon (TAA). Therefore, suppressor-free *E. coli* cells successfully transformed with pWhitescript appeared white on plates containing Luria agar, ampicillin, X-gal and IPTG.

However, pWhitescript can be mutated by PCR and mutagenic primers by replacing the TAA stop codon with the glutamine CAA codon (replacing thymidine with cytidine nucleotide), therefore restoring transcription of the full β-galactosidase gene. Mutant vector containing *E. coli* cells produce blue colonies under the conditions described above, thus serving as a positive control for the mutagenesis reaction. The pWhitescript PCR mutagenesis reaction contained the following components: 1 x Stratagene *Pfu* reaction buffer, 0.05 mM dATP, 0.05 mM dCTP, 0.05 mM dGTP, 0.05 mM dTTP, 125 ng control mutagenic forward primer, 125 ng control mutagenic reverse primer, 10 ng pWhitescript vector and 1 unit Stratagene *Pfu* in a total volume of 50 μl.

The PCR cycling reactions were run on a Perkin Elmer 2400 PCR machine as follows: 1). Denaturing step: 95°C for 30 seconds. 2). Denaturing step: 95°C for 30 seconds. 3). Annealing step: 45°C* for 1 minute. 4). Extension step: 68°C for 14 minutes. PCR steps 2-4 were cycled 16 times.
*: 55°C in the positive control.

The parental plasmid DNA produced by *E. coli* strains was methylated (DAM methylase) at GATC sequences. Therefore, mutated (non-methylated) PCR generated DNA was selected from the non-mutated (methylated) parental DNA by incubation with *Dpn* I endonuclease (recognises and cuts DNA at methylated GATC sequences). Thus, 1 unit of *Dpn* I endonuclease was incubated with each reaction at 37°C for 1 hour, digesting the methylated, non-mutated parental strand DNA. PCR reactions were transformed using the chemical transformation protocol directly into *E. coli* DH5α 10^8 competent cells (Gibco BRL, Paisley, Scotland). In addition to the mutagenesis positive control and mutagenesis reaction, a transformation positive control

(pLITMUS vector) was also used (1 μl mutagenesis positive control, 2.5 μl mutagenesis reaction and 1 ng of pLITMUS). Luria agar plates with 100 μg/ml ampicillin were prepared, the mutagenesis and transformation positive control plates were also treated with 2.5 mg of X-gal and 1 mM IPTG by incorporation to the agar upper surface with a 1 hour incubation at 37°C to dry the plates. White colonies from the mutagenesis reaction were selected at random and the insert cDNAs sequenced. Cloned cDNAs containing the mutation underwent further sequencing to confirm that no other mutations had been introduced into the cDNA.

Kir2.2 sequencing primers were designed by Dr Ian Ashmole of the Cell Physiology and Pharmacology Department, University of Leicester. The primers sequenced the non-coding strand from the following start sites:
1). 663-640: 5'-GCAGAGTCTGTGCGCGCTTCTTGG-3'. 2). 1148-1128: 5'-GCGGGGTGTAGATGGCACCTC-3'. 3). 1590-1565: 5'-CTCCTTGCCCACGGG TATACATCAGC-3'

2.1.6 Riboprobe Production by Transcript 'Run-Offs'

In situ hybridisation riboprobes were made by transcript 'run-off' from linearised DNA templates in the following reaction: 1 x transcription buffer, 1 μg linearised test or positive control template, 10 mM ATP, 10 mM CTP, 10mM GTP, 6.5 mM UTP, 3.5 mM DIG-UTP and 40 units of T7 RNA polymerase in a total volume of 20 μl in DEPC water. The reaction was incubated at 37°C for 2 hours.

2.2 Bacterial Transformation Using the Chemocompetent Protocol

E. coli XL1-Blue MRF' cells (originally obtained from Gibco BRL) were grown to an optical density of 0.3-0.4 at 600 nm. They were then aliquoted, centrifuged and resuspended in 100 μl volumes in polyethylene glycol and frozen at -80°C. Single aliquots were retrieved as required and thawed on ice over a 5 minute period. The following steps were then taken: 1). 1 μl of ligation mixture was added to 50 μl of cells. 2). The cells were incubated on ice for 30 minutes. 3). The cells were heat-shocked at 42°C for 45 seconds. 4). The cells were chilled on ice for 2 minutes. 5). 400 μl of LB was added to the cells, which were rescued at 37°C for 1 hour in an orbital shaker (minimum 200 rpm). 6). Each tube of cells was centrifuged at 14,000 g for 30 seconds in order to form a pellet. The LB was removed and replaced with 200 μl of fresh LB, 100 μl aliquots were pipetted onto Luria agar plates with the appropriate selection.

2.3 Colony PCR Screening for the pGEM-T and pLITMUS Vectors

PCR-based screening was used to differentiate between transformed colonies containing the vector with insert and those colonies that contained the religated vector. Screening took place on a Biometra TRIO-Thermoblock with 20 wells per block (3 blocks in total) so large numbers of colonies could be screened at once. A PCR 'master-mix' was made containing gene-specific forward and reverse primers, to span any insert present. Colonies without the insert did not give a DNA band. Fifty microlitres of master mix was used with each PCR reaction, containing the following components: 1 x *Taq* polymerase buffer (+1.5 mM $MgCl_2$), 0.1 mM dATP, 0.1 mM dCTP, 0.1 mM

dGTP, 0.1 mM dTTP, 32 nM gene specific forward primer, 32 nM gene specific reverse primer and 1 unit *Taq* polymerase.

The PCR cycling reactions were run on a Biometra TRIO-Thermoblock as follows: 1). Hot start: 94^{o}C for 4 minutes. 2). Denaturing step: 94^{o}C for 1 minute. 3). Annealing step: 55^{o}C for 1 minute. 4). Extension step: 72^{o}C for 1 minute. Typically, PCR steps 2-4 were cycled 35 times.

2.4 RNA Dot-Blots

Equilibrium centrifugation in caesium chloride gradients (Sambrook *et al.*, 1989) was used to purify plasmid DNA template suitable for transcript 'run-offs' (DIG RNA labelling kit (SP6/T7), Boehringer Mannheim). The pLITMUS RNA expression vector contains unique restriction sites on the T7 RNA polymerase promoter regions flanking the insert DNA. Linearisation with either *Afl* II or *Spe* I (New England Biolabs) restriction endonucleases produced template DNA that allowed transcription of either antisense or sense riboprobes. Transcription incorporated digoxigenin (DIG)-labelled UMP, producing labelled antisense and sense riboprobes. Transcription efficiency was assessed by titration of riboprobe onto positively charged nylon membranes (Boehringer Mannheim), followed by UV cross-linking as described in Materials and Methods section 2.1. The membranes were then rinsed in washing buffer (100 mM maleic acid pH 7.5/150 mM NaCl/0.3% Tween 20) for 1 minute and blocking buffer (100 mM maleic acid pH 7.5/150 mM NaCl/1% Boehringer Mannheim blocking reagent) for 30 minutes, both at room temperature. A sheep anti-DIG IgG antibody conjugated with alkaline phosphatase was diluted in blocking buffer (1:5000) and incubated with the

membranes for 30 minutes at room temperature. The membranes were washed twice in washing buffer for 15 minutes each and once in detection buffer (100 mM Tris HCl pH 9.5/100 mM NaCl) for 2 minutes, all at room temperature, followed by incubation with 20 ml of detection buffer containing 0.38 mg/ml NBT/0.18 mg/ml BCIP (Boehringer Mannheim) for 16 hours at room temperature in darkness.

Hybridisation of 25 ng/ml mKir2.2 riboprobe cocktails to a titration of UV cross-linked mouse brain total RNA and mKir2.2 DNA on positively charged nylon membranes, was carried out for 16 hours in 50% formamide/0.5 x SSC (standard saline citrate: 7.5 mM $Na_3C_6H_5O_7.2H_2O$/75 mM NaCl pH 7.0)/0.02% SDS (sodium dodecyl sulphate)/0.1% N lauroylsarcosine/2% Boehringer Mannheim blocking reagent at 42°C, followed by 3 post-hybridisation washes containing 40% formamide/0.5 x SSC for 10 minutes at 42°C. The membranes were then washed in NTE buffer (10 mM Tris HCl pH 7.5/0.5 M NaCl) for 3 minutes at 37°C, followed by a single wash with NTE buffer containing 20 μg/ml RNase A (Sigma, Poole, Dorset) for 30 minutes at 37°C. The membranes were then rinsed in washing buffer for 1 minute and blocking buffer for 30 minutes, both at room temperature. A sheep anti-DIG IgG antibody conjugated with alkaline phosphatase, was diluted in blocking buffer (1:20,000) and incubated with the membranes for 30 minutes at room temperature. The membranes were washed twice in washing buffer for 15 minutes each and once in detection buffer for 2 minutes, all at room temperature. The membranes were treated with a 1:100 dilution of CDP. STAR enhanced chemiluminescent substrate (Boehringer Mannheim) in detection buffer for 5 minutes at room temperature. The membranes were placed in Saran wrap and laid against X-ray hyperfilm (Amersham, Little

Chalfont, Bucks) for 1 minute and then developed. Similarly, hybridisation of 100 ng/ml β-actin riboprobes to a titration of UV cross-linked mouse brain total RNA and β-actin DNA on positively charged nylon membranes, was carried out for 16 hours with 40% formamide/4 x SSC/0.02% SDS/0.1% N lauroylsarcosine/2% Boehringer Mannheim blocking reagent at 37°C, followed by 3 post-hybridisation washes containing 50% formamide/0.5 x SSC for 10 minutes at 37°C. Other treatments and the detection system were identical to the details described in the previous paragraph.

2.5 Southern Blots

Double stranded DIG-11-dUTP labelled DNA probes were made by PCR amplification for β-actin and both mKir2.2 N- and C-terminal cDNAs. Mouse Kir2.0 and Kir3.0 cDNAs were determined to have the closest sequence homology to mKir2.2 of any known sequence as shown by BLAST2.0 software (Altschul *et al.,* 1997). Therefore Southern blotting (Sambrook *et al.,* 1989) was carried out using linearised plasmids (pCDNA3 cut with *Pvu* I/*Hind* III or pLITMUS cut with *Afl* II (New England Biolabs)) containing mKir2.2 and β-actin, together with 500 ng cDNA per lane of mouse Kir2.1, Kir2.3, Kir3.1, Kir3.2, Kir3.4 and the human NK-1 receptor. Nucleic acids were transferred onto a positively charged nylon membrane and UV cross-linked as described in Materials and Methods section 2.1. Mouse Kir2.2 DNA probe cocktail (10 ng/ml) was denatured by boiling for 10 minutes, followed by chilling on ice. Hybridisation to the membrane was carried out for 16 hours in 50% formamide/0.5 x SSC/0.02% SDS/0.1% N lauroylsarcosine/2% Boehringer Mannheim blocking reagent at 45.5°C. Stringent post-hybridisation washes were performed, containing 2 x SSC/0.1% SDS twice

for 5 minutes at room temperature and 0.1 x SSC/0.1% SDS twice for 15 minutes at 68°C.

Hybridisation of the denatured β-actin DNA probe (20 ng/ml) was carried out in a similar manner. The hybridisation conditions required 50% formamide/0.5 x SSC/0.02% SDS/0.1% N lauroylsarcosine/2% Boehringer Mannheim blocking reagent for 16 hours at 42°C, followed by post-hybridisation washes containing 2 x SSC/0.1% SDS twice for 5 minutes and 0.1 x SSC/0.1% SDS twice for 15 minutes at room temperature. Homologous probe hybridisation was defined as 10°C below theoretical Tm (melt temperature) for probe and target. Detection used sheep anti-DIG IgG antibodies (1:20,000) conjugated with alkaline phosphatase and the enhanced chemiluminescence system described in Materials and Methods section 2.4 (Boehringer Mannheim).

2.6 Tissue Preparation

Adult male Fisher rats were overdosed with 3% halothane anaesthetic in NO_2/O_2 and then decapitated. The brains were dissected and sectioned into coronal cerebellar and hippocampal blocks, and then fixed in 10% formal saline at room temperature for 48 hours. The blocks were subsequently paraffin-embedded and 4 μm sections cut on a microtome and mounted on silane coated glass slides. Sections were dewaxed in xylene and hydrated with 99%, 95% ethanol and finally water. Mayer's haematoxalin/eosin staining was used to indicate the condition of morphology and fixation within the tissue. In addition Weil-Davenport's technique was adopted for macroglial staining (Conn & Darrow, 1943).

Lister-Hooded rats (21 days old) were sacrificed by cervical dislocation, severing the carotid artery and finally decapitation. The brains were quickly dissected and the hippocampus, cerebellum/medulla regions removed. These tissues were rapidly frozen by immersion in iso-pentane, chilled by cardice. Frozen tissues were stored at -80^{o}C until required for Western blotting or *in vitro* dephosphorylation or deglycosylation studies.

2.7 *In Situ* Hybridisation

The β-actin and mKir2.2 specific *in situ* hybridisation conditions were determined by a procedure of increasing stringencies, until no hybridisation was seen. Stringency was then reduced until a homologous hybridisation between probe and target was seen as a strong signal in the antisense section, with the equivalent sense section remaining free of specific hybridisation. Cocktails of separate mKir2.2 antisense and sense riboprobes underwent homologous *in situ* hybridisation with the following empirically determined conditions: Coronal cerebellar sections containing the LC were dewaxed, hydrated and then immersed in 2 x SSC (30 mM $Na_3C_6H_5O_7.2H_2O$/0.3 M NaCl pH 7.0) for 10 minutes at 70^{o}C. Following a rinse in water, the sections were incubated in 2 μg/ml proteinase K for 1 hour at 37^{o}C. Sections were rinsed in water and post-fixed in 0.4% paraformaldehyde in 1 x phosphate buffered saline (PBS: 150 mM $NaPO_4$ pH 7.2/150 mM NaCl) for 20 minutes at 4^{o}C. Prehybridisation was carried out at 42^{o}C for 1 hour and contained the following: 50% formamide, 10% dextran sulphate, 1 x Denhardt's solution, 10 mM DTT, 0.5 x SSC, 1 mg/ml salmon sperm DNA and 1 mg/ml bakers' yeast transfer RNA. Subsequently sections were hybridised for 16 hours under the same conditions without riboprobe

(negative control), or 1.5 μg/ml antisense or sense mKir2.2 riboprobe cocktails on adjacent sections. After hybridisation, sections were washed 3 times in 40% formamide/0.5 x SSC for 10 minutes at 42°C. Sections were washed twice in NTE buffer (Materials and Methods section 2.4) for 3 minutes at 37°C, followed by a single wash with NTE buffer containing 20 μg/ml RNase A (Sigma) for 30 minutes at 37°C. The sections were then rinsed in blocking solution (3% BSA/0.1% Triton X-100 in Tris-HCl buffered saline (1 x TBS: 50 mM Tris-HCl pH 7.65/138 mM NaCl)) for 5 minutes at room temperature.

Detection involved a 1:600 dilution of sheep anti-DIG IgG antibodies conjugated with alkaline phosphatase (Boehringer Mannheim), in blocking solution for 30 minutes at room temperature. Sections were washed twice in TBS, followed by a single wash in substrate buffer (100 mM Tris-HCl pH 9.5/50 mM $MgCl_2$/100 mM NaCl) for 5 minutes at room temperature. Tissue sections were incubated with 100 μl of substrate buffer containing 0.38 mg/ml NBT/0.18 mg/ml BCIP/1 mM levamisole for 16 hours at room temperature in darkness. After detection the sections were preserved in aquamount (Sigma).

The β-actin antisense and sense riboprobes underwent homologous *in situ* hybridisation at different stringencies to mKir2.2, but the basic protocol remained the same as described earlier in this section. Prehybridisation/hybridisation was carried out at 37°C in the following solution: 40% formamide, 10% dextran sulphate, 1 x Denhardt's solution, 10 mM DTT, 4 x SSC, 1 mg/ml salmon sperm DNA and 1 mg/ml bakers' yeast transfer RNA. Hybridisation used 1 μg/ml antisense or sense β-actin

riboprobes on adjacent tissue sections. After hybridisation, sections were washed 3 times in 50% formamide/0.5 x SSC for 10 minutes at 37°C.

2.8 Preparation of Anti-Kir2.0 Polyclonal Antibodies

Antisera were raised by Dr Robert Norman of the Medicine Department, University of Leicester, to peptides corresponding to the C-terminal domains of the rat Kir2.1, Kir2.2 and Kir2.3 proteins. The peptides were synthesised in accordance with a standard methodology (Atherton & Sheppard, 1985) by the Protein and Nucleic Acid Chemistry Laboratory, Hodgkin Building, University of Leicester, and were composed of the following amino acid residues: Kir2.1: CHNQASVPLEPRPL (residues: 409-421), Kir2.2: CRLQASSGALERPY (residues: 409-421) and Kir2.3: CRMQAATLPLDNISY (residues: 427-440). N-terminal cysteine residues were added to the peptides to facilitate conjugation to ovalbumin carrier protein (Larochelle *et al.*, 1985), and then inoculated into New Zealand White rabbits. The antisera were purified by Dr Robert Norman, by affinity chromatography using peptide immobilised on Sulpho-Link coupling gels according to manufacturer's instructions (Pierce, Chester, Cheshire).

2.9 *In Vitro* Translation

Mouse Kir2.0 cDNAs in the pCDNA3 vector (Invitrogen) were transcribed and translated in the TNT rabbit reticulocyte lysate system (Promega), in the presence of 0.74 MBq [^{35}S]-Methionine (Amersham) and, for mKir2.1 and mKir2.2 only, canine pancreatic microsomal membranes (Promega). The reactions were incubated at 30°C for 90 minutes. 5 μl of each reaction

product (25 μl total) was loaded per lane on an 8% polyacrylamide gel (Laemmli, 1970), with low and high molecular weight protein standards in the same track (Sigma) at 1 μg/ml each. Gels were electrophoresed for 16 hours at 45 volts. Following electrophoresis the protein standard lanes were removed and stained in Fairbanks I stain (140 mg/litre each of G250/R250 Coomassie Blue stains/25% propan-2-ol/10% acetic acid), the main portion of the gel was fixed in 50% methanol/10% glacial acetic acid for 30 minutes. The gel was then treated with Amplify scintillant (Amersham) for a further 30 minutes before being vacuum dried at 80°C for 2 hours (Bio Rad, Hemel Hempstead, Herts). The dried gel was then placed against X-ray film (Sigma) and stored at -80°C, typically for 16 hours, before development of the film.

2.10 Immunoprecipitation

In vitro translated mKir2.0 proteins were treated with an equal volume of 2% Triton X-100/20 mM Tris-HCl pH 7.5 for 30 minutes at 4°C. Two-five microlitres of [^{35}S]-Methionine-labelled proteins were incubated for 16 hours at 4°C with 20 μl of protein specific antisera in a final volume of 1 ml made up in 20 mM Tris-HCl pH 7.5/1% BSA in TBS/100 mM KCl/0.2% Triton X-100. The protein/antibody complexes were immunoprecipitated by the addition of 5 mg/reaction of protein A Sepharose CL-4B (Sigma) with a 2 hour incubation with mixing at 4°C. The reactions were washed in 0.1% Triton X-100/20 mM Tris-HCl pH 7.5 followed by centrifugation by pulsing an MSE Micro Centaur microcentrifuge to 14,000 g for 5 seconds. Supernatants were removed and discarded, whilst the pellets were resuspended in fresh washing buffer as described above, this washing process was repeated 4 times. The protein/antibody complexes were recovered by the addition of denaturing

buffer (220 mM sucrose/2% SDS/6 mM DTT/62 mM Tris-HCl pH 6.8/Bromophenol Blue stain) and centrifugation as above. The supernatants were recovered and heated to 95°C for 5 minutes before being electrophoresed on an 8% polyacrylamide gel with 1 μg/ml low and high molecular weight standards (Laemmli, 1970). The protein standard lanes were removed and stained with Fairbanks I stain (Materials and Methods section 2.9): the main portion of the gel was treated with Amplify scintillant (Amersham), dried and placed against X-ray film as described in Materials and Methods section 2.9. Controls included omission of antibody, use of non-specific antibodies, and preabsorption of antibody solutions with 10 μg/ml of the specific or non-specific antigenic peptide for 16 hours at 4°C.

2.11 Western Blots

Rat brain tissue was homogenised (Ultraturrax) in homogenisation buffer at 4°C (320 mM sucrose/50 mM Tris-HCl pH 7.5), containing protease inhibitors (1 mM benzamidine, 1,10-phenanthroline and iodoacetamide, 0.1 mM phenylmethylsuphonyl fluoride, 2 μM leupeptin and pepstatin A). Centrifugation at 1,295 g for 10 minutes at 4°C yielded a nuclear pellet, and further centrifugation of the supernatant at 3,390 g for 10 minutes at 4°C yielded a mitochondrial pellet. This pellet was discarded and the supernatant was centrifuged at 44,800 g for 30 minutes at 4°C to obtain a plasma membrane pellet. Nuclear and plasma membrane protein pellets were resuspended in homogenisation buffer and protein concentration was determined using the bicinchoninic acid assay (Smith *et al.,* 1985). One hundred micrograms of protein was denatured and electrophoresed per lane on an 8% polyacrylamide gel (Laemmli, 1970). Protein was

transferred to nitrocellulose membranes (Hybond-C Super, Amersham) with a wet blot technique (Towbin & Gordon, 1984). Membranes containing standards were stained with Amido Black stain (0.1% Amido Black stain/45% methanol/10% acetic acid), followed by a destaining procedure which utilised 25% propan-2-ol/10% acetic acid. The test protein blots were incubated in blocking buffer (blots detected with rabbit IgG antibodies: 10 mM Tris-HCl pH 7.5/150 mM NaCl/0.05% Tween 20/5% milk powder; blots detected with mouse IgG PY99 antibody: 10 mM Tris-HCl pH 7.5/100 mM NaCl/0.1% Tween 20/3% BSA) for 1 hour at room temperature. The blots were then placed in a Decaprobe (Hoefer Scientific Instruments Ltd, San Francisco, CA), rinsed twice in Sarcosyl buffer (10 mM Tris-HCl pH 7.5/1 M NaCl/0.25% sodium sarcosine/0.25% Nonidet P40) and then treated with affinity purified antibodies (anti-Kir2.1: 9.3 μg/ml, anti-Kir2.2: 8.6 μg/ml, anti-Kir2.3: 8.4 μg/ml, 1:500 dilution of anti-NK-1 receptor or 0.2 μg/ml PY99 anti-phosphotyrosine antibody (Santa Cruz, Calne, Wilts)) in overlay buffer (10 mM Tris-HCl pH 7.5/150 mM NaCl/0.05% Tween 20) for 16 hours at 4^{o}C. This was followed by 2 washes in Sarcosyl buffer for 5 minutes at room temperature. An incubation for 1 hour was then carried out with a rabbit anti-mouse IgG antibody (for detection of PY99 primary antibody) or mouse anti-rabbit IgG antibody (for detection of other primary antibodies).

Colourimetric detection utilised secondary antibodies conjugated to alkaline phosphatase (Sigma) at a dilution of 1:1000 in overlay buffer. This was followed by two 5 minutes washes with Sarcosyl buffer and an incubation in 2.3 mg/ml NBT/BCIP in aqueous solution (Sigma). Enhanced chemiluminescence required an incubation in appropriate blocking buffers (described above) for 30 minutes at room temperature, followed by an

incubation for 1 hour with a rabbit anti-mouse IgG antibody (for detection of PY99 primary antibody) or mouse anti-rabbit IgG antibody (for detection of other primary antibodies), conjugated to horse radish peroxidase (Sigma) at a dilution of 1:2000 in overlay buffer. This was followed by two 5 minutes washes with Sarcosyl buffer. The blots were then placed face-up on Saran wrap, enhanced chemiluminescence reagent (Amersham) was incubated on the blots for 1 minute, before being drained. The blots were enclosed in Saran wrap and laid against X-ray hyperfilm (Amersham) for 1 minute and then developed. Controls consisted of primary antibody preabsorbed with 10 μg/ml specific antigenic peptide.

2.12 Immunohistochemistry

Paraffin-embedded 4 μm rat cerebellar and hippocampal brain sections were immunostained with the anti-Kir2.0 and anti-NK-1 receptor polyclonal antisera. The following generalised protocol was used with the addition of a 2 μg/ml proteinase K incubation for 1 hour at 37^{o}C, for the anti-Kir2.1 and anti-Kir2.3 antibodies. Tissue sections were dewaxed, hydrated to water and rinsed in TBS. The tissue sections were then blocked with 20% normal swine serum in blocking solution (Materials and Methods section 2.7) for 10 minutes at room temperature. Tissue sections were incubated with primary antibody, diluted in blocking solution for 16 hours at 4^{o}C (anti-Kir2.1: 5.3 μg/ml, anti-Kir2.2: 12μg/ml, anti-Kir2.3: 13μg/ml or 1:500 dilution of anti-NK-1 receptor affinity purified antibodies; or 1:500 dilution of anti-Kir2.1, 1:200 dilution of anti-Kir2.2 and anti-Kir2.3 antisera). The tissue sections were washed twice in TBS for 5 minutes at room temperature. Secondary detection involved the use of a 1:800 dilution of biotinylated swine anti-rabbit IgG

antibody (Dako, Cambridge) in blocking solution for 30 minutes at room temperature. The sections were washed twice in TBS for 5 minutes at room temperature, followed by 30 minutes incubation with 1.8% streptavidin-biotin (alkaline phosphatase) ABC-AP complex (Dako) at room temperature. The sections were washed twice in TBS and once in water for 5 minutes at room temperature. Finally, tissue sections were rinsed in substrate buffer for 5 minutes and detected colourimetrically with NBT/BCIP as described in Materials and Methods section 2.7. Preabsorption of primary antisera to specific and non-specific peptides (10 μg/ml) in blocking solution for 16 hours at 4^{o}C was sufficient to demonstrate specific peptide block of antisera binding. Controls included the absence of primary with secondary antibodies and the ABC-AP complex and also the absence of primary and secondary antibodies with the ABC-AP complex. Co-localisation on sequentially cut 4 μm coronal cerebellar sections was possible by colourising and overlaying 1 tissue section on top of the other, followed by merging of the images to produce the resultant co-localised image. This procedure was carried out by Dr Peter Furness of the Pathology Department, Leicester General Hospital, using a Zeiss photomicroscope and a CDHU 1912 monochrome video camera with the Macromedia XRES program on a Macintosh G3 computer.

2.13 Immunocytochemistry

Chinese hamster ovary (CHO) cells were grown on coverslips to 70-80% confluence in minimal essential media alpha with glutamax-1, without ribonucleosides or deoxyribonucleosides (Gibco BRL), and 10% foetal calf serum. The cells were then transiently transfected with 2 μg/ml mouse Kir2.1, Kir2.2 or Kir2.3 cDNAs in pCDNA3 vector using Fugene 6 (Boehringer

Mannheim). The cells were allowed to grow for 24 hours after transfection before being washed twice in calcium/magnesium free-phosphate buffered saline (CMFPBS (Sigma)). The cells were then fixed in methanol for 20 minutes, before being washed 5 times in CMFPBS. Cells were permeabilised with 0.1% Triton X-100/4% FCS/CMFPBS for 20 minutes and then washed again twice in CMFPBS before being blocked in 10% goat serum in CMFPBS for 15 minutes. Coverslips were transferred to blotting paper where they were left to dry for 5 minutes. The cells were then incubated with affinity purified primary antibodies (anti-Kir2.1: 5.3 μg/ml, anti-Kir2.2: 12 μg/ml and anti-Kir2.3: 13 μg/ml) in 10% normal goat serum/CMFPBS for 16 hours at room temperature. The coverslips were rinsed twice for 5 minutes and once for 30 minutes in CMFPBS.

Secondary detection involved an incubation with 4.9 mg/ml goat rhodamine labelled-anti-rabbit IgG antibody (Sigma), in 10% goat serum/CMFPBS for 1 hour at 37^{o}C. Cells were then washed twice for 2 minutes and once for 30 minutes in CMFPBS and stained with Hoechst 33342 (Sigma) nuclear stain (5 μg/ml in CMFPBS) for 10 minutes. Cells were again washed twice for 2 minutes and once for 30 minutes in CMFPBS. The coverslips were mounted in fluoromount (Sigma) and examined under a Leica TCS 4D confocal microscope with simultaneous detection in 2 channels, UV (excitation: 350 nm, emission: 420 nm) and rhodamine (excitation: 546 nm, emission: 590 nm). Controls included detection in the absence of primary with secondary antibody and detection in the absence of primary and secondary antibodies in transfected cells.

Although the Kir2.0 antisera were raised against rat peptides, the cells in this experiment were transfected with mouse Kir2.0 cDNAs. A peptide sequence alignment (MacVector 6.0.1, Oxford Molecular Group PLC) indicated no difference between rat and mouse Kir2.1 C-terminal peptide sequences or between rat and mouse Kir2.3 C-terminal peptide sequences. Rat and mouse Kir2.2 C-terminal peptide sequences varied by 2 amino acid residues (G for A and E for V, rat for mouse respectively. See Appendix 1).

Immunocytochemical staining of the SN56 and COS7 cell lines used the same protocol except for deviations in the following areas: The SN56 cells were grown in Dulbecco's minimal essential media containing glutamax-1, pyridoxine, 4500 mg/litre glucose without sodium pyruvate (Gibco BRL), with 10% foetal calf serum on laminin coated cover slips. The COS7 cells were grown in Dulbecco's minimal essential media containing glutamax-1, pyridoxine, sodium pyruvate, 1000 mg/litre glucose (Gibco BRL) and 10% foetal calf serum. The cell cultures were fixed by media dilution with 1% paraformaldehyde/0.1 M sodium cacodylate buffer, followed by washing 3 times for 15 minutes with 0.1 M cacodylate buffer. The cover slips were rinsed 3 times with 0.5% BSA/CMFPBS, permeabolised with 0.1% Triton X-100/0.5% BSA/CMFPBS for 20 minutes and blocked with 10% normal goat serum/CMFPBS for 15 minutes. Primary antibody detection included 1:500 dilution of the anti-NK-1 receptor antibody, in addition to the anti-Kir2.2 and anti-Kir2.3 antibodies as previously described (antibody dilutions were made in 0.5% BSA/CMFPBS). Secondary detection used goat anti-rabbit IgG conjugated to Cy3 fluorescent stain (1:200 (Amersham)) and cytoskeletal counter-staining was achieved with phalloidin toxin conjugated Cy2 fluorescent stain (1:200 (Molecular Probes, Leiden, The Netherlands)). In

addition, Hoechst 33342 (Sigma) nuclear stain (5 μg/ml) was also used. The confocal microscope with simultaneous detection in 3 channels was used, UV (excitation: 350 nm, emission: 420 nm), Cy2 (excitation: 490 nm, emission: 520 nm) and Cy3 (excitation: 546 nm, emission: 590 nm). Confocal microscopy was carried out by Mr Andrew Hubbard and Mr Kulvinder Sikand with the support of Dr Christopher Guerin of the Hodgkin Building, University of Leicester.

2.14 *In Vitro* Dephosphorylation

Native rat brain tissue was centrifuged into nuclear and plasma membrane fractions (Materials and Methods section 2.11). Two milligram aliquots of protein were dephosphorylated *in vitro* by incubation with calf intestinal alkaline phosphatase (CIAP (Sigma)). The *in vitro* dephosphorylation reactions included nuclear fraction proteins treated with or without CIAP, the reactions contained the following components: 1 x reaction buffer, 2 mg nuclear protein and 60 units CIAP in the test reaction only, in a final volume of 150 μl. Further *in vitro* dephosphorylation reactions included plasma membrane fraction proteins treated with or without CIAP, the reactions contained the following components: 1 x reaction buffer, 2 mg plasma membrane protein and 60 units CIAP in the test reaction only, in a final volume of 300 μl. Reactions were incubated at 37^{o}C for 1 hour.

2.15 *In Vitro* Deglycosylation

Native rat brain tissue was centrifuged into nuclear and plasma membrane fractions (Materials and Methods section 2.11). Two milligram aliquots of

protein were deglycosylated *in vitro* by incubation with endoglycosidase F (Sigma). The *in vitro* deglycosylation reactions included nuclear fraction proteins treated with or without endoglycosidase F, the reactions contained the following components: 2 mg nuclear protein and 0.5 unit of endoglycosidase F in the test reaction only, in a final volume of 200 µl. Further *in vitro* deglycosylation reactions included plasma membrane fraction proteins treated with or without endoglycosidase F, the reactions contained the following components: 2 mg plasma membrane protein and 0.5 unit of endoglycosidase F in the test reaction only, in a final volume of 300 µl. Reactions were incubated at 37°C for 16 hours.

2.16 *In Vitro* Phosphorylation

In vitro translated Kir2.2 protein was produced as described in Materials and Methods section 2.9 with either [^{35}S]-labelled-methionine or unlabelled methionine. Radiolabelled protein was phosphorylated *in vitro* with ATP and either PKA, PKCγ or PKC (all isoforms except PKCγ). Similarly, unlabelled Kir2.2 protein was phosphorylated with [γ^{32}P]-ATP and the previously described enzymes. The *in vitro* phosphorylation reactions are shown as follows:

2.16.1 Phosphorylation with [γ^{32}P]-ATP

The PKA and no-enzyme negative controls contained the following components: 5 µl Kir2.2 protein, 0.36 mCi [γ^{32}P]-ATP (>5000 Ci/mmol), 20 mM Tris pH 7.5 and 10 units cA-PK catalytic subunit in the test reaction only, in a final volume of 50 µl. Reactions were incubated at 37°C for 30 minutes.

The PKC reactions contained the following components: 1 x reaction buffer, 5 μl Kir2.2 protein, 0.36 mCi [γ^{32}P]-ATP (>5000 Ci/mmol), 660 ng phospholipid solution and either 17.5 ng PKC isoforms minus PKCγ or 0.225 ng PKCγ in a total volume of 36.5 μl. Reactions were incubated at 37°C for 30 minutes.

2.16.2 Phosphorylation with Unlabelled ATP

The PKA and no-enzyme negative controls contained the following components: 5μl Kir2.2 [^{35}S]-labelled protein, 1 mM ATP (disodium salt), 20 mM Tris pH 7.5 and 10 units cA-PK catalytic subunit in the test reaction only, in a final volume of 50 μl. Reactions were incubated at 37°C for 30 minutes.

The PKC reactions contained the following components: 1 x reaction buffer, 5μl Kir2.2 [^{35}S]-labelled protein, 1 mM ATP (disodium salt), 660 ng phospholipid solution and either 17.5 ng PKC isoforms minus PKCγ or 0.225 ng PKCγ in a total volume of 36.5 μl. Reactions were incubated at 37°C for 30 minutes.

Chapter 3: Localisation of the Kir2.2 and β-Actin mRNAs in the Locus Coeruleus by *In Situ* Hybridisation

3.1 Rationale for Using Digoxigenin-Labelled Riboprobes with *In Situ* Hybridisation

In situ hybridisation is the only technique currently available to allow the spatial distribution of specific RNA species to be assessed at the tissue, cellular and subcellular levels. The technique was first used in the 1960's and is based on the specific hybridisation of a labelled nucleic acid probe to a target RNA or DNA species (Gall & Pardue, 1969). An appropriate detection system then allows visualisation of the specific signal in the tissue section (Gall & Pardue, 1969 and Farquharson *et al.,* 1990). *In situ* hybridisation can be carried out with DNA or RNA probes (Komminoth, 1992 and Komminoth *et al.,* 1992). The decision to use RNA probes was based on the fact that, despite the fragility of RNA in an environment with considerable RNase activity, an RNA probe would bind to a mRNA target molecule with the strongest affinity of any nucleic acid-nucleic acid interaction. Because of the relatively high T_m (the mean thermal denaturation temperature at which 50% of the hybrids dissociate) of RNA:RNA hybrids, high stringency hybridisation conditions and post-hybridisation washes were possible, ensuring a low background and maximal signal strength (Komminoth, 1992 and Komminoth *et al.,* 1992).

In situ hybridisation originally utilised only radiolabelled probes, as this was the only labelling technology available (Gall & Pardue, 1969). Recently, the digoxigenin steroid hapten, derived from the plant cardiac glycoside digoxin,

has been used as a labelling molecule (Farquharson *et al.,* 1990). The decision to use digoxigenin-labelling over radiolabelling of probes was based on the following factors: 1). The specificity of the digoxigenin probes was equal to that of a radiolabelled probe of equal length but the former had the advantage of higher stability. 2). The rapid development speed of the enzymatic or fluorescent detection systems. 3). The use of radiolabelled probes often resulted in 'blooming' of the signal on the autoradiogram, yielding poor resolution of signal detection. 4). The use of digoxigenin removed the risks associated with use of radioactive materials, both to the researcher and to the environment (Komminoth, 1992 and Komminoth *et al.,* 1992).

Once the decision to use non-radioactive methods had been made, it was necessary to decide on the length of probe to be used in the *in situ* hybridisation. The simplest type of probe to manufacture is the digoxigenin-labelled deoxyoligonucleotide (Baldino & Lewis, 1989). These probes can be a maximum of 50 bp in length and incorporate a single type of digoxigenin-labelled nucleotide, such as digoxigenin-dUTP (Baldino & Lewis, 1989). Such synthetic DNA molecules are easy to manufacture and are robust to handle but suffer from a lack of specificity because of their shortness and comparative weakness of the RNA-DNA interaction (Komminoth, 1992 and Komminoth *et al.,* 1992). The chosen method for the production of a high specific activity digoxigenin-labelled riboprobe was *in vitro* transcription from cloned DNA templates contained in the pLITMUS RNA expression vector with T7 RNA polymerase, digoxigenin-UTP and other unlabelled ribonucleoside triphosphates (Komminoth, 1992 and Komminoth *et al.,* 1992). The size of the cloned cDNA fragments could be up to 500 bp. This was considered to

be the maximum length of polynucleotide that could effectively penetrate the surface of the *in situ* hybridisation section to bind to the target mRNA molecule (Komminoth, 1992 and Komminoth *et al.,* 1992). Therefore, probe sizes of between 199 bp and 359 bp were selected to allow both probe-penetration into the sections and maximum probe-specificity to the target (Komminoth, 1992 and Komminoth *et al.,* 1992). DNA templates were cloned from the N- and C-terminal coding regions of the mouse Kir2.2 cDNA and a single region of the mouse β-actin cDNA. These areas contained the most hypervariable regions within each gene family, thus providing the lowest possibility of non-specific hybridisation to mRNA from other members of the target gene's family as confirmed by BLAST2.0 search (Altschul *et al.,* 1997), (see Appendices 2 and 3).

3.2 Cloning a Mouse β-Actin cDNA Fragment

A 199 bp mouse β-actin cDNA fragment was cloned into the pLITMUS RNA expression vector to act as a positive control for the *in situ* hybridisation experiments. Mouse sequences were used for both β-actin and Kir2.2 probe templates, as they provided flexibility for other applications. The probes were utilised in this project to identify a Kir isoform expressed in rat LC. Sequence alignment of mouse and rat clones indicated tolerably few differences between the two species (see Appendix 4).

The PCR-generated cDNA fragment was cloned from mouse brain total RNA producing a mouse brain β-actin cDNA of 199 bp (accession number: X03672). This cDNA fragment had low homology to other sequences, as confirmed by BLAST2.0 search (Altschul *et al.,* 1997), (see Appendix 3). The

forward and reverse primers for this RT-PCR reaction were designed to anneal to the DNA in the fourth and fifth exons of the gene, respectively. In the genomic DNA the fragment would start at 1461 bp and proceed to 1785 bp to yield a product of 323 bp. However, because the DNA fragment was generated from a mRNA template, the fifth intron was missing and the resultant fragment was 199 bp in length as described in the Materials and Methods section 2.1.3.

The PCR-generated products where analysed by electrophoresis on a 1% (w/v) agarose gel (Figure 3-1).

Several unsuccessful attempts were made to blunt-end ligate the β-actin PCR fragment into the dephosphorylated (calf intestinal phosphatase) *Eco*R V site of the pLITMUS RNA expression vector. These blunt-end ligation attempts employed the following strategies: 1). Deep Vent proof-reading polymerase to produce a blunt-end PCR product. 2). *Pfu* polymerase to end-polish existing *Taq* PCR products via 'fill-in' and 'chew-back' reactions. 3). Mungbean nuclease end-polishing, to remove overhanging 3' ends from the PCR product.

The Pharmacia SureClone blunt-ending kit requires blunt-ended, dephosphorylated vector and fresh PCR fragment with 3' overhanging ends. This strategy is described in the Materials and Methods section 2.1.3. The PCR fragments were analysed by electrophoresis on a 1% (w/v) agarose gel (Figure 3-2). At the same time a fresh stock of pLITMUS was digested with *Eco*R V and dephosphorylated with calf intestinal phosphatase. The DNA was isolated on a 1% (w/v) agarose gel and all DNAs were extracted using

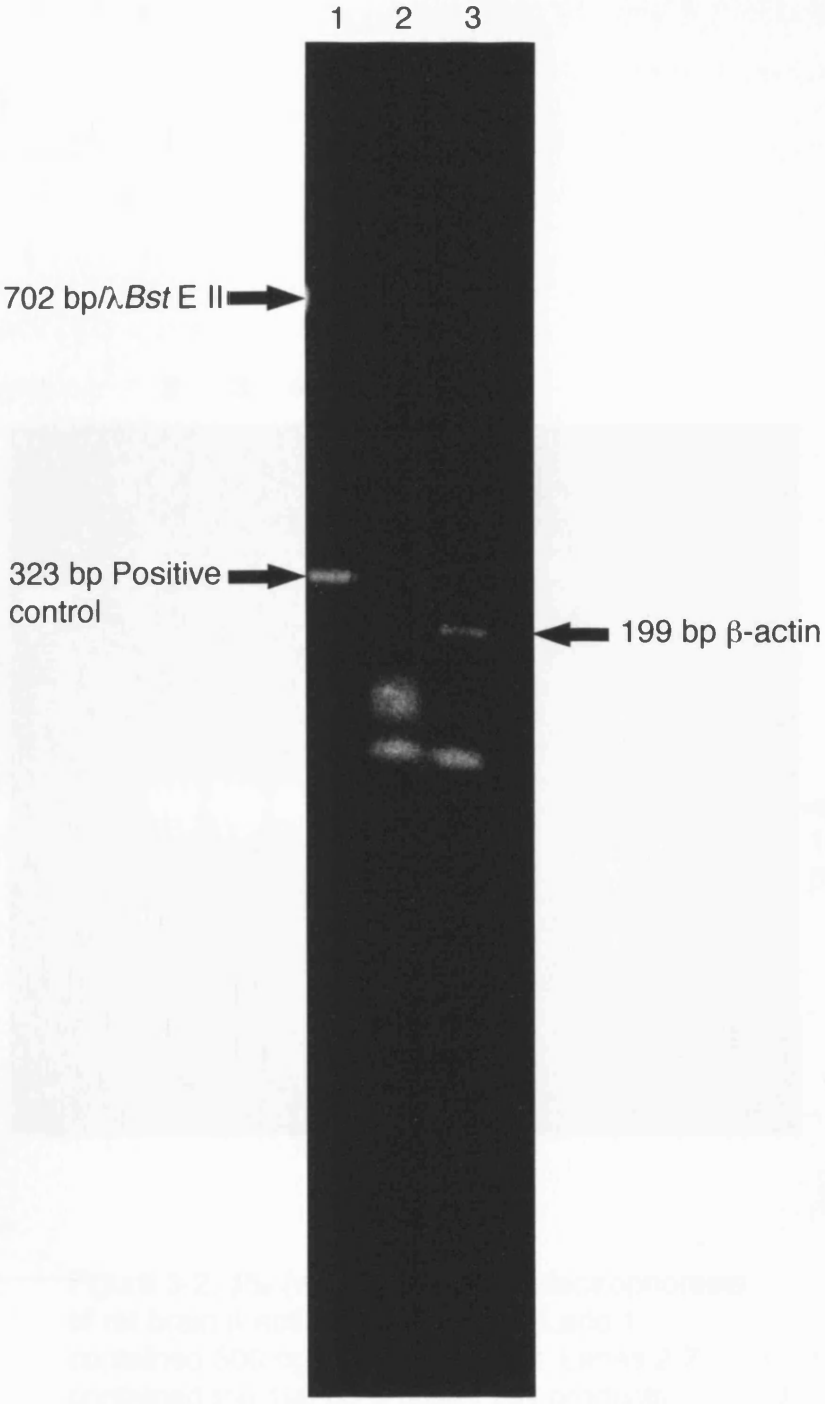

Figure 3-1. 1% (w/v) agarose gel electrophoresis of rat brain β-actin RT-PCR products with associated controls. Lane 1 contained the product of a control RNA and primer reaction, yielding a 323 bp CAT gene product. Lane 2 contained the product of the control RNA and β-actin specific primer reaction, this yielded a smear but no product as expected. Lane 3 contained the 199 bp rat brain β-actin gene fragment used as a positive control for *in situ* hybridisation.

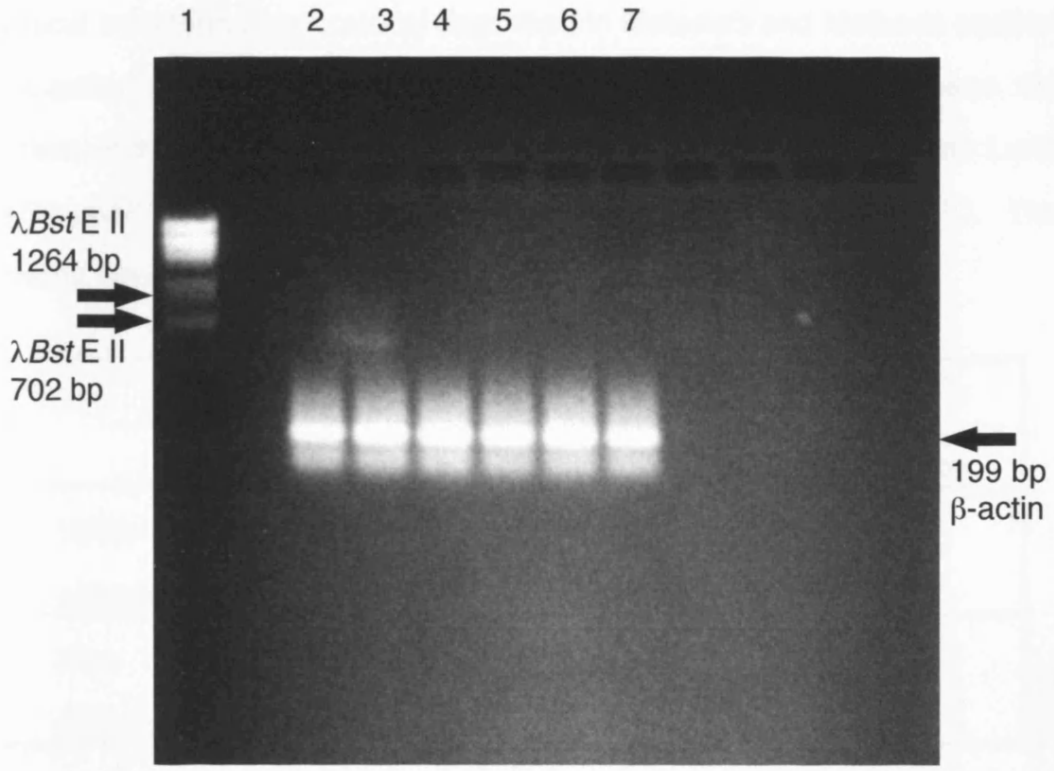

Figure 3-2. 1% (w/v) agarose gel electrophoresis of rat brain β-actin PCR products. Lane 1 contained 500 ng λ*Bst* E II marker. Lanes 2-7 contained the 199 bp β-actin PCR products.

the Genomed JETSORB system described in Materials and Methods section 2.1.2. The PCR-generated fragment was blunted with Klenow polymerase and 5' phosphorylated in a single reaction, then ligated with an equimolar concentration of the dephosphorylated, blunt-ended vector DNA.

The ligation products were transformed into *E. coli* TOP10F' cells using the chemical transformation protocol described in Materials and Methods section 2.2. Ligation and transformation (pUC18) controls were used to assess the success of their respective reactions. Transformants were plated onto Luria agar/X-gal/IPTG/ampicillin plates and grown for 16 hours at 37°C. The following results were obtained:

	Test ligation	Control ligation	Control transformation
White colonies	20	1440	-
Blue colonies	15	240	6000

Transformation efficiency: 3.6×10^8 colonies/μg of DNA

Eleven of the test white colonies were PCR screened as described in Materials and Methods section 2.3. The total PCR products were analysed by electrophoresis on a 1% (w/v) agarose gel (Figure 3-3). The results indicated that 10 out of the 11 PCR-screened, white colonies contained the β-actin insert. One false positive was detected, this was most likely to be a deletant

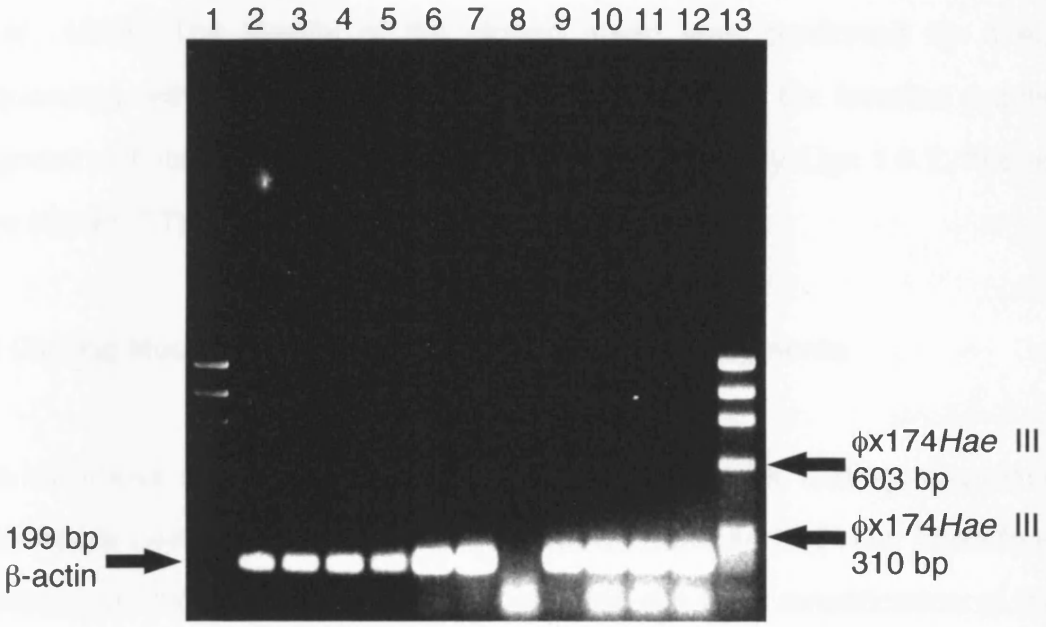

Figure 3-3.1% (w/v) agarose gel electrophoresis of colony PCR products for 11 rat brain β-actin/pLITMUS clones. Lanes 1 and 13 contained 500 ng ϕx174*Hae* III marker. Lanes 2-7 and 9-12 contained the 199 bp β-actin/pLITMUS colony PCR product, indicating successful ligation of the β-actin PCR product into the pLITMUS vector. Lane 8 contained religated vector, without the β-actin insert. The clone in lane 9 was cultured and the plasmid isolated using the caesium chloride gradient equilibrium centrifugation protocol (Sambrook *et al.*, 1989). The isolated plasmid DNA was then used as template for DNA sequencing and RNA transcript 'run-offs'.

whilst the β-actin positive control also produced a 199 bp band. Colony number 9 was selected and cultured in 100 ml of LB with 100 μg/ml ampicillin selection for 16 hours at 37°C. Plasmid DNA was isolated using the caesium chloride gradient equilibrium centrifugation protocol (Sambrook *et al.,* 1989). The identity of the cloned insert was confirmed by direct sequencing with the M13 reverse primer. This showed the inverted β-actin fragment with its junction in the pLITMUS vector (Assembly-Lign 1.0.7, Kodak, New Haven, CT), shown in Appendix 5.

3.3 Cloning Mouse Kir2.2 N- and C-Terminal cDNA Fragments

The intronless mouse Kir2.2 potassium inward rectifier coding sequence had already been cloned as a cDNA (accession number: X80417). Therefore, a cloning strategy was developed that required the PCR amplification of the regions of the cDNA encoding the N- and C-terminal regions. These avoided the areas of the gene encoding the M1, M2 and H5 domains, and were thus regions of lowest homology between the Kir family of ion channel genes as confirmed by BLAST2.0 search (Altschul *et al.,* 1997), (Appendix 2). The PCR-amplified regions were then cloned into the pLITMUS RNA expression vector, which had previously been used to clone the β-actin cDNA fragment.

Blunt-end ligations of the N-terminal: 71-430 bp (359 bp) and C-terminal: 1013 bp-1372 bp (359 bp) PCR fragments were attempted unsuccessfully using Pharmacia's SureClone kit with the pLITMUS vector, with linearisation and dephosphorylation at the *Eco*R V site. Therefore, a new directional cloning strategy was adopted, involving the use of the existing primers with redesigned 5' ends containing *Xho* I and *Xba* I sites. The resulting N- and C-

terminal coding regions had *Xho* I sites on their 5' ends and *Xba* I sites on their 3' ends. The N- and C-terminal coding regions were also checked to confirm that they did not contain any *Xba* I, *Xho* I, *Spe* I or *Afl* II sites. The conditions required for the generation of the PCR fragments are described in the Materials and Methods section 2.1.4.

The pLITMUS vector was digested with both *Xba* I and *Xho* I enzymes in order that the PCR fragments containing complementary termini could be ligated into the vector. The PCR fragments, together with pLITMUS digest products were analysed by electrophoresis on a 1% (w/v) agarose gel. The DNAs were extracted using the Genomed JETSORB system described in Materials and Methods section 2.1.2.

The recovered PCR and pLITMUS digest products were assessed for purity and recovery from the agarose gel by electrophoresis of small aliquots on a 1% (w/v) agarose gel. The recovered products were confirmed as being pure and their approximate concentrations estimated. The PCR products contained overhanging 3' adenines, complementary to the overhanging 3' thymines on the pGEM-T vector. The products were ligated into pGEM-T, then inserts were excised using *Xba* I and *Xho* I enzymes. The ends of the inserts were thus complementary to the *Xba* I and *Xho* I sites in the pLITMUS vector enabling a directional ligation to be carried out. The ligation products were transformed into *E. coli* XL1-Blue MRF' cells using the chemical transformation protocol in Materials and Methods section 2.2. A transformation (pUC18) control was used to assess the success of the transformation as shown overleaf:

	mKir2.2 N-terminal ligation	mKir2.2 C-terminal ligation	Control transformation
White colonies	16	14	-
Blue colonies	47	52	5500

Transformation efficiency: 3×10^8 colonies/μg DNA

A colony PCR screen was carried out on 9 N- and 9 C-terminal white colonies as described in the Materials and Methods section 2.3. The total PCR products were analysed by electrophoresis on a 1% (w/v) agarose gel. The results indicated that N-terminal clones 1, 2, 3, 5, 6, 7, 8 and 9 together with C-terminal clones 1 ,2, 3, 5, 6, 7 and 9 contained their respective inserts. The positive control, provided by mKir2.2 cDNA, and the negative control, provided by pLITMUS, both behaved as expected.

The PCR screening results from six clones were checked by isolation of plasmid DNA using the Promega Wizard® *Plus* SV miniprep system described in Materials and Methods section 2.1.1 (N-terminal clones: 1, 8 and 9. C-terminal clones: 1, 2 and 3). The recovered plasmid DNA was digested with *Xba* I and *Xho* I in order to release the inserts from the vector constructs. The digestion products were analysed by electrophoresis on a 1% (w/v) agarose gel (Figure 3-4). These data indicated that mKir2.2 N-

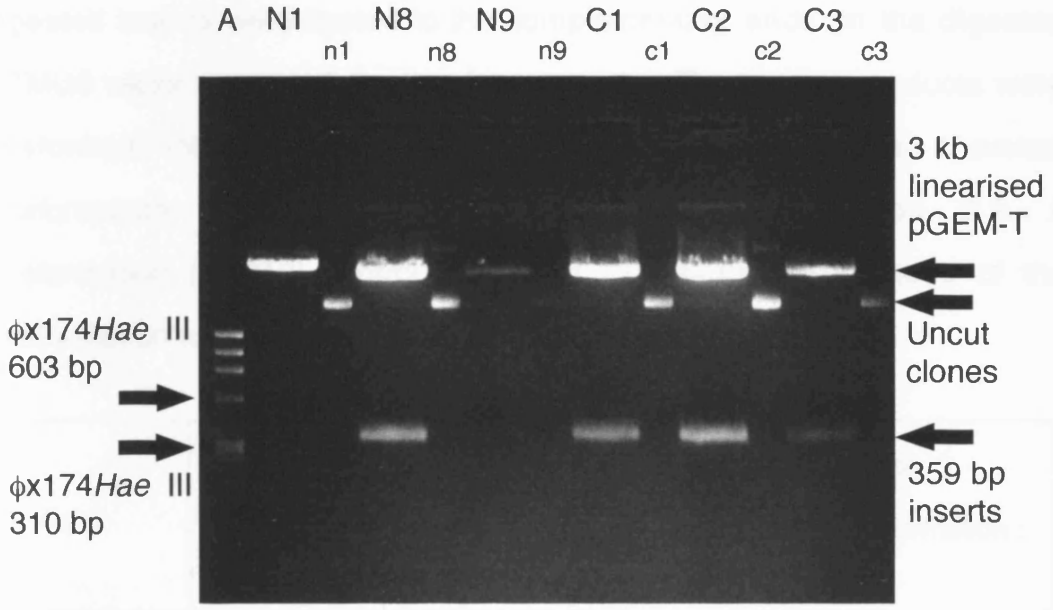

Figure 3-4. 1% (w/v) agarose gel electrophoresis of restriction digests from 6 mouse Kir2.2 N- and C-terminal/pGEM-T clones. Lane A contained 500 ng ϕx174*Hae* III marker. N-terminal clone N8 together with C-terminal clones C1, C2 and C3 contained the *Xba* I/*Xho* I restriction sites that allowed the 359 bp inserts to be cut from the pGEM-T vector. Uncut clones n1, n8 , n9, c1, c2 and c3 were electrophoresed on the right-hand side of each digested clone.

terminal clone 8 and mKir2.2 C-terminal clones 1, 2 and 3 contained the desired insert.

The insert bands were gel-extracted using the Genomed JETSORB system described in Materials and Methods section 2.1.2, and the concentrations of DNA assessed by electrophoresis on a 1% (w/v) agarose gel. The *Xba I*/*Xho* I digested inserts were ligated to the complementary ends on the digested pLITMUS vector, using a 5:1 ratio of insert:vector. The ligation products were transformed into *E. coli* XL1-Blue MRF' cells using the chemical transformation protocol in Materials and Methods section 2.2. A transformation (pUC18) control was used to assess the success of the transformation as shown below:

	mKir2.2 N-terminal ligation	mKir2.2 C-terminal ligation	Control transformation
White colonies	425	200	-
Blue colonies	22	25	5000

Transformation efficiency: 3×10^8 colonies/μg DNA

A colony PCR screen was carried out on 9 N- and 9 C-terminal white colonies as described in the Materials and Methods section 2.3. The total PCR products were analysed by electrophoresis on a 1% (w/v) agarose gel.

The results indicated that the N-terminal clones 1-9, and C-terminal clones 2-9 contained their respective inserts.

The PCR screening results from six clones were checked by isolation of plasmid DNA using the Promega Wizard® *Plus* SV miniprep system described in Materials and Methods section 2.1.1 (N-terminal clones: 1, 4 and 7. C-terminal clones: 2, 7 and 9). The recovered plasmid DNA was digested with *Xba* I and *Xho* I to remove the inserts from the vector constructs. Analysis of the digestion products by electrophoresis on a 1% (w/v) agarose gel indicated that mKir2.2 N-terminal/pLITMUS clones 1, 4 and 7 together with mKir2.2 C-terminal/pLITMUS clones 2, 7 and 9 all contained the correct inserts (Figure 3-5).

mKir2.2 colonies 'N-terminal 4' and 'C-terminal 9' were selected and cultured in 100 ml of LB supplemented with 100 μg/ml ampicillin selection for 16 hours at 37°C. The plasmid DNA was isolated using caesium chloride gradient equilibrium centrifugation (Sambrook *et al.,* 1989). The identities of the cloned inserts were confirmed by direct sequencing using the M13 reverse primer, which showed the mKir2.2 fragments with their junctions with the pLITMUS vector (Assembly-Lign 1.0.7, Kodak, New Haven, CT), shown in Appendix 6. A similar RT-PCR strategy was adopted to clone the N- and C-terminal coding regions of the mouse NK-1 receptor gene. Unfortunately, subsequent sequencing revealed that spurious DNA fragments had been cloned into the pLITMUS vector, and consequently neither clone could be used in the co-localisation of the NK-1 receptor and mKir2.2 genes in the LC.

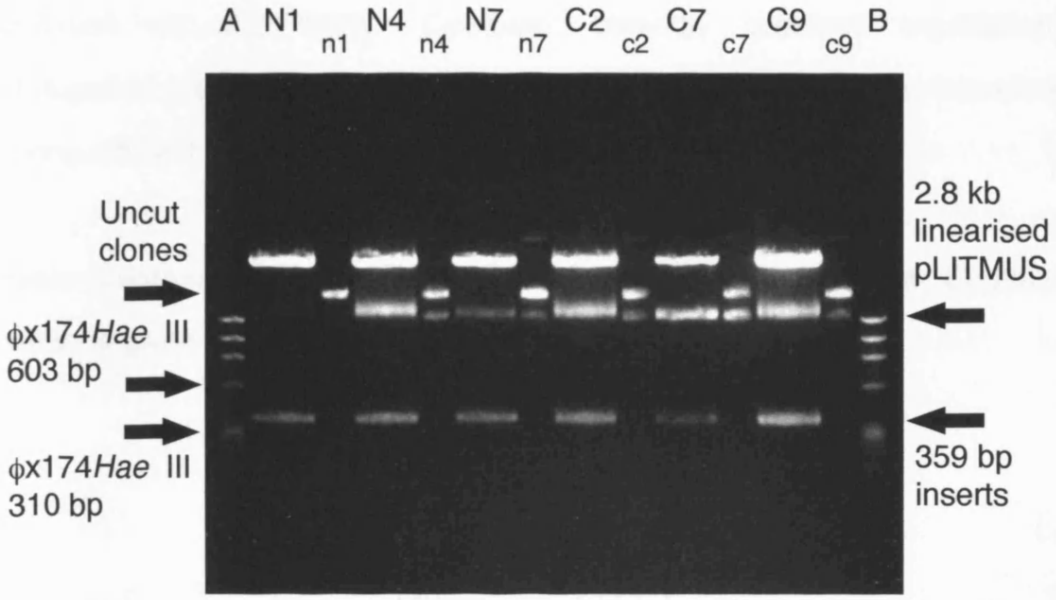

Figure 3-5. 1% (w/v) agarose gel electrophoresis of restriction digests from 6 mouse Kir2.2 N- and C-terminal/pLITMUS clones. Lanes A and B contained 500 ng ϕx174*Hae* III marker. N-terminal clones N1, N4 and N7 together with C-terminal clones C2, C7 and C9 contained the *Xba* I/*Xho* I restriction sites that allowed the 359 bp inserts to be cut from the pLITMUS vector. Uncut clones n1, n4 , n7, c2, c7 and c9 were electrophoresed on the right-hand side of each digested clone.

3.4 DIG-Labelled Riboprobes made by Transcript 'Run-Offs' from Cloned cDNA Templates

Initial experiments using plasmid DNA isolated using the Qiagen DNA prep gave low transcription efficiencies and, thus, low yields of probe. This problem was solved by preparing DNA using caesium chloride gradients (Sambrook *et al.,* 1989). Caesium chloride gradient equilibrium centrifugation prepared DNA was pure and lacked strand-breaks, therefore allowing efficient transcription and high probe yield.

A basic diagram of the pLITMUS RNA expression vector (New England Biolabs) is given in Figure 3-6:

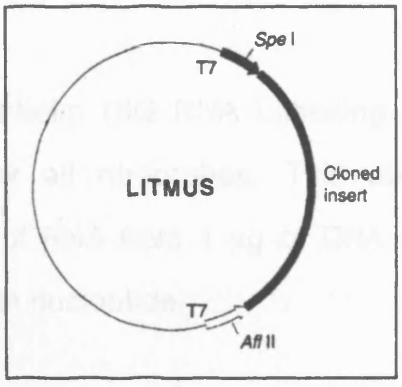

Figure 3-6. The pLITMUS RNA expression vector. The 2.8 kb vector contained a pUC origin of replication, an ampicillin resistance gene and the truncated *lac* operon for blue/white selection. pLITMUS allowed high efficiency transcription from T7 RNA polymerase promoter sites located on both sides of the cloned insert.

Linearisation of the vector was a prerequisite for transcript 'run-off', allowing production of either antisense or sense RNA. The pLITMUS vector could be linearised at *Spe* I or *Afl* II restriction sites, located in either of the T7 RNA

polymerase promoter sites, neither restriction enzyme site was found in the cloned inserts. Digestion of the pLITMUS vector DNA with either of these restriction enzymes resulted in linearisation in one or other of the promoter sites; ensuring transcription of antisense or sense RNA without leakage of one into the other.

The complete linearisation of the vectors by minimal concentrations of *Spe* I and *Afl* II restriction enzymes was desirable as single-strand DNA nicking was thus avoided. Therefore, a series of experiments was undertaken to assess the minimum required concentration of enzyme to achieve complete vector linearisation. This proved to be 1 unit/μg DNA for *Spe* I and 2 units/μg DNA for *Afl* II, as assessed by agarose gel electrophoresis (results not shown).

The Boehringer Mannheim DIG RNA Labelling kit was used to generate transcript 'run-offs' for all riboprobes. This allowed the transcription of approximately 10 μg of RNA from 1 μg of DNA template, with a DIG-UMP incorporated every 25th nucleotide.

The RNA was precipitated from unincorporated NTP's using the lithium chloride/ethanol protocol (Sambrook *et al.,* 1989). The recovered RNA pellets were dissolved in DEPC water, aliquoted into small volumes and stored at -80^{o}C. Quantitation of the DIG-labelled riboprobe was carried out using the Boehringer Mannheim alkaline phosphatase colourimetric detection system on Hybond-N dot-blots. This system required the spotting of a serial dilution of test and external/transcription DIG-labelled RNA controls. The system allowed the yield of riboprobe to be estimated as 70-75% of the transcription

control values for mKir2.2 (Figure 3-7a) and 100% of transcription control values for β-actin (Figure 3-7b). The limit of quantitation for both test probe families was therefore established as 1 pg (Figure 3-7)

3.5 Confirmation of Riboprobe Specificity in RNA Dot-Blots and Southern Blots

The specificities of the mKir2.2 and β-actin riboprobes were assessed by hybridisation to membrane bound serial dilutions of cloned DNA or brain total RNA in dot-blots, described in Materials and Methods section 2.4. Mouse Kir2.2 antisense and sense riboprobes were separately hybridised to titrated DNA (10 ng-1 pg) and total RNA (5 μg-0.5 μg). The results indicated that mKir2.2 N-terminal riboprobes (antisense and sense) detected cloned DNA to a limit of 1 pg. The antisense riboprobe was able to detect a signal within total RNA to a limit of 0.5 μg (Figure 3-8). The mKir2.2 C-terminal riboprobes (antisense and sense) were able to detect cloned DNA to a limit of 10 pg, whilst the antisense riboprobe detected a signal within total RNA to a limit of 0.5 μg. Both mKir2.2 N- and C-terminal coding sense riboprobes were unable to detect mKir2.2 mRNA within total RNA (Figure 3-8). The β-actin antisense and sense riboprobes were separately hybridised to titrated (10 ng-1 pg) cloned β-actin DNA and total RNA (5 μg-0.5 μg). The antisense riboprobe detected DNA to a limit of 10 pg and within total RNA to a limit of 0.5 μg (Figure 3-9). The sense riboprobe was able to detect DNA to a limit of 10 pg, but as expected could not detect a signal within total RNA (Figure 3-9), confirming a detection specificity for the antisense riboprobes.

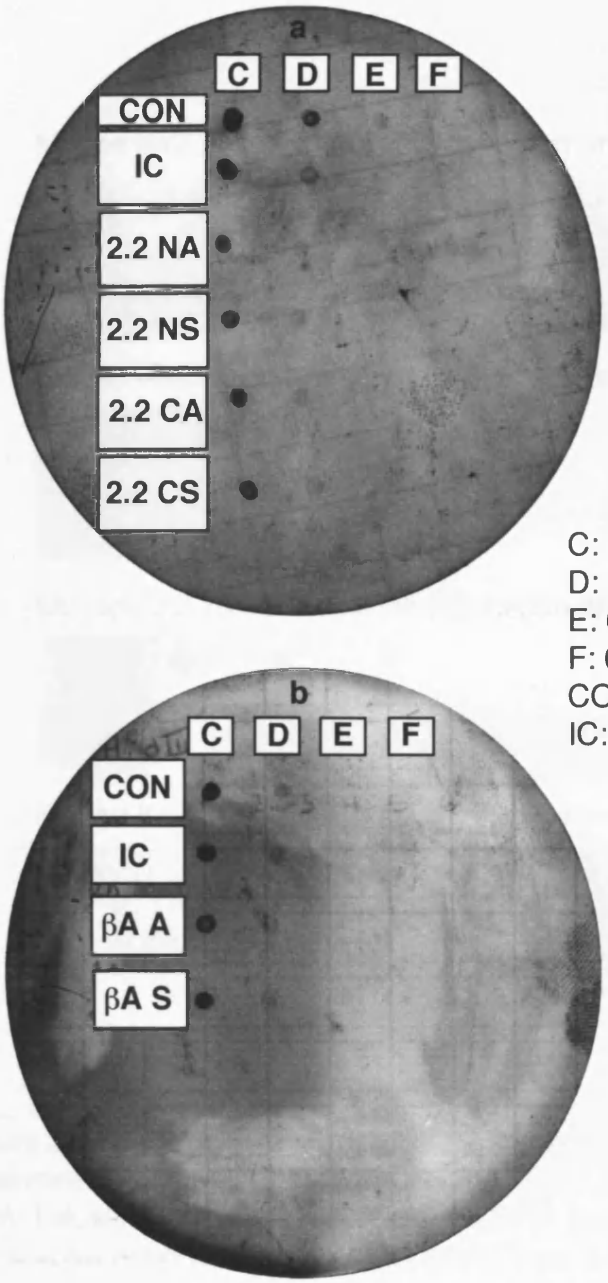

Kir2.2 riboprobe quantitation dot-blot

C: 10 pg RNA
D: 1 pg RNA
E: 0.1 pg RNA
F: 0.01 pg RNA
CON: external control
IC: transcription control

β-actin riboprobe quantitation dot-blot

Figure 3-7. Dot-blots for Kir2.2 and β-actin riboprobe quantitation. (a), Dot-blot for Kir2.2 riboprobe quantitation. All 4 test probes (2.2 NA, 2.2 NS: Kir2.2 N-terminal antisense and sense respectively, and 2.2 CA, 2.2 CS: Kir2.2 C-terminal antisense and sense respectively) could be detected to 1 pg (D). The transcription efficiency was approximately 70-75% of the transcription control. (b), Dot-blot for β-actin riboprobe quantitation indicated that the antisense (βA A) and sense probes (βA S) could be detected to 1 pg (D). The transcription efficiencies of the test and transcription controls were equivalent. Both the quantitation dotblots were detected with the alkaline phosphatase colourimetric system.

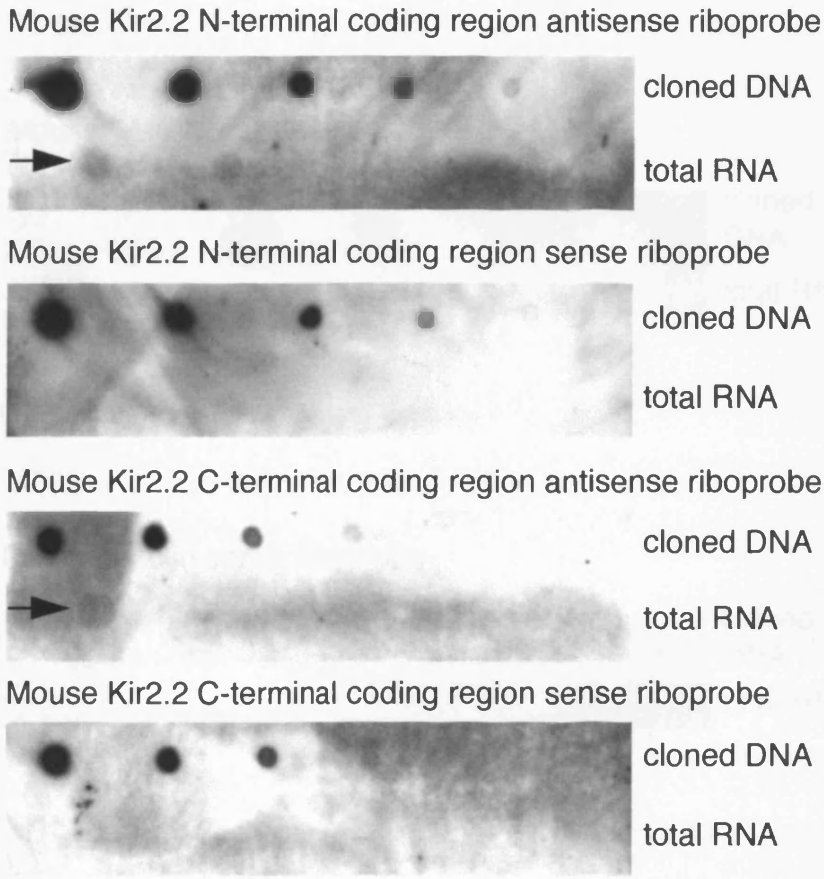

Figure 3-8. Specificity of mouse Kir2.2 N- and C-terminal riboprobes determined by dot-blots of titrated cloned DNA and rat brain total RNA. Dilutions of mouse Kir2.2 cloned DNA (upper rows; 10 ng-1 pg) and rat brain total RNA (lower rows; 5 μg-0.5 μg) were blotted on to membranes. The riboprobes were hybridised at optimum stringency (described in Materials and Methods section 2.4), with the result that the antisense riboprobes were able to detect both mouse Kir2.2 DNA and the complementary coding mRNA (arrows) to the following limits: 1 pg of DNA and 0.5 μg of total RNA (N-terminal coding region), 10 pg of DNA and 0.5 μg of total RNA (C-terminal coding region). The mouse Kir2.2 sense riboprobes detected cloned DNA to a limit of 1 pg (N-terminal coding region) and 10 pg (C-terminal coding region). The sense riboprobes were unable to detect total RNA as they were identical to the mouse Kir2.2 mRNA, confirming riboprobe sequence specificity.

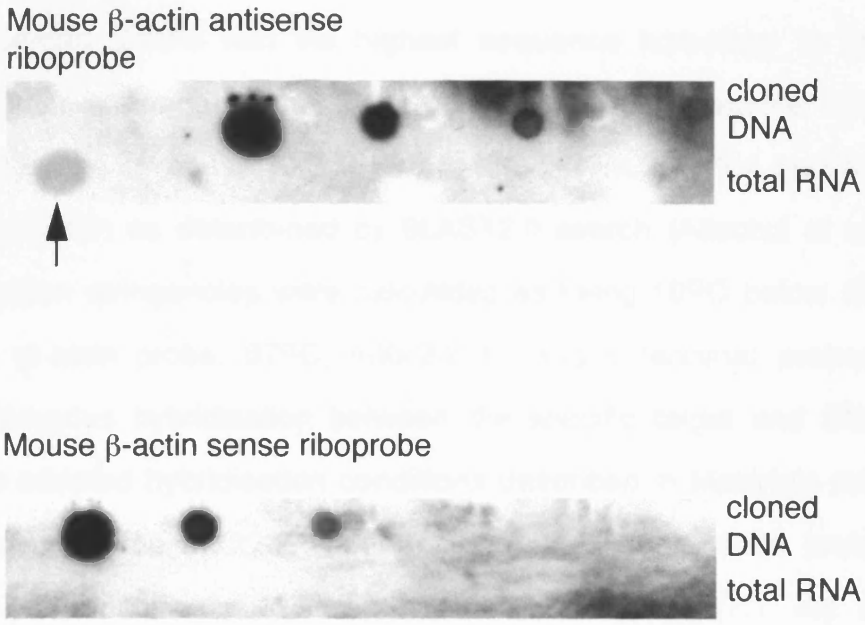

Figure 3-9. Specificity of mouse β-actin riboprobes determined by dot-blots of titrated cloned DNA and rat brain total RNA. Dilutions of mouse β-actin cloned DNA (upper rows; 10 ng-1 pg) and rat brain total RNA (lower rows; 5 μg-0.5 μg) were blotted on to membranes. The riboprobes were hybridised at optimum stringency (described in Materials and Methods section 2.4), with the result that the antisense riboprobe was able to detect both mouse β-actin DNA and the complementary coding mRNA (arrow) to the following limits: 10 pg of DNA and 0.5 μg of total RNA. The mouse β-actin sense riboprobe detected cloned DNA to a limit of 10 pg. The sense riboprobe was unable to detect total RNA as it was identical to the mouse β-actin mRNA, confirming riboprobe sequence specificity.

In order to further assess the specificity of the β-actin and mKir2.2 probes, DIG-labelled DNA probes were manufactured by specific PCR for each cDNA as described in Materials and Methods section 2.1.3 and 2.1.4 respectively. The probes were then separately hybridised to Southern blots (Sambrook *et al.,* 1989) containing cDNAs with the highest sequence homology to the mKir2.2 gene (Blots contained cDNA for mKir2.2 and β-actin, together with 500 ng cDNA per lane of mouse Kir2.1, Kir2.3, Kir3.1, Kir3.2, Kir3.4 and the human NK-1 receptor) as determined by BLAST2.0 search (Altschul *et al.,* 1997). Hybridisation stringencies were calculated as being 10^{o}C below the theoretical Tm (β-actin probe: 67^{o}C, mKir2.2 N- and C-terminal probes: 72^{o}C) for homologous hybridisation between the specific target and DNA probe using the adopted hybridisation conditions described in Materials and Methods section 2.5. The mKir2.2 N- and C-terminal coding DNA probe cocktail hybridised specifically to linearised mKir2.2 cDNA (7.1 kb) in pCDNA3 vector (Figure 3-10). The β-actin DNA probe hybridised specifically to linearised mouse β-actin cDNA fragment (3 kb) in pLITMUS vector (Figure 3-11). Probe hybridisation for both RNA dot-blots and Southern blots was detected by enhanced chemiluminescence and X-ray hyperfilm as described in Materials and Methods sections 2.4 and 2.5 respectively.

3.6 Localising the Locus Coeruleus in the Rat Brain

The LC was localised in 4 μm paraffin-embedded coronal cerebellar rat brain sections using either cresyl violet or Mayer's haematoxalin/eosin staining to indicate the condition of morphology and preservation within the tissue. The staining clearly indicated the positions of the LC regions on both the left and right-hand sides of the IVth ventricle in the medulla. The photograph in Figure

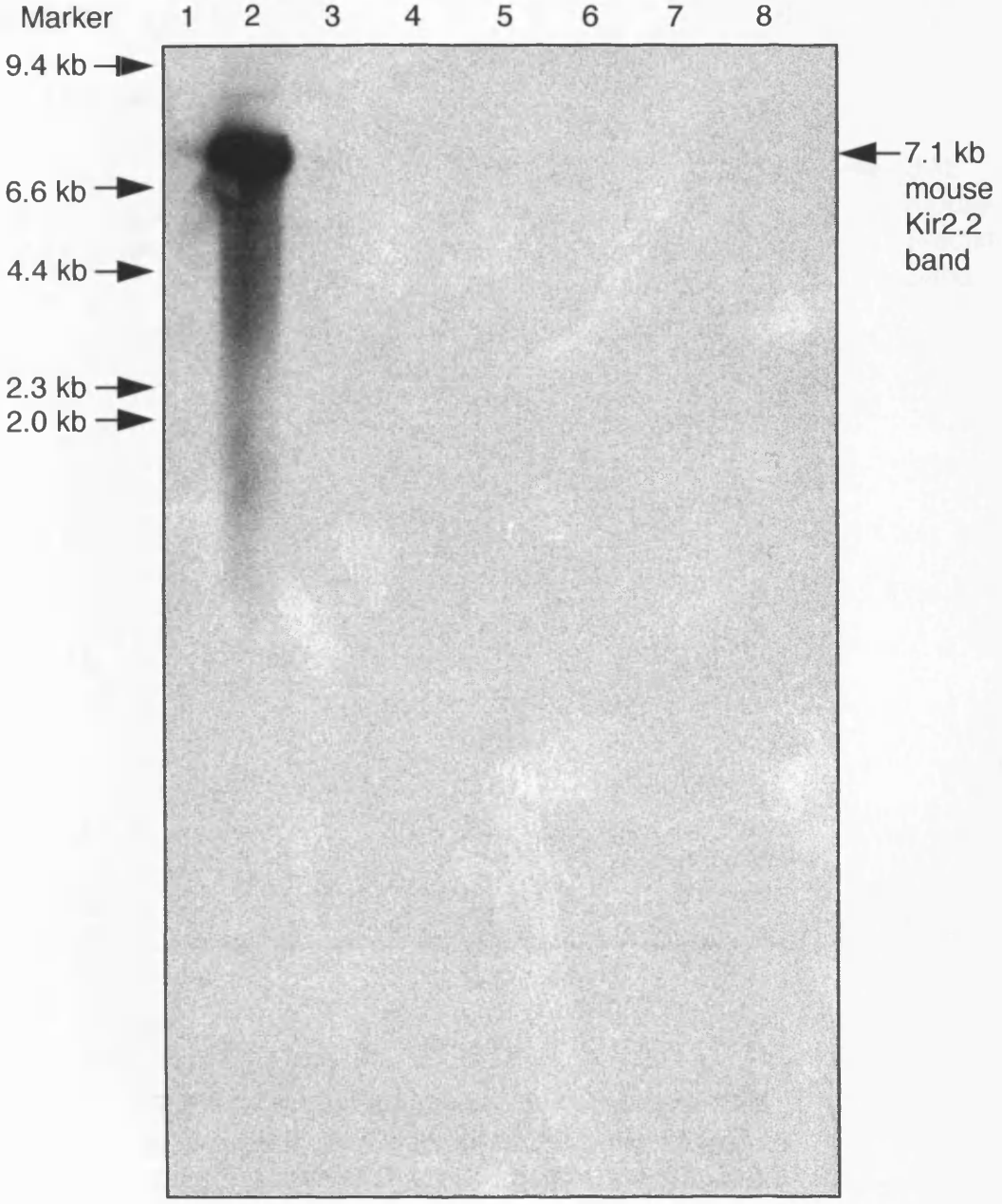

Figure 3-10. Confirmation of mouse Kir2.2 N- and C-terminal DNA probe specificity. Southern blotting was utilised to confirm Kir2.2 N- and C-terminal DNA probe specificity against the following panel of clones; lane 1: Kir2.1, lane 2: Kir2.2, lane 3: Kir2.3, lane 4: Kir3.1, lane 5: Kir3.2, lane 6: Kir3.4, lane 7: β-actin, lane 8: human NK-1 receptor. This blot indicated specific hybridisation between mouse Kir2.2 and the probe cocktail, yielding a band of 7.1 kb shown in lane 2.

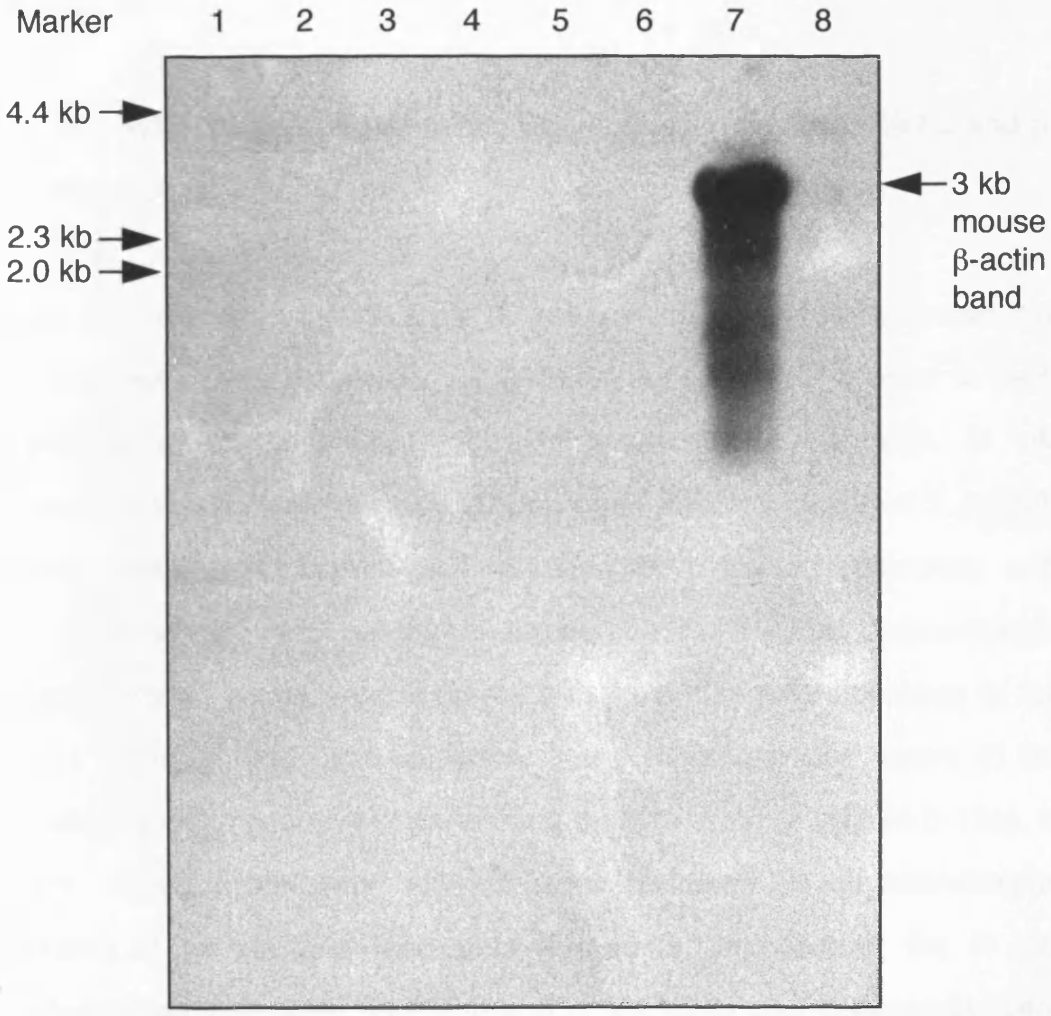

Figure 3-11. Confirmation of mouse β-actin DNA probe specificity. Southern blotting was utilised to confirm β-actin DNA probe specificity against the following panel of clones; lane 1: Kir2.1, lane 2: Kir2.2, lane 3: Kir2.3, lane 4: Kir3.1, lane 5: Kir3.2, lane 6: Kir3.4, lane 7: β-actin, lane 8: human NK-1 receptor. This blot indicated specific hybridisation between mouse β-actin and the probe cocktail, yielding a band of 3 kb shown in lane 7.

3-12 shows a typical cresyl violet stained rat brain section indicating the left-hand side LC.

3.7 *In Situ* Hybridisation on Rat Brain Tissue Sections with mKir2.2 and β-Actin Riboprobes

Studies of Kir expression in rat brain by *in situ* hybridisation have shown that mKir2.2 mRNA can be detected in LC (Karschin *et al.,* 1996). In order to verify the sites at which the mKir2.2 gene is expressed in rat brain, *in situ* hybridisation was carried out using riboprobes specific for mKir2.2 mRNA. Coronal cerebellar rat brain tissue sections were treated separately with mKir2.2 antisense and sense riboprobe cocktails. After colourimetric detection, strong signals were observed with the antisense riboprobes in the neurons of the LC, the Purkinje, granule and molecular cell layers of the cerebellum and the ependymal cells lining the IVth ventricle (Figure 3-13a). In addition, strong cytoplasmic signals were observed in oligodendroglia, particularly of the uncinate fasciculus (Figure 3-13a). Overall, the *in situ* hybridisation data reported here and that of Karschin and colleagues were similar (Karschin *et al.,* 1996). High magnification analysis of the LC stained with mKir2.2 antisense riboprobes indicated strong cytoplasmic signals in noradrenergic neurons, in addition to smaller oligodendroglia (Figure 3-13b). Sense riboprobes yielded a generally low background cytoplasmic signal, concentrated in some Purkinje cells (Figure 3-13c). Notably, there was no detectable signal in the LC using sense riboprobes. These non-specific signals were probably due to the expression of endogenous alkaline phosphatase in those cells during the 16 hour detection period, as indicated

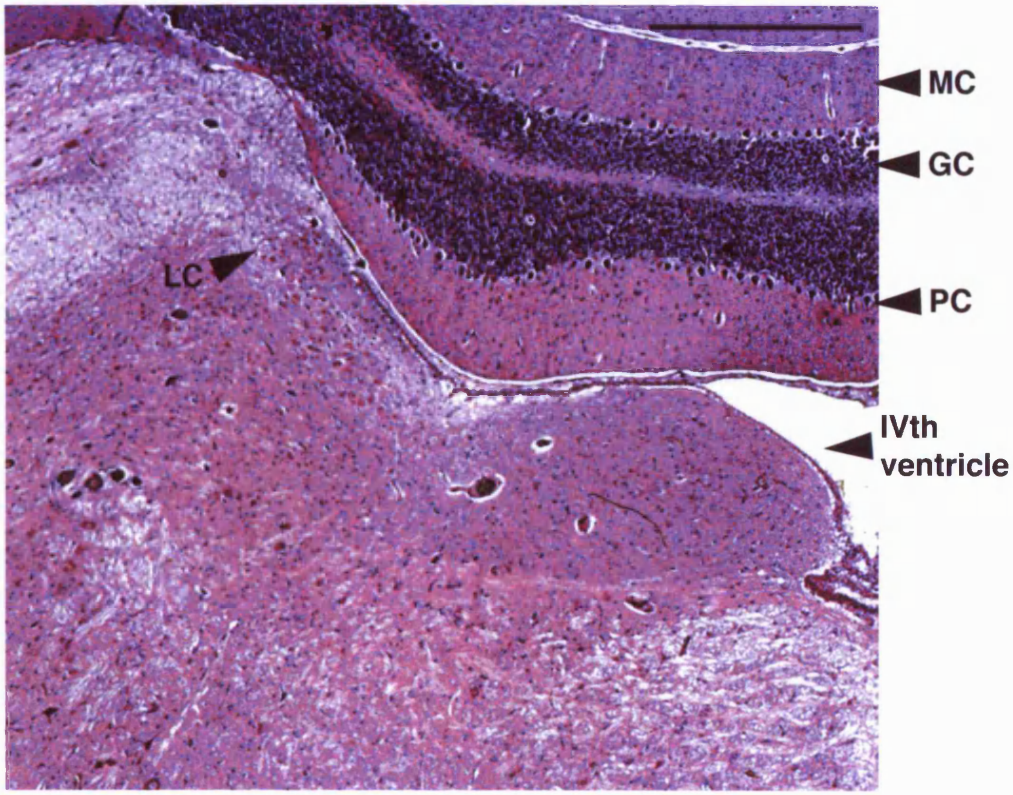

Figure 3-12. Cresyl violet stained coronal rat brain tissue section through the cerebellum and medulla. The tissue section provided evidence of good fixation and morphology within the paraffin-embedded brain block. Structures indicated include the locus coeruleus (LC), molecular cell layer (MC), granule cell layer (GC), Purkinje cell layer (PC) and the IVth ventricle. Scale bar represents 450 μm.

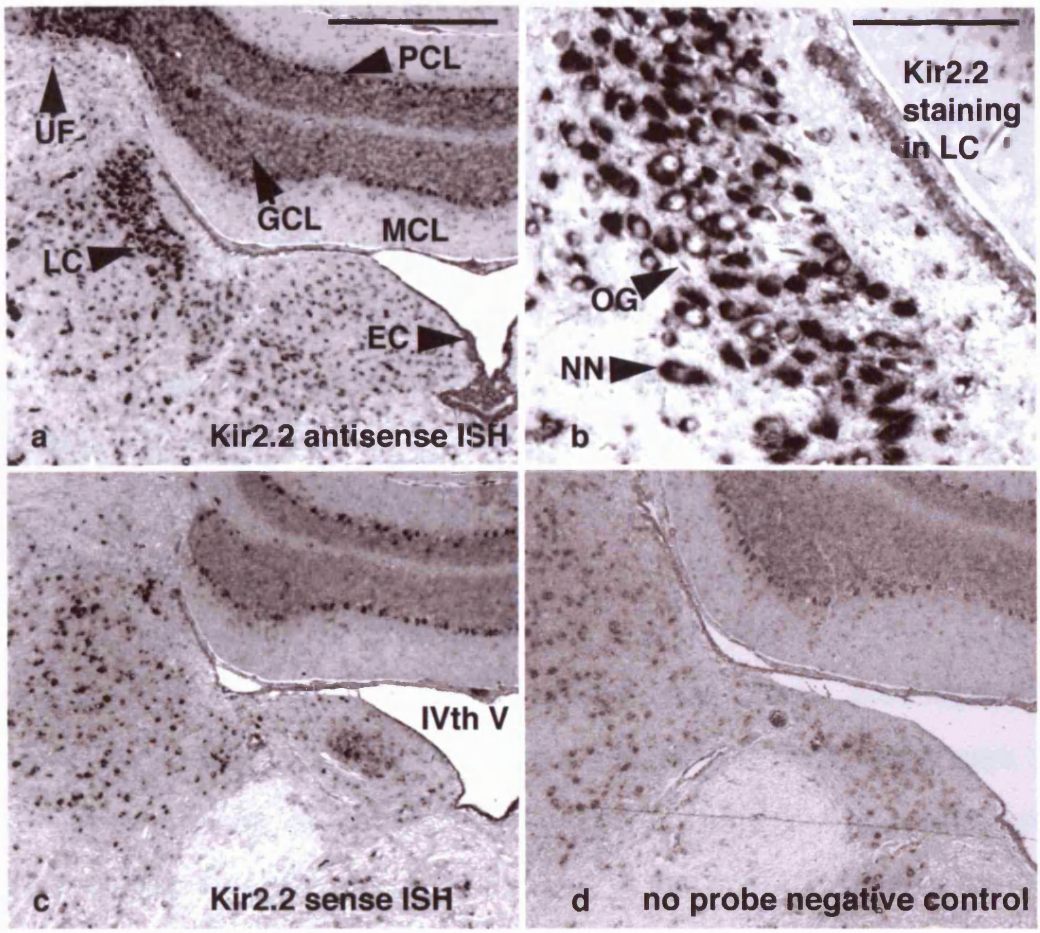

Figure 3-13. *In situ* hybridisation of Kir2.2 riboprobes on rat brain tissue sections. (a), Kir2.2 N- and C-terminal antisense riboprobe cocktails gave strong signals in neurons of the locus coeruleus (LC), Purkinje cell layer (PCL), granule cell layer (GCL), molecular cell layer (MCL), ependymal cells (EC) of the IVth ventricle (IVth V) and oligodendroglia of the uncinate fasciculus (UF). (b), Kir2.2 N- and C-terminal antisense riboprobe cocktail staining in the LC, showing noradrenergic neuron (NN) and oligodendroglia (OG) signals. (c), Kir2.2 N- and C-terminal sense riboprobe cocktails gave a weak background signal due to endogenous alkaline phosphatase activity, most notably some of the Purkinje cell layer, although fewer than in the antisense section. No staining was observed in the LC. (d), The negative control in the absence of probes indicated a low background signal associated with endogenous alkaline phosphatase activity. Tissue sections were taken from rat coronal cerebellar/medulla tissue blocks. Scale bars represents 450 μm (a, c, d) and 150 μm (b).

by the presence of staining in the Purkinje cell layer and mesencephalic trigeminal nucleus (Me5N) in the absence of probe (Figure 3-13d).

The β-actin positive control antisense riboprobe showed a different set of cytoplasmic signals which included the LC, Me5N, Purkinje and granule cell layers (Figure 3-14a). The β-actin sense riboprobe yielded barely detectable hybridisation signals (Figure 3-14b). The β-actin probe-free negative control was free of staining, indicating little endogenous alkaline phosphatase expression (Figure 3-14c).

3.8 Summary

Riboprobes specific to β-actin and mKir2.2 have been produced and characterised, using RNA dot-blotting and Southern blotting techniques. *In situ* hybridisation on rat brain tissue sections using mKir2.2 antisense riboprobes indicated very strong expression of the mKir2.2 gene in the LC. The Kir2.2 mRNA was also detected in the granule cell and molecular cell layers of the cerebellum, the oligodendroglia of the LC and uncinate fasciculus and ependymal cells lining the IVth ventricle. A separate subset of cells was detected by the β-actin antisense riboprobes, including the LC, Purkinje and granule cell layers.

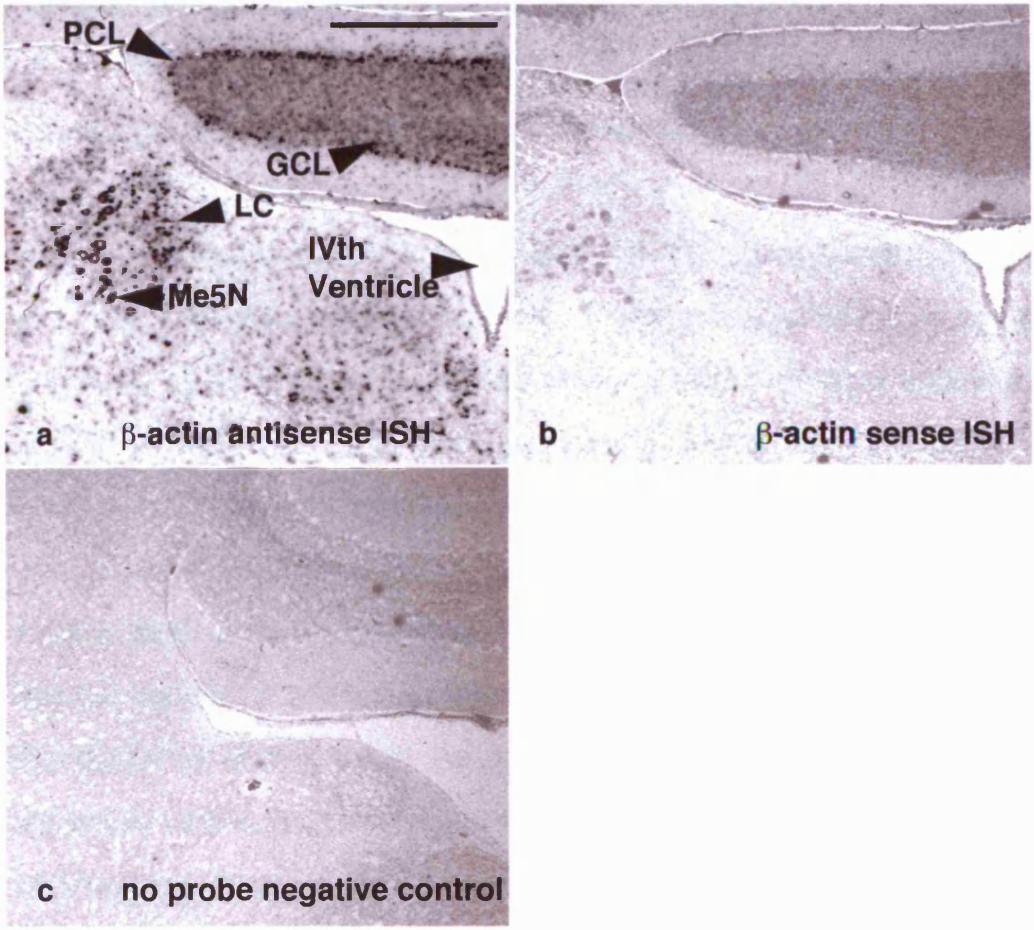

Figure 3-14. *In situ* hybridisation of β-actin riboprobes on rat brain tissue sections. (a), The β-actin antisense riboprobe gave a different staining pattern to the Kir2.2 antisense riboprobe. Although the locus coeruleus (LC), Purkinje cell layer (PCL) and granule cell layer (GCL) show signals, the neurons of the mesencephalic trigeminal nucleus (Me5N) also showed strong staining. (b), The β-actin sense riboprobe gave no specific signals, although there was a slight background staining in the granule cell layer and neurons of the mesencephalic trigeminal nucleus. (c), The negative control in the absence of probe showed no staining, indicating low background levels of endogenous alkaline phosphatase activity. Tissue sections were taken from rat coronal cerebellar/medulla tissue blocks. Scale bar represents 450 μm.

Chapter 4: Co-localisation of the Kir2.2 and NK-1 Receptor Proteins in Single Cells of the Locus Coeruleus by Immunohistochemistry

4.1 Production of Anti-Kir2.0 Polyclonal Antibodies

In order to co-localise Kir2.0 isoforms and the NK-1 receptor in single LC cells, it was necessary to generate anti-rat polyclonal antisera to several isoforms of the Kir2.0 subfamily. These antisera were important because of the failure to clone NK-1 receptor cDNA templates for the production of riboprobes, thus preventing co-localisation studies being carried out by *in situ* hybridisation. In addition, the antibodies allowed investigation of channel expression sites at the protein level. Finally, because anti-Kir2.1, anti-Kir2.3, as well as, anti-Kir2.2 antibodies were generated, a study of the distribution of this subfamily of Kirs could be made in the cerebellum, medulla and hippocampus of the rat brain for the first time. The anti-rat polyclonal NK-1 receptor antisera was provided by Dr Nigel Bunnett of the University of California, San Francisco (Vigna *et al.,* 1994). The Kir2.0 polyclonal antisera were raised by Dr Robert Norman of the Medicine Department, University of Leicester using C-terminal domain antigenic peptides as described in the Materials and Methods section 2.8. The antisera were affinity purified using antigenic peptide before use on tissue sections, cell cultures and Western blots. However, unpurified antisera were used in immunoprecipitation and the demonstration of antigenic peptide block on tissue sections.

4.2 Specificity of Anti-Kir2.0 Polyclonal Antibodies

4.2.1 Immunoprecipitation of Kir2.0 *In Vitro* Translated Proteins

Each anti-Kir2.0 antibody was displaced from antigen by competing specific antigenic peptide. This displacement could not be achieved by other non-specific Kir2.0 antigenic peptides in ELISA experiments. All antisera were positive in ELISA experiments against 20 ng of immunising peptide, to a dilution limit of 1×10^{-4}. The ELISA experiments were carried out by Dr Robert Norman of the Medicine Department, University of Leicester.

Wild type Kir2.1, Kir2.2 and Kir2.3 cDNAs were used as templates for reticulocyte lysate-coupled *in vitro* transcription/translation reactions to produce proteins labelled with [^{35}S]-Methionine. The reactions with Kir2.1 and Kir2.2 templates required the inclusion of canine pancreatic microsomal membranes in order to obtain high yields of protein. The endoplasmic reticulum membranes provided post-translational modification and protection against proteolysis, thus increasing the protein yield (see Materials and Methods section 2.9).

The *in vitro* translated [^{35}S]-Methionine-labelled Kir2.0 proteins were immunoprecipitated with specific antisera and electrophoresed in an 8% polyacrylamide gel as described in the Materials and Methods section 2.10. All three *in vitro* translated protein polypeptides were immunoprecipitated specifically (Figure 4-1, lanes 1, 3 and 5). Immunoprecipitation of these polypeptides was blocked in each case by preabsorption of the antiserum with 10 μg/ml of antigenic C-terminal peptide (Figure 4-1, lanes 2, 4 and 6).

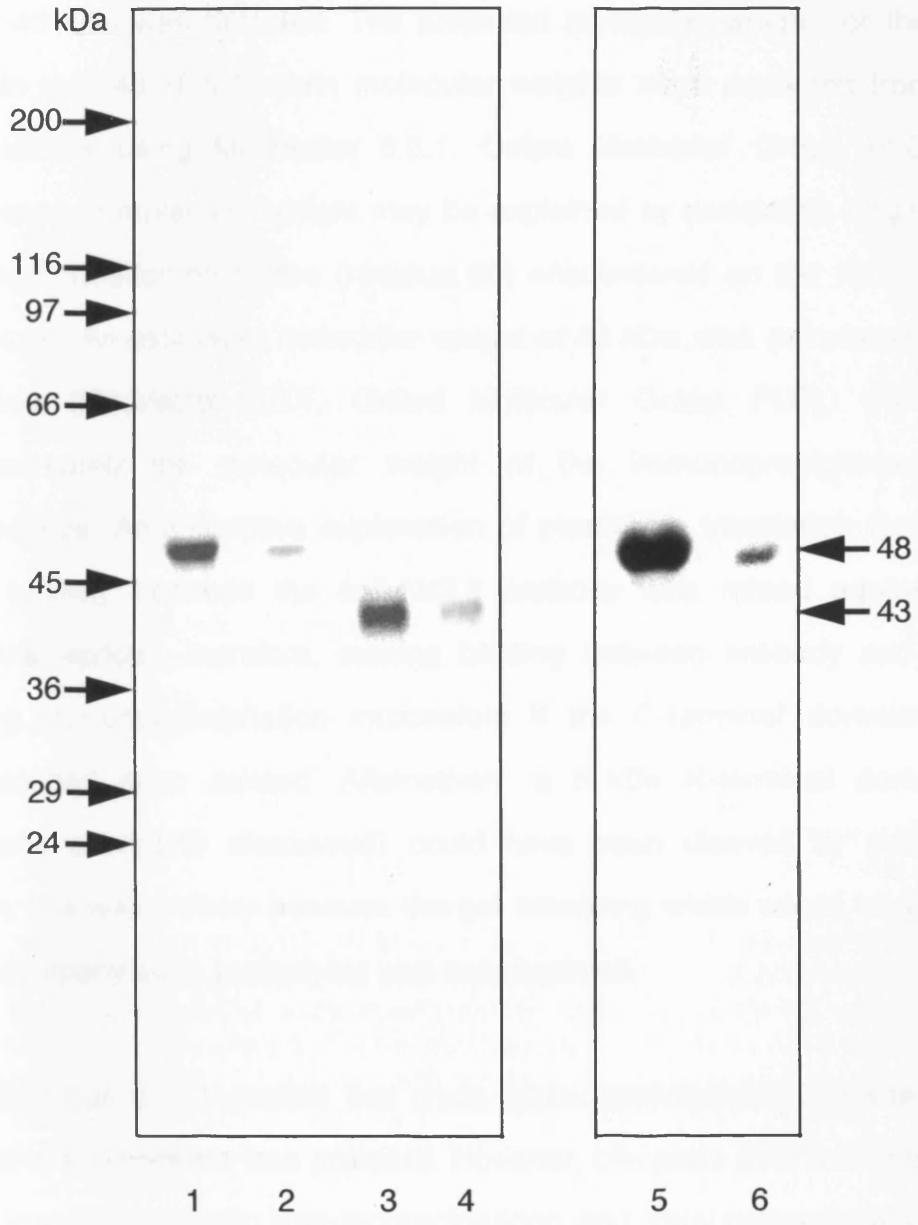

Figure 4-1. Immunoprecipitation of [^{35}S]–Methionine–labelled *in vitro* translated Kir2.0 proteins. Kir2.1 (lanes 1 and 2, molecular weight: 48 kDa), Kir2.2 (lanes 3 and 4, molecular weight: 43 kDa) and Kir2.3 (lanes 5 and 6, molecular weight: 48 kDa) were immunoprecipitated with corresponding specific antibodies either without (lanes 1, 3 and 5) or with preabsorption of the antibody with 10 μg/ml of the corresponding antigenic peptide.

In vitro translated protein bands were similar to the predicted molecular weights for Kir2.1 and Kir2.3 of 48-49 kDa. However, for Kir2.2 a polypeptide of 42-43 kDa was detected. The predicted molecular weight for the Kir2.2 protein was 48 kDa (protein molecular weights were predicted from cDNA translations using MacVector 6.0.1, Oxford Molecular Group PLC). This difference in molecular weight may be explained by translation beginning at the third methionine codon (residue 60) encountered on the Kir2.2 mRNA molecule. An estimated molecular weight of 42 kDa was calculated for this species (MacVector 6.0.1, Oxford Molecular Group PLC), which was approximately the molecular weight of the immunoprecipitated Kir2.2 polypeptide. An alternative explanation of premature translation termination was unlikely because the anti-Kir2.2 antibody was raised against a C-terminal epitope, therefore, making binding between antibody and protein during immunoprecipitation impossible if the C-terminal domain of the protein had been deleted. Alternatively, a 5 kDa N-terminal domain (for reasons previously discussed) could have been cleaved by proteolysis. Again, this was unlikely because the gel smearing which would be expected to accompany such proteolysis was not observed.

The previous data indicated that cross-immunoprecipitation between Kir2.0 proteins and antisera was possible. However, complete data were generated demonstrating specific immunoprecipitation and immunoprecipitation block by specific antigenic peptide (10 μg/ml). This was achieved in 1 ml reaction volumes by the addition of 1% bovine serum albumin carrier protein, 0.2% Triton X-100 and 100 mM potassium chloride to each immunoprecipitation reaction (Figure 4-2). The addition of salt blocked non-specific cross reactivity

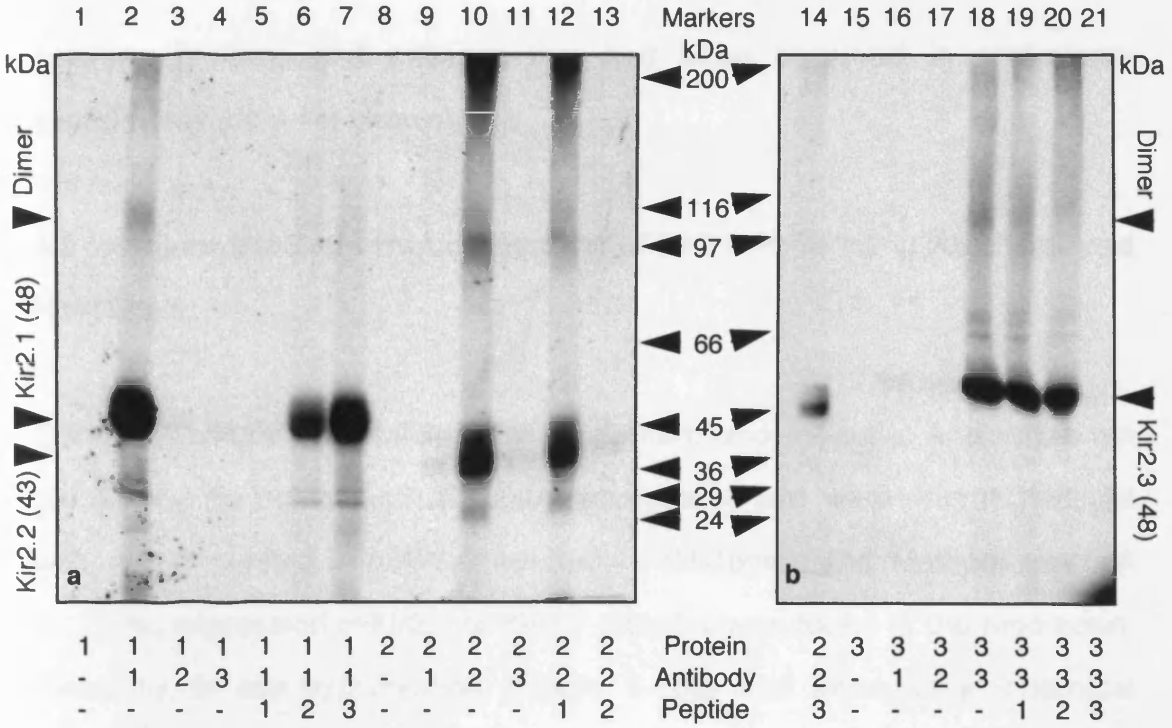

Kir2.1 protein, antibody and peptide: 1
Kir2.2 protein, antibody and peptide: 2
Kir2.3 protein, antibody and peptide: 3
No protein, antibody or peptide: -

Figure 4-2. Immunoprecipitation of [^{35}S]–Methionine–labelled *in vitro* translated Kir2.0 proteins with specific and non-specific antigenic peptide block. Kir2.1 protein (a, lanes 1-7, 48 kDa), Kir2.2 protein (a, b, lanes 8-14, 42 kDa), Kir2.3 protein (b, lanes 15-21, 48 kDa). Products were fractionated on an 8% polyacrylamide gel. Specificity was confirmed by immunoprecipitation of proteins by homologous antibodies (lanes 2, 10 and 18). Preabsorption of antibody with specific antigenic peptide (10 μg/ml) prevented immunoprecipitation of the homologous protein (lanes 5, 13 and 21). By contrast, preabsorption of antibody with non-specific antigenic peptide (10 μg/ml) failed to prevent immunoprecipitation of the homologous protein (lanes 6, 7, 12, 14, 19 and 20). Proteins could not be immunoprecipitated non-specifically without the homologous antibody (lane 1: Kir2.1, lane 8: Kir2.2 and lane 15: Kir2.3). All 3 Kir2.0 proteins may have formed dimers as indicated by the upper bands in lanes 2 (Kir2.1), 10 (Kir2.2) and 18 (Kir2.3). The Kir2.2 and Kir2.3 bands appear larger in Figure 4-2(b) than bands of equivalent molecular weight in Figure 4-2(a). This is due to the figures being taken from separate gels: however the standard markers indicated that Kir2.2 protein from both gels had a molecular weight of 43 kDa, whilst Kir2.1 (Figure 4-2(a)) and Kir2.3 (Figure 4-2(b)) both had molecular weights of 48 kDa.

between proteins and antisera that had been observed in preliminary experiments (data not shown).

4.3 Immunohistochemical Localisation of Kir2.0 Proteins in Rat Fore- and Hind-Brain

Coronal hind-brain (containing the cerebellum and medulla) and fore-brain (containing the hippocampus) tissue sections (4 μm) were immunostained with affinity purified anti-Kir2.0 antibodies (Materials and Methods section 2.12). No expression of Kir2.1 or Kir2.3 proteins was found in the hind-brain. Generally, *in situ* hybridisation (Figure 3-13a) and immunohistochemical (Figure 4-3a) data for Kir2.2 reported here for the rat cerebellum and medulla were mutually supporting. Immunostaining of Kir2.2 protein in the cerebellum and medulla of the hind-brain was detected in locus coeruleus, mesencephalic trigeminal nuclei, cerebellar molecular and granule layers and oligodendroglia (Figure 4-3a). Immunostaining of Kir2.1 (Figure 4-3b), Kir2.2 (Figure 4-3c) and Kir2.3 (Figure 4-3d) proteins in the hippocampus of the fore-brain was detected in CA1-CA3 pyramidal neurons and granule layer cells. Kir2.1 protein was also detected in astrocytes and oligodendroglia (Figure 4-4a), but Kir2.2 and Kir2.3 proteins were detected only in oligodendroglia (Figure 4-4b and Figure 4-4c, respectively) of the corpus callosum (as identified with Weil-Davenport's stain, data not shown). In addition, Kir2.1 protein was also expressed in fore-brain vascular smooth muscle cells (middle cerebral artery-Figure 4-4d), capillary endothelia and lateral ventricle ependyma (Figure 4-3b). Kir2.2 protein was expressed in fore-brain (middle cerebral artery-Figure 4-4e) and hind-brain (basilar artery-data not shown), vascular smooth muscle cells, capillary endothelia and IVth

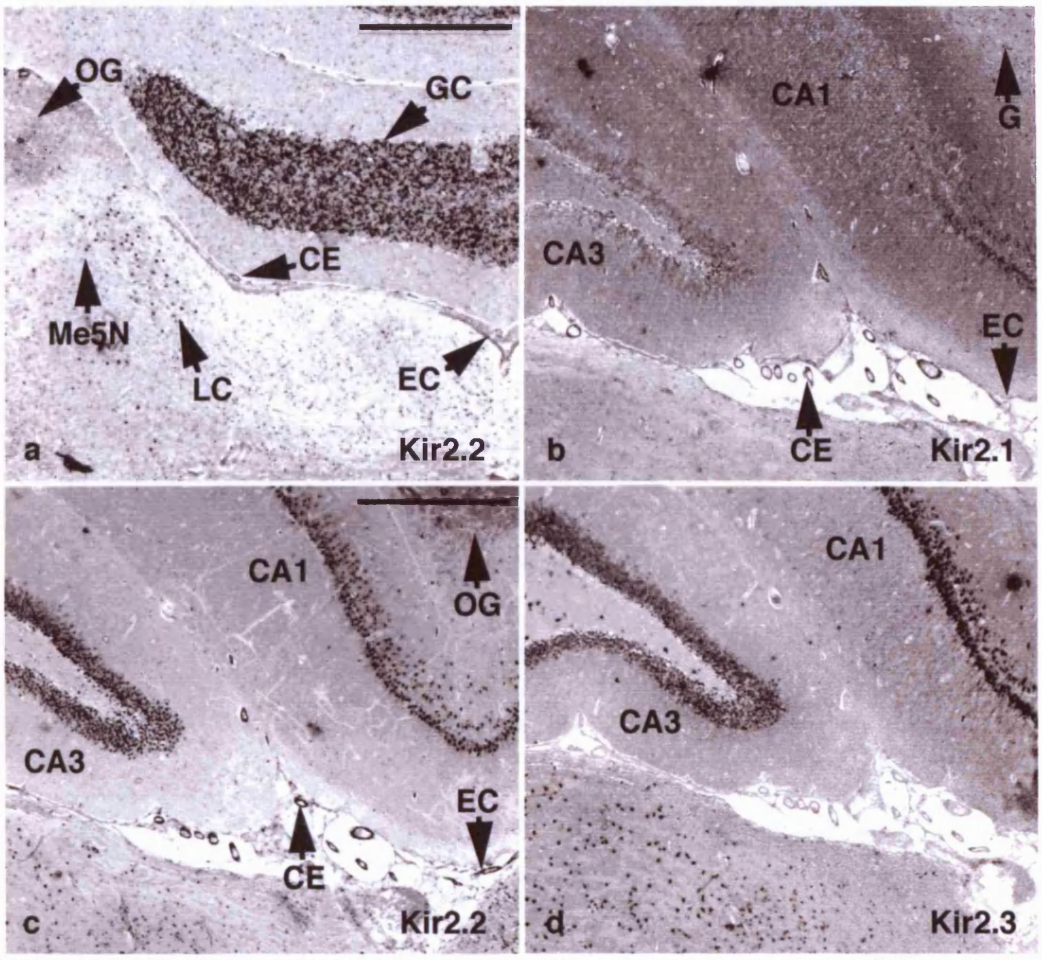

Figure 4-3. Kir2.0 immunostaining in rat brain tissue sections. (a), Anti-Kir2.2 immunostaining in cerebellar neurons of the locus coeruleus (LC), mesencephalic trigeminal nucleus (Me5N), granule cell layer (GC), oligodendroglia (OG), ependymal cells (EC) of the IVth ventricle and capillary endothelial cells (CE). (b), Anti-Kir2.1 immunostaining in hippocampal pyramidal CA1 and CA3 neurons, capillary endothelial cells (CE), oligodendroglia and astrocytes (G) and lateral ventricle ependymal cells (EC). (c), Anti-Kir2.2 immunostaining in hippocampal pyramidal CA1 and CA3 neurons, capillary endothelial cells (CE), oligodendroglia of the corpus callosum (OG) and lateral ventricle ependymal cells (EC). (d), Anti-Kir2.3 immunostaining of hippocampal CA1 and CA3 neurons and oligodendroglia (OG). Scale bars represent 450 μm (a) and 350 μm (b, c, d).

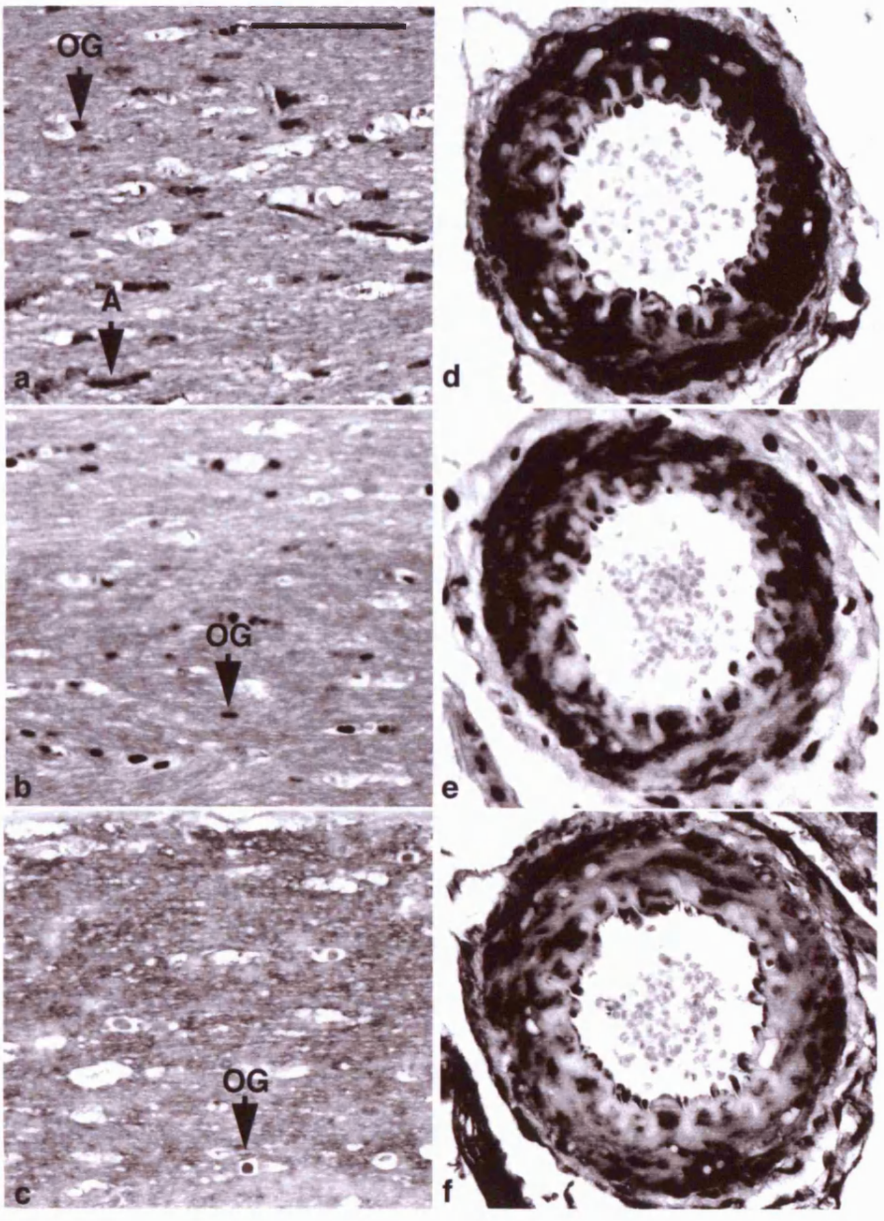

Figure 4-4. Kir2.0 immunostaining in rat brain macroglia and vascular smooth muscle. (a), Anti-Kir2.1 staining in oligodendroglia (OG) and astrocytes (A) of the corpus callosum. (b), Anti-Kir2.2 staining in oligodendroglia (OG) of the corpus callosum. (c), Anti-Kir2.3 staining also in oligodendroglia (OG) of the corpus callosum. (d), Anti-Kir2.1 staining was also found in vascular smooth muscle in the fore-brain (middle cerebral artery). (e), Anti-Kir2.2 staining was also found in vascular smooth muscle (middle cerebral artery) of the fore-brain. (f), Weak expression of Kir2.3 protein was detected in vascular smooth muscle (middle cerebral artery) in the fore-brain area. Scale bars represent 75 μm.

and lateral ventricle ependyma (Figure 4-3a and Figure 4-3c). Weak expression of Kir2.3 protein was found in fore-brain vascular smooth muscle cells (middle cerebral artery-Figure 4-4f), but not capillary endothelia or lateral ventricle ependyma (Figure 4-3d).

The observations presented here are in agreement with the *in situ* hybridisation data of Karschin and colleagues for brain regions investigated in both studies (Karschin *et al.,* 1996). For example, the data shown here indicate that Kir2.1 and Kir2.3 protein expression was not detectable in the cerebellum, supporting the earlier published data (Karschin *et al.,* 1996). However, presented here for the first time is a detailed immunohistochemical study of Kir2.0 protein distribution in fore-brain (hippocampus) and hind-brain (cerebellum and medulla), including the non-neuronal cell types. In addition, high magnification photomicrographs of anti-Kir2.1 (Figure 4-5a), anti-Kir2.2 (Figure 4-5b) and anti-Kir2.3 (Figure 4-5c) immunostaining in CA3 pyramidal neurons of the hippocampus, demonstrate for the first time a nuclear, as well as plasma membrane localisation in rat brain tissue sections. Table 4-1 provides a summary of the cell types and subcellular localisations of the NK-1 receptor and Kir2.0 channel proteins.

Tissue sections stained in the absence of primary antibody with the ABC-AP colourimetric detection system (hind-brain, Figure 4-6b; fore-brain, Figure 4-6d), and in the absence of primary and secondary antibodies with the ABC-AP colourimetric detection system (hind-brain, Figure 4-6c; fore-brain, Figure 4-6e) indicated background levels of immunostaining.

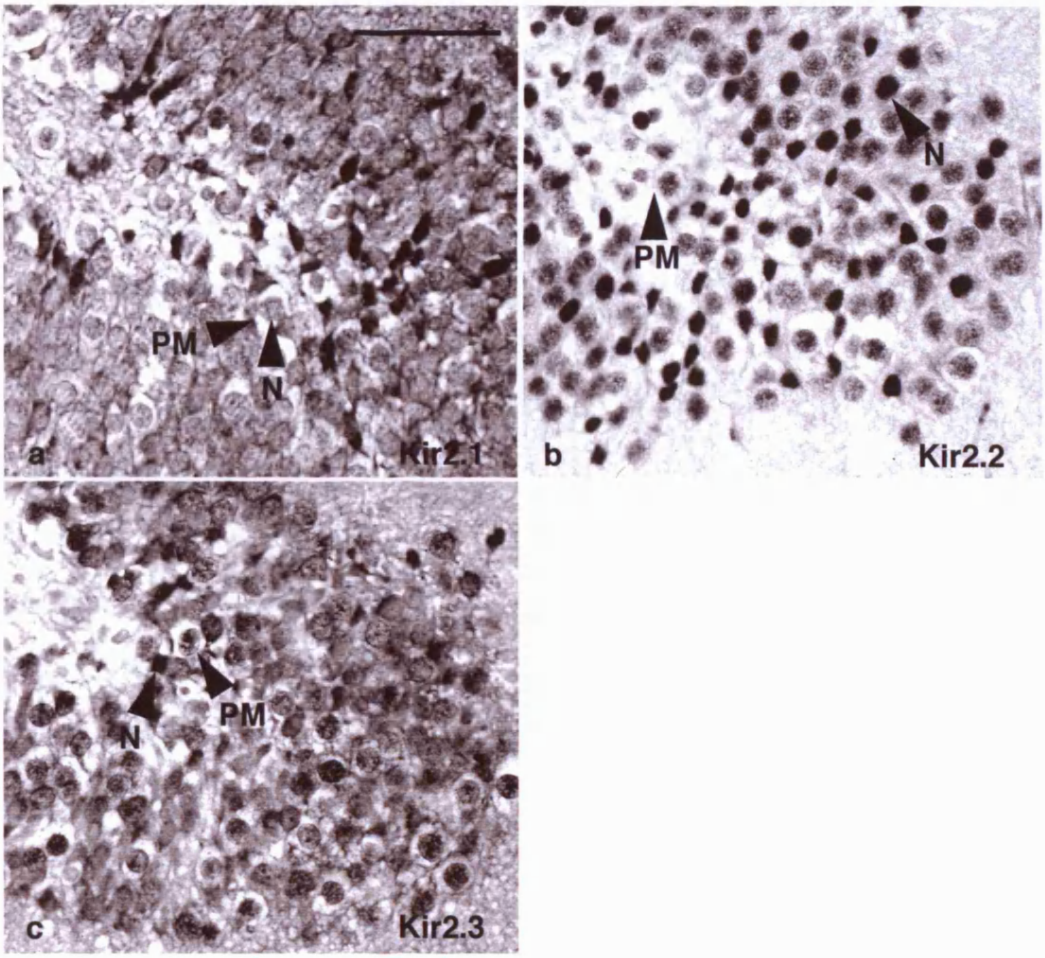

Figure 4-5. Kir2.0 immunostaining in rat brain hippocampal tissue sections. (a), Anti-Kir2.1. (b), Anti-Kir2.2. (c), Anti-Kir2.3 all demonstrated immunostaining in CA3 pyramidal neurons of the hippocampus. The immunostaining indicated channel proteins were located in nucleus (N) and plasma membrane (PM). Scale bar represents 25 μm.

Table 4-1. NK-1 R/Kir2.0 Proteins in Rat Hind- and Fore-Brain

Hind-brain	Kir2.1	Kir2.2	Kir2.3	NK-1 R
neurons- locus coeruleus	-	+*	-	+
Me5N	-	+*	-	-
cerebellar Purkinje cell layer	-	-	-	-
molecular cell layer	-	+	-	-
granule cell layer	-	+	-	-
macroglia- astrocytes	-	-	-	-
oligodendroglia	-	+	-	+
capillary endothelia	-	+	-	-
vascular smooth muscle	-	+	-	-
IVth ventricle ependyma	-	+	-	-
Fore-brain				
neurons- CA1-CA3 pyramidal	+*	+*	+*	-
granule cell layer	+*	+*	+*	-
macroglia- astrocytes	+	-	-	-
oligodendroglia	+	+	+	-
capillary endothelia	+	+	-	-
vascular smooth muscle	+	+	+	-
lateral ventricle ependyma	+	+	-	-

+ positive immunostaining; +* positive immunostaining with distinct nuclear and plasma membrane subcellular localisation; - negative immunostaining.

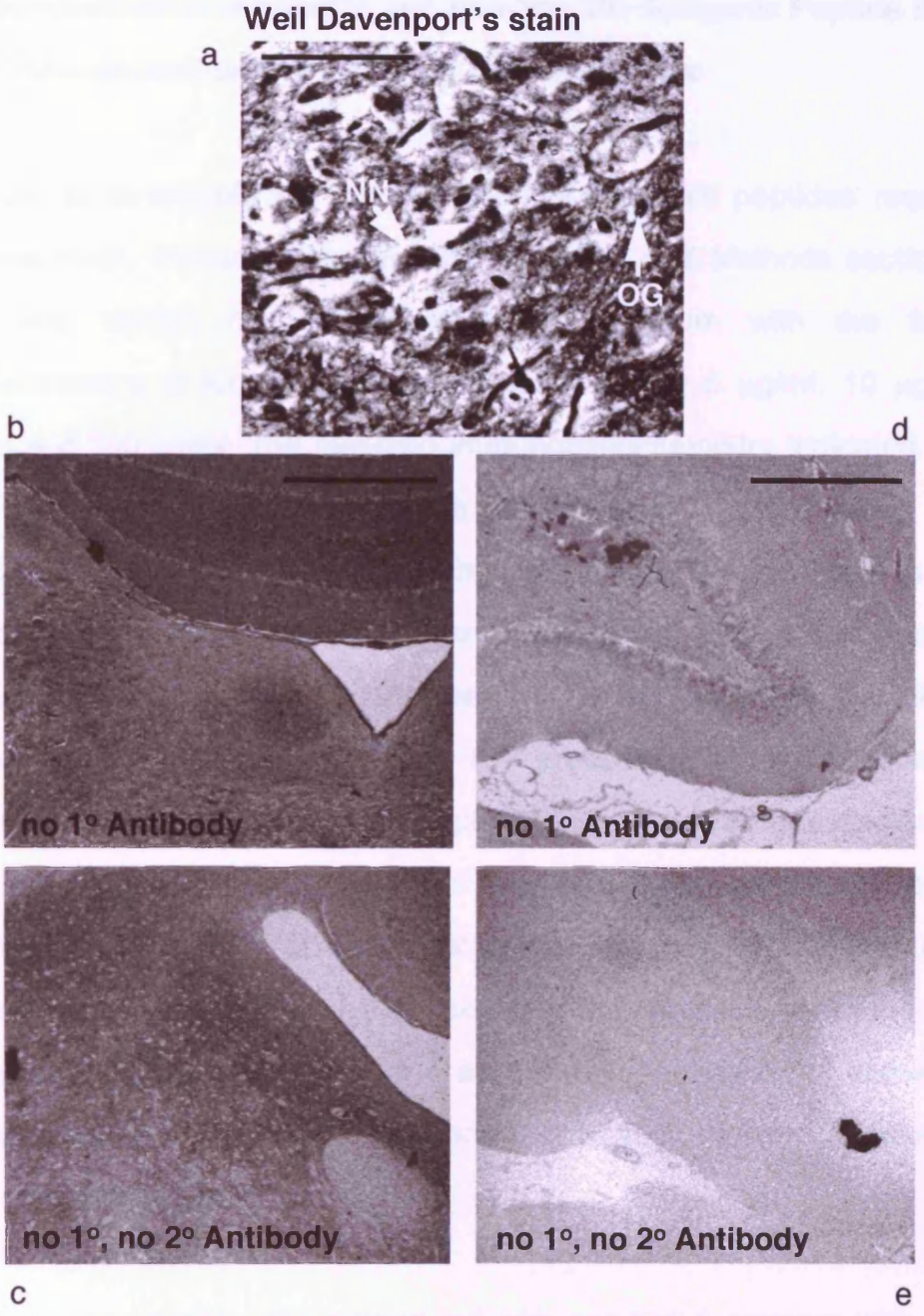

Figure 4-6. Antibody negative controls and Weil Davenport's histological stain in rat brain tissue sections. (a), Weil Davenport's staining of the locus coeruleus, indicating the outline of large noradrenergic neurons (NN) and small densely staining oligodendroglia (OG). (b), Negative control in the absence of primary antibody in rat hind-brain. (c), Negative control in the absence of primary and secondary antibodies in rat hind-brain. (d), Negative control in the absence of primary antibody in rat fore-brain. (e), Negative control in the absence of primary and secondary antibodies in rat fore-brain. Scale bars represent 100 μm (a), 450 μm (b, c) and 350 μm (d, e).

4.4 Demonstration of Specific and Non-Specific Antigenic Peptide Block of Kir2.0 Immunostaining on Rat Brain Tissue Sections

In order to investigate the concentration of antigenic peptides required to achieve block, immunohistochemistry (Materials and Methods section 2.12) was first carried out using anti-Kir2.2 antiserum with the following concentrations of Kir2.2 antigenic peptide: 1 μg/ml, 5 μg/ml, 10 μg/ml, 50 μg/ml and 100 μg/ml. The resulting immunohistochemistry indicated that the use of 1 μg/ml or 5 μg/ml antigenic peptide did not reduce tissue section immunostaining. The use of 10 μg/ml antigenic peptide resulted in almost complete block of tissue section immunostaining (Figure 4-8b). The use of 50 μg/ml or 100 μg/ml antigenic peptide caused very strong background immunostaining, possibly due to the production of immunocomplexes formed by an excess of antigenic peptide binding to specific antiserum (data not shown). The immunocomplexes then bound non-specifically to the rat brain tissue sections, allowing detection with the ABC-AP colourimetric system. Therefore, from these experiments, specific and non-specific antigenic peptide block of all three anti-Kir2.0 antisera in immunohistochemistry, immunoprecipitation and Western blotting were carried out at 10 μg/ml.

Further experiments were carried out with anti-Kir2.0 antisera with specific and non-specific antigenic peptide block (10 μg/ml) on rat fore-brain tissue sections. Immunostaining with anti-Kir2.1 antiserum (1:500) and Kir2.1 antigenic peptide (Figure 4-7a) produced staining that was retained in CA1 and CA3 pyramidal neurons, capillary endothelia and lateral ventricle ependyma. However, the staining strength was reduced by approximately

20% in comparison to non-specific antigenic peptide block in the presence of Kir2.2 or Kir2.3 antigenic peptide. Immunostaining with anti-Kir2.1 antiserum (1:500) and Kir2.2 antigenic peptide (Figure 4-7b) produced very strong staining, in particular CA1 and CA3 pyramidal neurons, capillary endothelia and lateral ventricle ependyma. Immunostaining with anti-Kir2.1 antiserum (1:500) and Kir2.3 antigenic peptide (Figure 4-7c) was very strong (stronger than the Kir2.2 antigenic peptide block), particularly in the CA1 and CA3 pyramidal neurons, capillary endothelia and lateral ventricle ependyma.

Immunostaining with anti-Kir2.2 antiserum (1:200) and Kir2.1 antigenic peptide (Figure 4-8a) produced staining in CA1 and CA3 pyramidal neurons, capillary endothelia and lateral ventricle ependyma. Anti-Kir2.2 antiserum (1:200) and Kir2.2 antigenic peptide (Figure 4-8b) abolished immunostaining on the tissue section, with the exception of slight staining in the capillary endothelia. Anti-Kir2.2 antiserum (1:200) and Kir2.3 antigenic peptide (Figure 4-8c) yielded immunostaining in the CA1 and CA3 pyramidal neurons, capillary endothelia and lateral ventricle ependyma of a similar strength to the Kir2.1 antigenic peptide block.

Immunostaining with anti-Kir2.3 antiserum (1:200) and Kir2.1 antigenic peptide (Figure 4-9a) produced very strong background staining. Background immunostaining with anti-Kir2.3 antiserum (1:200) and Kir2.2 antigenic peptide (Figure 4-9b) was slightly weaker than block with Kir2.1 antigenic peptide. However, immunostaining strength was similar in the CA1 and CA3 pyramidal neurons in both tissue sections. Immunostaining with anti-Kir2.3 antiserum (1:200) and Kir2.3 antigenic peptide (Figure 4-9c) resulted in a reduction of background by approximately 50%, revealing unblocked

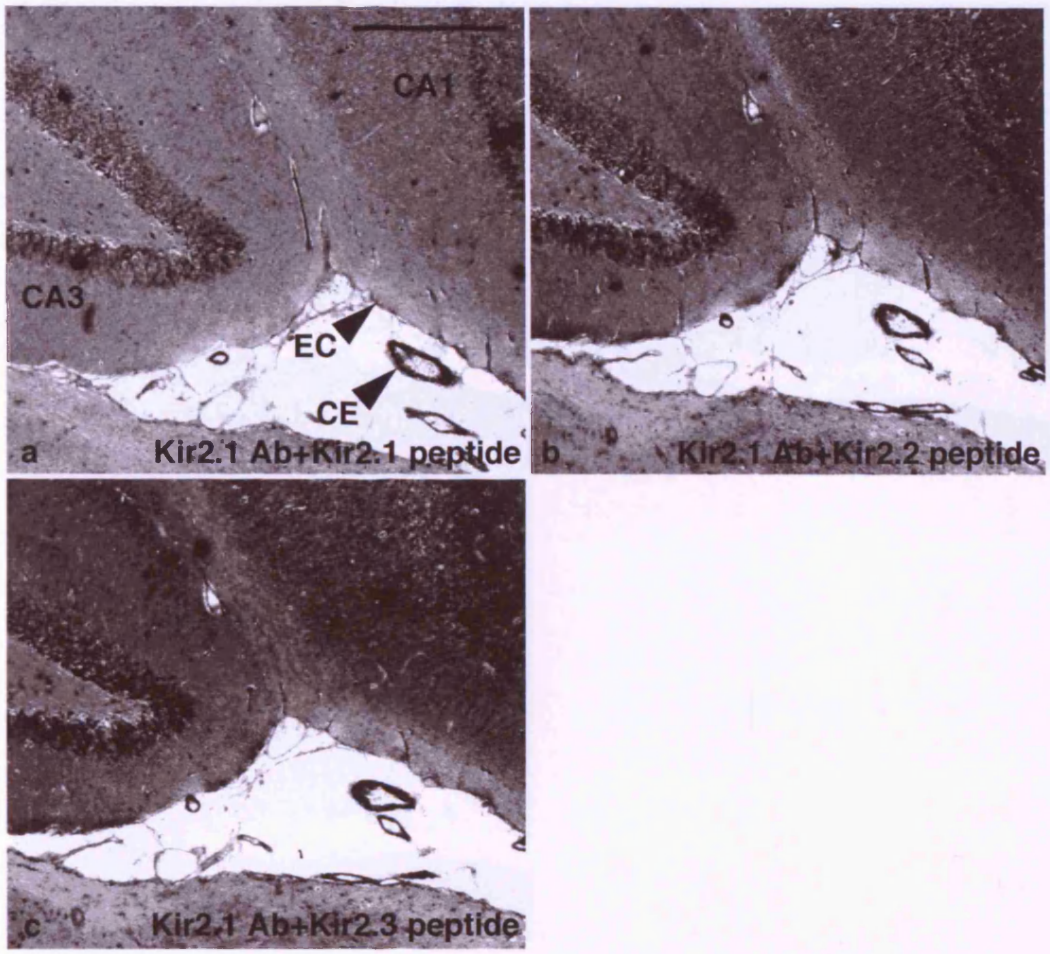

Figure 4-7. Kir2.1 immunostaining with specific and non-specific antigenic peptides in rat brain tissue sections. (a), Rat fore-brain tissue section, immunostained with anti-Kir2.1 antiserum, preabsorbed for 16 hours with 10 μg/ml Kir2.1 antigenic peptide prior to immunostaining. Immunostaining was retained in CA1 and CA3 pyramidal neurons, capillary endothelia (CE) and lateral ventricle ependyma (EC), however the staining strength was reduced by approximately 20% in comparison to non-specific peptide block in the presence of Kir2.2 or Kir2.3 peptide. (b), Rat fore-brain tissue section, immunostained with anti-Kir2.1 antiserum, preabsorbed for 16 hours with 10 μg/ml Kir2.2 antigenic peptide prior to immunostaining. Overall, very strong immunostaining was observed in the tissue section, in particular CA1 and CA3 pyramidal neurons, capillary endothelia (CE) and lateral ventricle ependyma (EC). (c), Rat fore-brain tissue section, immunostained with anti-Kir2.1 antiserum, preabsorbed for 16 hours with 10 μg/ml Kir2.3 antigenic peptide prior to immunostaining. Again the overall immunostaining in this tissue section was very strong (stronger than the Kir2.2 antigenic peptide block), particularly in the CA1 and CA3 pyramidal neurons, capillary endothelia (CE) and lateral ventricle ependyma (EC). Scale bar represents 350 μm.

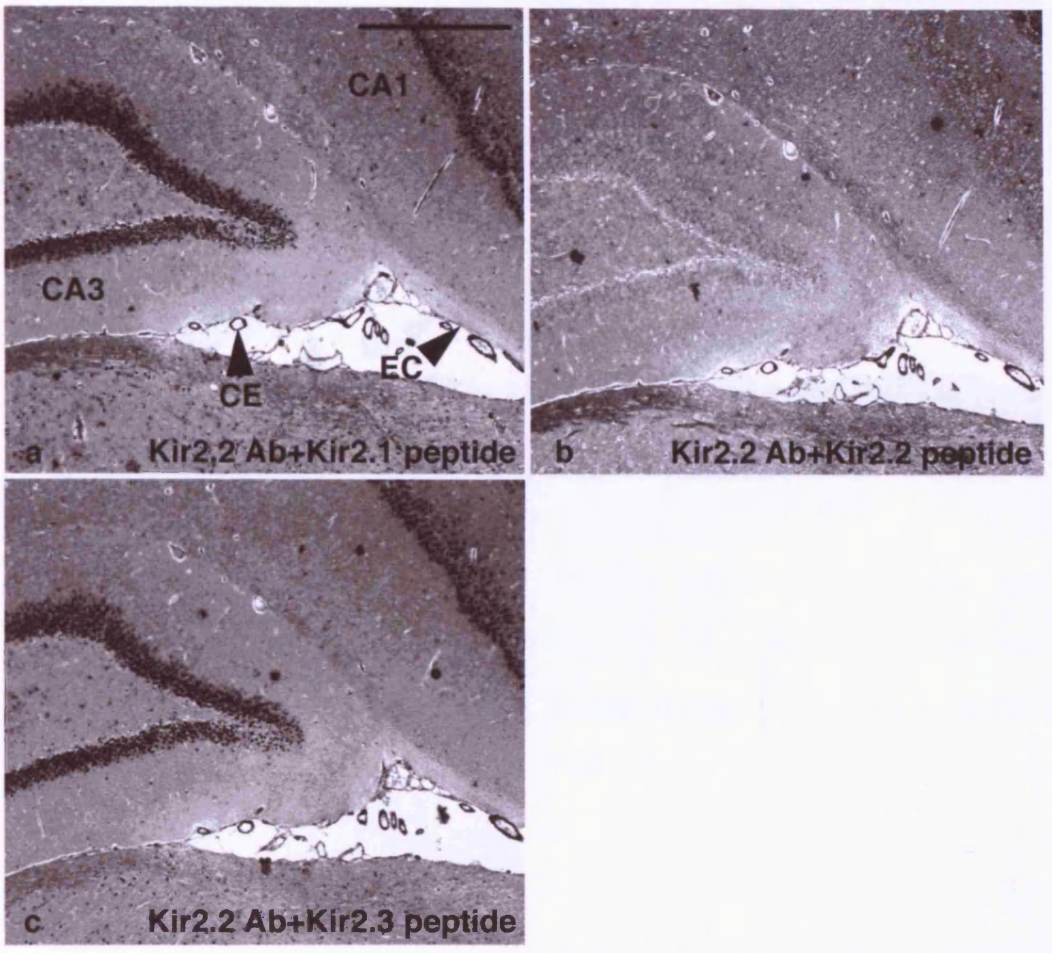

Figure 4-8. Kir2.2 immunostaining with specific and non-specific antigenic peptides in rat brain tissue sections. (a), Rat fore-brain tissue section, immunostained with anti-Kir2.2 antiserum, preabsorbed for 16 hours with 10 μg/ml Kir2.1 antigenic peptide prior to immunostaining. Immunostaining was observed in CA1 and CA3 pyramidal neurons, capillary endothelia (CE) and lateral ventricle ependyma (EC). (b), Rat fore-brain tissue section, immunostained with anti-Kir2.2 antiserum, preabsorbed for 16 hours with 10 μg/ml Kir2.2 antigenic peptide prior to immunostaining. Immunostaining was abolished on the tissue section, with the exception of slight immunostaining in the capillary endothelia (CE). (c), Rat fore-brain tissue section, immunostained with anti-Kir2.2 antiserum, preabsorbed for 16 hours with 10 μg/ml Kir2.3 antigenic peptide prior to immunostaining. Again, immunostaining in this tissue section was observed in the CA1 and CA3 pyramidal neurons, capillary endothelia (CE) and lateral ventricle ependyma (EC). Scale bar represents 350 μm.

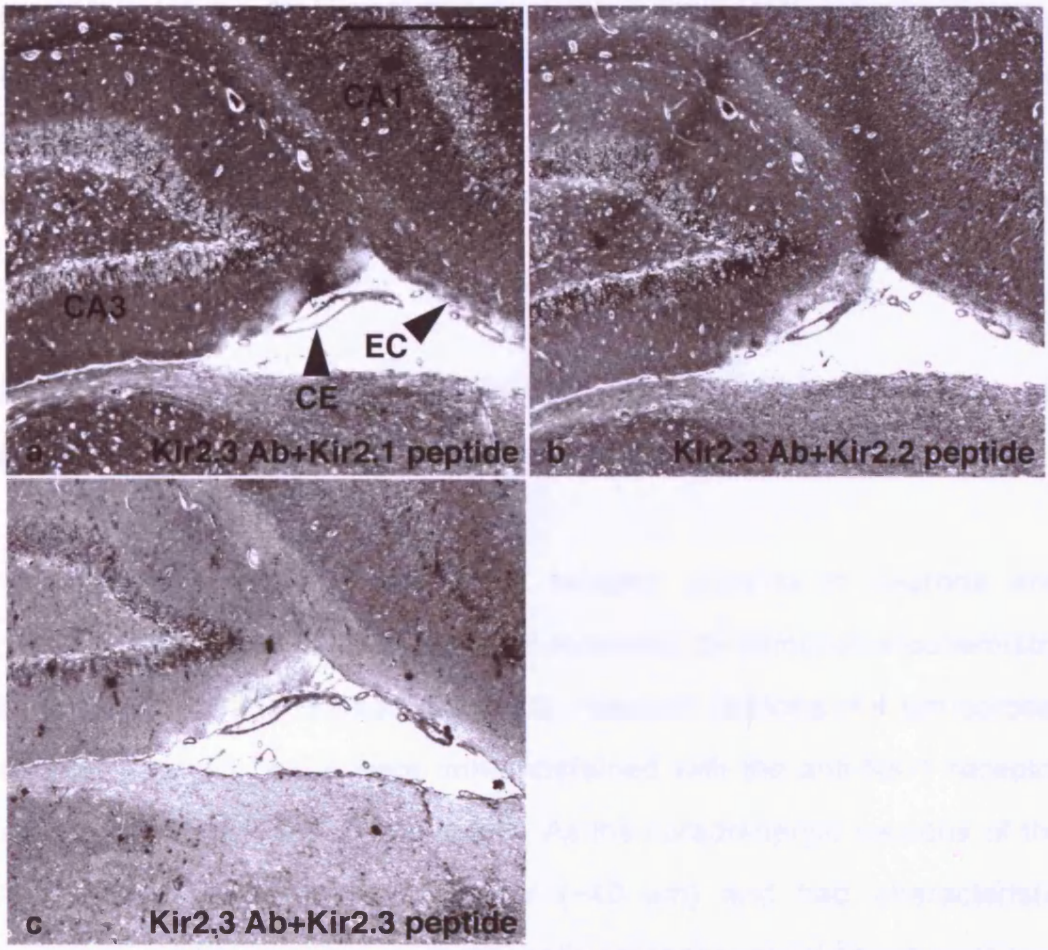

Figure 4-9. Kir2.3 immunostaining with specific and non-specific antigenic peptides in rat brain tissue sections. (a), Rat fore-brain tissue section, immunostained with anti-Kir2.3 antiserum, preabsorbed for 16 hours with 10 μg/ml Kir2.1 antigenic peptide prior to immunostaining. A very strong background immunostaining was observed, particularly in CA1 and CA3 pyramidal neurons. (b), Rat fore-brain tissue section, immunostained with anti-Kir2.3 antiserum, preabsorbed for 16 hours with 10 μg/ml Kir2.2 antigenic peptide prior to immunostaining. Immunostaining strength of the CA1 and CA3 pyramidal neurons was similar to block with Kir2.1 antigenic peptide. However, background was reduced by approximately 20% in comparison to block with Kir2.1 antigenic peptide. (c), Rat fore-brain tissue section, immunostained with anti-Kir2.3 antiserum, preabsorbed for 16 hours with 10 μg/ml Kir2.3 antigenic peptide prior to immunostaining. The background immunostaining was reduced by approximately 50%, revealing unblocked immunostaining in CA1 and CA3 pyramidal neurons and also capillary endothelia (CE) and lateral ventricle ependyma (EC). The latter 2 types of structure were not stained by the affinity purified antibodies, leading to the conclusion that the staining was due to a non-specific component of the unpurified antiserum. Scale bar represents 350 μm.

immunostaining in CA1 and CA3 pyramidal neurons and also capillary endothelia and lateral ventricle ependyma. The latter two types of structure were not stained by the affinity purified antibodies, leading to the conclusion that the staining was due to a non-specific component of the unpurified anti-Kir2.3 antiserum.

4.5 Co-Localisation of Kir2.2 and NK-1 Receptor Proteins in Neurons and Oligodendroglia of the LC by Immunohistochemistry

The expression of Kir2.2 and NK-1 receptor proteins in neurons and oligodendroglia of the LC has been co-localised by immunohistochemistry (see Materials and Methods section 2.12). Adjacent sections of 4 μm coronal cerebellar rat brain tissue were immunostained with the anti-NK-1 receptor or anti-Kir2.2 affinity purified antibodies. As the noradrenergic neurons of the LC were relatively large in diameter (~40 μm) and had characteristic morphology, it was possible to identify cells present in serial tissue sections. Adjacent tissue sections containing the same group of cells within the LC were stained with anti-Kir2.2 and anti-NK-1 receptor antibodies. Strong nuclear and weaker plasma membrane signals in neurons were observed for Kir2.2 protein, with immunostaining in oligodendroglia (identified by Weil Davenport's stain (Figure 4-6a)) but not astrocytes (Figure 4-10a). NK-1 receptor protein was strongly expressed on the plasma membranes of neurons, oligodendroglia and fibres but not astrocytes within the LC (Figure 4-10b). Generally the observations presented in this chapter on the NK-1 receptor protein localisation are in agreement with published *in situ* hybridisation data (Maeno *et al.,* 1993) and immunohistochemical data (Nakaya *et al.,* 1994). However, this study has expanded on the detail of their

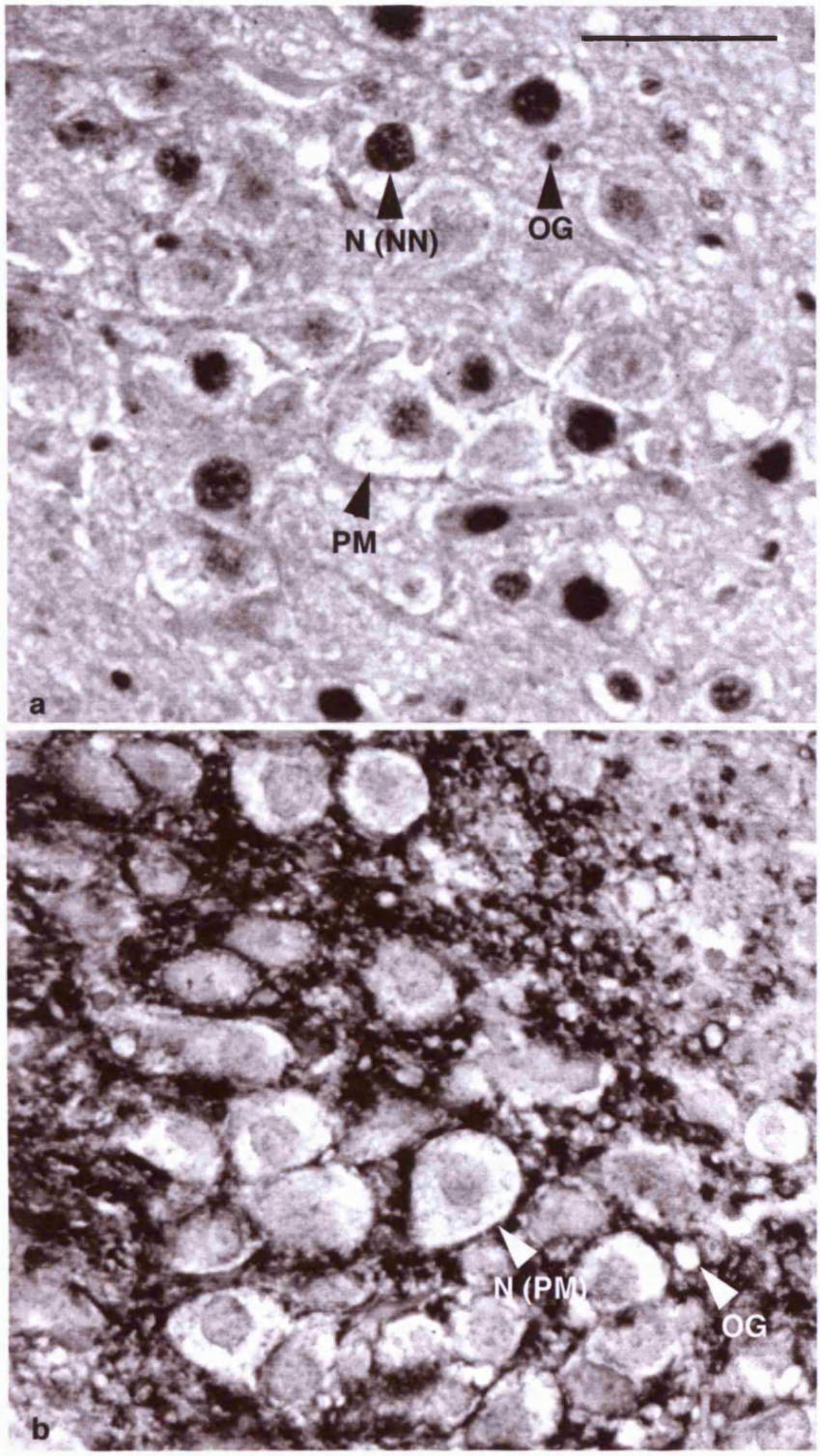

Figure 4-10. Anti-Kir2.2 and anti-NK-1 receptor immunostaining in the LC. (a), Anti-Kir2.2 immunostaining in rat hind-brain tissue sections. Nuclear (NN) and weaker plasma membrane (PM) staining was seen in noradrenergic neurons (N) and oligodendroglia (OG). (b), Anti-NK-1 receptor immunostaining was detected on plasma membranes of noradrenergic neurons (N), oligodendroglia (OG) and neural processes. Scale bar represents 75 μm.

findings, which identified structures that were positively stained for the NK-1 receptor protein within the CNS. In this study immunostaining in neurons and oligodendroglia has been identified.

In order to establish co-expression of Kir2.2 and NK-1 receptor proteins, the Macromedia XRES program was used to overlay two adjacent tissue sections (immunostained with anti-Kir2.2 (Figure 4-11a) and anti-NK-1 receptor (Figure 4-11b) respectively). This overlay demonstrated a co-localisation of NK-1 receptor and Kir2.2 proteins in single neurons and oligodendroglia of the LC (Figure 4-11c).

4.6 Subcellular Localisation of Kir2.0 Proteins in Transiently Transfected Chinese Hamster Ovary Cells by Immunocytochemistry

In order to further investigate the unexpected intracellular localisation of Kir2.0 proteins, mouse Kir2.0 cDNAs were transiently transfected into Chinese hamster ovary (CHO) cells, grown by Ms Penny Spencer, Hodgkin Building, University of Leicester. The localisation of Kir2.0 isoforms was investigated by immunocytochemistry with rhodamine detection (see Materials and Methods section 2.13). Strong cytoplasmic and plasma membrane signals were observed for anti-Kir2.1 (Figure 4-12a), with apparent cytoplasmic (trafficking) staining. Predominantly, nuclear signals were observed for anti-Kir2.2 (Figure 4-12b) and anti-Kir2.3 (Figure 4-12c). Negative controls included the absence of primary antibody with secondary antibody treatment on transfected cells (Kir2.1 transfected, Figure 4-13a; Kir2.2 transfected, Figure 4-13b; Kir2.3 transfected, Figure 4-13c), yielding a very low background stain attributable to the secondary antibody. Negative

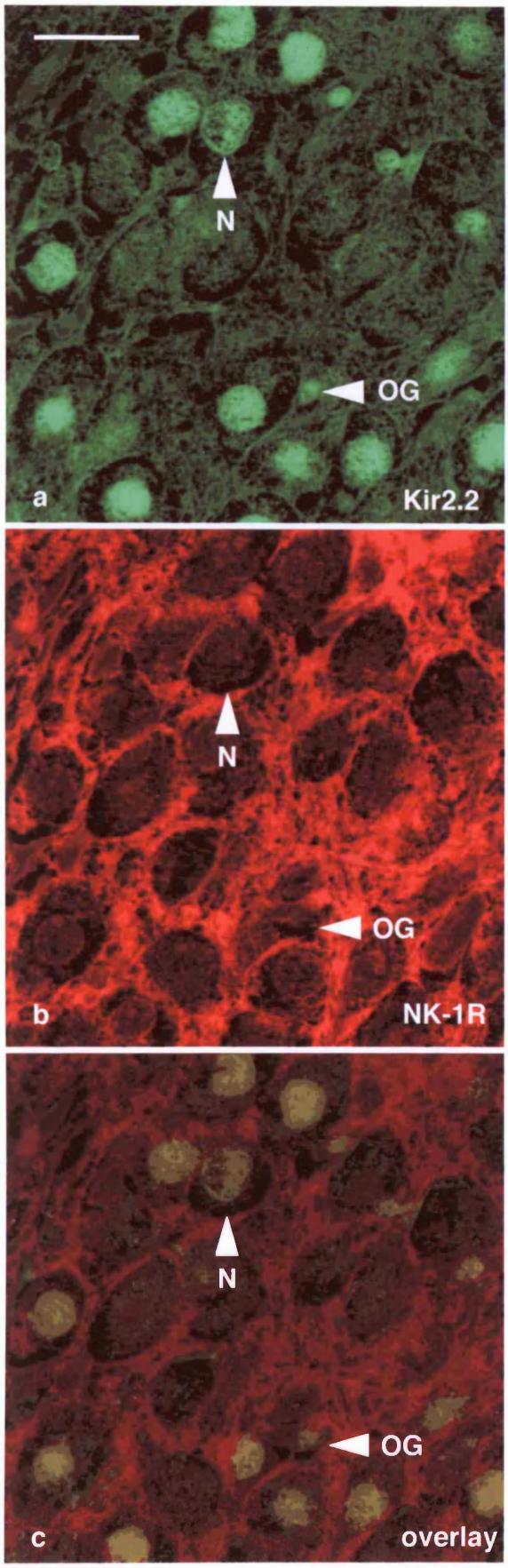

Figure 4-11. Co-localisation of Kir2.2 and NK-1 receptor in 2 sequentially cut tissue sections from rat hind-brain. The sections were individually immunostained for Kir2.2 and NK-1 receptor proteins. The sections were artificially coloured (XRES program) with FITC (a), and rhodamine (b), respectively and then overlayed: co-localisation was indicated by dark red plasma membrane NK-1 receptor staining surrounding dark green nuclear Kir2.2 staining (c). The co-localisation included both neurons (N) and oligodendroglia (OG) as identified by Weil-Davenport's stain. Scale bar represents 75 μm.

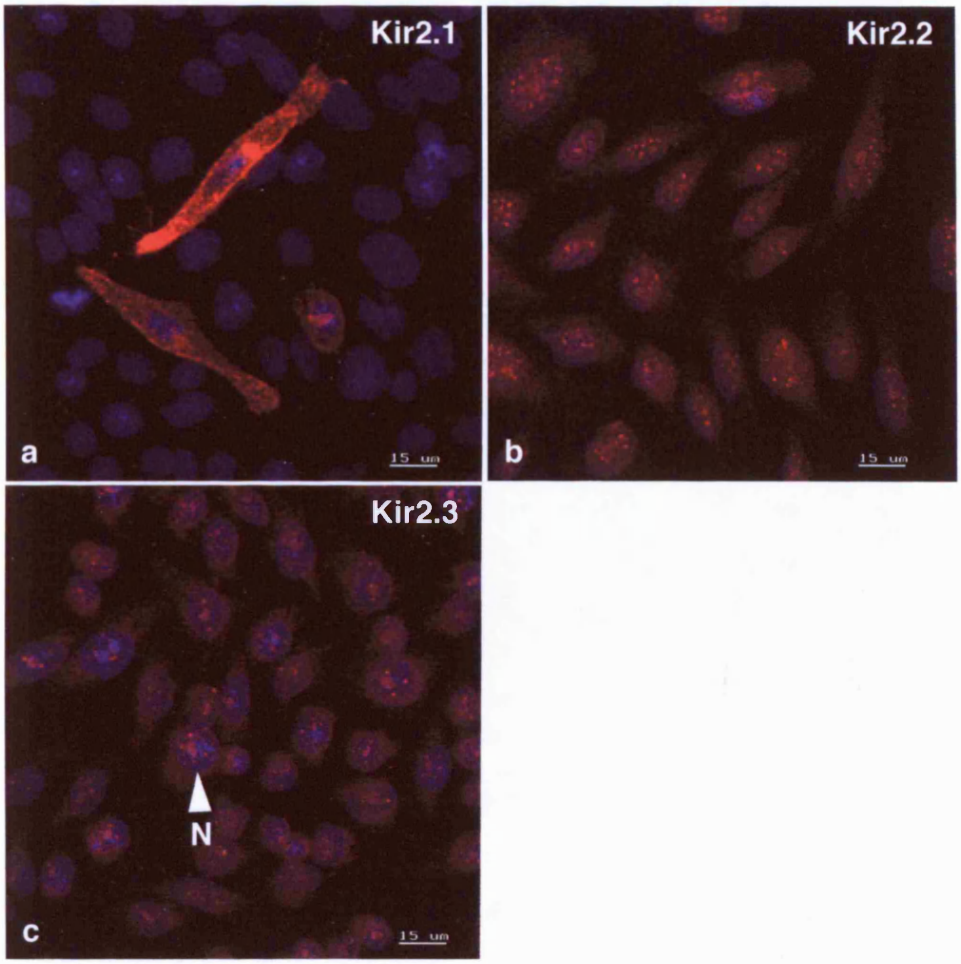

Figure 4-12. Immunolocalisation of Kir2.0 channel proteins in CHO cells, transiently transfected with (a) Kir2.1, (b) Kir2.2 and (c) Kir2.3 cDNAs. (a), Anti-Kir2.1 exhibited cytoplasmic and plasma membrane immunostaining. (b), Anti-Kir2.2 displayed nuclear and cytoplasmic (trafficking) immunostaining. (c), Anti-Kir2.3 also displayed nuclear and cytoplasmic (trafficking) immunostaining. Nuclei (N) were stained purple with Hoechst 33342.

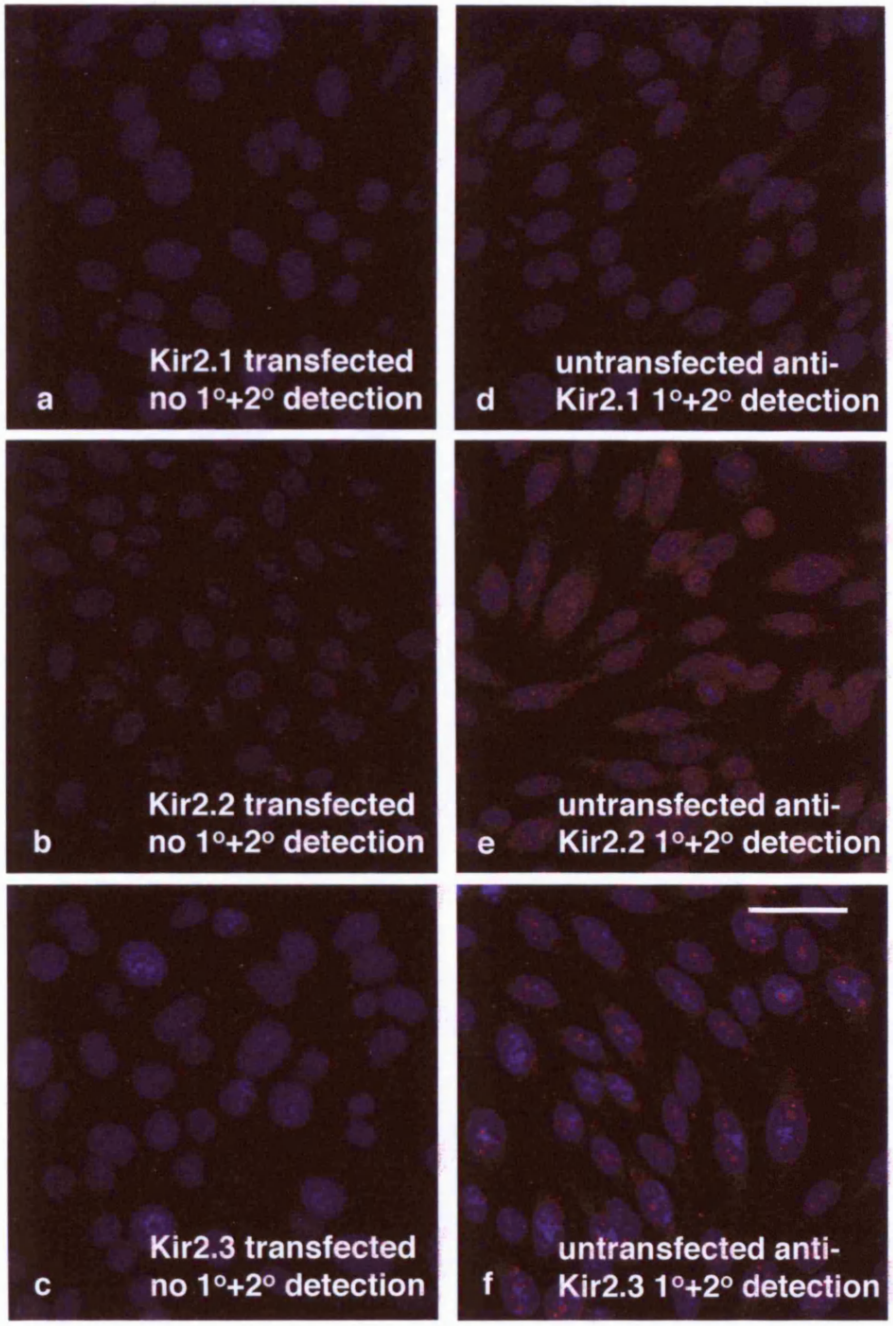

Figure 4-13. Negative controls for the detection of Kir2.0 channel proteins in transfected and untransfected CHO cells. (a) Kir2.1, (b) Kir2.2 and (c) Kir2.3 transfections revealed background staining in fluorometric detection of cells stained in the absence of primary, but with secondary antibody. These data implied that a low level of staining was due to the secondary antibody. Untransfected cells stained with (d) anti-Kir2.1, (e) anti-Kir2.2 and (f) anti-Kir2.3 primary and secondary antibodies respectively. Again, some background staining was seen, particularly for anti-Kir2.2 (e) and anti-Kir2.3 (f). However, there was a clear difference in the cell staining in untransfected cells compared to transfected cells (Figure 4-12), (Kir2.2 and Kir2.3 staining was nuclear, Kir2.1 staining was cytoplasmic) and the general cytoplasmic staining shown in this figure. Nuclei are shown in purple with Hoechst 33342. Scale bar represents 30 μm.

controls also included treatment of untransfected cells with primary and secondary antibodies (anti-Kir2.1 antibody, Figure 4-13d; anti-Kir2.2 antibody, Figure 4-13e; anti-Kir2.3 antibody, Figure 4-13f). These negative controls indicated that Kir2.1 protein (Figure 4-13d) could not be detected in untransfected CHO cells. However, low levels of nuclear staining were detected in untransfected CHO cells after detection with anti-Kir2.2 (Figure 4-13e) and anti-Kir2.3 (Figure 4-13f) antibodies. The Kir2.2 and Kir2.3 nuclear staining proteins in untransfected CHO cells were approximately 25% of the strength found in transfected cells. In addition, it was noted that non-transfected cells within the test populations showed no background staining (anti-Kir2.1 staining in Figure 4-12a).

4.7 Western Blotting of Kir2.2 on Rat Brain Proteins

In order to fully investigate the nuclear distribution pattern observed in rat brain tissue sections by immunohistochemistry and transfected CHO cells by immunocytochemistry, Western blotting was conducted on nuclear and plasma membranes of rat brain tissues (Materials and Methods section 2.11, nuclear proteins were obtained by centrifugation, but were not quantified as being nuclear in origin prior to Western blotting). In immunoblots using 8.6 μg/ml of affinity purified anti-Kir2.2 antibody a single polypeptide was recognised in plasma and nuclear membrane extracts from rat brain tissue of 62 kDa (Figure 4-14, lanes 2 and 4). These single bands were obtained in 8% polyacrylamide gels and concurred with published size estimates of 55 kDa (6% gel) and 64 kDa (10% gel) (Raab-Graham & Vandenberg, 1998). Detection of the 62 kDa polypeptide was blocked by

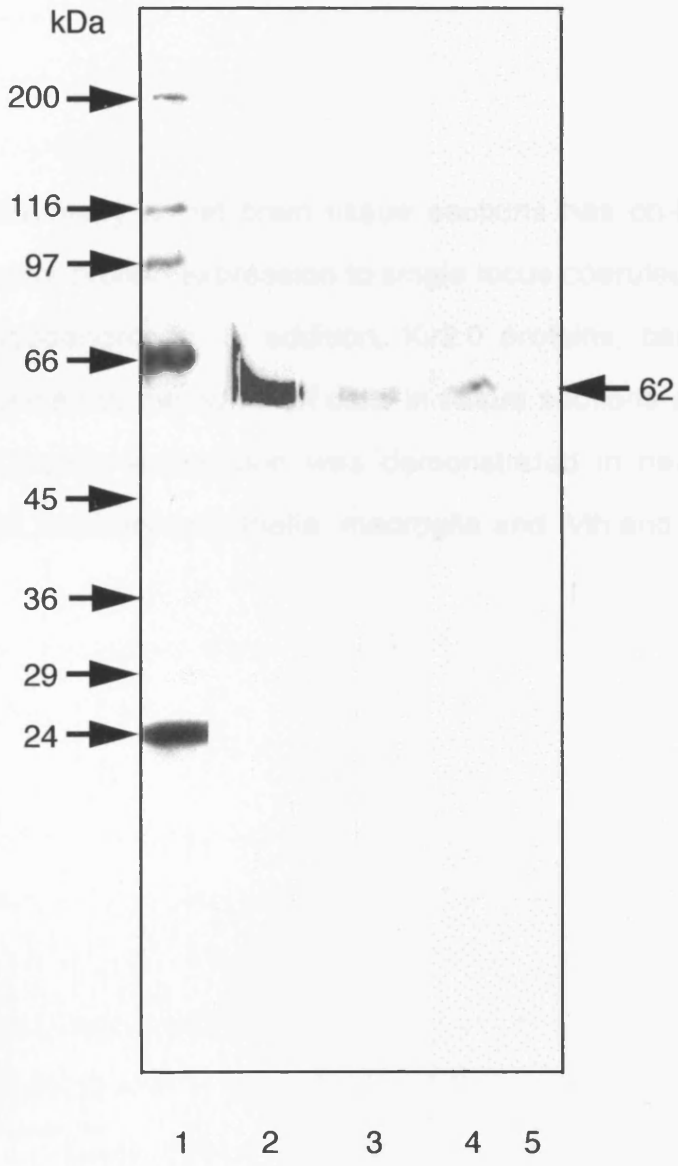

Figure 4-14. Detection of Kir2.2 channel protein in Western blots of fractionated rat cerebellar proteins (1 mg of protein per lane) produced a 62 kDa polypeptide. Lanes 2 and 3 plasma membrane, lanes 4 and 5 nuclear membrane, without (lanes 2 and 4) and with (lanes 3 and 5) preabsorption of the Kir2.2 antibody with 10 μg/ml Kir2.2 C-terminal antigenic peptide. Migration of protein standards (lane 1) is indicated by arrows.

preabsorption of the anti-Kir2.2 antibody with 10 μg/ml Kir2.2 C-terminal antigenic peptide (Figure 4-14, lanes 3 and 5).

4.8 Summary

Immunohistochemistry on rat brain tissue sections has co-localised Kir2.2 and NK-1 receptor protein expression to single locus coeruleus neurons and associated oligodendroglia. In addition, Kir2.0 proteins, particularly Kir2.2, have been localised to the nuclei of cells in tissue sections and cell culture. Finally, Kir2.0 protein expression was demonstrated in neurons, vascular smooth muscle, capillary endothelia, macroglia and IVth and lateral ventricle ependyma.

Chapter 5: Kir2.2 Protein as a Substrate for Protein Kinase-Mediated Phosphorylation

The co-localisation of the Kir2.2 ion channel isoform with the NK-1 receptor in single locus coeruleus noradrenergic neurons raised the need to explore a further question; that of a functional link between the two proteins. Although there was indirect electrophysiological evidence from the nucleus basilis of Meynert, implicating a PKC-mediated phosphorylation of an unidentified Kir isoform in response to binding of substance P (SP) to the NK-1 receptor (Takano *et al.,* 1995), no direct evidence has yet linked NK-1 receptor activity to suppression of a specific Kir2.0 isoform.

5.1.1 *In Vitro* Phosphorylation of Unlabelled *In Vitro* Translated Kir2.2 Protein by PKA and PKC

This experiment was carried out in order to demonstrate Kir2.2 protein as a PKA/PKC substrate for *in vitro* phosphorylation with [γ^{32}P]-ATP.

In vitro phosphorylation with PKA or PKC isoforms and unradiolabelled *in vitro* translated Kir2.2 with [γ^{32}P]-ATP (Materials and Methods section 2.16.1), resulted in the production of a radiolabelled Kir2.2 protein of a molecular weight slightly higher than the unphosphorylated negative control (Figure 5-1).

In vitro translated Kir2.2 protein was made, incorporating unlabelled methionine (Materials and Methods section 2.9). In addition 10 nM okadaic acid, a protein phosphatase 1 and 2A inhibitor, was added into each *in vitro*

translated reaction to block any phosphatase activity in the transcription/translation system. Unlabelled Kir2.2 protein was phosphorylated by PKA, a mixture of isoforms of PKC other than PKCγ and PKCγ alone in the presence of [γ^{32}P]-ATP. In order to inhibit the activity of the protein kinases, the following inhibitors were used: 100 nM staurosporine in the PKC reactions and 20 μg protein kinase A inhibitor in the PKA reactions. Inhibitors were not administered to negative control reactions lacking protein kinases, thus enabling an assessment of the endogenous protein kinase activity in the *in vitro* translation reactions to be made. The total phosphorylation reactions were denatured and electrophoresed in an 8% polyacrylamide gel and the distribution of radioactivity analysed by autoradiography.

A 40 kDa band was observed in the phosphorylation reactions containing unlabelled Kir2.2 protein and [γ^{32}P]-ATP. This was strongest in the PKA reaction (Figure 5-1, lane 1), but also present in the PKC multi-isoform reaction (Figure 5-1, lane 3). It was also present but weaker in the PKCγ isoform reaction (Figure 5-1, lane 2) and absent in the negative control reaction lacking protein kinases (Figure 5-1, lane 4). These results indicated that a polypeptide of the molecular weight of Kir2.2 could be phosphorylated *in vitro* by PKA and PKC isoforms. In addition, the presence of [γ^{32}P]-ATP in the negative control reaction lacking protein kinases indicated that no significant kinase was present in the *in vitro* translation reaction and that the [γ^{32}P]-ATP was not simply binding to the Kir2.2 protein.

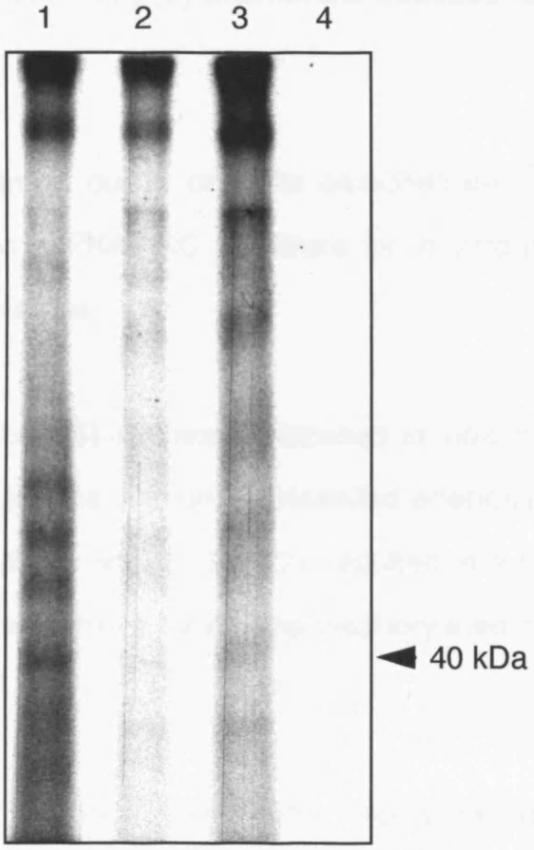

Figure 5-1. *In vitro* phosphorylation of unlabelled *in vitro* translated Kir2.2 protein with [γ^{32}P]-ATP. Lane 1, PKA. Lane 2, PKCγ. Lane 3, other isoforms of PKC. Lane 4, kinase-free negative control. A 40 kDa, potentially Kir2.2 phosphorylated band was detected in lanes 1-3.

5.1.2 *In Vitro* Phosphorylation of [^{35}S]-Methionine-Labelled Kir2.2 Protein by PKA and PKC

This experiment was carried out in order to demonstrate [^{35}S]-Methionine-labelled Kir2.2 protein as a PKA/PKC substrate for *in vitro* phosphorylation with ATP by band-shift analysis.

In vitro phosphorylation of [^{35}S]-Methionine-labelled *in vitro* translated Kir2.2 protein by PKA or PKC isoforms with unradiolabelled adenosine triphosphate (ATP) (Materials and Methods section 2.16.2), resulted in a slight band-shift with lower mobility in comparison to an unphosphorylated negative control (Figure 5-2).

In vitro translated Kir2.2 protein was made, incorporating [^{35}S]-labelled-methionine (Materials and Methods section 2.9). In addition 10 nM okadaic acid, a protein phosphatase 1 and 2A inhibitor, was added into each *in vitro* translated reaction to block any phosphatase activity in the transcription/translation system.

[^{35}S]-Methionine-labelled Kir2.2 protein was phosphorylated by PKA, a mixture of isoforms of PKC other than PKCγ and PKCγ alone with unlabelled ATP. After the phosphorylation reactions were completed, inhibitors were added and the reactions electrophoresed as described in section 5.1.1.

Bands of 42 kDa were observed on analysis of the phosphorylation reactions containing [^{35}S]-Methionine-labelled Kir2.2 protein and unlabelled ATP (Figure 5-2, lane 1 (PKA), lane 2 (PKCγ), lane 3 (PKC multi-isoforms)). All

three phosphorylation reactions appeared to produce a shift in the electrophoretic mobility of the Kir2.2 protein, when compared with the unphosphorylated (no enzyme) negative control, which yielded a 38 kDa band (Figure 5-2, lane 4), indicating a 4 kDa band-shift between phosphorylated and unphosphorylated proteins. Although these experiments (*in vitro* phosphorylation of unlabelled (section 5.1.1) and [^{35}S]-labelled (section 5.1.2) Kir2.2 protein) indicated that Kir2.2 protein could be phosphorylated *in vitro*, there can be no guarantee that a similar reaction could be repeated *in vivo* under physiological conditions. Therefore, *in vivo* phosphorylation of Kir2.2 channel protein was investigated.

5.2 *In Vivo* Phosphorylation State of Kir2.2 in the SN56 Cholinergic Neuronal Cell Line

In order to be able to study the biochemical events associated with the possible suppression of Kir2.0 activity *in vivo*, it was necessary to characterise a cell line in which receptor-induced channel suppression might be achieved or mimicked in transfected cells. The SN56 mouse cholinergic neuronal cell line (Hammond *et al.,* 1986 and Lee *et al.,* 1990) was investigated as a possible example of a immortal 'native' cell-type as it was analogous to the rat nucleus basalis of Meynert in which suppression of an unidentified Kir by SP had been demonstrated (Stanfield *et al.,* 1985). Therefore, investigations were carried out to assess whether the ion channel and cognate receptor were expressed in this cell line. Immunocytochemistry and Western blotting were carried out to provide evidence for Kir2.0 isoform and NK-1 receptor protein co-expression. Once co-expression had been confirmed, a series of single experiments were conducted to investigate the

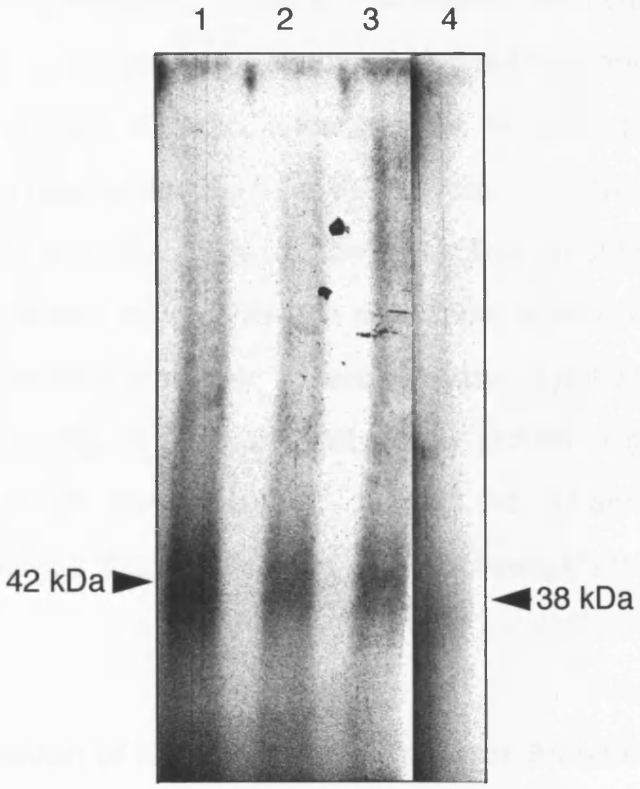

Figure 5-2. *In vitro* phosphorylation of [^{35}S]-Methionine-labelled Kir2.2 protein with unlabelled ATP. Lane 1, PKA. Lane 2, PKCγ. Lane 3, other isoforms of PKC. Lane 4, kinase-free negative control. A 4 kDa band shift was observed between phosphorylated and unphosphorylated Kir2.2 species.

possibility of a signalling link between the receptor and channel proteins by investigation of Kir2.2 protein phosphorylation/dephosphorylation events in response to treatment of cell cultures with SP. Recently published findings indicated that phosphorylation of the Kir2.1 isoform on tyrosine residue 242 (phosphorylation site: Glu-Tyr-Ile), following application of nerve growth factor to cells, was sufficient for suppression of channel activity (Wischmeyer *et al.*, 1998). Kir2.2 contains a similar potential phosphorylation site on tyrosine residue 243, making, it possible that Kir2.2 protein might also undergo phosphorylation at this residue, leading to channel suppression. Experiments using a Kir2.2 (Y243F) mutant to investigate this possibility were also initiated.

5.2.1 Determination of Kir2.2 and NK-1 Receptor Protein Co-expression in the SN56 Cholinergic Neuronal Cell Line by Immunocytochemistry

To investigate the presence of Kir isoforms and NK-1 receptor by immunocytochemistry, SN56 cells were cultured on laminin-coated glass cover slips until 70-80% confluent (Ms Penny Spencer, Hodgkin Building, University of Leicester) and then fixed in 1% paraformaldehyde/0.1 M cacodylate buffer. The cells were stained with anti-Kir2.2 (12 μg/ml), anti-Kir2.3 (13 μg/ml) or anti-NK-1 receptor (1:500) affinity purified antibodies. In addition, the cultures were counter-stained with a 1:200 dilution of phalloidin toxin conjugated Cy2 (green fluorescence), to stain the cytoskeleton of the cells and 5 μg/ml Hoechst 33342 nuclear stain. The channel and receptor primary antibodies were detected with goat anti-rabbit IgG Cy3 conjugate (red fluorescence) (Materials and Methods section 2.13).

Fixation with 1% paraformaldehyde/0.1 M cacodylate buffer preserved the neuronal morphology of the SN56 cells (Figure 5-3). This was important to permit future studies involving the differential distribution of ion channel proteins in neural processes. Kir2.2 protein expression was exclusively nuclear (red fluorescence) and overlapped the Hoechst 33342 nuclear stain, whilst the phalloidin toxin (green fluorescence) stained the actin cytoskeleton on the interior of the plasma membrane and neural processes (Figure 5-3a, Kir2.2 and actin; Figure 5-3b, Hoechst 33342 nuclear stain). No evidence of Kir2.3 protein expression above background levels of fluorescence could be detected: however, the anti-actin and nuclear counter-staining was successful as above (Figure 5-3c, actin; Figure 5-3d, Hoechst 33342 nuclear stain). NK-1 receptor protein was found in punctate vesicles in the cytoplasm, as well as on the plasma membrane (red fluorescence), possibly indicating *de novo* synthesis or receptor stimulation leading to receptor-ligand internalisation and deactivation (Abbadie *et al.,* 1997, McConalogue *et al.,* 1998 and Barak *et al.,* 1999); (Figure 5-3e, NK-1 receptor and actin). Counter-staining was again performed as previously described (data not shown). Negative controls lacked either primary channel or receptor antibodies (Figure 5-3f) or both primary and secondary goat anti-rabbit IgG Cy3 conjugated (red fluorescence) antibodies (Figure 5-3g). Both of these controls contained very low levels of non-specific fluorescence.

These results confirmed that both Kir2.2 channel and NK-1 receptor proteins were expressed in the differentiated SN56 neuronal cell line. In addition, Kir2.2 protein was located largely in the nucleus, supporting previous localisation results in transiently transfected CHO cells (Figure 4-12) and immunohistochemistry on tissue sections (Figure 4-3). Optical sections

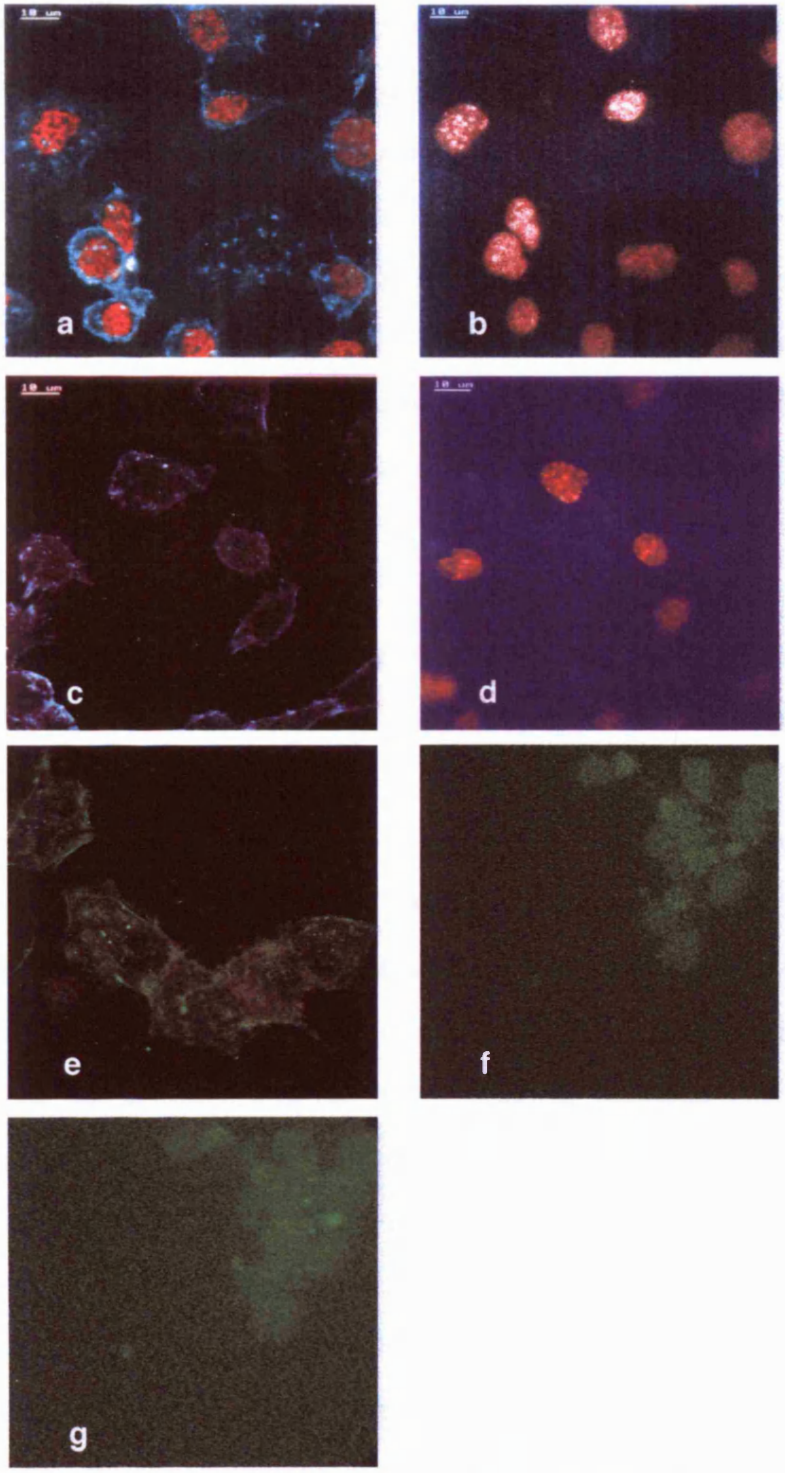

Figure 5-3. Immunocytochemistry in SN56 cells. (a), Kir2.2 (red) nuclear and actin (green) cytoskeletal staining. (b), Co-localised nuclear stain (red) with Hoechst 33342. (c), Actin (green) cytoskeletal staining, no evidence of Kir2.3 staining. (d), Hoechst 33342 co-localised (with (c)) red nuclear stain. (e), Punctate NK-1 receptor (red) and actin (green) cytoskeletal staining. (f), Detection with secondary antibody only and (g), detection in the absence of primary and secondary antibodies revealed extremely low levels of non-specific staining.

through the body of the nucleus confirmed that the Kir2.2 fluorescence was present throughout the nucleus, rather than being present only on the nuclear membrane. Finally, protein expression was found in all cells within each culture, when stained with either the anti-Kir2.2 or anti-NK-1 receptor antibody. This indicated expression of these proteins was universal within the SN56 cell line population and that, at least for these two proteins no subsets of cells existed with different expression patterns. This experiment was carried out jointly with Ms Penny Spencer, Hodgkin Building, University of Leicester.

5.2.2 Confirmation of Kir2.2 and NK-1 Receptor Protein Co-expression in the SN56 Cholinergic Neuronal Cell Line by Western Blotting

Further to the immunocytochemical investigation of NK-1 receptor and Kir2.0 expression in the SN56 cell line, Western blotting was carried out in order to confirm the earlier results and obtain a quantitative estimate of the relative abundance of the proteins. A single large flask of SN56 cells (25 ml) was grown to 80% confluence by Ms Penny Spencer, Hodgkin Building, University of Leicester. The cells were transferred to a sterile 50 ml tube and centrifuged at 750 g for 2 minutes at 37^{o}C. The supernatant was decanted and the cell pellet frozen by immersion in iso-pentane, chilled by cardice and stored at -80^{o}C. The pellet was defrosted and immediately resuspended in 1.5% SDS without protease inhibitors. An estimation of protein concentration was made using a ratiometric method of the readings of absorbance at 260 nm and 280 nm. An estimated 36 μg of protein per lane was subjected to electrophoresis in an 8% polyacrylamide gel. Gel electrophoresis and Western blotting were carried out as described in the Materials and Methods

section 2.11. Primary antibody detection used 9.3 μg/ml anti-Kir2.1 antibody, 8.6 μg/ml anti-Kir2.2 antibody, 8.4 μg/ml anti-Kir2.3 antibody, 1:500 dilution of anti-NK-1 receptor antibody and 1 μg/ml MCTrks mouse monoclonal antibody against nerve growth factor (NGFR) as a positive control (Santa Cruz catalogue number: SC-414). Antigenic peptide blocking reactions were carried out for each of the anti-Kir2.0 antibodies by preabsorption of the antibody with 10 μg/ml of the specific antigenic peptide. Secondary detection of the MCTrks antibody required the use of rabbit anti-mouse antibody (whole antibody) conjugated to alkaline phosphatase at a dilution of 1:1000.

The anti-Kir2.1 antibody failed to detect the presence of Kir2.1 protein in SN56 cells (Figure 5-4, lane 1). The Kir2.2 antibody detected a strongly stained 62 kDa polypeptide and several smaller, weaker bands which were likely to have been proteolytic cleavage products (Figure 5-4, lane 3). The weaker bands were abolished by the antigenic peptide block, and only a very weak staining of the polypeptide of 62 kDa was retained (Figure 5-4, lane 4). Anti-Kir2.3 antibody detected a weak band at 52 kDa, similar to the 49 kDa theoretical size of the Kir2.3 protein. This was the first time that Kir2.3 protein had been Western blotted successfully (Figure 5-4, lane 5). The 52 kDa band was completely abolished by preabsorption of the antibody with antigenic peptide (Figure 5-4, lane 6). The anti-NK-1 receptor antibody detected a 93 kDa polypeptide, which was within the published 70-150 kDa range obtained by Western blotting using the anti-NK-1 receptor antisera (Vigna *et al.,* 1994) (Figure 5-4, lane 7). The NGFR antibody detected a number of polypeptides, the strongest of which was at 54 kDa (Figure 5-4, lane 8). However, there were also fainter bands representing polypeptides at higher and lower molecular weights. The theoretical molecular weight for NGFR (*trk*A) was 140

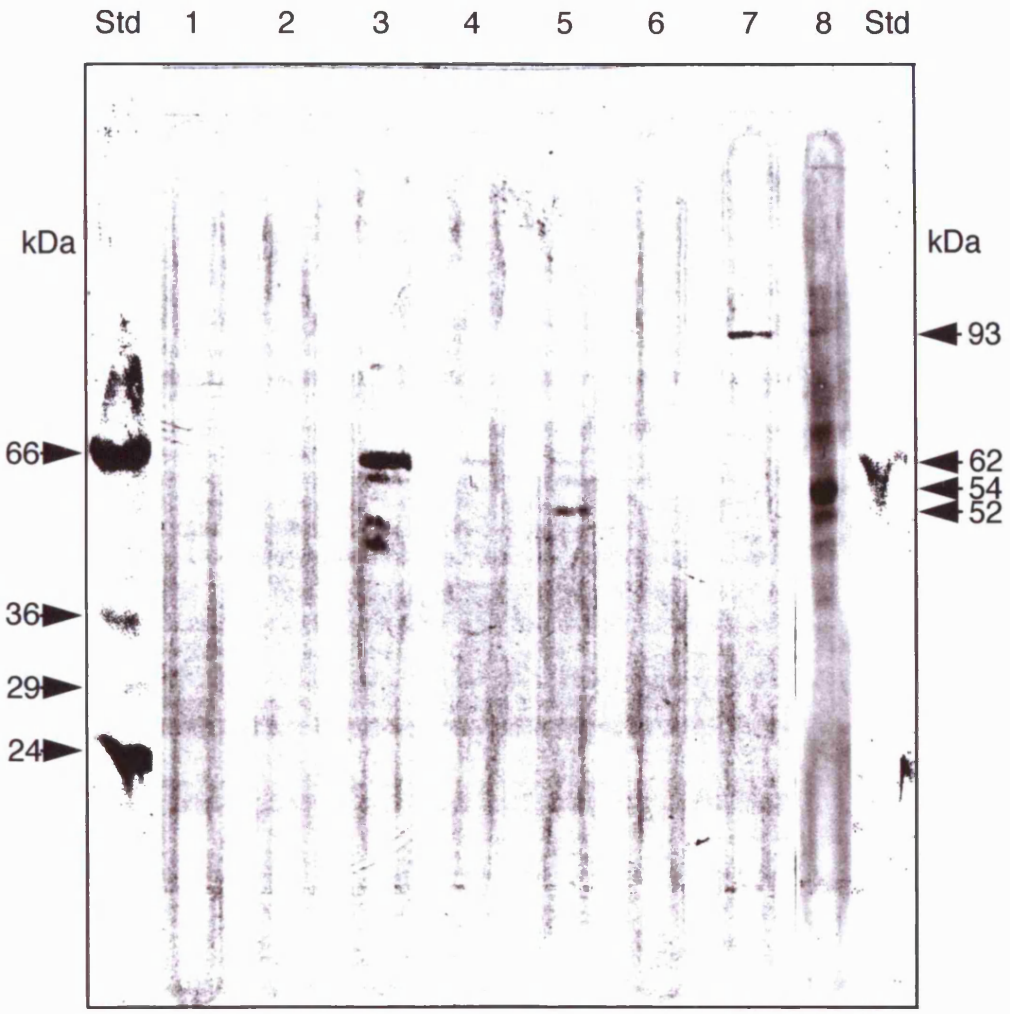

Figure 5-4. Western blotting of SN56 cell lysates. Lane 1, anti-Kir2.1 antibody. Lane 2, anti-Kir2.1 antibody with antigenic peptide. Lane 3, anti-Kir2.2 antibody. Lane 4, anti-Kir2.2 antibody with antigenic peptide. Lane 5, anti-Kir2.3 antibody. Lane 6, anti-Kir2.3 antibody with antigenic peptide. Lane 7, anti-NK-1 receptor antibody. Lane 8, anti-NGF receptor antibody. Kir2.2 protein was strongly expressed, with a major band detected at 62 kDa (lane 3). Incubation of anti-Kir2.2 antibody with antigenic peptide resulted in inhibition of the 62 kDa band staining (lane 4). Kir2.3 protein was weakly expressed as a 52 kDa band (lane 5). The 52 kDa band was abolished by incubation of anti-Kir2.3 antibody with antigenic peptide (lane 6). The anti-NK-1 receptor antibody detected a 93 kDa band (lane 7). The positive control NGF receptor antibody detected a number of bands, the major one being 54 kDa (lane 8).

kDa (Martin-Zanca *et al.,* 1989), and the largest observed band in this Western blot was at 125 kDa. The NGFR is apparently highly susceptible to proteolytic cleavage and this may be the reason for the smaller than anticipated molecular weight of the major polypeptide (personal communication from Dr Martin Dickens of the Biochemistry Department, University of Leicester).

These results confirmed, by an alternative method to immunocytochemistry, that the Kir2.2 and NK-1 receptor proteins were expressed in the SN56 neuronal cell line. In addition, no evidence of Kir2.1 protein expression was observed and weak expression of Kir2.3 was confirmed. Protease inhibitors were used in analyses of all subsequent SN56 cell preparations, as results for the NGFR detection suggested that 1.5% SDS was insufficient to denature all endogenous proteases.

5.2.3 Experiments to Investigate Tyrosine Residue Phosphorylation in Kir2.2 Channels in Response to Treatment of SN56 Cells with SP

As the SN56 cell line expressed both Kir2.2 channel and NK-1 receptor proteins, it was considered to be an appropriate *in vivo* system in which to assess the tyrosine phosphorylation of Kir2.2 channel, after treatment with SP. Therefore, experiments were designed and carried out in which cell cultures were treated with SP, lysed and immunoprecipitated by anti-Kir2.2 antibody, then Western blotted and probed with PY99 anti-phosphotyrosine antibody. These experiments consistently produced an 80 kDa tyrosine phosphorylated polypeptide band, which was not observed in lysates from untreated cell cultures (data not shown). The 80 kDa polypeptide, potentially

a tyrosine phosphorylated Kir2.2 species, was further investigated by repeating the previously described experiment, with the inclusion of 10 μg/ml, 50 μg/ml or 100 μg/ml Kir2.2 antigenic peptide in the immunoprecipitation step. Western blotting with detection by PY99 anti-phosphotyrosine antibody indicated that the 80 kDa polypeptide was not blocked by the addition of Kir2.2 antigenic peptide up to a concentration of 100 μg/ml (data not shown). As a result of these data, it is unlikely that the 80 kDa tyrosine phosphorylated polypeptide was Kir2.2 or an associated co-immunoprecipitating species. It is possible that activation of the NK-1 receptor by binding of SP leads to activation of tyrosine kinases and phosphorylation of channel specific tyrosine residues (Wischmeyer *et al.,* 1998), and to the activation of a PKC isoform (Takano *et al.,* 1995). Phosphorylation by PKC may occur on a C-terminal phosphorylation site (residues: 423-425, Arg-Glu-Ser) resulting in disruption of antibody binding, preventing immunoprecipitation. This possibility was investigated in section 5.5, and if confirmed would indicate that the 80 kDa tyrosine phosphorylated polypeptide detected in these experiments was artifactual due to non-specific adsorption to immunomatrices during immunoprecipitation.

5.3 Mutagenesis of Kir2.2 to Produce a Y243F Mutant

Karschin and colleagues found that Kir2.1 protein activity could be suppressed by administration of NGF to COS7 cells after co-transfection of Kir2.1 and NGFR cDNAs (Wischmeyer *et al.,* 1998). Mutation of a consensus tyrosine phosphorylation site (tyrosine: 242) to phenylalanine in Kir2.1 resulted in the abolition of channel suppression in response to administration of NGF, suggesting that Kir2.1 protein was phosphorylated at

tyrosine residue 242, leading to channel suppression (Wischmeyer *et al.*, 1998). The corresponding tyrosine consensus phosphorylation site in Kir2.2 (tyrosine: 243) was eliminated by mutating the tyrosine codon to a phenylalanine codon using the Stratagene QuikChange system (Materials and Methods section 2.1.5). The mutant Kir2.2 protein was therefore unable to undergo tyrosine phosphorylation at residue 243 and was used to seek evidence that tyrosine 243 was the key target for channel phosphorylation after treatment with SP. The QuikChange strategy required mutagenic primers designed across the tyrosine residue (codon: TAC), replacing it with phenylalanine (codon: TTC). PCR with *Pfu* proof-reading polymerase was then used to amplify the whole cDNA (Kir2.2 assession number: X80417) and vector (pCDNA3). The methylated parental strand (containing the tyrosine codon) was then digested with *Dpn* I. PCR reactions were transformed using the chemical transformation protocol directly into *E. coli* DH5α (10^8 competent cells) as described in the Materials and Methods section 2.2. The results of the transformation are as follows:

	Kir2.2 mutagenesis	Mutagenesis positive control	Control transformation
White colonies	100	3	-
Blue colonies	-	50	250

Transformation efficiency: 2.8×10^7 colonies/μg DNA

DNA sequencing was carried out on six candidate colonies, using sequencing primers provided by Dr Ian Ashmole of the Cell Physiology and Pharmacology Department, University of Leicester. This confirmed that clones 2 and 4 contained the Y243F mutation. Further sequencing of the whole cDNA confirmed that there were no further mutations in the sequence except for the conservative mutation of phenylalanine 375 from codon: TTC into TTT. Clone 2 was selected and cultured in 100 ml of LB with 100 μg/ml ampicillin selection for 16 hours at 37°C. Plasmid DNA was prepared using the caesium chloride gradient equilibrium centrifugation protocol (Sambrook *et al.*, 1989).

The mutant and wild type Kir2.2 cDNAs were separately co-transfected into the COS7 cell line, each with the wild type human NK-1 receptor cDNA (accession number: M84425). Subsequent treatment with SP, followed by immunoprecipitation with anti-Kir2.2 antisera and Western blotting using anti-Kir2.2 and PY99 anti-phosphotyrosine antibodies indicated the following: 1). Kir2.2 protein was immunoprecipitated and detected on Western blots from transfected cell lysates: detection was blocked by preabsorption of the anti-Kir2.2 antibody with Kir2.2 antigenic peptide (data not shown). 2). There was no evidence for Kir2.2 tyrosine phosphorylation in response to SP treatment using the PY99 antibody to probe the blot (data not shown).

In a subsequent experiment, Western blot analysis of untransfected COS7 cell lysate with anti-Kir2.2 antibody indicated the unexpected presence of an endogenous Kir2.2 channel protein as a 62 kDa immunostaining polypeptide band (Figure 5-5, lane 1). This cell line is routinely used for transient transfection and electrophysiology because of its 'null' Kir background

(Wischmeyer *et al.,* 1998). These data implied that the Kir2.2 protein identified in COS7 cells was expressed at some site other than the plasma membrane, possibly the nucleus. Similar Western blot analysis of untransfected COS7 cell lysate with anti-NK-1 receptor antibody, indicated the absence of NK-1 receptor protein (Figure 5-5, lane 2). Western blotting of the Kir2.2 and NK-1 receptor co-transfected cell lysates with the anti-NK-1 receptor antibody did not detect any protein (Figure 5-5, lanes 3-6), suggesting that the NK-1 receptor cDNA transfection was unsuccessful.

Overall, this experiment was inconclusive due to unsuccessful co-transfections of Kir2.2 channel and NK-1 receptor cDNAs and the presence of an apparent endogenous Kir2.2 protein. Thus, the question of whether tyrosine phosphorylation could be prevented in the Kir2.2 (Y243F) mutant remained unresolved.

5.4 Immunocytochemical Demonstration of a Nuclear Localisation for Kir2.2 Protein Expressed in the COS7 Cell Line

Immunocytochemistry was carried out on COS7 cells in order to characterise the subcellular localisation of Kir2.2 protein. COS7 cells were cultured on glass cover slips until 90% confluent (Dr Caroline Dart of the Cell Physiology and Pharmacology Department, University of Leicester) and then fixed in 1% paraformaldehyde/0.1 M cacodylate buffer. The cells were stained with anti-Kir2.2 antibody (12 μg/ml) and counter-stained with a 1:200 dilution of phalloidin toxin conjugated Cy2 (green fluorescence), to stain cellular actin and 5 μg/ml Hoechst 33342 nuclear stain. The primary anti-channel antibody

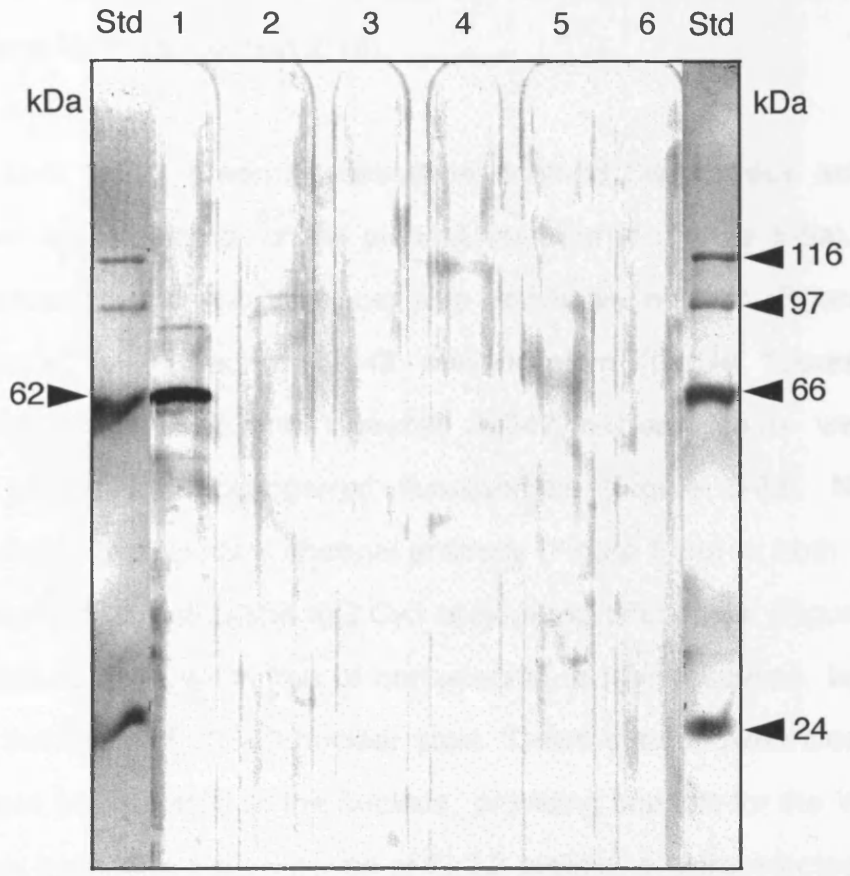

Figure 5-5. Western blotting of untransfected and NK-1 receptor transfected COS7 cell lysates. Lane 1, anti-Kir2.2 antibody. Lanes 2-6, anti-NK-1 receptor antibody. Untransfected cell lysates were Western blotted and probed with anti-Kir2.2 antibody, detecting a 62 kDa band (lane 1). Similarly, probing untransfected cell lysates with anti-NK-1 receptor antibody failed to detect endogenous protein (lane 2). Western blotting of COS7 cell lysates after transfection with NK-1 receptor cDNA failed to detect NK-1 receptor protein expression, suggesting that the transfection was unsuccessful (lanes 3-6).

was detected with goat anti-rabbit IgG Cy3 conjugate (red fluorescence) (Materials and Methods section 2.13).

Phalloidin toxin (weak green fluorescence) stained the nucleus and actin cytoskeleton on the interior of the plasma membrane (Figure 5-6a). Kir2.2 protein expression (red fluorescence) was exclusively nuclear (Figure 5-6b) and overlapped the Hoechst 33342 nuclear stain (purple fluorescence, Figure 5-6c). The Kir2.2 and Hoechst 33342 nuclear stains were co-localised, producing a orange/red fluorescence (Figure 5-6d). Negative controls lacked either primary channel antibody (Figure 5-6e) or both primary and secondary goat anti-rabbit IgG Cy3 conjugated antibodies (Figure 5-6f). Both of these controls were free of non-specific red fluorescence, but were stained by the Hoechst 33342 nuclear stain. These data showed clearly that Kir2.2 protein was located in the nucleus, providing support for the Western blot analysis indicating the presence of Kir2.2 protein in untransfected COS7 cells (section 5.3).

5.5 Immunoprecipitation of *In Vitro* Phosphorylated Kir2.2 Protein by Kir2.2 Antibody

An experiment was undertaken to assess the ability of Kir2.2 antibody to immunoprecipitate Kir2.2 protein following *in vitro* phosphorylation by PKA and PKC isoforms. The literature indicated that both PKC and tyrosine kinases were potentially involved in phosphorylation of Kir2.0, contributing to channel suppression (Takano *et al.*, 1995 and Wischmeyer *et al.*, 1998). Phosphorylation on tyrosine and serine/threonine channel residues may result in protein conformational changes in such a way that the C-terminal

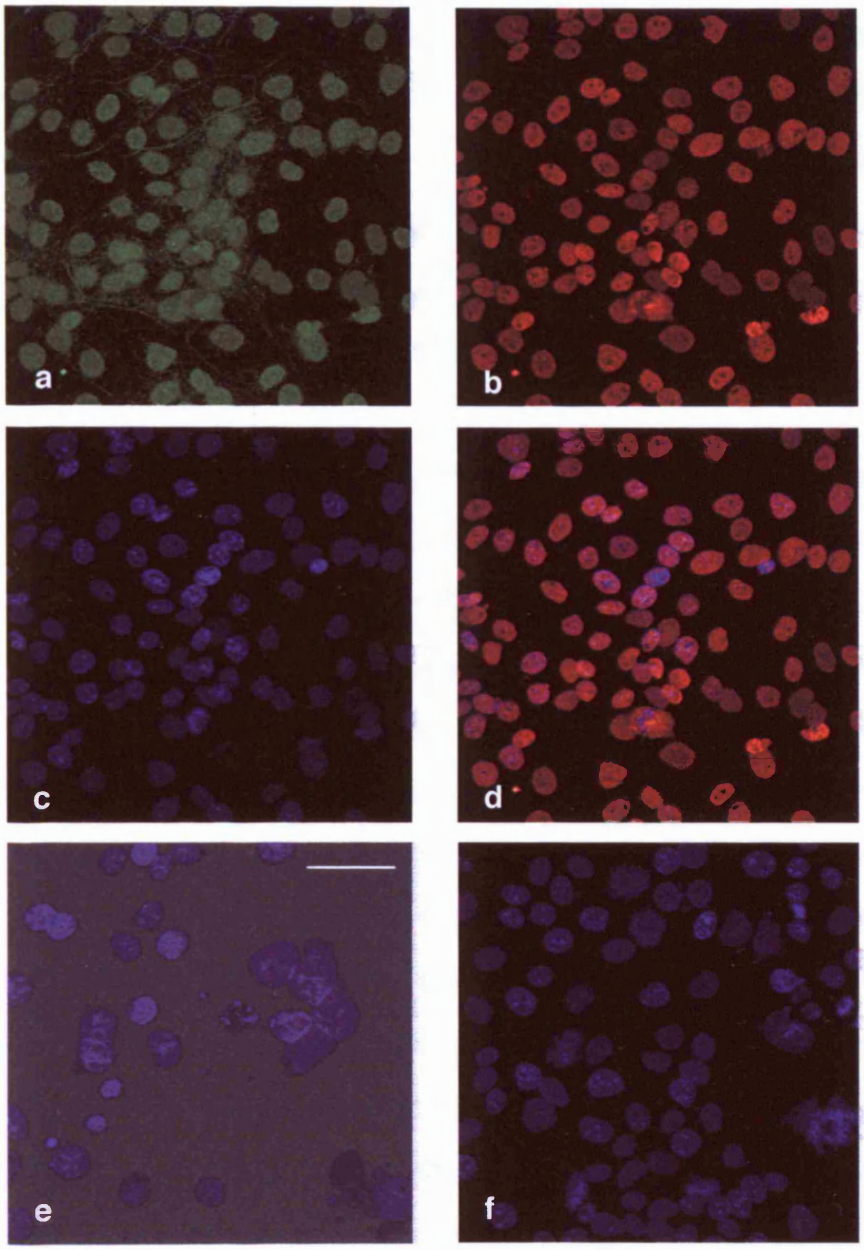

Figure 5-6. Immunocytochemistry in COS7 cells. (a), Nuclear and cytoskeletal anti-actin staining (green). (b), Kir2.2 nuclear stain (red). (c), Hoechst 33342 nuclear stain (purple). (d), Co-localised Kir2.2 and Hoechst 33342 nuclear stains (orange/red). (e), Hoechst 33342 nuclear staining in the absence of primary Kir2.2 antibody (purple). (f), Hoechst 33342 nuclear staining in the absence of primary Kir2.2 and secondary antibodies (purple). Scale bar represents 20 μm.

epitope is not available for antibody binding. In addition to a consensus tyrosine phosphorylation site (Residues: 241-243, Glu-Tyr-Ile), Kir2.2 also contains five consensus PKA/PKC (Arg-Arg-x-Ser/Thr) phosphorylation sites (Residues: 219-221, Arg-Lys-Ser. Residues: 236-238, Arg-Val-Thr. Residues: 313-315, Arg-Ser-Ser. Residues: 356-358, Arg-Cys-Ser. Residues: 423-425, Arg-Glu-Ser (on C-terminal epitope)).

In order to test the effects of serine/threonine phosphorylation on antibody-recognition, *in vitro* translated [^{35}S]-Methionine-labelled Kir2.2 protein was prepared and phosphorylated *in vitro* using PKA, PKCγ and PKC (all other isoforms) in the presence of unlabelled ATP (Materials and Methods section 2.16.2). Aliquots of phosphorylated protein were immunoprecipitated with anti-Kir2.2 antibody and samples were electrophoresed on an 8% polyacrylamide gel (Materials and Methods section 2.10). The results of this experiment indicated that the *in vitro* translation reaction was successful yielding a 43 kDa, Kir2.2 protein band (Figure 5-7, lane 2). The *in vitro* translated negative control, containing no DNA template did not produce any bands (Figure 5-7, lane 1). Phosphorylated (but not immunoprecipitated) Kir2.2 protein produced bands with slightly reduced mobility in the 8% polyacrylamide gel with apparent molecular weights of 44 kDa-45 kDa when phosphorylated by PKA, PKCγ and a mixture of other PKC isoforms. The slight change in electrophoretic mobility of the phosphorylation suggested that the Kir2.2 polypeptide may have been subject to phosphorylation under each condition (Figure 5-7, lanes 3, 4 and 5).

Similar phosphorylated protein preparations were immunoprecipitated with anti-Kir2.2 antibody but resulted in no visible bands after electrophoresis and

autoradiography, suggesting that proteins phosphorylated *in vitro* by PKA and PKC could not be immunoprecipitated by the anti-Kir2.2 antibody (Figure 5-7, lanes 6, 7 and 8). The kinase-free, phosphorylation negative control was also immunoprecipitated with anti-Kir2.2 antibody and produced a band of 43 kDa, showing that unphosphorylated protein could be immunoprecipitated (Figure 5-7, lane 9). Finally, immunoprecipitation of the Kir2.2 protein in the absence of anti-Kir2.2 antibody failed to produce a band, indicating that non-specific binding did not occur between the protein A Sepharose CL-4B and the Kir2.2 protein (Figure 5-7, lane 10).

These results indicated that Kir2.2 channel protein serine/threonine can not be immunoprecipitated by the anti-Kir2.2 antibody following serine/threonine phosphorylation, suggesting either steric hindrance of antibody binding or a conformational change in the epitope sequence in response to protein phosphorylation. This result may explain why phosphorylated Kir2.2 species were not observed in earlier *in vivo* phosphorylation experiments and further indicates that the 80 kDa tyrosine phosphorylated protein seen in SN56 cells after treatment with SP was an experimental artifact (section 5.2.3).

5.6 Western Blotting of SN56 Cell Protein after Substance P Treatment

To investigate SP-induced tyrosine phosphorylation of Kir2.2 protein in SN56 cells and to take account that the current anti-Kir2.2 antibody was unable to immunoprecipitate Kir2.2 protein the following experiment, omitting immunoprecipitation, was designed. Three large flasks (25 ml) of SN56 cells, cultured to approximately 70% confluence were grown by Ms Penny Spencer, Hodgkin Building, University of Leicester. Flasks 1 and 2 were

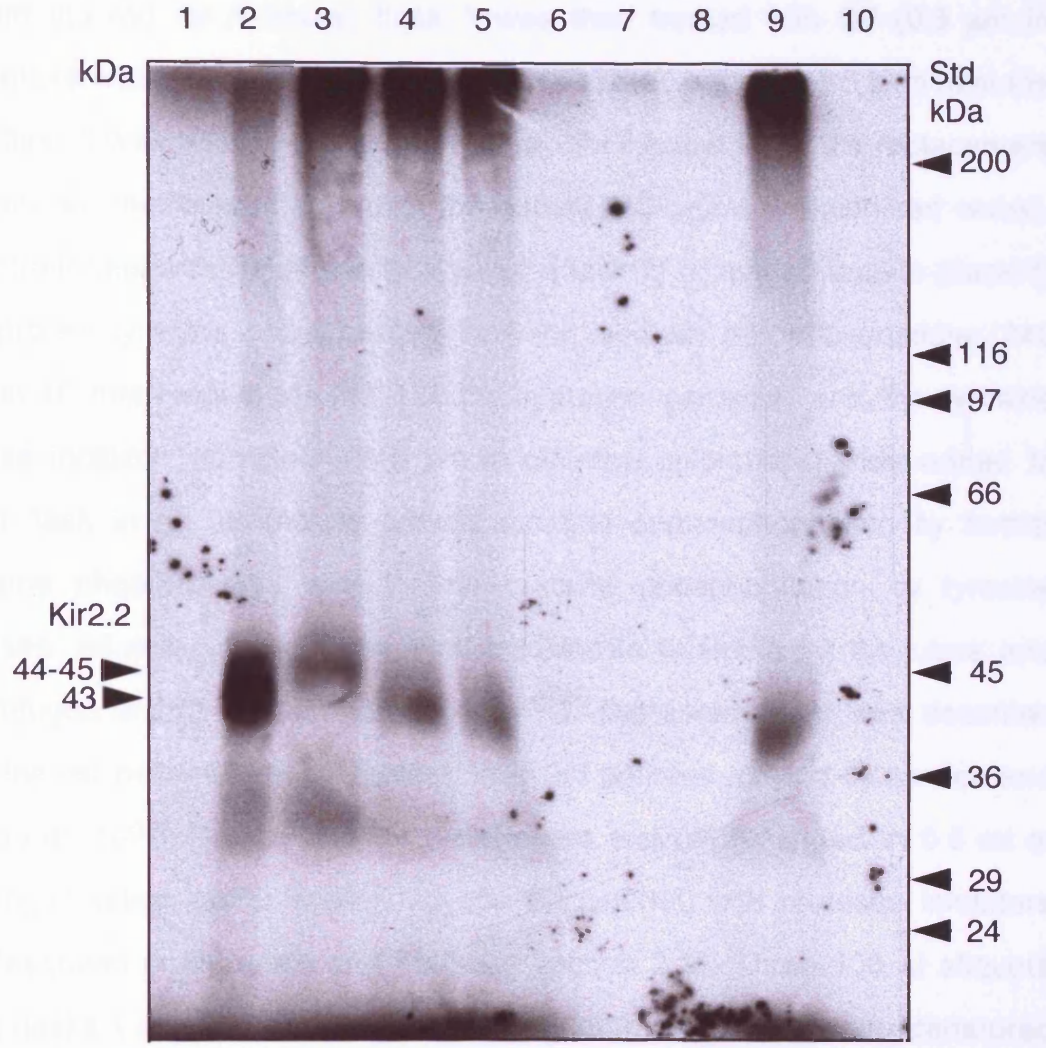

Figure 5-7. Autoradiography of an 8% polyacrylamide gel analysis of phosphorylated PKA/PKC [^{35}S]-Methionine-labelled *in vitro* translated Kir2.2 protein, either with or without immunoprecipitation by anti-Kir2.2 antibody. Lane 1, *in vitro* translation negative control. Lane 2, *in vitro* translated Kir2.2 protein (43 kDa). *In vitro* translated Kir2.2 protein (44-45 kDa) phosphorylated *in vitro* by PKA (lane 3), PKCγ (lane 4) and a mixture of other isoforms of PKC (lane 5) . *In vitro* translated Kir2.2 protein phosphorylated *in vitro* by PKA and immunoprecipitated by anti-Kir2.2 antibody (lane 6), phosphorylated by PKCγ and immunoprecipitated by anti-Kir2.2 antibody (lane 7) and phosphorylated by a mixture of other isoforms of PKC and immunoprecipitated by anti-Kir2.2 antibody (lane 8). Lane 9, *in vitro* translated Kir2.2 kinase-free negative control after immunoprecipitation (43 kDa). Lane 10, Kir2.2 protein immunoprecipitation negative control, lacking anti-Kir2.2 antibody.

serum starved for 4 hours; flask 1 was then treated with SP (0.3 μm in deionised water) for 5 minutes; flask 2 was treated with 1 x PBS for 5 minutes and flask 3 was treated with human insulin for 4 hours when the replacement serum-free media was added to the culture (10 μg/ml in deionised water). After treatment with SP (flask 1), 1 x PBS (flask 2) or human insulin (flask 3) the protein tyrosine phosphatase inhibitor, sodium perorthovanadate (240 μm in 40 mM Hepes pH 7.4/0.003% hydrogen peroxide) and the tyrosine kinase inhibitor, genistein (240 μm in dimethyl sulphoxide) were added to each flask in an attempt to prevent tyrosine dephosphorylation by further tyrosine phosphatases and further tyrosine phosphorylation by tyrosine kinases. All cell cultures were then transferred to sterile 50 ml tubes and centrifuged at 750 g for 2 minutes at 37°C. The supernatant was decanted and the cell pellet frozen by immersion in iso-pentane, chilled by cardice and stored at -80°C. Cell pellets were defrosted and resuspended in 0.5 ml of homogenisation buffer containing 1% Triton X-100 with protease inhibitors as described in Materials and Methods section 2.11. Three 100 μl aliquots from flasks 1 and 2, and a single 100 μl aliquot from flask 3 were denatured in denaturing buffer and electrophoresed in an 8% polyacrylamide gel, followed by Western blotting as described in Materials and Methods section 2.11 (Figure 5-8: flask 1, lanes 1, 3 and 5; Figure 5-8: flask 2, lanes 2, 4 and 6; Figure 5-8: flask 3, lane 7). The Western blot was probed with 8.6 μg/ml anti-Kir2.2 antibody, 8.6 μg/ml anti-Kir2.2 antibody with 10 μg/ml antigenic peptide or 0.2 μg/ml PY99 anti-phosphotyrosine antibody. Both SP treated (Figure 5-8, lane 1) and untreated cell (Figure 5-8, lane 2) preparations, when probed with anti-Kir2.2 antibody, yielded polypeptides of 62 kDa and 80 kDa. These polypeptides were blocked by incubation with the anti-Kir2.2 antibody with antigenic peptide (Figure 5-8, SP treated: lane 3 and SP untreated: lane

4). The PY99 antibody detected a number of high molecular weight polypeptides in the SP treated cell preparation (Figure 5-8, lane 5). Significantly, a 62 kDa polypeptide was clearly observed, potentially representing a tyrosine phosphorylated Kir2.2 species (Figure 5-8, lane 5). The band profile from untreated cells was very similar to the treated cells, with the exception that the 62 kDa polypeptide was not present in the untreated cell preparation (Figure 5-8, lane 6). Finally, an insulin treated cell lysate was probed with the PY99 antibody, again indicating a spread of tyrosine phosphorylated high molecular weight species, but lacking a 62 kDa polypeptide (Figure 5-8, lane 7). These data indicated that Kir2.2 is potentially phosphorylated by SP treatment of SN56 cells. However, the exact nature of the 62 kDa band detected by the PY99 antibody in this experiment is not clear and will require further investigation. The 80 kDa band detected by the anti-Kir2.2 antibody was not detected by the PY99 antibody and therefore can not be regarded as a tyrosine phosphorylated Kir2.2 species.

5.7 Assessment of the *In Vivo* Phosphorylation and Glycosylation States of the Kir2.2 Channel Protein in Rat Brain

The basal state of Kir2.2 *in vivo* phosphorylation was assessed in a band-shift experiment by the incubation of native rat brain membrane proteins with calf intestinal alkaline phosphatase (CIAP) (Figure 5-9). This together with attempts to deglycosylate the native rat brain protein with endoglycosidase F (Figure 5-9) resulted in the following observations: 1). Dephosphorylation of native protein resulted in no change in molecular weight of the Kir2.2 protein. This was taken tentatively to indicate that the basal condition of the Kir2.2 protein was unphosphorylated. 2). Deglycosylation of native protein similarly

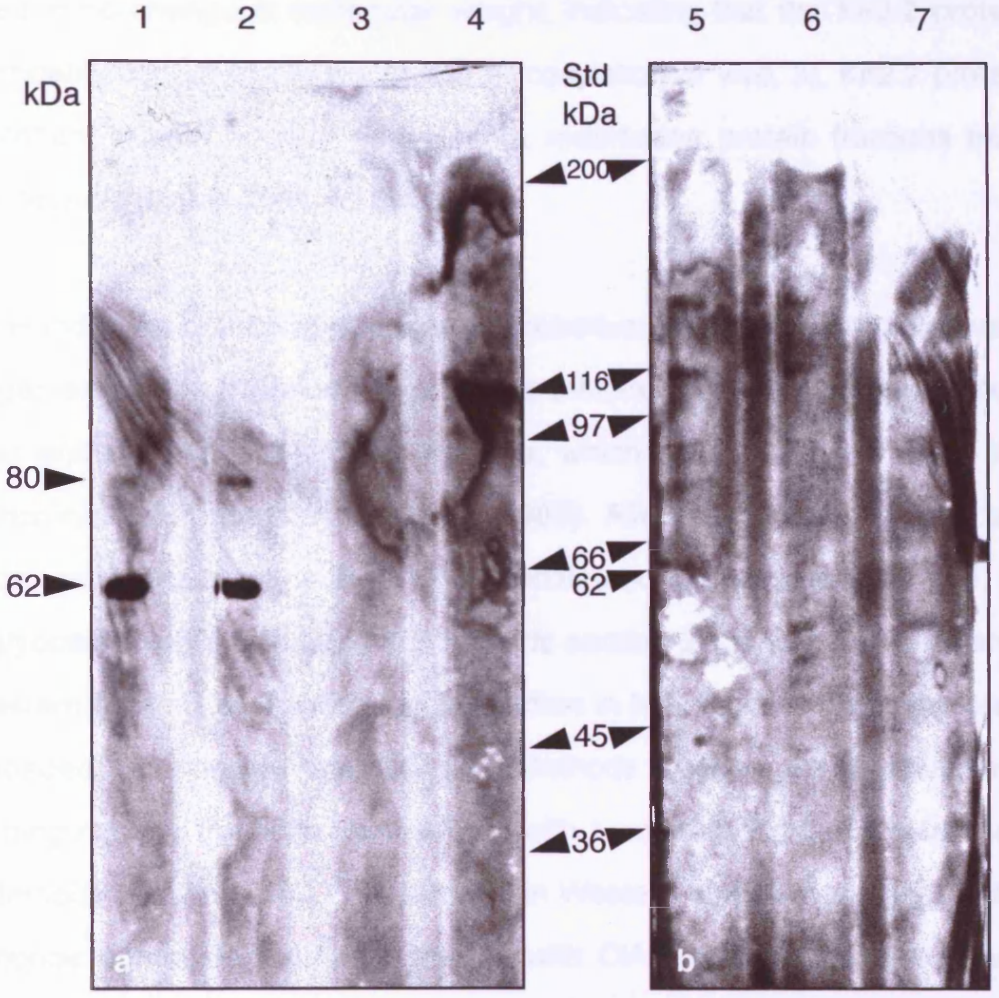

Figure 5-8. Western blotting of SN56 cell lysates, with and without earlier SP treatment. Lane 1, anti-Kir2.2 antibody (+SP). Lane 2, anti-Kir2.2 antibody (-SP). Lane 3, anti-Kir2.2 antibody with Kir2.2 antigenic peptide (+SP). Lane 4, anti-Kir2.2 antibody with Kir2.2 antigenic peptide (-SP). Lane 5, PY99 anti-phosphotyrosine antibody (+SP). Lane 6, PY99 anti-phosphotyrosine antibody (-SP). Lane 7, PY99 anti-phosphotyrosine antibody (+insulin). Both SP stimulated and unstimulated cell lysates produced Kir2.2 bands of 62 kDa and 80 kDa (lanes 1 and 2, respectively). A 62 kDa band was also detected from the SP stimulated cell lysate when probed with the PY99 anti-phosphotyrosine antibody (lane 5). This was not detected in unstimulated cells (lane 6).

resulted in no change in molecular weight, indicating that the Kir2.2 protein was probably not subject to significant glycosylation *in vivo*. 3). Kir2.2 protein was present in both nuclear and plasma membrane protein fractions from native rat brain tissue (data not shown).

Lister-Hooded rat brain hippocampus, cerebellum and medulla regions were homogenised in the presence of protease inhibitors and centrifuged to yield nuclear and plasma membrane fractions, which were quantified using the bicinchoninic acid assay (Smith *et al.,* 1985). Aliquots (2 mg of protein per reaction) were incubated with CIAP (Materials and Methods section 2.14) or endoglycosidase F (Materials and Methods section 2.15) and then prepared for Western blotting by splitting each reaction in half, so that 1 mg of protein was loaded per lane (Materials and Methods section 2.11). Reactions containing nuclear fractions were treated with 1 x denaturing buffer (Materials and Methods section 2.10). This resulted in Western blots containing 62 kDa polypeptide bands, for samples treated with CIAP, endoglycosidase F and untreated negative controls when probed with 8.6 μg/ml of anti-Kir2.2 affinity purified antibody (Figure 5-9, lanes 1, 3, 5 and 7). Detection of the 62 kDa polypeptides was blocked by preabsorption of 8.6 μg/ml of anti-Kir2.2 affinity purified antibody with 10 μg/ml Kir2.2 antigenic peptide (Figure 5-9, lanes 2, 4, 6 and 8). This experiment was repeated with 0.5 x denaturing buffer with native rat brain plasma membrane and nuclear fraction proteins. Western blots were probed with 8.6 μg/ml of anti-Kir2.2 affinity purified antibody, detecting a 120 kDa polypeptide band (data not shown). Incubation of the Western blot with 8.6 μg/ml anti-Kir2.2 affinity purified antibody and 10 μg/ml Kir2.2 antigenic peptide, prevented detection of the 120 kDa polypeptide band (data not shown). The apparent dimerisation observed from native protein

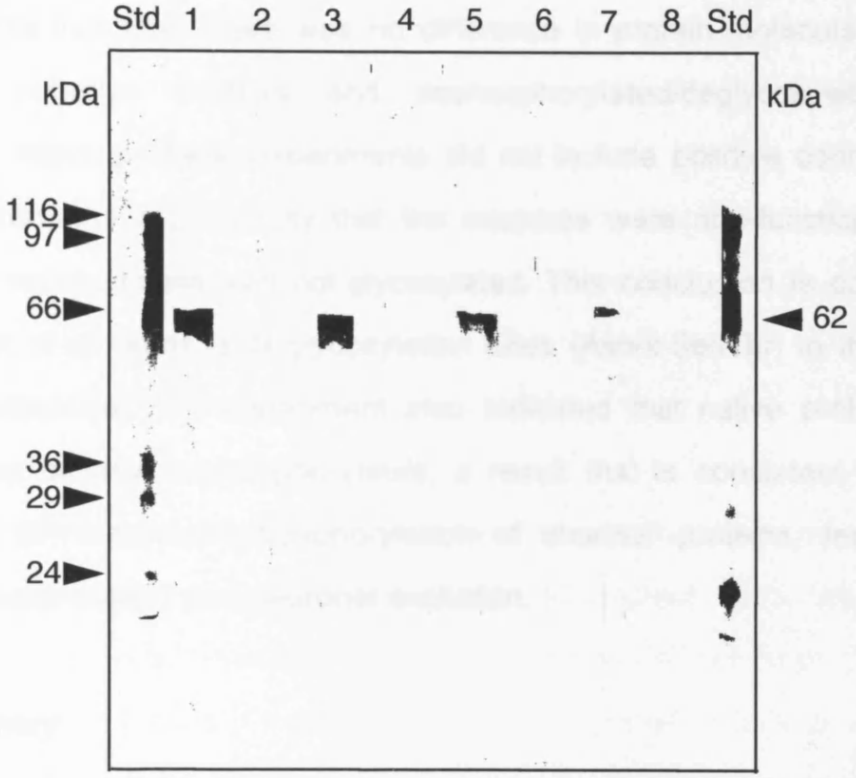

Figure 5-9. Band shift analysis of attempts to enzymatically dephosphorylate and deglycosylate rat brain nuclear fraction proteins. Lane 1, anti-Kir2.2 antibody (CIAP treated). Lane 2, anti-Kir2.2 antibody with Kir2.2 antigenic peptide (CIAP treated). Lane 3, anti-Kir2.2 antibody (untreated control). Lane 4, anti-Kir2.2 antibody with Kir2.2 antigenic peptide (untreated control). Lane 5, anti-Kir2.2 antibody (deglycosylated). Lane 6, anti-Kir2.2 antibody with Kir2.2 antigenic peptide (deglycosylated). Lane 7, anti-Kir2.2 antibody (untreated control). Lane 8, anti-Kir2.2 antibody with Kir2.2 antigenic peptide (untreated control). There were no apparent changes in the molecular weight of Kir2.2 protein (62 kDa) after attempts to enzymatically dephosphorylate and deglycosylate.

samples treated with 0.5 x denaturing buffer, could serve as the basis of a method for mapping the channel protein dimerisation sites. These experiments indicated there was no difference in protein molecular weight between negative controls and dephosphorylated/deglycosylated test reactions. Although these experiments did not include positive controls and so there remains a possibility that the enzymes were non-functional, it is likely that native protein was not glycosylated. This conclusion is consistent with a lack of consensus N-glycosylation sites (Asn-x-Ser/Thr) in the Kir2.2 protein sequence. The experiment also indicated that native protein was likely to be basally unphosphorylated, a result that is consistent with the model of SP mediated phosphorylation of channel proteins, leading to channel suppression and neuronal excitation.

5.8 Summary

Band-shift after serine/threonine phosphorylation with [γ^{32}P]-ATP on unlabelled Kir2.2 protein and unlabelled ATP on [^{35}S]-Methionine-labelled Kir2.2 protein, suggested that Kir2.2 was a substrate for *in vitro* phosphorylation. Further, Kir2.2 *in vivo* phosphorylation was investigated using the SN56 cell line and treatment with SP, suggested that Kir2.2 protein could be tyrosine phosphorylated *in vivo*.

In addition, the site of Kir2.2 protein expression in untransfected COS7 cells was determined to be the nucleus. Finally, attempts to dephosphorylate and deglycosylate native Kir2.2 protein were unsuccessful, suggesting that the Kir2.2 channel protein is basally unphosphorylated and unglycosylated.

Further experiments involving the *in vivo* phosphorylation and expression sites of Kir2.2 protein are suggested in section 6.4.

Results Analysis

Further analysis of the *in situ* hybridisation and immunohistochemical data has been requested and will be dealt with in the following sections.

***In Situ* Hybridisation Data**

Kir2.2 antisense riboprobes generated signals on rat coronal medulla/cerebellar tissue sections. Cytoplasmic signals were observed in the granule cell layer (including Golgi cells), molecular cell layer (including stellate and basket cells), Purkinje cell layer, noradrenergic cells of the locus coeruleus, oligodendroglia of the uncinate fasciculus and ependymal cells of the IVth ventricle (Figure 3-13a). Further, higher magnification analysis of the locus coeruleus indicated that many large nuclei and smaller cells (macroglia) contained intense cytoplasmic staining (Figure 3-13b).

The ABC-AP development system utilised to detect hybridisation required a development time of 16 hours. The associated Kir2.2 sense negative control riboprobes developed a cytoplasmic background staining present in the Purkinje cell layer and large nuclei of the medulla (Figure 3-13c). This background staining was similar to that observed on the no probe negative control tissue section (Figure 3-13d). Because the ABC-AP development period was 16 hours, it appeared that the background staining on the no probe control may be due to endogenous alkaline phosphatase activity. The

similar distribution on the sense negative control may also be due to endogenous alkaline phosphatase, however, an alternative explanation for this staining may be due to genuine signals resulting from the hybridisation of the sense riboprobes to an unknown mRNA.

In contrast, the β-actin antisense riboprobe stained the cytoplasm of a different subset of cells in the medulla and cerebellum (Figure 3-14a). These included the Purkinje, molecular and granule cell layers, the locus coeruleus and the mesencephalic trigeminal nuclei. No staining was observed in either the sense riboprobe (Figure 3-14b) or no probe negative controls (Figure 3-14c). Thus indicating that endogenous alkaline phosphatase was not present in the tissue section, and that the sense riboprobe did not hybridise to an unknown mRNA species.

Immunohistochemical Data

The immunohistochemistry on hippocampal and medulla/cerebellar tissue sections utilised affinity-purified antisera. However, the initial experiments to achieve specific peptide block on tissue sections utilised unpurified antisera (as this was the only material available at the time). Therefore, whilst non-specific peptide block did not reduce staining by any of the antisera, the specific peptide block of anti-Kir2.1 antibody by Kir2.1 peptide (Figure 4-7a) and anti-Kir2.3 antibody by Kir2.3 peptide (Figure 4-9c) yielded only a weak reduction in staining intensity.

In addition, high magnification analysis of the locus coeruleus revealed that not every large nuclei stained with anti-Kir2.2 antibody (Figure 4-10a),

indicating that a non-staining subset of nuclei may exist within the locus coeruleus (possibly cholinergic neurons). The anti-NK-1 receptor antibody stained the locus coeruleus and the periventricular grey area in the medulla. High magnification analysis of the locus coeruleus indicated that the large nuclei and smaller cells of macroglial origin were surrounded by intense staining. In addition, this staining extended into the extracellular space and could be due to extensive receptor expression in dendritic processes (Figure 4-11b). Alternatively, this staining may be due to the ABC-AP detection system which may have produced such a colour density that intercellular spaces were stained artifactually.

In general, staining with the affinity-purified Kir2.0 antisera produced very strong nuclear and weak plasma membrane signals on tissue sections. Figures could have been produced, such that the corresponding negative controls for each of the stained tissue sections were adjacent to each other for easy comparison. In addition, staining in the vascular smooth muscle was very strong and could potentially have been improved by reducing the primary antibody concentration (Figure 4-4d,e,f).

Chapter 6: Discussion

The studies presented in this thesis have shown that the Kir2.2 channel and NK-1 receptor proteins are co-localised in the noradrenergic neurons of the locus coeruleus (section 4.5). Preliminary experiments have provided evidence of *in vitro* PKC phosphorylation (sections 5.1.1 and 5.1.2), and *in vivo* tyrosine kinase phosphorylation of Kir2.2 channel protein in response to NK-1 receptor activation (section 5.6). These studies strengthen published data implicating both PKC (Takano *et al.*, 1995) and an unidentified transactivated tyrosine kinase (Wischmeyer *et al.*, 1998) in phosphorylation and suppression of Kir channel activity. In addition, the identification of Kir2.0 isoforms in macroglia (section 4.3) and vascular smooth muscle (section 4.3) may contribute to the understanding of potassium buffering in both of these cell types. Further, the nuclear localisation of Kir2.0 isoforms (sections 4.3 and 4.6) may have implications as to the function of the nuclear envelope lumen.

6.1 Kir2.0 Expression and Function in Macroglia

In this study astrocytes and oligodendroglia have been shown to express Kir2.0 channel isoforms in rat-fore and hind-brain regions (section 4.3). A potential role for Kir2.0 channels in these macroglia is to buffer neuronally derived extracellular potassium. Buffering in macroglia is vital to neurons because the latter produce localised high concentrations of potassium. Such concentrations may result in a potassium-induced depolarisation of the neuron. Therefore, it is important to remove these localised concentrations of extracellular potassium (expelled from repolarising neurons via Kv and K_{Ca}

channels), in order to prevent an undesirable neuronal depolarisation. Kirs are strongly implicated in macroglial potassium buffering because of the effect of high extracellular potassium on Kir activity. This effect is to shift a typical Kir current-voltage relationship (section 1.1) to the right, resulting in a strong inward flow of potassium ions into the macroglial cell at relatively positive membrane potentials. This high level of buffered potassium can then be released from the macroglial cell by Kirs at sites where the extracellular potassium concentration is lower (Brew *et al.,* 1986).

Macroglial potassium buffering by Kirs was first described in retinal Müller cells by electrophysiological recordings (Brew *et al.,* 1986). Interestingly, an uneven distribution of Kir channels was discovered over the plasma membrane. The vast majority of Kirs (94%) were found on the terminal endfoot of the cell (in close proximity to the neuron in this radial form of macroglia), an observation consistent with the idea of buffering high localised concentrations of potassium from neurons. In addition, although the specific isoform of Kir expressed in Müller cells was not identified, Kir expression in all areas of the plasma membrane was confirmed to be of a single type electrophysiologically (Brew *et al.,* 1986). Similar electrophysiological studies have implicated Kirs in the uptake of extracellular potassium into Müller cells (Brew *et al.,* 1986 and Ishii *et al.,* 1997), oligodendroglia (Karschin *et al.,* 1995 and Horio *et al.,* 1997) and astrocytes (MacFarlane & Sontheimer, 1997).

The generation of a pan-Kir2.0 specific polyclonal antibody, used with immunoelectron microscopy, allowed the assessment of Kir2.0 sites of expression in rat sciatic nerve Schwann cells. Kir2.0 isoforms were

specifically expressed in the microvilli of the nodes of Ranvier, indicating these were the sites of potassium buffering (Mi *et al.,* 1996).

6.2 Kir2.0 Expression and Function in Vascular Smooth Muscle

In this thesis, the expression of Kir2.0 channel isoforms has been demonstrated in vascular smooth muscle of rat brain cerebral arteries (section 4.3). Unidentified Kir isoforms have been characterised electrophysiologically in smooth muscle of small cerebral and coronary arteries and arterioles (reviewed by Quayle *et al.,* 1997). Therefore, the data presented in this thesis are consistent with earlier published work. However, details of the Kir isoforms involved have not previously been available, and for the first time Kir2.0 isoform expression has been described in vascular smooth muscle. The potential function of these Kir2.0 channels in vascular smooth muscle is in the determination of membrane potential and thus control of vascular tone (Edwards *et al.,* 1988).

Recently, endothelial derived hyperpolarising factor (EDHF) has been postulated to be potassium (Edwards *et al.,* 1998). EDHF-induced hyperpolarisation of smooth muscle is linked to the activities of endothelial potassium channels. Increases in the extracellular potassium concentration as small as 5 mM are able to mimic the effects of EDHF in an endothelium-independent manner, indicating that endothelium derived potassium is EDHF. Neurotransmitters, such as acetycholine, hyperpolarise endothelial cells by inducing an efflux of potassium through K_{Ca} and Kv channels, thus increasing the concentration of potassium in the myoendothelial space. This small increase in myoendothelial potassium concentration hyperpolarises

and relaxes vascular smooth muscle cells due to a slight shift in the Kir channel current-voltage relationship to the right, resulting in an efflux of potassium through a muscle cell Kir channel. This potassium efflux is then followed by the removal of extracellular potassium by a muscle cell Na^+/K^+ ATPase (Edwards *et al.,* 1998). The variations in potassium concentration are generated within the blood vessel wall itself, and therefore imply that vasodilation via hyperpolarisation and smooth muscle relaxation can be produced by the blood vessel itself (Edwards *et al.,* 1998).

The unidentified Kir channel(s) described electrophysiologically in vascular smooth muscle may have been identified here as Kir2.1, Kir2.2 and Kir2.3 (Edwards *et al.,* 1998). All three channel isoforms are constitutively active and therefore would be available to conduct the efflux of potassium. In addition, other data in this thesis indicate that Kir2.0 isoforms are expressed in the endothelia of capillaries and possibly cerebral artery walls as well, again consistent with a possible role in the model that EDHF is potassium.

6.3 Ion Channel Nuclear Localisation and Function

In this thesis it has been demonstrated for the first time that nuclear localisation of Kir2.0 channel proteins occurs in both native cells and cells transfected with channel cDNAs (sections 4.3 and 4.6). At present it is unknown whether the channel proteins are expressed on either the inner or outer nuclear envelopes (or both): however the data presented here indicate that Kir2.0 channel protein is found throughout the nucleoplasm. Further definition of the channel protein location could be obtained by immunoelectron microscopy.

The nucleoplasm and cytoplasm are segregated by the nuclear envelope. This has similar characteristics to leaky epithelium due to the presence of nuclear pore complexes. These supramolecular assemblies (125 mDa) contain up to 100 separate protein components known as nucleoporins. Nuclear pore complexes are permeable to solutes of a molecular mass of up 20 kDa. Larger molecules (e.g., RNAs) are actively removed from the nucleoplasm by nuclear pore associated and cytoplasmic proteins. Surprisingly, there appears to be an electrical potential gradient between the nucleoplasm and cytoplasm (Draguhn *et al.,* 1997), indicating that the nucleus can be considered as a separate compartment with its own membrane potential. The outer nuclear envelope and nuclear envelope lumen are continuous with the endoplasmic reticulum (ER), and the outer nuclear envelope membrane can be therefore considered to have similar properties to ER membrane (Gerasimenko *et al.,* 1996). In contrast, the inner nuclear membrane has a different protein composition and is unrelated to ER membrane (Gerasimenko *et al.,* 1996).

Although the potential function of these nuclear channels remains unclear, there is firm evidence for the presence of other ion channel proteins in the nuclear membrane (Gerasimenko *et al.,* 1995, Maruyama *et al.,* 1995, Gerasimenko *et al.,* 1996 and Draguhn *et al.,* 1997). These studies used electrophysiological methods involving patch clamping, or the activation of calcium-sensitive fluorescent probes in isolated nuclei. Studies using isolated mouse liver nuclei and calcium-sensitive fluorescent probes indicated that an ATP-dependent calcium channel was present on the outer nuclear envelope, whilst an inositol 1, 4, 5-trisphosphate-activated calcium channel was present on the inner nuclear envelope (Gerasimenko *et al.,*

1995). This study suggested that calcium transport was limited to the nuclear envelope lumen, with final release of calcium into the nucleoplasm followed by diffusion from the nucleus via the nuclear pore complexes. Similar studies using isolated nuclei from rat pancreatic acinar cells with electrophysiological recordings from the outer nuclear envelope, revealed the presence of both voltage-activated and calcium-activated potassium channels. These observations suggested that the channels were activated by positive potentials and high calcium concentrations in the nuclear envelope lumen (Maruyama *et al.,* 1995). Electrophysiological recordings from isolated nuclei of rat cerebral cortex neurons have also demonstrated the presence of voltage-dependent ion channels, selective for monovalent (sodium and potassium) cations, on the outer nuclear envelope (Draguhn *et al.,* 1997).

Overall, these data indicate that the nuclear envelope lumen forms a calcium storage pool (Gerasimenko *et al.,* 1995), by a combination of the activities of calcium and potassium channels. The function of this polarised compartment may be to aid the transmission of calcium fluxes from the cell membrane to the nucleus where changes in gene expression may result (Gerasimenko *et al.,* 1996). The whole area of control of ion flux across the two nuclear envelope membranes is under development. Therefore, the potential functions of Kir2.0 channels in the nuclear envelope will remain uncertain, until precise information becomes available for the location and orientation of the channel proteins within the nuclear envelope.

The consensus nuclear localisation sequence in Kir2.2-Kir2.4 channel proteins has been identified as a string of basic arginine and lysine residues (underlined) in the N-terminus of the protein sequence (Arg-Arg-Arg/Lys-X-

Arg/His-Asn-Arg-Phe-Val-Lys-Lys). The Kir2.1 protein nuclear localisation sequence is weaker than the other Kir2.0 isoforms (see the sequence below), and this may reflect the cytoplasmic/plasma membrane staining pattern seen in this study in Kir2.1 transfected CHO cells. The nuclear localisation sequences are present in the following positions; Kir2.1 residues: 44-50 (Arg-Ser-Arg-Phe-Val-Lys-Lys), Kir2.2 residues: 39-49 (Arg-Arg-Arg-Cys-Arg-Asn-Arg-Phe-Val-Lys-Lys), Kir2.3 residues: 14-24 (Arg-Arg-Lys-Arg-Arg-Asn-Arg-Phe-Val-Lys-Lys) and Kir2.4 residues: 39-49 (Arg-Arg-Arg-Cys-His-Asn-Arg-Phe-Val-Lys-Lys) (Noselli & Vincent, 1991 and Kügler *et al.*, 1996).

There is precedence for intracellular targeting sequences amongst members of the potassium channel family; for example K_{ATP} (Kir6.1/Kir6.2 and SUR1) channels have been described as containing an endoplasmic reticulum retention sequence (Zerangue *et al.*, 1999). This sequence (Arg-Lys-Arg) is found within 36 residues of the Kir6.2 C-terminus, and is responsible for the prevention of incomplete channel (Kir6.2 tetramer and SUR1 monomer subunit) expression on the plasma membrane. The Arg-Lys-Arg sequence appears to have both a subcellular targeting and a quality control function. If the tetrameric Kir6.2, Arg-Lys-Arg sequences are not masked by surrounding SUR1 subunits then the channel tetramer is retained in the ER. Similarly, all four SUR1 subunits must be in position in order for their own Arg-Lys-Arg sequences to be masked. Therefore, only correctly assembled K_{ATP} channels can be trafficked to the plasma membrane (Zerangue *et al.*, 1999).

This Arg-Lys-Arg sequence, when identified in K_{ATP} channels, was subsequently shown to be position-independent within the Kir6.2/SUR1 sequences. Interestingly, the Arg-Lys-Arg sequence was also found in Kir2.0 channels (Kir2.3 residues: 15-17). In addition to the Arg-Lys-Arg sequence, similar basic residue sequences were also observed in Kir2.2 and Kir2.4 residues: 39-41 (Arg-Arg-Arg). If the Arg-Lys-Arg containing C-terminal 36 residues of Kir6.2 are transplanted onto either the N- or C-termini of Kir2.1, then the channel protein does not traffic to the plasma membrane, as assessed by electrophysiological recordings (Zerangue *et al.,* 1999). Kir2.1 does not contain Arg-Lys-Arg or Arg-Arg-Arg ER retention sequences and thus should traffic successfully to the plasma membrane. However, the Kir2.2, Kir2.3 and Kir2.4 isoforms all contain one of these sequences and, therefore, may be expected to be retained in the ER unless: 1). The nuclear localisation sequence overrides the ER localisation sequence: 2). The tetrameric structure of Kir2.0 channels masks the ER localisation sequence, as does the octameric structure in K_{ATP}, allowing the Kir2.0 channel proteins to leave the ER only when correctly assembled.

Recently, other work has been published concerning the control of the subcellular localisation of Kir3.0 channel protein. The acetylcholine-activated potassium current found in cardiac pacemaker cells (I_{KACh}), is due to a heterotetrameric channel protein composed of Kir3.1 and Kir3.4 subunits (Krapivinsky *et al.,* 1995). Kir3.1 is unable to form functional homomultimer channels and must, therefore, combine with other Kir3.0 subfamily channels. In addition, Kir3.1-tagged subunits were found to require association with Kir3.4 subunits in order to achieve plasma membrane localisation (Kennedy *et al.,* 1999). Chimeric channel subunits (Kir3.1/Kir3.4) containing the C-

terminal of Kir3.4 (residues: 400-419) were localised to the plasma membrane, whilst a chimera containing the C-terminal (residues: 374-501) of Kir3.1 had an intracellular localisation consistent with the ER. This work indicated that a plasma membrane localisation sequence was present in the C-terminus of Kir3.4 and that further, the Kir3.4 subunit was required for correct trafficking of the I_{KACh} channel heterotetramer to the plasma membrane.

6.4 Potential Mechanisms of Kir2.2 Phosphorylation and Suppression by Substance P

Previously published data indicate that excitability of noradrenergic neurons of the locus coeruleus is at least partially controlled by the activity of unidentified Kir isoforms, which are modulated by the neurokinin, substance P (Shen & North, 1992 and Koyano *et al.* 1993). Similar observations have been made in cholinergic neurons of the nucleus basalis of Meynert (Stanfield *et al.,* 1985, Yamaguchi *et al.,* 1990, Takano *et al.,* 1995 and 1996).

Studies describing the modulation of the Kir channel (most likely Kir2.2, in locus coeruleus neurons from channel localisations performed in this study) by the NK-1 receptor have until recently implied that phosphorylation by PKC is the main signal transduction mechanism involved (Takano *et al.,* 1995). Certainly the data presented in this thesis indicate that Kir2.2 protein can be phosphorylated *in vitro* by all PKC isoforms and also by PKA. This does not, however, guarantee that similar phosphorylation reactions occur *in vivo*. In fact, the data published by Nakajima and colleagues indicated that PKC phosphorylated an unidentified target protein, which may or may not be a Kir

channel protein (Takano *et al.,* 1995). If PKC phosphorylated an unidentified intermediary protein, this could initiate a series of events that eventually could cause suppression of a Kir channel protein. However, recently published data support the view of direct PKC modulation of Kirs (Zhu *et al.,* 1999). These data were generated by the mutagenesis of phosphorylation sites on Kir2.3, leading to the conclusion that threonine residue 53 was the site of PKC phosphorylation responsible for channel suppression. The introduction of an analogous threonine residue into Kir2.1 made the latter channel susceptible to PKC-dependent suppression (Zhu *et al.,* 1999).

In addition to the data indicating that modulation of Kir activity was due to phosphorylation by PKC, more recent data have implicated an unidentified tyrosine kinase in the phosphorylation and suppression of Kir2.1 (Wischmeyer *et al.,* 1998). The work of Karschin and colleagues indicated that tyrosine residue 242 in Kir2.1 was phosphorylated and channel activity suppressed by the activation of nerve growth factor receptor (NGFR) or epidermal growth factor receptor (EGFR). Mutation of the tyrosine 242 into phenylalanine abolished this suppression in co-transfected COS7 cells (Wischmeyer *et al.,* 1998). The tyrosine phosphorylation site on Kir2.1 is also present in the other three members of the Kir2.0 channel subfamily: therefore the potential involvement of tyrosine phosphorylation in the modulation of Kir2.2 activity by substance P was investigated in this study.

From investigation of the SN56 cholinergic mouse neuronal cell line, it was concluded that both Kir2.2 and the NK-1 receptor were endogenously expressed, making this cell line an ideal vehicle for channel modulation studies. In preliminary experiments, treatment of these cells with substance

P followed by immunoprecipitation (anti-Kir2.2 antibody) and Western blotting (anti-phosphotyrosine antibody) revealed an 80 kDa tyrosine-phosphorylated polypeptide. The identity of this polypeptide was not characterised but was potentially a phosphorylated Kir2.2 dimer or co-immunoprecipitated channel-associated protein. Subsequent investigation of the ability of the anti-Kir2.2 antibody to immunoprecipitate PKC phosphorylated protein *in vitro*, revealed that conformational changes associated with PKC phosphorylation prevented immunoprecipitation. Therefore, the 80 kDa band seen after substance P treatment of SN56 cells, followed by immunoprecipitation and Western blotting was probably artifactual (section 5.5). In order to obtain evidence of tyrosine phosphorylation of Kir2.2 in SN56 cells, similar experiments were carried out without the immunoprecipitation step (section 5.6). This resulted in the detection of a 62 kDa band in substance P treated cells (but not in untreated negative control cells), when probed with anti-phosphotyrosine antibody. This finding provides some evidence for a tyrosine phosphorylation of Kir2.2 triggered by substance P *in vivo*, thus still consistent with the model of Kir2.2/NK-1 receptor co-localisation in locus coeruleus.

In order to further characterise the tyrosine phosphorylation of Kir2.2 induced by substance P, a Kir2.2 mutant was made in which the tyrosine residue in the consensus tyrosine kinase site at position 243 was mutated to phenylalanine (similar to the experiment carried out by Wischmeyer *et al.*, 1998). Co-transfection of the Kir2.2 (Y243F) mutant with the NK-1 receptor in COS7 cells was unsuccessful, so any effect of the tyrosine mutation on tyrosine phosphorylation could not be observed. However, prevention of tyrosine phosphorylation may not be reflected in a prevention of channel

suppression, as it is likely that PKC phosphorylation of channel protein is working in tandem.

The observation that substance P binding to the NK-1 receptor causes Kir channel phosphorylation (and suppression) via two probable signal transduction mechanisms, is known as receptor 'transactivation'. In addition to activation of PKC (Takano *et al.,* 1995), NK-1 receptor activation leads to phosphorylation of the mitogen-activated protein (MAP) kinase, ERK (Luo *et al.,* 1996). ERK (extracellular-signal-regulated kinase) cascades used by receptor tyrosine kinases (e.g., EGFR) can also be transactivated by G-protein-coupled receptors, yielding a Ras-activating core mitogenic signalling complex (Daub *et al.,* 1996). G-protein-coupled receptor-transactivated tyrosine receptor kinases (e.g., EGFR), have been characterised as being able to phosphorylate tyrosine residues in adaptor proteins such as the SH2 domain-containing Shc, followed by the recruitment of the non-receptor tyrosine kinase Src, leading to ERK activation by the Ras/MAP kinase signalling cascade (Daub *et al.,* 1996). An overview of receptor transactivation involving G-protein-coupled receptor and tyrosine receptor kinases is shown in Figure 6-1:

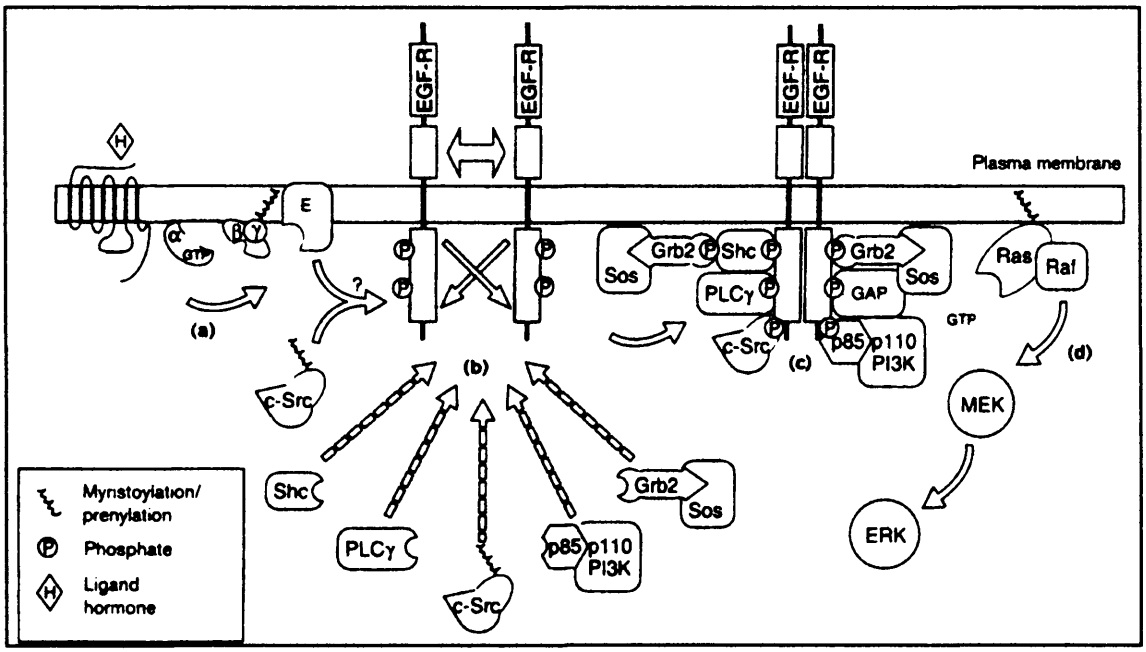

Figure 6-1. Receptor transactivation. This figure and legend are taken from Luttrell *et al.*, 1999. (a), G-protein-coupled receptors activation results in dissociation of the Gα.GTP and Gβγ subunits and effector (E) activation. (b), Working via unidentified effectors that are probably Gβγ-subunit-regulated, G-protein-coupled receptors induce epidermal growth factor (EGF)-independent activation of EGF receptor kinase. (c), EGF receptor tyrosine phosphorylation promotes its association with phosphotyrosine-binding SH2 domain-containing adaptor proteins, such as Shc and Grb2, and signalling proteins such as c-Src, phospholipase Cγ, Ras.GTPase activating protein (GAP) to form a membrane-associated Ras activation complex. (d), Grb2-Sos1 recruited to the EGF receptor complex catalyses Ras.GTP exchange. There is then an association of Ras with the MAP kinase cascade.

Recently, the m1 muscarinic acetylcholine receptor has been shown to cause suppression of the voltage-gated potassium ion channel Kv1.2, by activation of the EGFR tyrosine kinase in stably transfected human 293 cells (Tsai *et al.*, 1997). Binding of acetylcholine to the m1 muscarinic acetylcholine receptor leads to release of $G\alpha_q$ subunits and subsequent activation of PKC. PKC phosphorylates EGFR on threonine residue 654

resulting in receptor dimerisation and autophosphorylation (Hunter *et al.*, 1984), allowing the recruitment and tyrosine phosphorylation of the Ras-activating core mitogenic signalling complex. Previously published data indicated that the m1 muscarinic acetylcholine receptor suppressed the Kv1.2 channel, via a tyrosine kinase mechanism (Huang *et al.*, 1993). The transactivated EGFR tyrosine kinase was assessed as being capable of directly phosphorylating and partially suppressing Kv1.2 channels, a response that was repeated by treatment of the cells with EGF (Tsai *et al.*, 1997).

There are obvious parallels between the suppression of Kv1.2 and that of Kir2.2: both are modulated via the activation of G-protein-coupled receptors (m1 muscarinic acetylcholine receptor and NK-1 receptor, respectively), resulting in the release of $G\alpha_q$ and $G\alpha_{q/11}$ subunits (Takano *et al.*, 1996) respectively, and the activation of PKC. There is also evidence that activated NK-1 receptor results in activation of the MAP kinase ERK, suggesting that the receptor may be linked with the activity of a growth factor tyrosine kinase receptor (Luo *et al.*, 1996).

Nakajima and colleagues have described either direct or indirect PKC phosphorylation of an unidentified Kir, leading to channel suppression (Takano *et al.*, 1995). Evidence is presented in this thesis that Kir2.2 can be directly phosphorylated by PKC (sections 5.1.1 and 5.1.2): however, an additional phosphorylation target may be a growth factor receptor such as EGFR. A possible future investigation could centre on Kir2.2 suppression by EGF, a result which would strongly support a receptor tyrosine kinase transactivation hypothesis. Such an investigation has already been

performed with Kir2.1, resulting in channel tyrosine phosphorylation and suppression (Wischmeyer *et al.,* 1998). A potential hypothesis for activated NK-1 receptor suppression of Kir2.2 involves PKC activation, phosphorylation of EGFR (or other growth factor receptor e.g., NGFR) leading to dimerisation and tyrosine auto/transphosphorylation, followed by tyrosine phosphorylation and suppression of Kir2.2. A parallel pathway may involve direct phosphorylation and suppression of Kir2.2 by PKC itself. The tyrosine kinase responsible for channel phosphorylation may be transactivated EGFR. However, it is most likely that channel phosphorylation is carried out by an unidentified, soluble cytoplasmic tyrosine kinase. The identity of this tyrosine kinase could be investigated by co-immunoprecipitation of Kir2.2 without reducing agents, or use of the yeast-two-hybrid system (Fields & Song, 1989 and Chein *et al.,* 1991) with Kir2.2 protein as bait.

The following experiments could also be employed to further investigate the signal transduction mechanisms involved in NK-1 receptor modulation of Kirs;

1). Production of a pan-N-terminal Kir2.0 polyclonal antibody for the purposes of immunoprecipitation and assessment of channel phosphorylation states.

2). Successful co-transfection of the Kir2.2 (Y243F) mutant with the NK-1 receptor cDNAs in a cell line, without endogenous Kir2.2 protein expression, therefore enabling assessment of channel phosphorylation states after substance P treatment.

3). Examination of the potential dual signal transduction mechanisms controlling Kir2.2 activity by channel suppression measured electrophysiologically in CHO cells, after co-transfection with Kir2.2 (or Kir2.2 (Y243F) mutant) and NK-1 receptor cDNAs. This experiment would require the inhibition of PKC (by staurosporine), in order to examine the divergence position of the proposed parallel signal transduction mechanisms.

4). Investigation of the substance P stimulated, immunoprecipitated and Western blotted 80 kDa band by removal from the blot, followed by treatment with high concentrations of sodium dodecyl sulphate and β-mercaptoethanol. Gel electrophoresis would then assess whether the polypeptide band size could be reduced to 62 kDa (Kir2.2).

5). Removal of both the Western blotted/immunoprecipitated and Western blotted 80 kDa polypeptide bands for protein sequencing.

6). Investigation of *in vivo* Kir2.2 phosphorylation states by the production of a *c-myc*-Kir2.2 fusion. This fusion would be transiently transfected into COS7 cells, treated with [^{32}P] and phorbol esters, resulting in protein phosphorylation by PKC. Immunoprecipitation with an anti-*c-myc* antibody would then recover the Kir2.2 protein from cell lysates. Recovered Kir2.2 protein would be subjected to proteolytic digest, followed by purification with 1-dimensional thin-layer chromatography and analysis by mass spectrometry.

7). Investigation of the subcellular protein distribution of N- and C-terminal Kir2.2-GFP (green fluorescent protein) fusions in transiently transfected

COS7 cells. These experiments would allow the detection of fluorescent protein, without the need for antibodies.

6.5 Regulation of Voltage-Gated Potassium Ion Channels by Phosphorylation

A description of the structure and function of voltage-gated potassium channels can be found in section 1.3. Although the activity of this family of ion channels is predominantly controlled by voltage sensitivity to changes in transmembrane potential, many voltage-gated potassium channels are also influenced by protein phosphorylation. The *Drosophila* voltage-gated potassium channels belonging to the 'Shaker', 'Shab', 'Shaw' and 'Shal' subfamilies (Butler *et al.,* 1990, Wei *et al.,* 1990 and Covarrubias *et al.,* 1991) are related to the Kvα subunits belonging respectively, to the Kv1, Kv2, Kv3 and Kv4 subfamilies of vertebrate voltage-gated potassium channels (Baumann *et al.,* 1988, Butler *et al.,* 1990, Wei *et al.,* 1990, Covarrubias *et al.,* 1991, MacKinnon, 1991, McCormack *et al.,* 1992, Salkoff *et al.,* 1992 and Ranganathan, 1994).

Phosphorylation of the Kvα subunits results in changes in channel current amplitude and voltage-dependence of gating. These changes in channel activity lead to modulation of calcium entry and action potential firing (Levitan, 1985, Shearman *et al.,* 1989 and Jonas & Kaczmarek, 1996). The activation of neurotransmitter receptors leads to changes in channel subunit phosphorylation states by signal transduction pathways resulting in the activation of protein kinases and phosphatases (Levitan, 1985, Shearman *et al.,* 1989 and Jonas & Kaczmarek, 1996).

There is evidence of channel protein phosphorylation by PKA, PKC and tyrosine kinases in the Kv1 subfamily, for example: 1). Rat Kv1.1 can be phosphorylated *in vitro* by PKA (Baumann *et al.,* 1988 and Ivanina *et al.,* 1994). 2). Activation of the β-adrenergic receptor co-expressed in *Xenopus* oocytes with rat Kv1.2 resulted in activation of PKA, and an increase in channel current (McKinnon, 1989 and Huang *et al.,* 1994). Co-expression of the m1 muscarinic acetylcholine receptor with the rat Kv1.2 channel in *Xenopus* oocytes resulted in channel suppression after receptor activation (Paulmichl *et al.,* 1991 and Huang *et al.,* 1993). The suppression of rat Kv1.2 is also observed with the activation of PKC. This study lead to the discovery of a PKC or calcium activated tyrosine kinase (Huang *et al.,* 1993 and Lev *et al.,* 1995). 3). Human Kv1.3 channel protein is phosphorylated by both PKA and PKC on serine residues as determined by phosphopeptide mapping (Attali *et al.,* 1992 and Cai & Douglass, 1993). The co-expression of Kv1.3 and v-Src (constitutively active non-receptor tyrosine kinase) in HEK 293 cells resulted in channel tyrosine phosphorylation and suppression of channel activity (Holmes *et al.,* 1996a). 4). Phosphorylation of human Kv1.4 by PKC resulted in a partial reduction in channel activity. In addition, human Kv1.4 can be phosphorylated *in vitro* by PKC (Kamb *et al.,* 1989, Ramaswami & Tanouye, 1989 and Fahrig *et al.,* 1992). 5). Phosphorylation by PKA is detected on serine residues of human Kv1.5 isoforms (Philipson *et al.,* 1990, Swanson *et al.,* 1990 and Curran *et al.,* 1992). In addition, tyrosine phosphorylation of human Kv1.5 can be demonstrated in human myocardium by Src, resulting in suppression of channel activity (Philipson *et al.,* 1990 and Holmes *et al.,* 1996b).

There is evidence of channel protein phosphorylation by PKA in the Kv2 subfamily: for example rat Kv2.1 and Kv2.2 channel isoforms both contain C-terminal PKA phosphorylation sites (Frech *et al.,* 1989 and Wilson *et al.,* 1994).

The Kv3 subfamily of voltage-gated potassium channels all contain putative PKA and PKC phosphorylation sites. There is currently little evidence suggesting that Kv3 channel activity can be modulated by protein phosphorylation, however, the available evidence suggests the following: 1). The use of phorbol esters to stimulate PKC resulted in a limited degree of Kv3.1 channel suppression and a reduction in the open channel probability (Kanemasa *et al.,* 1995). 2). Kv3.2 channels were phosphorylated and suppressed by PKA (Moreno *et al.,* 1995).

There is a limited amount of information available concerning the regulation of the Kv4 subfamily by protein phosphorylation. However, it appears that PKA, PKC and tyrosine kinases are potentially involved as consensus phosphorylation sites are found in Kv4.2 between the S4 and H4 loops (Baldwin *et al.,* 1991, Roberds & Tamkun, 1991 and Blair *et al.,* 1992). In addition, Kvβ regulatory subunits are found to contain consensus phosphorylation sites for both PKA and PKC (Rettig *et al.,* 1994 and Scott *et al.,* 1994).

6.6 Ion Channel Clustering with PSD-95

Some ion channels appear to be anchored to specific sites on the plasma membrane of neurons. Ion channel clustering is mediated by proteins such

as mammalian post-synaptic density protein-95 (PSD-95), a protein originally purified from both the pre- and post-synaptic densities of synaptosomes (Cho *et al.,* 1992). The protein had similarities to the *Drosophila* discs large (*D*lg) tumour suppressor protein (Woods & Bryant, 1991) and zonula occludentes-1 (*Z*O-1), a vertebrate tight junction protein (Willott *et al.,* 1993). Consequently the three regions of homology per protein, or PDZ domains, were named after the three previously described proteins, all of which were found at cellular junctions. These 90 amino acid regions of homology are capable of binding to the far C-terminal regions of ion channels containing a Glu-Ser/Thr-Asp-Val consensus sequence. Examples of PDZ-binding ion channels include the Kv1.4 'Shaker' voltage-gated potassium channel, which binds two of the three PDZ domains in PSD-95 (Kim *et al.,* 1995), and the Kir2.3 and Kir4.1 inwardly rectifying channels. The Kir2.3 channel, containing a Glu-Ser-Ala-Ile sequence in the far C-terminus of the protein, is able to bind to PSD-95. The serine residue in this sequence can also be phosphorylated by PKA, preventing binding of the ion channel and PSD-95 (Cohen *et al.,* 1996a). Thus, PKA phosphorylation and potentially associated suppression of channel activity prevents channel clustering, implying that only active channels are able to cluster. Related sequences are found in the other three members of the Kir2.0 subfamily, but the alanine residue in the sequence is replaced with glutamic acid (a non-polar to acidic substitution), probably preventing binding to PDZ domains. However, unpublished observations indicate that Kir2.1 channel and PSD-95 proteins are able to bind in co-transfected COS7 cells causing channel suppression (personal communication from Dr Mark Leyland and Dr Caroline Dart of the Cell Physiology and Pharmacology Department, University of Leicester). The Kir4.1 channel, containing a Ser-Asn-Val sequence in the C-terminus, is also

capable of binding to PSD-95, increasing both whole-cell currents and clustering the channel protein in the plasma membrane (Horio *et al.*, 1997). The Kir3.2c splice variant containing the Glu-Ser-Lys-Val C-terminal sequence is capable of binding and co-immunoprecipitating PSD-95 protein from brain extracts. In comparison the Kir3.2a isoform is not, implying specialised functions for splice variants within a single channel isoform (Inanobe *et al.*, 1999).

The PDZ family of proteins may be important for the localisation of receptors and channels in clusters, therefore increasing the efficiency with which receptor mediated changes in ion channel activity are seen: for example, PSD-95 may localise receptor/ion channel complexes to the post-synaptic membrane in neurons (Cho *et al.*, 1992).

6.7 Summary and Conclusions

The data presented in this thesis describe the production and characterisation of high specificity riboprobes for the Kir2.2 channel mRNA. These results indicated that Kir2.2 mRNA was strongly expressed in the locus coeruleus, complementing earlier published data. In addition, anti-Kir2.1, anti-Kir2.2 and anti-Kir2.3 polyclonal antibodies were generated and characterised. New information was produced with these antibodies, indicating that Kir2.0 isoform expression was distinct, but at times overlapping in the examined brain regions. In addition, a nuclear localisation of Kir2.0 channel isoforms was encountered in tissue sections and transfected cells (Kir2.2 and Kir2.3 only). The anti-Kir2.2 antibody was used

in conjunction with the anti-NK-1 receptor polyclonal antibody to show protein co-localisation in single cells in the locus coeruleus.

Attempts were made to establish the existence of a signal transduction mechanism, linking the NK-1 receptor and Kir2.2 channel proteins. *In vitro* phosphorylation of Kir2.2 protein by PKC was demonstrated. In addition, an unidentified tyrosine kinase was shown to be capable of phosphorylating the Kir2.2 channel protein *in vivo*.

These studies suggest that it is probable that the Kir isoform suppressed by the NK-1 receptor in locus coeruleus (Shen & North, 1992 and Koyano *et al.*, 1993) is the constitutively active Kir2.2. The channel activity is probably modulated by a combination of direct PKC phosphorylation and PKC transactivation of a growth factor receptor signalling pathway, resulting in tyrosine phosphorylation and suppression of the Kir channel protein.

Appendices

Appendix 1: Alignment of Rat and Mouse Kir2.2 Proteins

Identical residues are indicated by bold letters contained within dark grey boxes. Conservative substitutions are also lettered in bold, but are contained within pale grey boxes. Non-identical and non-conserved substitutions are represented in normal capital typeface, on a white background.

There are five differences between the rat and mouse Kir2.2 proteins, the most significant are present in the C-terminus of the protein, forming the polyclonal antibody epitope site (changes are: G for A and E for V, rat for mouse respectively). By contrast, rat and mouse Kir2.1 and Kir2.3 proteins have no differences in their C-terminal regions (alignment was made using MacVector 6.0.1, Oxford Molecular Group PLC).

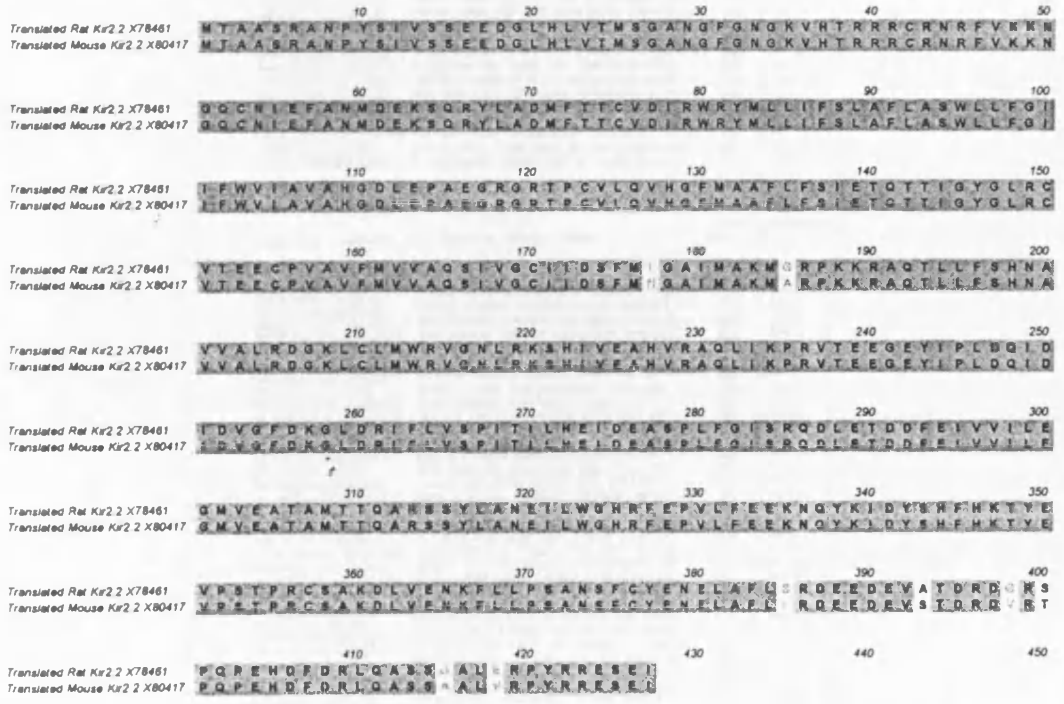

Appendix 2: Kir2.2 N- and C-Terminal Riboprobe Template BLAST2.0 Searches

BLAST2.0 searches confirm the high specificity of Kir2.2 riboprobe templates by comparison to other similar sequences (N-terminal: upper panel. C-terminal: lower panel).

Sequences producing High-scoring Segment Pairs:		High Score	Smallest Sum Probability P(N)	N
emb|X80417|MMRBIRK2	M.musculus MB-IRK2 mRNA	1790	7.2e-139	1
emb|X78461|RNRBIRK2	R. norvegicus RB-IRK2 cDNA	1491	1.2e-130	1
gb|L36049|HUMMCIR	Human high conductance inward rectif...	1306	3.0e-115	1
gb|U53143|HSU53143	Human inward rectifying K+ channel a...	1474	1.4e-112	1
gb|U24054|HSU24054	Human inward rectifier K+ channel pr...	704	1.6e-48	1
gb|U07364|HSU07364	Human inwardly rectifying potassium ...	695	8.7e-48	1
gb|S72501|S72501	IRK1=inward rectifier potassium chan...	666	4.9e-47	1
emb|X81580|RNIRPC|1	R.norvegicus mRNA for inward rectifi...	660	1.5e-46	1
emb|X87435|RNBIRK1	R.norvegicus mRNA for inwardly recti...	660	1.5e-46	1
gb|AF020792|AF020792	Bos taurus inward rectifier potassiu...	676	3.3e-46	1
gb|U55369|BTU55369	Bos taurus inward rectifier potassiu...	667	1.9e-45	1
gb|S81771|S81771	Inwardly rectifying K+ channel IRK3[...	659	8.6e-45	1
gb|S71182|S71182	MB-[RK]=class 3 inward rectifier pot...	644	1.5e-43	1
gb|U11075|MMU11075	Mus musculus inwardly-rectifying K+ ...	644	1.5e-43	1
db|D21057|RABPC	Rabbit mRNA for potassium channel, c...	627	4.0e-42	1
gb|AF021138|AF021138	Oryctolagus cuniculus inward rectifi...	627	4.0e-42	1
gb|AF021137|AF021137	Rattus norvegicus inward rectifier p...	618	2.2e-41	1
gb|L48498|RATRBIR	Rattus norvegicus inwardly rectifyin...	618	2.2e-41	1
gb|U27582|RNU27582	Rattus norvegicus brain inwardly rec...	581	5.7e-40	2
gb|AF021135|AF021135	Macaca mulatta inward rectifier pota...	596	1.5e-39	1
emb|X71052|MMIRK1	M. musculus mRNA for inward rectifie...	591	3.9e-39	1
gb|AF021136|AF021136	Mus musculus inward rectifier potass...	591	3.9e-39	1
gb|AF021142|AF021142	Cavia porcellus inward rectifier pot...	583	1.8e-38	1
emb|Z48971|CCIRK1	C.cobaya gene for inward rectifier p...	583	1.8e-38	1
gb|U12507|HSU12507	Human cardiac inward rectifier potas...	578	4.7e-38	1
gb|U16861|HSU16861	Human inward rectifying potassium ch...	578	4.7e-38	1
gb|AF011904|AF011904	Homo sapiens inwardly rectifying pot...	578	4.7e-38	1
gb|AF021139|AF021139	Homo sapiens inward rectifier potass...	578	4.7e-38	1
gb|U22411|HSU22411	Human inward rectifier potassium cha...	578	4.7e-38	1
gb|U24055|HSU24055	Human inward rectifier K+ channel pr...	569	2.6e-37	1
gb|AF021141|AF021141	Gallus gallus inward rectifier potas...	551	8.3e-36	1
gb|U20216|GGU20216	Gallus gallus inward rectifier potas...	551	8.3e-36	1
gb|AF008262|AF008262	Oryctolagus cuniculus ATP-sensitive ...	179	1.7e-21	1
db|D50582|HUMIRKCB	Human gene for inward rectifier K ch...	116	9.3e-18	1
gb|U90581|HSU90581	Human 86Kb contig from chromosome 11...	116	9.3e-18	1
db|D88159|D88159	Mouse mRNA for ATP-sensitive inwardl...	104	2.9e-15	1
db|D42145|RATUKATP1	Rat mRNA for ATP-sensitive potasium ...	295	1.6e-14	1
gb|U27558|RNU27558	Rattus norvegicus brain-specific inw...	289	5.2e-14	1
emb|X86818|RSKBAB|GFX	R.norvegicus mRNA for inward rectifi...	280	2.9e-13	1
emb|X83585|RNIRPC|0	R.norvegicus mRNA for inward rectifi...	280	2.9e-13	1
gb|U21917|MAU21917	Mesocricetus auratus potassium chann...	251	5.1e-11	1
gb|U51239|MMU51239	Mus musculus lysosomal-associated mu...	125	0.98	1
gb|U29539|MMU29539	Mus musculus retinoic acid-inducible...	125	0.98	1
emb|Z74771|SCYOL031C	S.cerevisiae chromosome XV reading f...	124	0.94	1
emb|Z74772|SCYOL01CW	S.cerevisiae chromosome XV reading f...	124	0.94	1
emb|X71807|ANUAPA	A.nidulans uapA gene for uric acid-x...	121	0.992	1
gb|M61676|SERERYAA	S.erythraea first ORF of eryA gene, ...	109	0.999	2

Sequences producing High-scoring Segment Pairs:		High Score	Smallest Sum Probability P(N)	N
emb|X80417|MMRBIRK2	M.musculus MB-IRK2 mRNA	1795	2.8e-139	1
emb|X78461|RNRBIRK2	R. norvegicus RB-IRK2 cDNA	1578	2.6e-121	1
gb|L36049|HUMMCIR	Human high conductance inward recti...	1076	9.0e-80	2
gb|U53143|HSU53143	Human inward rectifying K+ channel ...	758	4.4e-75	3
gb|U55369|BTU55369	Bos taurus inward rectifier potassi...	630	5.0e-44	2
gb|AF021140|AF021140	Sus scrofa inward rectifier potassi...	619	4.0e-43	1
gb|AF020792|AF020792	Bos taurus inward rectifier potassi...	621	1.3e-41	1
gb|U20216|GGU20216	Gallus gallus inward rectifier pota...	607	1.8e-40	1
gb|AF021141|AF021141	Gallus gallus inward rectifier pota...	607	1.8e-40	1
db|D21057|RABPC	Rabbit mRNA for potassium channel, ...	576	6.9e-38	1
gb|AF021138|AF021138	Oryctolagus cuniculus inward rectif...	576	6.9e-38	1
gb|AF021135|AF021135	Macaca mulatta inward rectifier pot...	558	1.9e-37	2
gb|U24055|HSU24055	Human inward rectifier K+ channel p...	549	3.2e-37	2
gb|U12507|HSU12507	Human cardiac inward rectifier pota...	549	3.5e-37	2
gb|U16861|HSU16861	Human inward rectifying potassium c...	549	3.6e-37	2
gb|S72501|S72501	HRK1=inward rectifier potassium cha...	545	5.7e-37	1
gb|U07364|HSU07364	Human inwardly rectifying potassium...	545	5.7e-37	1
gb|AF021139|AF021139	Homo sapiens inward rectifier potas...	549	1.0e-36	2
gb|U24054|HSU24054	Human inward rectifier K+ channel p...	554	3.2e-36	1
gb|AF011904|AF011904	Homo sapiens inwardly rectifying po...	531	1.0e-35	2
emb|X71052|MMIRK1	M. musculus mRNA for inward rectifi...	550	1.0e-35	1
gb|AF021136|AF021136	Mus musculus inward rectifier potas...	550	1.0e-35	1
gb|U22411|HSU22411	Human inward rectifier potassium ch...	549	1.2e-35	1
gb|AF021142|AF021142	Cavia porcellus inward rectifier po...	547	1.8e-35	1
emb|Z48971|CCIRK1	C.cobaya gene for inward rectifier ...	547	1.8e-35	1
gb|U11075|MMU11075	Mus musculus inwardly-rectifying K+...	502	9.9e-32	1
gb|S81771|S81771	Inwardly rectifying K+ channel IRK3...	502	9.9e-32	1
emb|X81580|RNIRPC|1	R.norvegicus mRNA for inward rectif...	502	9.9e-32	1
emb|X87435|RNBIRK1	R.norvegicus mRNA for inwardly rect...	502	9.9e-32	1
gb|S71182|S71182	MB-[RK]=class 3 inward rectifier po...	502	9.9e-32	1
gb|U27582|RNU27582	Rattus norvegicus brain inwardly re...	491	5.6e-31	1
gb|U52152|HSU52152	Human inwardly rectifying potassium...	269	2.4e-12	1
gb|U92801|OCU92801	Oryctolagus cuniculus K-ATP channel...	266	4.2e-12	1
db|D50582|HUMIRKCB	Human gene for inward rectifier K c...	262	9.1e-12	1
gb|U90581|HSU90581	Human 86Kb contig from chromosome 1...	262	9.1e-12	1
gb|AF008262|AF008262	Oryctolagus cuniculus ATP-sensitive...	244	2.9e-10	1
db|D50111|D50111	Porcine mRNA for inward rectifying ...	211	2.3e-08	1
gb|U52154|HSU52154	Human G protein-coupled inwardly re...	217	5.0e-08	1
gb|U19195|HSU19195	Human clone KGP G-protein coupled i...	217	5.0e-08	1
emb|X81582|HSKATP	H.sapiens mRNA for KATP (cardiac)	217	5.0e-08	1
db|D50114|D50114	Human mRNA for inward rectifying K ...	217	5.0e-08	1
gb|L27929|RATRK1C	Rattus norvegicus G protein-activat...	215	7.4e-08	1
gb|L47208|HUMGIRK	Human G protein-activated inwardly ...	208	2.8e-07	1
gb|U52153|HSU52153	Human inwardly rectifying potassium...	199	1.6e-06	1
db|D87127|D87127	Human mRNA for G protein-coupled in...	199	1.6e-06	1
gb|L78480|HUMKIR1B	Homo sapiens inwardly rectifying po...	199	1.6e-06	1
gb|U78485|U78485	KCNJ6/BIR1=ATP-sensitive inwardly r...	199	1.6e-06	1
gb|U24440|HSU24440	Human G protein coupled inward rect...	199	1.6e-06	1
gb|U21082|RNU21082	Rattus norvegicus potassium channel...	190	8.9e-06	1

Appendix 3: β-Actin Riboprobe Template BLAST2.0 Search

BLAST2.0 search confirming high specificity of the β-actin riboprobe template by comparison to other similar sequences.

Sequences producing High-scoring Segment Pairs:		High Score	Smallest Sum Probability P(N)	N
emb|X03672|MMACTBR	Mouse cytoskeletal mRNA for beta-actin	958	6.7e-70	1
gb|J04181|MUSACTMEL	Mouse A-X actin mRNA, complete cds.	958	6.7e-70	1
emb|X03765|MMACTBR2	Mouse mRNA for cytoplasmatic beta-a...	949	3.8e-69	1
gb|M12481|MUSACCYB	Mouse cytoplasmic beta-actin mRNA.	949	3.8e-69	1
gb|J00691|RATACCYB	Rat cytoplasmic beta-actin gene, co...	807	3.0e-66	2
emb|V01217|RNAC01	Rat gene encoding cytoplasmic beta-...	807	3.0e-66	2
dbj|AB004047|AB004047	Human mRNA for beta-actin, complete...	886	6.5e-64	1
gb|AF014364|AF014364	Cricetinae gen. sp. beta actin mRNA...	886	6.5e-64	1
gb|AF014363|AF014363	Cricetinae gen. sp. beta actin mRNA...	886	6.5e-64	1
emb|V00478|HSAC01	Human mRNA fragment encoding cytopl...	841	3.6e-60	1
emb|X00351|HSAC07	Human mRNA for beta-actin	841	3.6e-60	1
gb|U20114|CGU20114	Cricetulus griseus beta-actin (ACTB...	726	1.5e-59	2
emb|X63432|HSACTB	H.sapiens ACTB mRNA for mutant beta...	832	2.0e-59	1
gb|AF035774|AF035774	Equus caballus beta actin mRNA, com...	823	1.1e-58	1
gb|L08165|CHKBACTN	Gallus gallus beta-actin mRNA, comp...	805	3.6e-57	1
emb|X52815|RRGAMACT	Rat mRNA for cytoplasmic-gamma isof...	805	3.6e-57	1
gb|U39357|OAU39357	Ovis aries beta actin mRNA, complet...	805	3.6e-57	1
gb|M21495|MUSACTGCS	Mouse cytoskeletal gamma-actin mRNA...	796	2.0e-56	1
gb|U67202|CFU67202	Canis familiaris beta-actin mRNA, p...	796	2.0e-56	1
emb|X13055|MMGACTR	Murine mRNA for cytoplasmic gamma-a...	796	2.0e-56	1
emb|X13053|MMPG36	Murine cytoskeletal gamma-36-actin ...	787	1.1e-55	1
gb|M10142|MUSACTPSE	Mouse cytoplasmic gamma-actin proce...	787	1.1e-55	1
emb|X02443|MMACTG1	Mouse processed gene related to cyt...	787	1.1e-55	1
emb|X13049|MMPG14LH	Murine DNA for cytoskeletal gamma-a...	769	3.5e-54	1
emb|X04098|HSACTCGR	Human mRNA for cytoskeletal gamma-a...	769	3.5e-54	1
gb|U07786|SSU07786	Sus scrofa beta actin mRNA, partial...	760	2.0e-53	1
gb|M16247|HUMACTGAA	Human gamma-actin mRNA, partial cds.	760	2.0e-53	1
gb|AF025305|AF025305	Danio rerio beta actin mRNA, comple...	760	2.0e-53	1
emb|X16940|HSSMGA	Human mRNA for enteric smooth muscl...	760	2.0e-53	1
emb|X13056|MMPG118	Murine gamma-118-actin pseudogene	751	1.1e-52	1
gb|AF035422|AF035422	Ovis aries beta-actin mRNA, partial...	751	1.1e-52	1
gb|M24770|XELACTIN8A	Xenopus laevis cytoskeletal actin t...	751	1.1e-52	1
gb|M26689|MUSGAAC	Mus musculus smooth muscle gamma ac...	751	1.1e-52	1
emb|Z38130|LPACT3	L.polyphemus mRNA for actin.	742	6.2e-52	1
gb|AF057040|AF057040	Danio rerio beta-actin mRNA, comple...	742	6.2e-52	1
emb|V00481|HSAC04	Human beta-actin related pseudogene...	742	6.2e-52	1
emb|X02648|GG5ACT1	Chicken gene for type 5 nonmuscle a...	742	6.2e-52	1
gb|L36342|MOZBEAC	Morone saxatilis (striped bass) bet...	733	3.5e-51	1
gb|AF038150|AF038150	Mustela putorius furo beta-actin mR...	733	3.5e-51	1
emb|X60733|OCRNAGNMA	O.cuniculus mRNA for gamma-non musc...	733	3.5e-51	1
emb|X89920|SABTACTIN	S.aurata mRNA for beta-actin protein	733	3.5e-51	1
gb|M22323|RATACTGE	Rat gamma-enteric smooth muscle act...	733	3.5e-51	1
gb|L21996|MUSGA	Mouse cytoplasmic gamma-actin gene,...	651	4.4e-51	2
gb|M28424|HUMACTA1	Human beta-actin mRNA, partial cds	730	6.2e-51	1
gb|L07775|ECCACT	Echinococcus granulosus actin mRNA,...	724	2.0e-50	1
gb|U02283|DDU02283	Diphyllobothrium dendriticum clone ...	724	2.0e-50	1
gb|K00667|DROACT5CX	D.melanogaster actin gene, complete...	724	2.0e-50	1
gb|M26111|GOOACTB	Goose beta-actin mRNA, complete cds.	724	2.0e-50	1
gb|M24769|XELACTIN5A	Xenopus laevis cytoskeletal actin t...	724	2.0e-50	1
gb|U02282|DDU02282	Diphyllobothrium dendriticum clone ...	724	2.0e-50	1
gb|M55083|HUMACTGXPS	Human gamma actin-like pseudogene, ...	718	6.2e-50	1
gb|U27835|DDU27835	Diphyllobothrium dendriticum clone ...	715	1.1e-49	1
emb|Y13663|BLY13663	Branchiostoma lanceolatum mRNA for ...	715	1.1e-49	1
emb|X05106|PWAACTR	Salamander mRNA fragment for skelet...	715	1.1e-49	1
gb|AF012125|AF012125	Salmo salar beta actin mRNA, comple...	706	6.1e-49	1
gb|U27833|DDU27833	Diphyllobothrium dendriticum clone ...	706	6.1e-49	1
gb|M28996|TAEACTA	Taenia solium (clone pAT5) actin ge...	706	6.1e-49	1
dbj|D87738|D87738	Amphioxus mRNA for cytoplasmic acti...	706	6.1e-49	1
gb|AF019887|AF019887	Mus musculus metalloprotease-disint...	706	6.1e-49	1
emb|X13297|MMACTASM	Mouse mRNA for vascular smooth musc...	706	6.1e-49	1
gb|M19283|HUMACTGA	Human cytoskeletal gamma-actin gene...	637	1.5e-48	2

Appendix 4: Alignment of Rat and Mouse Kir2.2 cDNAs

BLAST2.0 searching indicates that rat and mouse Kir2.2 cDNAs have the highest degree of homology within the database. This is shown by a BLAST2.0 programme print out and an alignment of rat and mouse Kir2.2 cDNAs. The sequences corresponding to the Kir2.2 N- and C-terminal riboprobe templates are indicated by lines. Identical bases are indicated by bold letters contained within dark grey boxes. Non-identical bases are represented in normal capital typeface, on a white background (alignment was made using MacVector 6.0.1, Oxford Molecular Group PLC).

Sequences producing High-scoring Segment Pairs:		High Score	Smallest Sum Probability P(N)	N
emb|X80417|MMMBIRK2	M.musculus MB-IRK2 mRNA	8745	0.0	1
emb|X78461|RNRBIRK2	R. norvegicus RB-IRK2 cDNA	7441	0.0	1
gb|U53143|HSU53143	Human inward rectifying K+ channe...	4033	0.0	3
gi|4504844	Homo sapiens potassium inwardly-r...	4003	0.0	3
gb|L36069|HUMHCIR	Human high conductance inward rec...	3703	0.0	5
gb|AF005214|AF005214	Homo sapiens inward rectifying K+...	2231	3.9e-249	5
gb|U24056|HSU24056	Human inward rectifier K+ channel...	2406	2.1e-239	2
gi|4826797	Homo sapiens potassium inwardly-r...	2415	2.2e-239	2
gb|S72503|S72503	HRK1=inward rectifier potassium c...	2415	1.2e-238	2
emb|X83580|RNIRPC11	R.norvegicus mRNA for inward rect...	2403	2.7e-237	2
emb|X87635|RNRIRK3	R.norvegicus mRNA for inwardly re...	2403	5.5e-237	2
dbj|AB024304.1|AB024304	Mus musculus mRNA for inward rect...	2411	9.7e-236	2
emb|Z97056|HS434P1	Human DNA sequence from PAC 434P1...	2415	1.5e-235	4
gb|U95369|BTU95369	Bos taurus inward rectifier potas...	2386	4.6e-235	3
gb|U11075|MMU11075	Mus musculus inwardly-rectifying ...	2411	7.1e-235	2
gb|AF020792|AF020792	Bos taurus inward rectifier potas...	2377	7.9e-235	2
gb|S71382|S71382	MB-IRK3=class 3 inward rectifier ...	2411	9.3e-235	2
gb|S81773|S81773	inwardly rectifying K+ channel IR...	2280	3.3e-225	2
gb|AF021138|AF021138	Oryctolagus cuniculus inward rect...	2152	4.4e-212	2
dbj|D21057|RABPC	Rabbit mRNA for potassium channel...	2152	8.3e-212	2
gb|AF021136|AF021136	Mus musculus inward rectifier pot...	2144	2.0e-208	2
gb|L48490|RATRBIR	Rattus norvegicus inwardly rectif...	2116	2.4e-208	2
emb|X73052|MMIRK1	M. musculus mRNA for inward recti...	2144	3.5e-208	2
gb|AF021137|AF021137	Rattus norvegicus inward rectifie...	2107	1.3e-207	2
gb|AF021141|AF021141	Gallus gallus inward rectifier po...	2155	5.1e-206	2
gb|U20216|GGU20216	Gallus gallus inward rectifier po...	2146	4.8e-205	2
gb|AF021135|AF021135	Macaca mulatta inward rectifier p...	2080	8.4e-204	3
gi|4504834	Homo sapiens potassium inwardly-r...	2080	1.2e-202	3
gb|U16861|HSU16861	Human inward rectifying potassium...	2080	1.2e-202	3
gb|AF021139|AF021139	Homo sapiens inward rectifier pot...	2080	2.6e-202	3
gb|U22413|HSU22413	Human inward rectifier potassium ...	2080	4.9e-202	2
gb|U24055|HSU24055	Human inward rectifier K+ channel...	2080	5.4e-202	3
emb|Z48971|CCIRK1	C.cobaya gene for inward rectifie...	2071	1.2e-201	2
gb|AF011904|AF011904	Homo sapiens inwardly rectifying ...	2062	2.6e-201	3
gb|AF021142|AF021142	Cavia porcellus inward rectifier ...	2062	5.9e-201	2
gb|AC005242|AC005242	Homo sapiens chromosome 17, clone...	2080	4.4e-199	4
gb|U27582|RNU27582	Rattus norvegicus brain inwardly ...	1548	1.0e-189	4
gb|AF021140|AF021140	Sus scrofa inward rectifier potas...	2215	4.0e-173	1
emb|AJ003065|RNAJ3065	Rattus norvegicus mRNA for Kir2.4...	1756	3.5e-165	2
gi|4826803	Homo sapiens potassium inwardly-r...	1757	5.0e-135	1
dbj|D50133|D50133	Porcine mRNA for inward rectifyin...	1719	7.2e-132	1
gb|AF130860.1|AF130860	Mus musculus GIRK3 (Kir3.3) mRNA,...	1703	1.5e-130	1
gb|U11860|MMU11860	Mus musculus G protein coupled in...	1685	4.9e-129	1
gb|L77929|RATRK3G	Rattus norvegicus G protein-activ...	1649	4.8e-126	1
gb|U39195|HSU39195	Human clone KGP G-protein coupled...	1634	8.5e-125	1
emb|X83582|HSKATP	H.sapiens mRNA for KATP (cardiac)	1634	8.5e-125	1
gi|4826799	Homo sapiens potassium inwardly-r...	1634	8.5e-125	1
dbj|D50134|D50134	Homo sapiens mRNA for inward rect...	1616	2.7e-123	1
gb|L47208|HUMGIRK	Human G protein-activated inwardl...	1607	1.5e-122	1
dbj|D50135|D50135	Rattus norvegicus mRNA for inward...	1540	5.6e-117	1
gb|L35771|RATKCHANN	Rattus norvegicus potassium chann...	1531	3.1e-116	1
gb|L35555|CHKGIRK	Gallus gallus GIRK1 mRNA, complet...	1520	2.6e-115	1
emb|X83584|RNKATP	R.norvegicus mRNA for KATP (cardiac)	1504	5.5e-114	1
dbj|AB019560|AB019560	Mus musculus mRNA for G-protein-a...	1504	5.5e-114	1
gb|U39196|HSU39196	Human clone hGIRK1 G-protein coup...	1459	3.1e-110	1

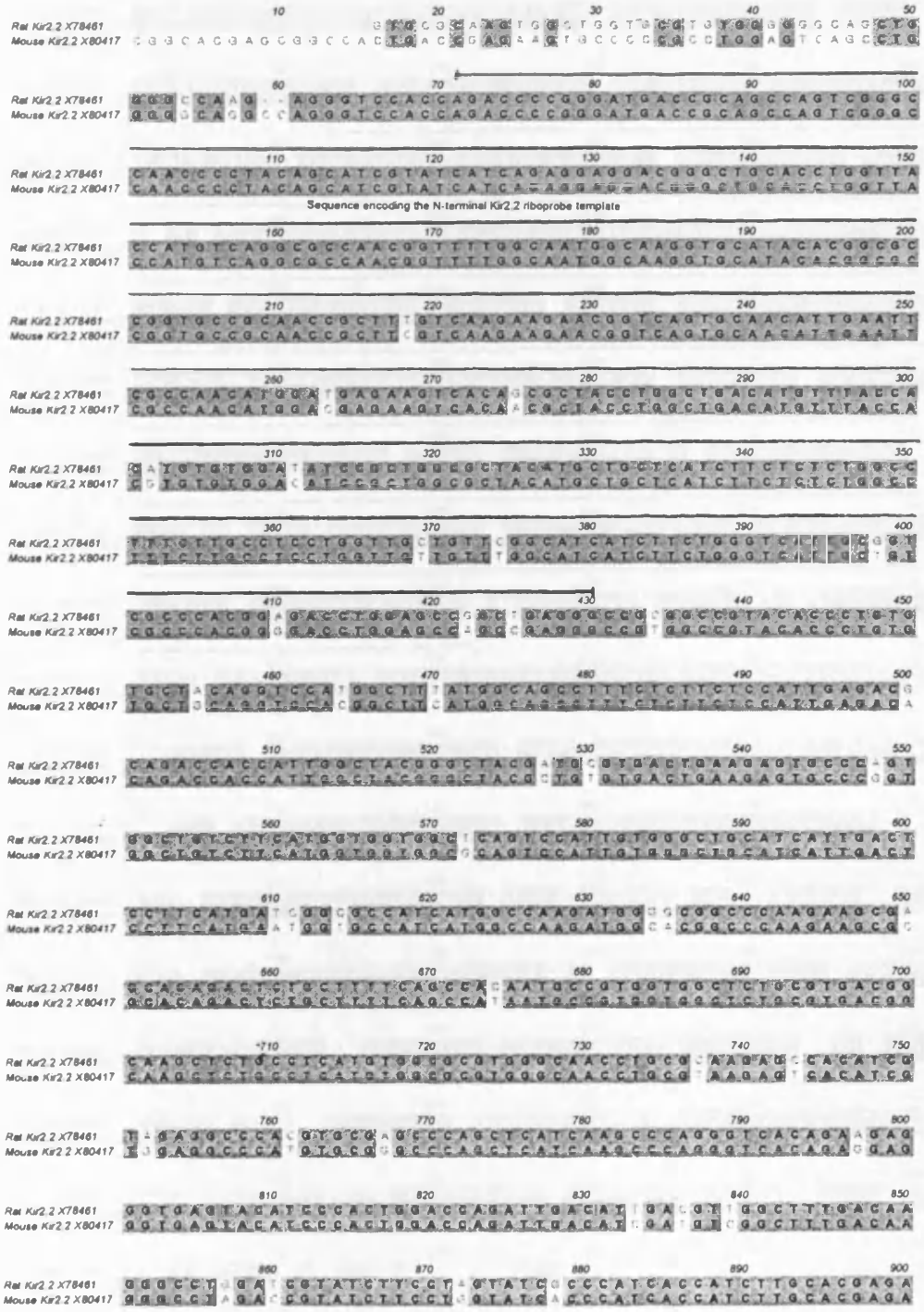
Rat Kir2.2 X78461
Mouse Kir2.2 X80417
Sequence encoding the N-terminal Kir2.2 riboprobe template

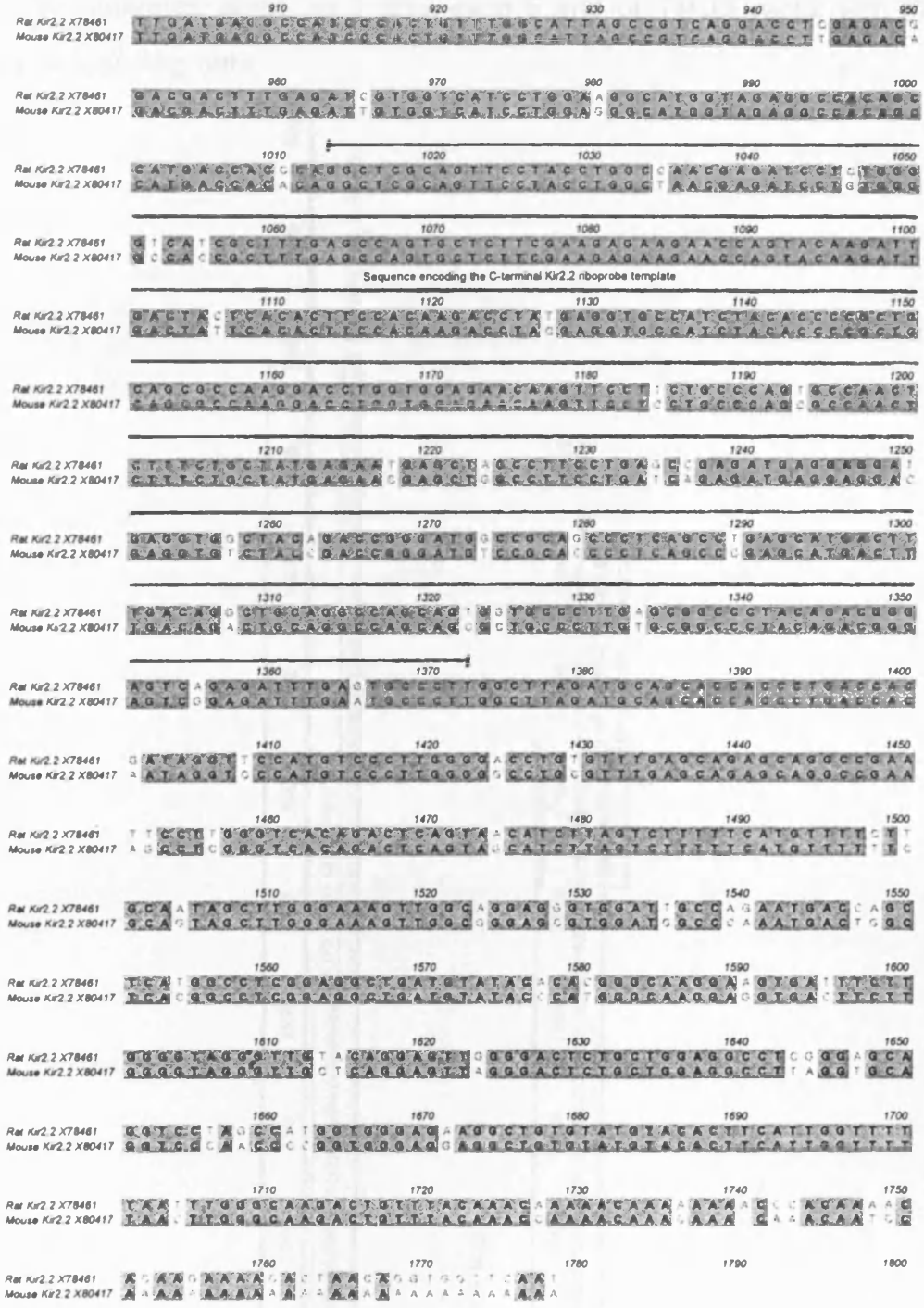
Rat Kir2.2 X78461
Mouse Kir2.2 X80417
Sequence encoding the C-terminal Kir2.2 riboprobe template

Appendix 5: β-Actin cDNA Fragment Sequencing

The Assembly-Lign programme (version 1.0.7, Kodak, New Haven, CT) was used to separately align the β-actin exon 5 and pLITMUS vector with the β-actin sequencing data.

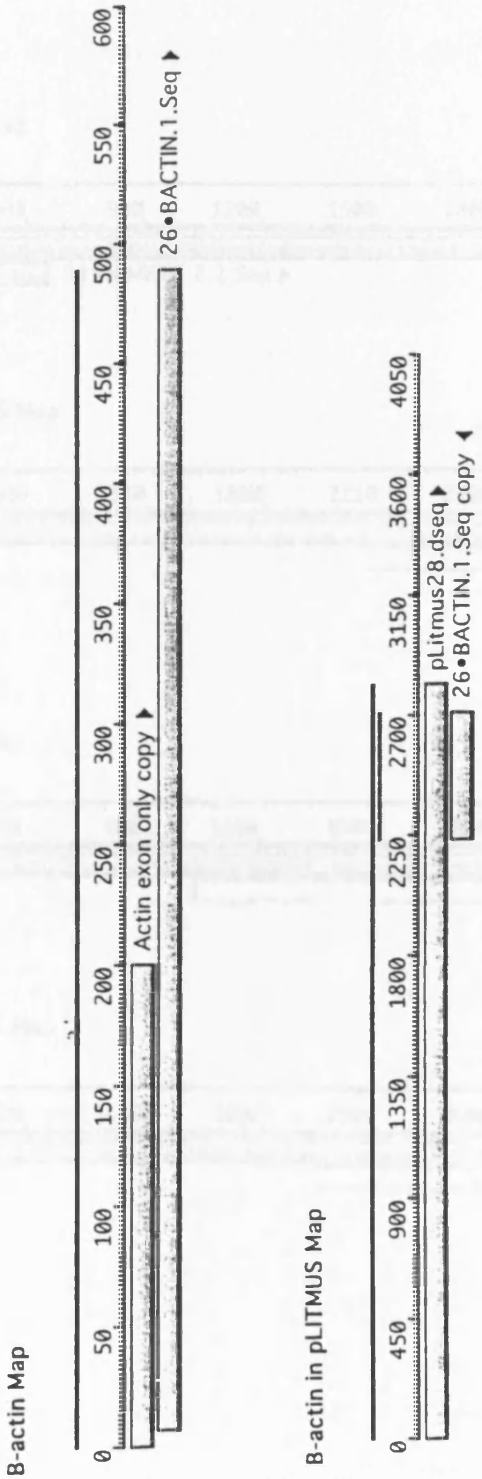

Appendix 6: Kir2.2 N- and C-Terminal cDNA Fragment Sequencing

The Assembly-Lign programme (version 1.0.7, Kodak, New Haven, CT) was used to separately align the Kir2.2 cDNA and pLITMUS vector with the Kir2.2 N- and C-terminal cDNA sequencing data.

Nterm Kir2.2 probe Map

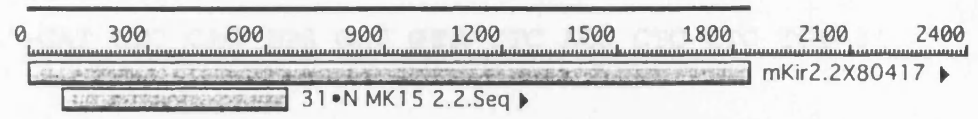

Nterm Kir2.2 pLITMUS Map

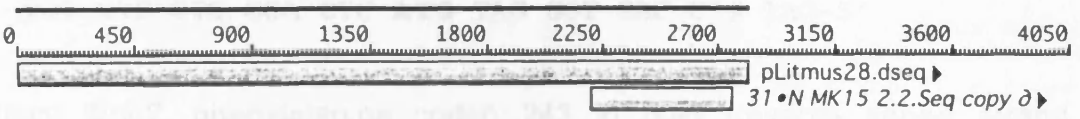

Cterm Kir2.2 probe Map

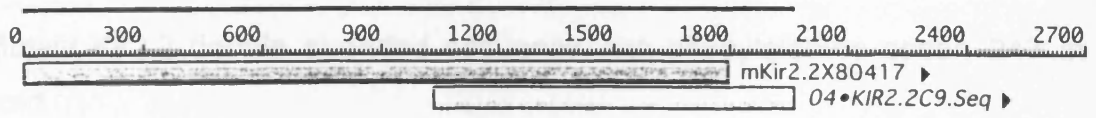

Cterm Kir2.2 pLITMUS Map

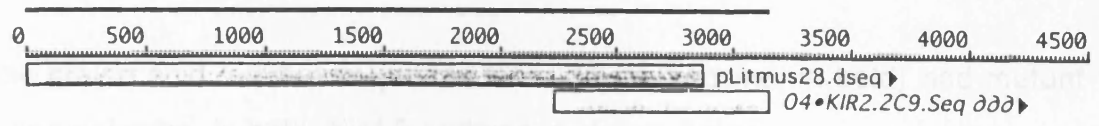

Appendix 7: Kir2.2 (Y243F) cDNA Sequencing

The entire Kir2.2 (Y243F) mutant cDNA was sequenced, revealing no further mutations from wild type. The mutated tyrosine to phenylalanine codon, flanked by five non-mutated codons on either side is shown below.

Wild type Kir2.2: tyrosine codon 243 in bold (reverse sense strand sequence).

5′-GAT GTC CAG TGG GAT **GTA** CTC ACC CTC CTC TGT-3′

Wild type Kir2.2 double stranded sequence with tyrosine codon 243 in bold.

5′-ACA GAG GAG GGT GAG **TAC** ATC CCA CTG GAC ATC-3′
3′-TGT CTC CTC CCA CTC **ATG** TAG GGT GAC CTG TAG-5′

Mutant Kir2.2: phenylalanine codon 243 in bold (reverse sense strand sequence).

5′-GAT GTC CAG TGG GAT **GAA** CTC ACC CTC CTC TGT-3′

Mutant Kir2.2 double stranded sequence with phenylalanine codon 243 in bold.

5′-ACA GAG GAG GGT GAG **TTC** ATC CCA CTG GAC ATC-3′
3′-TGT CTC CTC CCA CTC **AAG** TAG GGT GAC CTG TAG-5′

The amino acid residue sequence for wild type (tyrosine, in bold) and mutant (phenylalanine, in bold) Kir2.2 proteins is shown below:

NH_2-Thr-Glu-Glu-Gly-Glu-**Tyr**-Ile-Pro-Leu-Glu-Ile-COOH

NH_2-Thr-Glu-Glu-Gly-Glu-**Phe**-Ile-Pro-Leu-Glu-Ile-COOH

References

Abbadie, C., Trafton, J., Liu, H., Mantyh, P. and Basbaum, A. (1997) Inflammation increases the distribution of dorsal horn neurons that internalise the neurokinin-1 receptor in response to noxious and non-noxious stimulation. *The Journal of Neuroscience*, **17**, 8049-8060.

Abrams, C., Davies, N., Shelton, P. and Stanfield, P. (1996) The role of a single aspartate residue in ionic selectivity and block of a murine inward rectifier K^+ channel Kir2.1. *Journal of Physiology*, **493**, 643-649.

Ali, S., Chen, X., Lu, M., Xu, J., Lerea, K. and Hebert, S. (1998) The A kinase anchoring protein is required for mediating the effect of protein kinase A on ROMK1 channels. *Proceedings of the National Academy of Sciences USA*, **95**, 10274-10278.

Altschul, S., Madden, T., Shaffer, A., Zhang, J., Miller, W. and Lipman, D. (1997) Gapped BLAST and PSI-BLAST: a new generation of protein database search programs. *Nucleic Acids Research*, **25**, 3389-3402.

Armstrong, C. and Bezanilla, F. (1977) Inactivation of the sodium channel. II Gating current experiments. *Journal of General Physiology*, **70**, 567-690.

Aston-Jones, G., Ennis, M., Pieribone, V., Nickell, W. and Shipley, M. (1986) The brain nucleus locus coeruleus: Restricted afferent control of a broad efferent network. *Science*, **234**, 734-737.

Aston-Jones, G., Shipley, M., Chouvet, G., Ennis, M., van Bockstaele, E., Pieribone, V., Shiekhattar, R., Akaoka, H., Drolet, G., Astier, B., Charlety, P., Valentino, R. and Williams, J. (1991) Afferent regulation of locus coeruleus neurons: Anatomy, physiology and pharmacology. *Progress in Brain Research*, **88**, 47-76.

Atherton, E. and Sheppard, R. (1985) Solid-phase peptide-synthesis using N-alpha-fluorenylmethoxycarbonylamino acid pentafluorophenyl esters. *Journal of the Chemical Society*, **3**, 165-166.

Attali, B., Romey, G., Honore, E., Schmid-Alliana, A., Mattei, M., Lesage, F., Ricard, P., Barhanin, J. and Lazdunski, M. (1992) Cloning, functional expression, and regulation of two K^+ channels in human T lymphocytes. *Journal of Biological Chemistry*, **267**, 8650-8657.

Baldino, F. and Lewis, M. (1989) Nonradioactive *in situ* hybridisation histochemistry with digoxigenin-deoxyuridin 5'-triphosphate-labelled oligonucleotides. *Methods in Neuroscience. Gene Probes.* San Diego, CA: Academic. pp. 282-292.

Baldwin, T., Tsaur, M., Lopez, G., Jan, Y. and Jan, L. (1991) Characterisation of a mammalian cDNA for an inactivating voltage-sensitive K^+ channel. *Neuron*, **7**, 471-483.

Barak, L., Warabi, K., Feng, X., Caron, M. and Kwatra, M. (1999) Real-time visualisation of the cellular redistribution of G protein-coupled receptor

kinase 2 and β-arrestin 2 during homologous desensitization of the substance P receptor. *Journal of Biological Chemistry*, **274**, 7565-7569.

Baumann, A., Grupe, A., Ackermann, A. and Pongs, O. (1988) Structure of the voltage-dependent potassium channel is highly conserved from Drosophila to vertebrate central nervous systems. *EMBO Journal*, **7**, 2457-2463.

Bausch, S., Patterson, T., Ehrengruber, M., Lester, H., Davidson, N. and Chavkin, C. (1995) Colocalisation of mu opioid receptors with GIRK1 potassium channels in the rat brain: An immunocytochemical study. *Receptors and Channels*, **3**, 221-241.

Bezanilla, F. and Stefani, E. (1994) Voltage-dependent gating of ionic channels. *Annual Review of Biophysics and Biomolecular Structure*, **23**, 819-846.

Blair, T., Roberds, S., Tamkun, M. and Hartshorne, R. (1992) Protein kinase C modulates the RK5 K^+ current. *Biophysical Journal*, **61**, A2199.

Bond, C., Pessia, M., Xia, X., Lagrutta, A., Kavanaugh, M. and Adelman, J. (1994) Cloning and expression of a family of inward rectifier potassium channels. *Receptors and Channels*, **2**, 183-191.

Brew, H., Gray, P., Mobbs, P. and Attwell, D. (1986) Endfeet of retinal glial cells have higher densities of ion channels that mediate K^+ buffering. *Nature*, **324**, 466-468.

Butler, A., Wei, A. and Salkoff, L. (1990) Shal, Shab, and Shaw: three genes encoding potassium channels in Drosophila. *Nucleic Acids Research*, **18**, 2173-2174.

Cai, Y. and Douglass, J. (1993) *In-vivo* and *in-vitro* phosphorylation of the T-lymphocyte type-N (Kv1.3) potassium channel. *Journal of Biological Chemistry*, **268**, 23720-23727.

Cao, Y., Mantyh, P., Carlson, E., Gillespie, A., Epstein, C. and Basbaum, A. (1998) Primary afferent tachykinins are required to experience moderate to intense pain. *Nature*, **392**, 390-393.

Chein, C., Bartel, P., Sternglanz, R. and Fields, S. (1991) The two hybrid system: a method to identify and clone genes for proteins that interact with a protein of interest. *Proceedings of the National Academy of Sciences USA*, **88**, 9578-9582.

Cho, K., Hunt, C. and Kennedy, M. (1992) The rat brain postsynaptic density fraction contains a homolog of the *Drosophila* discs-large tumor suppressor protein. *Neuron*, **9**, 929-942.

Choi, K., Aldrich, R. and Yellen, G. (1991) Tetraethylammonium blockade distinguishes two inactivation mechanisms in voltage-activated K^+ channels. *Proceedings of the National Academy of Sciences USA*, **88**, 5092-5095.

Cirelli, C., Pompeiano, M. and Tononi, G. (1996) Neuronal gene expression in the waking state: a role for the locus coeruleus. *Science*, **274**, 1211-1215.

Cohen, N., Brenman, J., Snyder, S. and Bredt, D. (1996a) Binding of the inward rectifier K^+ channel Kir 2.3 to PSD-95 is regulated by protein kinase A phosphorylation. *Neuron*, **17**, 759-767.

Cohen, N., Sha, Q., Makhina, E., Lopatin, A., Linder, M., Snyder, S. and Nichols, C. (1996b) Inhibition of an inward rectifier potassium channel (Kir2.3) by G-protein $\beta\gamma$ subunits. *Journal of Biological Chemistry*, **271**, 32301-32305.

Conklin, B. and Bourne, H. (1993) Structural elements of $G\alpha$ subunits that interact with $G\beta\gamma$, receptor, and effectors. *Cell*, **73**, 631-641.

Conn, H. and Darrow, M. (1943) *Staining Procedures*. Geneva: N.Y. Biotech Publications.

Covarrubias, M., Wei, A. and Salkoff, L. (1991) Shaker, Shal, Shab, and Shaw express independent K^+ current. *Neuron*, **7**, 763-773.

Curran, M., Landes, G. and Keating, M. (1992) Molecular-cloning, characterisation, and genomic localisation of a human potassium channel gene. *Genomics*, **12**, 729-737.

Dascal, N., Lim, N., Schreibmayer, W., Wang, W., Davidson, N. and Lester, H. (1993a) Expression of an atrial G-protein-activated potassium channel in *Xenopus* oocytes. *Proceedings of the National Academy of Sciences USA*, **90**, 6596-6600.

Dascal, N., Scheibmayer, W., Lim, N., Wang, W., Chavkin, C., DiMagno, L., Labarca, C., Kieffer, B., Gaveriaux-Ruff, C., Trollinger, D., Lester, H. and Davidson, N. (1993b) Atrial G protein-activated K^+ channel: Expression cloning and molecular properties. *Proceedings of the National Academy of Sciences USA*, **90**, 10235-10239.

Daub, H., Weiss, F., Wallasch, C. and Ullrich, A. (1996) Role of transactivation of the EGF receptor in signalling by G-protein-coupled receptors. *Nature*, **379**, 557-560.

De Felipe, C., Herrero, J., O'Brien, J., Palmer, J., Doyle, C., Smith, A., Laird, J., Belmonte, C., Cervero, F. and Hunt, S. (1998) Altered nociception, analgesia and aggression in mice lacking the receptor for substance P. *Nature*, **392**, 394-397.

Doupnik, C., Davidson, N. and Lester, H. (1995) The inward rectifier potassium channel family. *Current Opinion in Neurobiology*, **5**, 268-277.

Doyle, D., Cabral, J., Pfuetzner, R., Kuo, A., Gulbis, J., Cohen, S., Chait, B. and MacKinnon, R. (1998) The structure of the potassium channel: Molecular basis of K^+ conduction and selectivity. *Science*, **280**, 69-76.

Draguhn, A., Borner, G., Beckmann, R., Buchner, K., Heinemann, U. and Hucho, F. (1997) Large-conductance cation channels in the envelope of nuclei from rat cerebral cortex. *Journal of Membrane Biology*, **158**, 159-166.

Edwards, F., Hirst, G. and Silverberg, G. (1988) Inward rectification in rat cerebral arterioles; involvement of potassium ions in autoregulation. *Journal of Physiology*, **404**, 455-466.

Edwards, G., Dora, K., Gardner, M., Garland, C. and Weston, A. (1998) K^+ is an endothelium-derived hyperpolarising factor in rat arteries. *Nature*, **396**, 269-272.

Fahrig, S., Snyders, D., Knoth, K., Tamkun, M. and Murray, K. (1992) Depression of a human cardiac K^+ current by stimulation of protein kinase C. *Biophysical Journal*, **61**, A2208.

Falk, T., Meyerhof, W., Corrette, B., Schafer, J., Bauer, C., Schwarz, J. and Richter, D. (1995) Cloning, functional expression and mRNA distribution of an inwardly rectifying potassium channel protein. *FEBS Letters*, **367**, 127-131.

Farquharson, M., Harvie, R. and McNicol, A. (1990) Detection of messenger RNA using a digoxigenin end labelled oligodeoxynucleotide probe. *Journal of Clinical Pathology*, **42**, 424-428.

Fields, S. and Song, O. (1989) A novel genetic system to detect protein-protein interactions. *Nature*, **340**, 245-246.

Foote, S., Berridge, C., Adams, L. and Pineda, J. (1991) Electrophysiological evidence for the involvement of locus coeruleus in alert, orienting and attending. *Progress in Brain Research*, **88**, 521-532.

Fraser, I. and Scott, J. (1999) Modulation of ion channels: a "current" view of AKAPs. *Neuron*, **23**, 423-246.

Frech, G., Vandongen, A., Schuster, G., Brown, A. and Joho, R. (1989) A novel potassium channel with delayed rectifier properties isolated from rat brain by expression cloning. *Nature*, **340**, 642-645.

Futami, T., Hatanaka, Y., Matsushita, K. and Furuya, S. (1998) Expression of substance P receptor in the substantia nigra. *Molecular Brain Research*, **54**, 183-198.

Gall, G. and Pardue, M. (1969) Formation and detection of RNA-DNA hybrid molecules in cytological preparations. *Proceedings of the National Academy of Sciences USA*, **63**, 378-81.

Gerasimenko, O., Gerasimenko, J., Tepikin, A. and Petersen, O. (1995) ATP-dependent accumulation and inositol trisphosphate- or cyclic ADP-ribose-mediated release of Ca^{2+} from the nuclear envelope. *Cell*, **80**, 439-444.

Gerasimenko, O., Gerasimenko, J., Tepikin, A. and Petersen, O. (1996) Calcium transport pathways in the nucleus. *Pflugers Archiv-European Journal of Physiology*, **432**, 1-6.

Gerfen, C. (1991) Substance P (neurokinin -1) receptor mRNA is selectively expressed in cholinergic neurons in the striatum and basal forebrain. *Brain Research*, **556**, 165-170.

Grissmer, S. and Cahalan, M. (1989) TEA prevents inactivation while blocking open K^+ channels in human lymphocytes *Biophysical Journal*, **55**, 203-206.

Gudermann, T., Kalkbrenner, F. and Schultz, G. (1996) Diversity and selectivity of receptor-G protein interaction. *Annual Review of Pharmacology and Toxicology*, **36**, 429-459.

Hammond, D., Wainer, B., Tonsgard, J. and Heller, A. (1986) Neuronal properties of clonal hybrid cell-lines derived from central cholinergic neurons. *Science*, **234**, 1237-1240.

Harley, C. (1991) Noradrenergic and locus coeruleus modulation of the perforant path-evoked potential in rat dentate gyrus supports a role for locus coeruleus in attentional and memorial processes. *Progress in Brain Research*, **88**, 307-322.

He, Z., Zhang, H., Mirshahi, T. and Logothetis, D. (1999) Identification of a potassium channel site that interacts with $G\beta\gamma$ subunits to mediate agonist-induced signalling. *Journal of Biological Chemistry*, **274**, 12517-12524.

Helke, C., Krause, J., Mantyh, P., Couture, R. and Bannon, M. (1990) Diversity in mammalian tachykinin peptidergic neurons: multiple peptides, receptors, and regulatory mechanisms. *FASEB Journal*, **4**, 1606-1615.

Hille, B. (1992) *Ionic Channels of Excitable Membranes.* Sunderland, Mass: Sinauer. 2nd Edition.

Ho, K., Nichols, C., Lederer, W., Lytton, J., Vassilev, P., Kanazirska, M. and Herbert, S. (1993) Cloning and expression of an inwardly rectifying ATP-regulated potassium channel. *Nature*, **362**, 31-38.

Hodgkin, A. and Huxley, A. (1952) A quantitative description of membrane current and its application to conduction and excitation in nerve. *Journal of Physiology*, **117**, 500-544.

Holmes, T., Fadool, D. and Levitan, I. (1996a) Tyrosine phosphorylation of the Kv1.3 potassium channel. *Journal of Neuroscience*, **16**, 1581-1590.

Holmes, T., Fadool, D., Ren, R. and Levitan, I. (1996b) Association of Src tyrosine kinase with a human potassium channel mediated by SH3 domain. *Science*, **274**, 2089-2091.

Horio, Y., Hibino, H., Inanobe, A., Yamada, M., Ishii, M., Tada, Y., Satoh, E., Hata, Y., Takai, Y. and Kurachi, Y. (1997) Clustered and enhanced activity of an inwardly rectifying potassium channel, Kir4.1, by an anchoring protein PSD-95/SAP90. *Journal of Biological Chemistry*, **272**, 12885-12888.

Horio, Y., Morishige, K., Takahashi, N. and Kurachi, Y. (1996) Differential distribution of classical inwardly rectifying potassium channel mRNAs in the brain: comparison of IRK2 with IRK1 and IRK3. *FEBS Letters*, **379**, 239-243.

Huang, C., Feng, S. and Hilgemann, D. (1998) Direct activation of inward rectifier potassium channels by PIP_2 and its stabilisation by $G\beta\gamma$. *Nature*, **391**, 803-806.

Huang, C., Slesinger, P., Casey, P., Jan, Y. and Jan, L. (1995) Evidence that direct binding of Gβγ to the GIRK1 G protein-gated inwardly rectifying K^+ channel is important for channel activation. *Neuron*, **15**, 1133-1143.

Huang, X., Morielli, A. and Peralta, E. (1993) Tyrosine kinase-dependent suppression of a potassium channel by the G protein-coupled m1 muscarinic acetylcholine receptor. *Cell*, **75**, 1145-1156.

Huang, X., Morielli, A. and Peralta, E. (1994) Molecular basis of cardiac potassium channel stimulation by protein kinase A. *Proceedings of the National Academy of Sciences USA*, **91**, 624-628.

Hunter, T., Ling, N. and Cooper, J. (1984) Protein kinase C phosphorylation of the EGF receptor at a threonine residue close to the cytoplasmic face of the plasma membrane. *Nature*, **311**, 480-483.

Inagaki, N., Tsuura, Y., Namba, N., Masuda, K., Gonoi, T., Horie, M., Seino, Y., Mizuta, M. and Seino, S. (1995) Cloning and functional characterisation of a novel ATP-sensitive potassium channel ubiquitously expressed in rat tissues, including pancreatic islets, pituitary, skeletal muscle, and heart. *Journal of Biological Chemistry*, **270**, 5691-5694.

Inanobe, A., Yoshimoto, Y., Horio, Y., Morishige, K., Hibino, H., Matsumoto, S., Tokunaga, Y., Maeda, T., Hata, Y., Takai, Y. and Kurachi, Y. (1999) Characterisation of G-protein-gated K^+ channels composed of Kir3.2 subunits in dopaminergic neurons of the substantia nigra. *Journal of Neuroscience*, **19**, 1006-1017.

Inoue, K., Nakazawa, K., Inoue, K. and Fujimori, K. (1995) Non-selective cation channels coupled with tachykinin receptors in rat sensory neurons. *Journal of Neurophysiology*, **73**, 736-742.

Inoue, M., Nakajima, S. and Nakajima, Y. (1988) Somatostatin induces an inward rectification in rat locus coeruleus neurones through a pertussis toxin-sensitive mechanism. *Journal of Physiology*, **407**, 177-198.

Ishii, M., Horio, Y., Tada, Y., Hibino, H., Inanobe, A., Ito, M., Yamada, M., Gotow, T., Uchiyama, Y. and Kurachi, Y. (1997) Expression and clustered distribution of an inwardly rectifying potassium channel, K_{AB}-2/Kir4.1, on mammalian retinal Müller Cell Membrane: Their regulation by insulin and laminin signals. *Journal of Neuroscience*, **17**, 7725-7735.

Ivanina, T., Perets, T., Thornhill, W., Levin, G., Dascal, N. and Lotan, I. (1994) Phosphorylation by protein-kinase-A of RCK1 K^+ channels expressed in Xenopus oocytes. *Biochemistry*, **33**, 8786-8792.

Jonas, E. and Kaczmarek, L. (1996) Regulation of potassium channels by protein kinases. *Current Opinion in Neurobiology*, **6**, 318-323.

Jones, S. (1991) Descending noradrenergic influences on pain. *Progress in Brain Research*, **88**, 381-394.

Kamb, A., Weir, M., Rudy, B., Varmus, H. and Kenyon, C. (1989) Identification of genes from pattern formation, tyrosine kinase, and potassium channel

families by DNA amplification. *Proceedings of the National Academy of Sciences USA*, **86**, 4372-4376.

Kanemasa, T., Gan, L., Perney, T., Wang, L. and Kaczmarek, L. (1995) Electrophysiological and pharmacological characterisation of a mammalian Shaw channel expressed in NIH 3T3 fibroblasts. *Journal of Neurophysiology*, **74**, 207-217.

Karschin, A. and Wischmeyer, E. (1995) Identification of G protein-regulated inwardly rectifying K^+ channels in rat brain oligodendrocytes. *Neuroscience Letters*, **183**, 135-138.

Karschin, C., Dissmann, E., Stuhmer, W. and Karschin, A. (1996) IRK (1-3) and GIRK (1-4) inwardly rectifying K^+ channel mRNAs are differentially expressed in the adult rat brain. *Journal of Neuroscience*, **16**, 3559-3570.

Karschin, C. and Karschin, A. (1997) Ontogeny of gene expression of Kir channel subunits in the rat. *Molecular and Cellular Neuroscience*, **10**, 131-148.

Karschin, C., Schreibmayer, W., Dascal, N., Lester, H., Davidson, N. and Karschin, A. (1994) Distribution and localisation of a G protein-coupled inwardly rectifying K^+ channel in the rat. *FEBS Letters*, **348**, 139-144.

Kennedy, M., Nemec, J., Corey, S., Wickman, K. and Clapham, D. (1999) GIRK4 confers appropriate processing and cell surface localisation to G-

protein-gated potassium channels. *Journal of Biological Chemistry*, **274**, 2571-2582.

Kim, E., Niethammer, M., Rothschild, A., Jan, Y. and Sheng, M. (1995) Clustering of Shaker-type K^+ channels by interaction with a family of membrane-associated guanylate kinases. *Nature*, **378**, 85-88.

King, A., Ackley, M. and Slack, J. (1997) Profile of neuronal excitation following selective activation of the neurokinin-1 receptor in rat deep dorsal horn *in vitro*. *Brain Research*, **767**, 55-63.

Kobayashi, T., Ikeda, K., Ichikawa, T., Abe, S., Togashi, S. and Kumanishi, T. (1995) Molecular cloning of a mouse G-protein-activated K^+ channel (mGIRK1) and distinct distributions of three GIRK (GIRK1,2 and 3) mRNA's in mouse brain. *Biochemical and Biophysical Research Communications*, **208**, 1166-1173.

Kofuji, P., Davidson, N. and Lester, H. (1995) Evidence that neuronal G-protein-gated inwardly rectifying K^+ channels are activated by $G\beta\gamma$ subunits and function as heteromultimers. *Proceedings of the National Academy of Sciences USA*, **92**, 6542-6546.

Komminoth (1992) Digoxigenin as an alternative probe labelling for *in situ* hybridisation. *Diagnostic Molecular Pathology*, **1**, 142-150.

Komminoth, P., Merk, F., Leav, I., Wolfe, H. and Roth, J. (1992) Comparison of ^{35}S- and digoxigenin-labelled RNA and oligonucleotide probes for *in situ* hybridisation. *Histochemistry*, **98**, 217-228.

Koyama, H., Morishige, K., Takahashi, N., Zanelli, J., Fass, D. and Kurachi, Y. (1994) Molecular cloning, functional expression and localisation of a novel inward rectifier potassium channel in the rat brain. *FEBS Letters*, **341**, 303-307.

Koyano, K., Velimirovic, B., Grigg, J., Nakajima, S. and Nakajima, Y. (1993) Two signal transduction mechanisms of substance P-induced depolarisation in locus coeruleus neurons. *European Journal of Neuroscience*, **5**, 1189-1197.

Krapivinsky, G., Gordon, E., Wickman, K., Velimirovic, B., Krapivinsky, L. and Clapham, D. (1995) The G-protein-gated atrial K^+ channel I_{KACh} is a heteromultimer of two inwardly rectifying K^+ channel proteins. *Nature*, **374**, 135-141.

Krapivinsky, G., Kennedy, M., Nemec, J., Medina, I., Krapivinsky, L. and Clapham, D. (1998b) $G\beta\gamma$ binding to GIRK4 subunit is critical for G protein-gated K^+ channel activation. *Journal of Biological Chemistry*, **273**, 16946-16952.

Krapivinsky, G., Medina, I., Eng, L., Krapivinsky, L., Yang, Y. and Clapham, D. (1998a) A novel inward rectifier K^+ channel with unique pore properties. *Neuron*, **20**, 995-1005.

Kubo, Y., Baldwin, T., Jan, Y. and Jan, L. (1993a) Primary structure and functional expression of a mouse inward rectifier potassium channel. *Nature*, **362,** 127-133.

Kubo, Y., Reuveny, E., Slesinger, P., Jan, Y. and Jan, L. (1993b) Primary structure and functional expression of a rat G protein-coupled muscarinic potassium channel. *Nature*, **364,** 802-806.

Kugler, S., Grunweller, A., Probst, C., Klinger, M., Muller, P. and Kruse, C. (1996) Vigilin contains a functional nuclear localisation sequence and is present in both the cytoplasm and the nucleus. *FEBS Letters*, **382,** 330-334.

Kumar, G., Yan, D., Swaminathan, A., Yuan, Y., Sharma, A., Swaroop, A. and Hughes, B. (1999) Localisation and functional expression of a human inward rectifier K^+ channel, hKir2.4. *Investigative Ophthalmology & Visual Science*, **40,** 1131-B39.

Kunkel, M. and Peralta, E. (1995) Identification of domains conferring G protein regulation on inward rectifier potassium channels. *Cell*, **83,** 443-449.

Laemmli, U. (1970) Cleavage of structural proteins during the assembly of the head of bacteriophage T4. *Nature*, **227,** 680-685.

Larochelle, W., Wray, B., Sealock, R. and Froehner, S. (1985) Immunochemical demonstration that amino-acids 360-377 of the acetylcholine-receptor γ-subunit are cytoplasmic. *Journal of Cell Biology*, **100,** 684-691.

Lee, H., Hammond, D., Large, T. and Wainer, B. (1990) Immortalised young-adult neurons from the septal region-generation and characterisation. *Developmental Brain Research*, **52**, 219-228.

Lesage, F., Duprat, F., Fink, M., Guillemare, E., Coppola, T., Lazdunski, M. and Hugnot, J. (1994) Cloning provides evidence for a family of inward rectifier and G-protein coupled K^+ channels in the brain. *FEBS Letters*, **353**, 37-42.

Lev, S., Moreno, H., Martinez, R., Canoll, P., Peles, E. and Musacchio, J. (1995) Protein-tyrosine kinase PYK2 involved in Ca^{2+}-induced regulation of ion-channel and MAP kinase functions. *Nature*, **376**, 737-745.

Levitan, I. (1985) Phosphorylation of ion channels. *Journal of Membrane Biology*, **87**, 177-190.

Li, M., Jan, Y. and Jan, L. (1992) Specification of subunit assembly by the hydrophilic amino-terminal domain of the Shaker potassium channel. *Science*, **257**, 1225-1230.

Lieberman, D. and Mody, I. (1998) Substance P enhances NMDA channel function in hippocampal dentate gyrus granule cells. *Journal of Neurophysiology*, **80**, 113-119.

Liu, H., Mazarati, M., Katsumori, H., Sankar, R. and Wasterlain, C. (1999) Substance P is expressed in hippocampal principal neurons during status epilepticus and plays a critical role in the maintenance of status epilepticus. *Proceedings of the National Academy of Sciences USA*, **96**, 5286-5291.

Lopatin, A., Makhina, E. and Nichols, C. (1994) Potassium channel block by cytoplasmic polyamines as the mechanism of intrinsic rectification. *Nature*, **372**, 366-369.

Loughlin, S. and Fallon, J. (1985) *Locus coeruleus. The Rat Nervous System.* Academic Press Australia. pp. 79-93.

Luchian, T. and Shreibmayer, W. (1998) Ion permeation through a G-protein activated (GIRK1/GIRK5) inwardly rectifying potassium channel. *Biochemica et Biophysica Acta-Biomembranes*, **1368**, 167-170.

Luo, W., Sharif, T. and Sharif, M. (1996) Substance P-induced mitogenesis in human astrocytoma cells correlates with activation of the mitogen-activated protein kinase signalling pathway. *Cancer Research*, **56**, 4983-4991.

Luttrell, L., Daaka, Y. and Lefkowitz, R. (1999) Regulation of tyrosine kinase cascades by G-protein-coupled receptors. *Current Opinion in Cell Biology*, **11**, 177-183.

Ma, W., Zhang, L., Xing, G., Hu, Z., Iwasa, K. and Clay, J. (1998) Prenatal expression of inwardly rectifying potassium channel mRNA (Kir4.1) in rat brain. *Neuroreport*, **9**, 223-227.

MacFarlane, S. and Sontheimer, H. (1997) Electrophysiological changes that accompany reactive gliosis *in vitro*. *Journal of Neuroscience*, **17**, 7316-7329.

MacKinnon, R. (1991) Determination of the subunit stoichiometry of a voltage-activated potassium channel. *Nature*, **350**, 232-235.

Maeno, H., Kiyama, H. and Tohyama, M. (1993) Distribution of the substance P receptor (NK-1 receptor) in the central nervous system. *Molecular Brain Research*, **18**, 43-58.

Malmberg, A., Chen, C., Tonegawa, S. and Basbaum, A. (1997) Preserved acute pain and reduced neuropathic pain in mice lacking PKCγ. *Science*, **278**, 279-283.

Martin-Zanca, D., Oskam, R., Mitra, G., Copeland, T. and Barbacid, M. (1989) Molecular and biochemical characterisation of the human *trk* proto-oncogene. *Molecular Cell Biology*, **9**, 24-33.

Maruyama, Y., Shimada, H. and Taniguchi, J. (1995) Ca^{2+}- activated K^{+}-channels in the nuclear envelope isolated from single pancreatic acinar cells. *Pflugers Archiv-European Journal of Physiology*, **430**, 148-150.

McConalogue, K., Corvera, C., Gamp, P., Grady, E. and Bunnett, N. (1998) Desensitization of the neurokinin-1 receptor (NK1-R) in neurons: Effects of substance P on the distribution of NK1-R, $G(\alpha_{q11})$ G-protein receptor kinase - 2/3, and β-arrestin-1/2. *Molecular Biology of the Cell*, **9**, 2305-2324.

McCormack, K., Lin, L., Iverson, L., Tanouye, M. and Sigworth, F. (1992) Tandem linkage of Shaker K^{+} channel subunits does not ensure the stoichiometry of expressed channels. *Biophysical Journal*, **63**, 1406-1411.

McKinnon, D. (1989) Isolation of cDNA clone coding for a putative second potassium channel indicates the existance of a gene family. *Journal of Biological Chemistry*, **264**, 8230-8236.

Mi, H., Deerinck, T., Ellisman, M. and Schwarz, T. (1996) Inwardly rectifying K^+ channels that may participate in K^+ buffering in microvilli of Schwann-cells. *Journal of Neuroscience*, **16**, 2421-2429.

Minor, D., Masseling, S., Jan, Y. and Jan, L. (1999) Transmembrane structure of an inwardly rectifying potassium channel. *Cell*, **96**, 879-891.

Moreno, H., Kentros, C., Bueno, E., Weiser, M., Hernandez, A., Vega-Saenz de Miera, E., Ponce, A., Thornhill, W. and Rudy, B. (1995) Thalamocortical projections have a K^+ channel that is phosphorylated and modulated by cAMP-dependent protein-kinase. *Journal of Neuroscience*, **15**, 5486-5501.

Morin, X., Cremer, H., Hirsch, M., Kapur, R., Goridis, C. and Brunet, J.-F. (1997) Defects in sensory and autonomic ganglia and absence of locus coeruleus in mice deficient for the homeobox gene *Phox*2a. *Neuron*, **18**, 411-423.

Morishige, K., Takahashi, N., Findlay, I., Koyama, H., Zanelli, J., Peterson, C., Jenkins, N., Copeland, N., Mori, N. and Kurachi, Y. (1993) Molecular cloning, functional expression and localisation of an inward rectifier potassium channel in the mouse brain. *FEBS Letters*, **336**, 375-380.

Morishige, K., Takahashi, N., Jahangir, A., Yamada, M., Koyama, H., Zanelli, J. and Kurachi, Y. (1994) Molecular cloning and functional expression of a novel brain-specific inward rectifier potassium channel. *FEBS Letters*, **346**, 251-256.

Nakajima, Y., Tsuchida, K., Negishi, M., Ito, S. and Nakanishi, S. (1992) Direct linkage of three tachykinin receptors to stimulation of both phosphatidylinositol hydrolysis and cyclic AMP cascades in transfected chinese hamster ovary cells. *Journal of Biological Chemistry*, **267**, 2437-2442.

Nakanishi, S. (1991) Mammalian tachykinin receptors. *Annual Review of Neuroscience*, **14**, 123-136.

Nakaya, Y., Kaneko, T., Shigemoto, R., Nakanishi, S. and Mizuno, N. (1994) Immunohistochemical localisation of substance P receptor in the central nervous system of the adult rat. *The Journal of Comparative Neurology*, **347**, 249-274.

Neer, E. (1995) Heterotrimeric G proteins: Organisers of transmembrane signals. *Cell*, **80**, 249-257.

Nestler, E. (1996) Under siege: The brain on opiates. *Neuron*, **16**, 897-900.

Nichols, C. and Lopatin, A. (1997) Inward rectifier potassium channels. *Annual Review of Physiology*, **59**, 171-191.

Nishimura, K., Frederick, J. and Kwatra, M. (1998a) Human substance P receptor expressed in Sf9 cells couples with multiple endogenous G proteins. *Journal of Receptor and Signal Transduction Research*, **18**, 51-65.

Nishimura, K., Warabi, K., Roush, E., Frederick, J., Schwinn, D. and Kwatra, M. (1998b) Characterisation of GRK2-catalysed phosphorylation of the human substance P receptor in Sf9 membranes. *Biochemistry*, **37**, 1192-1198.

Noselli, S. and Vincent, A. (1991) A *Drosophila* nuclear localisation signal included in an 18 amino acid fragment from the *serendipity* δ zinc finger protein. *FEBS Letters*, **280**, 167-170.

Otsuka, M. and Yoshioka, K. (1993) Neurotransmitter functions of mammalian tachykinins. *Physiological Reviews*, **73**, 229-308.

Oyamada, Y., Ballantyne, D., Muckenhoff, K. and Scheid, P. (1998) Respiration-modulated membrane potential and chemosensitivity of locus coeruleus neurones in the *in vitro* brainstem-spinal cord of the neonatal rat. *Journal of Physiology*, **513**, 381-398.

Patil, N., Cox, D., Bhat, D., Faham, M., Myers, R. and Peterson, A. (1995) A potassium channel mutation in weaver mice implicates membrane excitability in granule cell differentiation. *Nature Genetics*, **11**, 126-129.

Paulmichl, M., Nasmith, P., Hellmiss, R., Reed, K., Boyle, W., Nerbonne, J., Peralta, E. and Clapham, D. (1991) Cloning and expression of a rat cardiac

delayed rectifier potassium channel. *Proceedings of the National Academy of Sciences USA*, **88**, 7892-7895.

Perozo, E., Cortes, D. and Cuello, L. (1999) Structural rearrangements underlying K^+-channel activation gating. *Science*, **285**, 73-78.

Pessia, M., Tucker, S., Lee, K., Bond, C. and Adelman, J. (1996) Subunit positional effects revealed by novel heteromeric inwardly rectifying K^+ channels. *EMBO Journal*, **15**, 2980-2987.

Philipson, L., Hice, R., Schaefer, K., Lamendola, J., Bell, G., Nelson, D. and Steiner, D. (1991) Sequence and functional expression in Xenopus oocytes of a human insulinoma and islet potassium channel. *Proceedings of the National Academy of Sciences USA*, **88**, 53-57.

Pieribone, V. and Aston-Jones, G. (1991) Adrenergic innervation of the rat locus coeruleus arises from the C1 and C3 cell groups in the rostral medulla: An anatomic study combining retrograde transport and immunofluorescence. *Neuroscience*, **41**, 525-542.

Quayle, J., Nelson, M. and Standen, N. (1997) ATP-sensitive and inwardly rectifying potassium channels in smooth muscle. *Physiological Reviews*, **77**, 1165-1232.

Raab-Graham, K. and Vandenberg, C. (1998) Tetrameric subunit structure of the native brain inwardly rectifying potassium channel Kir2.2. *Journal of Biological Chemistry*, **273**, 19699-19707.

Ramaswami, M. and Tanouye, M. (1989) Two sodium channel genes in Drosophila: Implications for channel diversity. *Proceedings of the National Academy of Sciences USA*, **86**, 2079-2082.

Ranganathan, R. (1994) Evolutionary origins of ion channels. *Proceedings of the National Academy of Sciences USA*, **91**, 3484-3486.

Reimann, F. and Ashcroft, F. (1999) Inwardly rectifying potassium channels. *Current Opinion in Cell Biology*, **11**, 503-508.

Rens-Domiano, S. and Hamm, H. (1995) Structural and functional relationships of heterotrimeric G-proteins. *FASEB Journal*, **9**, 1059-1066.

Rettig, J., Heinemann, S., Wunder, F., Lorra, C., Parcej, D., Dolly, J. and Pongs, O. (1994) Inactivation properties of voltage-gated K^+ channels altered by presence of β-subunit. *Nature*, **369**, 289-294.

Roberds, S. and Tamkun, M. (1991) Cloning and tissue-specific expression of five voltage-gated potassium channel cDNAs expressed in rat-heart. *Proceedings of the National Academy of Sciences USA*, **88**, 1798-1802.

Rossi, P., DeFilippi, G., Armano, S., Taglietti, V. and D'Angelo, E. (1998) The weaver mutation causes a loss of inward rectifier current regulation in premigratory granule cells of the mouse cerebellum. *Journal of Neuroscience*, **18**, 3537-3547.

Roush, E. and Kwatra, M. (1998) Human substance P receptor expressed in Chinese hamster ovary cells directly activates $G\alpha_{q11}$, $G\alpha_s$ and $G\alpha_o$. *FEBS Letters*, **428**, 291-294.

Saitoh, O., Kubo, Y., Miyatani, Y., Asano, T. and Nakata, H. (1997) RGS8 accelerates G-protein-mediated modulation of K^+ currents. *Nature*, **390**, 525-529.

Saitoh, O., Kubo, Y., Odagiri, M., Ichikawa, M., Yamagata, K. and Sekine, T. (1999) RGS7 and RGS8 differentially accelerate G protein-mediated modulation of K^+ currents. *Journal of Biological Chemistry*, **274**, 9899-9904.

Sakai, K. (1991) Physiological properties and afferent connections of the locus coeruleus and adjacent tegmental neurons involved in the generation of paradoxical sleep in the cat. *Progress in Brain Research*, **88**, 31-46.

Salkoff, L., Baker, K., Butler, A., Covarrubias, M., Pak, M. and Wei, A. (1992) An essential set of K^+ channels conserved in flies, mice and humans. *Trends in Neurosciences*, **15**, 161-166.

Sambrook, J., Fritsch, E. and Maniatis, T. (1989) *Molecular Cloning: A Laboratory Manual.* Cold Spring Harbour. Second Edition.

Scott, V., Rettig, J., Parcej, D., Keen, J., Findlay, J., Pongs, O. and Dolly, J. (1994) Primary structure of a β subunit and α-dendrotoxin-sensitive K^+ channels from bovine brain. *Proceedings of the National Academy of Sciences USA*, **91**, 1637-1641.

Shearman, M., Sekiguchi, K. and Nishizuka, Y. (1989) Modulation of ion channel activity: A key function of the protein kinase C enzyme family. *Pharmacological Reviews*, **41**, 211-237.

Shen, K. and North, R. (1992) Substance P opens cation channels and closes potassium channels in rat locus coeruleus neurons. *Neuroscience*, **50**, 345-353.

Smith, P., Krohn, R., Hermanson, G., Mallia, A., Gartner, F., Provenzano, M., Fujimoto, E., Goete, N., Olson, B. and Klenk, D. (1985) Measurement of protein using bicinchoninic acid. *Analytical Biochemistry*, **150**, 76-85.

Smrcka, A. and Sternweis, P. (1993) Regulation of purified subtypes of phosphotidylinositol-specific phospholipase Cβ by G protein α and βγ subunits. *Journal of Biological Chemistry*, **268**, 9667-9674.

Spauschus, A., Lentes, K., Wischmeyer, E., Diβmann, E., Karschin, C. and Karschin, A. (1996) G-protein-activated inwardly rectifying K^+ channel (GIRK4) from human hippocampus associates with other GIRK channels. *Journal of Neuroscience*, **16**, 930-938.

Stanfield, P., Davies, N., Shelton, P., Khan, I., Brammar, W., Standen, N. and Conley, E. (1994a) The intrinsic gating of inward rectifier K^+ channels expressed from murine IRK1 gene depends on voltage, K^+ and Mg^{2+}. *Journal of Physiology*, **475**, 1-7.

Stanfield, P., Davies, N., Shelton, P., Sutcliffe, M., Khan, I., Brammar, W. and Conley, E. (1994b) A single aspartate residue is involved in both intrinsic gating and blockage by Mg^{2+} of the inward rectifier, IRK1. *Journal of Physiology*, **478**, 1-6.

Stanfield, P., Nakajima, Y. and Yamaguchi, K. (1985) Substance P raises neuronal membrane excitability by reducing inward rectification. *Nature*, **315**, 498-501.

Surmeier, D., Mermelstein, P. and Goldowitz, D. (1996) The weaver mutation of GIRK2 results in a loss of inwardly rectifying K^+ current in cerebellar granule cells. *Proceedings of the National Academy of Sciences USA*, **93**, 11191-11195.

Sutin, E. and Jacobowitz, D. (1991) Neurochemicals in the dorsal pontine tegmentum. *Progress in Brain Research*, **88**, 3-14.

Swanson, R., Marshall, J., Smith, J., Williams, J., Boyle, M., Folander, K., Luneau, C., Antanavage, J., Oliva, C., Buhrow, S., Bennett, C., Stein, R. and Kaczmarek, L. (1990) Cloning and expression of cDNA and genomic clones encoding three delayed rectifier potassium channels in rat brain. *Neuron*, **4**, 929-939.

Takahashi, N., Morishige, K., Jahangir, A., Yamada, M., Findlay, I., Koyama, H. and Kurachi, Y. (1994) Molecular cloning and functional expression of cDNA encoding a second class of inward rectifier potassium channel in the mouse brain. *Journal of Biological Chemistry*, **269**, 23274-23279.

Takano, K., Stanfield, P., Nakajima, S. and Nakajima, Y. (1995) Protein kinase C-mediated inhibition of an inward rectifier potassium channel by substance P in nucleus basalis neurons. *Neuron*, **14,** 999-1008.

Takano, K., Yasufuku-Takano, J., Kozasa, T., Nakajima, S. and Nakajima, Y. (1997) Different G proteins mediate somatostatin-induced inward rectifier K^+ currents in murine brain and endocrine cells. *Journal of Physiology*, **502,** 559-567.

Takano, K., Yasufuku-Takano, J., Kozasa, T., Singer, W., Nakajima, S. and Nakajima, Y. (1996) $G\alpha_{q/11}$ and PLCβ1 mediate the substance P-induced inhibition of an inward rectifier K^+ channel in brain neurons. *Journal of Neurophysiology*, **76,** 2131-2136.

Takumi, T., Ishii, T., Horio, Y., Morishige, K., Takahashi, N., Yamada, M., Yamashita, T., Kiyama, H., Sohmiya, K., Nakanishi, S. and Kurachi, Y. (1995) A novel ATP-dependent inward rectifier potassium channel expressed predominantly in glial cells. *Journal of Biological Chemistry*, **270,** 16339-16346.

Tinker, A., Jan, Y. and Jan, L. (1996) Regions responsible for the assembly of inwardly rectifying potassium channels. *Cell*, **87,** 857-868.

Topert, C., Doring, F., Wischmeyer, E., Karschin, C., Brockhaus, J., Ballanyi, K., Derst, C. and Karschin, A. (1998) Kir2.4: A novel K^+ inward rectifier channel associated with motoneurons of cranial nerve nuclei. *Journal of Neuroscience*, **18,** 4096-4105.

Towbin, H. and Gordon, J. (1984) Immunoblotting and dot immunobinding-current status and outlook. *Journal of Immunological Methods*, **72**, 313-340.

Tsai, W., Morielli, A. and Peralta, E. (1997) The m1 muscarinic acetylcholine receptor transactivates the EGF receptor to modulate ion channel activity. *EMBO Journal*, **16**, 4597-4605.

Tseng, J., Kolb, P., Raskind, M. and Miller, M. (1997) Estrogen regulates galanin but not tyrosine hydroxylase gene expression in the rat locus coeruleus. *Molecular Brain Research*, **50**, 100-106.

Velimirovic, B., Koyano, K., Nakajima, S. and Nakajima, Y. (1995) Opposing mechanisms of regulation of a G-protein-coupled inward rectifier K^+ channel in rat brain neurons. *Proceedings of the National Academy of Sciences USA*, **92**, 1590-1594.

Vigna, S., Bowden, J., McDonald, D., Fisher, J., Okamoto, A., McVey, D., Payan, D. and Bunnett, N. (1994) Characterisation of antibodies to the substance P (NK-1) receptor and to a chimeric substance P receptor expressed in mammalian cells. *Journal of Neuroscience*, **14**, 834-845.

Wei, A., Covarrubias, M., Butler, A., Baker, K., Pak, M. and Salkoff, L. (1990) K^+ current diversity is produced by an extended gene family conserved in Drosophila and mouse. *Science*, **248**, 599-603.

Williams, K. (1997) Interaction of polyamines with ion channels. *Biochemical Journal*, **325**, 289-297.

Willott, E., Balda, M., Fanning, A., Jameson, B., Van Itallie, C. and Anderson, J. (1993) The tight junction protein ZO-1 is homologous to the *Drosophila* discs-large tumor suppressor protein of septate junctions. *Proceedings of the National Academy of Sciences USA*, **90**, 7834-7838.

Wilson, G., O'Neill, C., Sivaprasadarao, A., Findlay, J. and Wray, D. (1994) Modulation by protein kinase A of a cloned rat brain potassium channel expressed in Xenopus oocytes. *Pflugers Archiv-European Journal of Physiology*, **428**, 186-193.

Wischmeyer, E., Doring, F. and Karschin, A. (1998) Acute suppression of inwardly rectifying Kir2.1 channels by direct tyrosine kinase phosphorylation. *Journal of Biological Chemistry*, **273**, 34063-34068.

Woods, D. and Bryant, P. (1991) The discs-large tumor suppressor gene of *Drosophila* encodes a guanylate kinase homolog localized at septate junctions. *Cell*, **66**, 451-464.

Yamaguchi, K., Nakajima, Y., Nakajima, S. and Stanfield, P. (1990) Modulation of inwardly rectifying channels by substance P in cholinergic neurons from rat brain in culture. *Journal of Physiology*, **426**, 499-520.

Yang, J., Jan, Y. and Jan, L. (1995) Determination of the subunit stoichiometry of an inwardly rectifying potassium channel. *Neuron*, **15**, 1441-1447.

Yang, J., Yu, M., Jan, Y. and Jan, L. (1997) Stabilisation of ion selectivity filter by pore loop ion pairs in an inwardly rectifying potassium channel. *Proceedings of the National Academy of Sciences USA*, **94,** 1568-1572.

Yellen, G., Sodickson, D., Chen, T. and Jurman, M. (1994) An engineered cysteine in the external mouth of a K^+ channel allows inactivation to be modulated by metal binding. *Biophysical Journal*, **66,** 1068-1075.

Yokota, Y., Sasai, Y., Tanaka, K., Fujiwara, T., Tsuchida, K., Shigemoto, R., Kakizuka, A., Ohkubo, H. and Nakanishi, S. (1989) Molecular characterisation of a functional cDNA for rat substance P receptor. *Journal of Biological Chemistry*, **264,** 17649-17652.

Zerangue, N., Schwappach, B., Jan, Y. and Jan, L. (1999) A new ER trafficking signal regulates the subunit stoichiometry of plasma membrane K_{ATP} channels. *Neuron*, **22,** 537-548.

Zhu, G., Qu, Z., Cui, N. and Jiang, C. (1999) Suppression of Kir2.3 activity by protein kinase C phosphorylation of the channel protein at threonine 53. *Journal of Biological Chemistry*, **274,** 11643-11646.

Published in The Journal of Physiology (1999) 518:129P

Demonstration of inwardly rectifying potassium ion channel: Kir2.2 and substance P receptor expression in the CNS using polyclonal antibodies.

A.H. Stonehouse[1], J.H. Pringle[2], R.I. Norman[3], P.R. Stanfield[4], E.C. Conley[2] and W.J. Brammar[1].

Departments of [1]Biochemistry, [2]Pathology, [3]Medicine and [4]Cell Physiology and Pharmacology, University of Leicester, Leicester LE1 7RH, England, UK.

Potassium currents flowing through open channels of the Kir2.0 and Kir3.0 subfamilies of inward rectifier channels contribute to resting membrane potential in many cell types. Suppression of inward rectifier (Kir) activity by neurokinin neurotransmitters increases neuronal excitability. Despite many functional studies reporting the specific modulation of whole-cell Kir current in the locus coeruleus (LC) nucleus, little information is available describing the specific molecules that may be involved. Here we demonstrate by immunohistochemistry the co-localisation of the substance P receptor (SPR) and the Kir2.2 isoform of the Kir2.0 subfamily of inwardly rectifying potassium channels in the neurons and also in oligodendroglia of the rat LC.

Adult male F344 rats were killed by anaesthetic (halothane in N_2O/O_2) overdose, followed by immersion fixation in 10% formal saline for 48 hours. Immunohistochemistry using affinity purified Kir2.2 polyclonal antibodies and 10μm paraffin-embedded rat cerebellum/medulla and hippocampus tissue sections revealed consistent immunostaining patterns in neurons, oligodendroglia, capillary endothelia, ventricle ependyma and vascular smooth muscle cells as confirmed by *in situ* hybridisation with Kir2.2 specific riboprobes. In direct comparison, the SPR and Kir2.0 channel proteins showed a remarkable difference in subcellular distribution pattern in native membranes: while the SPR was localised exclusively to plasma membranes of neurons, neuronal processes and to the oligodendroglia, Kir2.2 channels appeared to be distributed both on neuronal plasma membranes and within the nucleus.

This nuclear expression pattern was mimicked in Chinese hamster ovary (CHO) cells, transiently transfected with the Kir2.2 cDNA. In untransfected CHO cells no Kir2.2 protein was detected. Western blotting of plasma membrane and nuclear fractions from native rat brain preparations yielded single bands of 64kDa which were blocked by incubation with 10μg/ml of the Kir2.2 antigenic peptide.

Karschin, C., Diβmann, E., Stuhmer, W., Karschin, A. (1996) *J. Neurosci.* **16**,3559-3570.
Koyano, K., Velimirovic, B.M., Grigg, J.J., Nakajima, S., Nakajima, Y. (1993) *Euro. J. Neurosci.* **5**,1189-1197.
Maeno, H., Kiyama, H., Tohyama, M. (1993) *Mol. Brain Res.* **18**,43-58.
Nakaya, Y., Kaneto, T., Shigemoto, R., Nakanishi, S., Mizuno, N. (1994) *J. Comp. Neuro.* **347**,249-274.
Shen, K-Z., & North, R.A. (1992) *Neurosci.* **50**,345-353.
Stanfield, P.R., Nakajima, Y., Yamaguchi, K. (1985) *Nature* **315**,498-501.
Takano, K., Stanfield, P.R., Nakajima, S., Nakajima, Y. (1995) *Neuron* **14**,999-1008.
Yamaguchi, K., Nakajima, Y., Nakajima, S., Stanfield, P.R. (1990) *J. Physiol.* **426**,499-520.

We thank Dr N.W. Bunnett (University of California, San Francisco) for the kind gift of the rat substance P receptor polyclonal antibody.

Published in The Journal of Physiology (1999) 518:167-168P

The distribution of the inwardly rectifying potassium channel, Kir 2.3, in a population of rat dorsal root ganglion neurones.

Chopra B[1], Manolopoulos J[1], Stanfield PR[1], Norman RI[2], Stonehouse A[3], Giblett S[1], Evans RJ[1] & Grubb BD[1]. Departments of Cell Physiology and Pharmacology[1], Medicine[2] and Biochemistry[3], University of Leicester, Leicester. LE1 9HN

Inwardly rectifying potassium channels (Kir) regulate membrane potential and action potential firing in neurones. Molecular cloning techniques have identified at least six Kir subfamilies (Kir 1-6) whose inward rectification properties are regulated by a voltage dependent Mg^{2+} block and by polyamines (Nichols & Lopatin, 1997). Kir currents have been recorded previously from primary sensory neurones but little is known of the Kir subtypes involved. The aim of this study was to examine the properties of Kir in dorsal root ganglion neurones using electrophysiological and immunocytochemical methods.

Adult male Wistar rats (250-350g) were killed by cervical dislocation and the lumbar dorsal root ganglia (DRG) were dissected and either enzymatically dissociated or frozen. Whole cell patch clamp recordings were made from acutely dissociated neurones (1-2 days) which were maintained in standard culture medium supplemented with nerve growth factor. Current-voltage relationships were determined in 140mM KCl based solution (pipette containing 140mM potassium gluconate based solution) from a holding potential of 0mV. Barium sensitive (Ba^{2+}, 1mM) currents were obtained by subtraction. Ten micrometer frozen sections of intact ganglia were cut from lumbar (L5) ganglia, fixed in paraformaldehyde (2%, 10 mins) and incubated in rabbit anti-rat Kir 2.3 polyclonal antibody and visualised with a FITC conjugated secondary antibody using an epifluorescence microscope. Preabsorption of this antibody with Kir 2.3 peptide reduced immunolabelling to background levels. Cell areas were measured using NIH Image and all values are reported are mean ± sem.

Strong inwardly rectifying barium sensitive currents which showed characteristics of the Kir 2.0 subfamily were identified in >90% of DRG neurones (mean diameter 34.1 ± 3.2 μm). The mean steady state inward current at -140mV was -1474 ± 281pA (range=-321 to -2944, n=9). In the L5 DRG (n=5) 52.0 ± 1.8% of cell bodies were labelled by the Kir 2.3 antibody. An examination of the size distribution of Kir positive neurones revealed that labelling was strongest in the cytoplasm and the perinuclear region of small to intermediate sized cells (mean area=484 ± 31μm^2). Cyclooxygenase (cox)-1 is a marker for small-medium sized DRG neurones and is co-localised extensively with CGRP, a marker for peptidergic nociceptors (Grubb et al, 1997). In dual labelling experiments cox-1 was identified in 75% of Kir 2.3 labelled neurones. These data suggest that Kir 2.3 channels may be expressed in nociceptive neurones and might contribute to the strongly rectifying inward currents that regulate membrane potential or firing rate.

Supported the Wellcome Trust and the MRC

Nichols CG & Lopatin AN (1997) Ann. Rev Physiol. 59, 171-191.
Grubb BD, Giblett S, McLymont N & Goodsell S (1997) J. Physiol. 504, 100P.

In Press with: The Annals of the New York Academy of Sciences

Co-localisation of the inwardly rectifying potassium ion channel, Kir2.2 and the substance P receptor in single locus coeruleus neurons

Anthony H. Stonehouse[a], J. Howard Pringle[b], Robert I. Norman[c], Peter R. Stanfield[d], Edward C. Conley[b] and William J. Brammar[a]

Department of [a]Biochemistry, Adrian Building, University of Leicester, Leicester LE1 7RH, England, UK. The Departments of [b]Pathology, [c]Medicine, (Leicester, LE2 7LX) and [d]Cell Physiology and Pharmacology, (Leicester, LE1 9HN) University of Leicester. Anthony H. Stonehouse is the corresponding author. Telephone: +44 116 252 5586, Fax: +44 116 5616, Email: ahs6@le.ac.uk

Inwardly rectifying potassium (Kir) channels are expressed in a wide range of excitable and non-excitable cells, where they set the resting membrane potential. Because Kirs are open in the range of the resting potential, their modulation is an important factor in the regulation of cellular excitability. In the noradrenergic neurons of locus coeruleus (LC), the neuropeptide substance P (SP) has been shown to suppress Kir activity (1,2). In this report we demonstrate, by immunohistochemistry with site-directed polyclonal antibodies, the co-localisation of Kir2.2 and substance P receptor (SPR) proteins in single LC neurons and associated oligodendroglia. In addition, we show a nuclear localisation in LC neurons for Kir2.2 protein. This was supported by a nuclear signal with Kir2.2 antibodies obtained in Chinese hamster ovary (CHO) cells transiently transfected with Kir2.2. Expression of Kir2.2 protein could not be detected in untransfected cells. The Kir2.2 antibody detected a single 64kDa band on Western blots containing rat brain nuclear and plasma membrane protein fractions. This band was blocked by incubation with the 10μg/ml Kir2.2 antigenic peptide (data not shown). Similarly Kir2.2 immunostaining on rat brain tissue sections was also blocked by incubation with the Kir2.2 antigenic peptide (data not shown).

Adjacent coronal cerebellar rat brain tissue sections (10μm deep, paraffin-embedded) were immunostained with the affinity purified SPR antibody (1:500), or the affinity purified Kir2.2 antibody (12μg/ml). The large diameter (~40μm) of LC neurons, made it possible to identify cells present in serial tissue sections. Strong nuclear and plasma membrane signals in neurons were observed for Kir2.2, with a clear nuclear signal also in oligodendroglia (FIG 1A). SPR was strongly expressed on the plasma membranes of neurons and oligodendroglia, as well as neural processes within the LC (FIG 1B). In order to establish co-expression of Kir2.2 and SPR, the Macromedia XRES program was used to overlay the two adjacent tissue sections. This overlay demonstrated a co-localisation of SPR and Kir2.2 proteins in single neurons and oligodendroglia of the LC (FIG 1C). This is consistent with previous studies using *in situ* hybridisation (3) and immunohistochemistry (4) for SPR and *in situ* hybridisation (5) for Kir2.2, showing expression in the LC.

In order to confirm the unexpected intracellular localisation of Kir2.2, mouse Kir2.2 cDNA was transiently transfected into CHO cells. The localisation of the Kir2.2 isoform was investigated by immunocytochemistry with rhodamine detection. Kir2.2 protein was detected as nuclear and cytoplasmic (trafficking) signals (FIG 2). The negative controls and untransfected cells in the test population were free of non-specific background staining (data not shown). Although the Kir2.2 antibody was raised against rat protein, the cells in this experiment were transfected with mouse Kir2.2 cDNA. A peptide sequence alignment (MacVector) indicated that rat and mouse Kir2.2 C- terminal peptide sequences varied by two amino acid residues (G 415 A and E 418 V, rat for mouse respectively).

In summary, Kir2.2 and SPR proteins are co-localised to single locus coeruleus neurons, where Kir2.2 expression is found on both the plasma membrane and the nucleus. This co-localisation may indicate that the suppression of Kir2.2 by SP is responsible for the increase in neuronal excitability seen in previous studies. Although such a functional connection between Kir2.2 and SP remains to be demonstrated and the signal transduction pathway linking the SPR to Kir2.2 remains unresolved.

The presence of Kir2.2 proteins in the nucleus may help regulate ionic fluxes across nuclear membranes (6) and is the subject of further studies. The expression of Kir2.2 and SPR in oligodendroglia is consistent with the proposed potassium buffering role of glial cells (7).

ACKNOWLEDGEMENT

We thank Dr N.W. Bunnett (University of California, San Francisco) for the gift of the rat SPR polyclonal antibody.

REFERENCES

1. Shen, K-Z. & R.A. North. 1992. Substance P opens cation channels and closes potassium channels in rat locus coeruleus neurons. Neurosci. **50**: 345-353.

2. Koyano, K., B.M. Velimirovic, J.J. Grigg, S. Nakajima & Y. Nakajima. 1993. Two signal transduction mechanisms of substance P-induced depolarisation in locus coeruleus neurons. Euro. J. Neurosci. **5**: 1189-1197.

3. Maeno, H., H. Kiyama & M. Tohyama. 1993. Distribution of substance P receptor (NK-1 receptor) in the central nervous system. Mol. Brain Res. **18**: 43-58.

4. Nakaya, Y., T. Kaneto, R. Shigemoto, S. Nakanishi & N. Mizuno. 1994. Immunohistochemical localisation of the substance P receptor in the central nervous system of the adult rat. J. Comp. Neuro. **347**: 249-274.

5. Karschin, C., E. Diβmann, W. Stuhmer & A. Karschin. 1996. IRK(1-3) and GIRK(1-4) inwardly rectifying K^+ channel mRNAs are differentially expressed in the adult rat brain. J. Neurosci. **16**: 3559-3570.

6. Gerasimenko, O.V., J.V. Gerasimenko, A.V. Tepikin & O.H. Petersen. 1996. Calcium transport pathways in the nucleus. Pflugers Arch **432**: 1-6.

7. Brew, H., P.T.A. Gray, P. Mobbs & D. Attwell. 1986 Endfeet of retinal glial cells have higher densities of ion channels that mediate K+ buffering. Nature **324**: 446-468.

FIGURE 1. Co-localisation of Kir2.2 and SPR in two sequentially cut tissue sections from rat brain cerebellum. The sections were individually immunostained for Kir2.2 and SPR proteins. The sections were artificially coloured (XRES program) with FITC **(A)**, and rhodamine **(B)**, respectively and then overlayed, co-localised signals were coloured orange **(C)**. The co-localisation included both neurons (N) and oligodendroglia (OG) as identified by Weil-Davenports stain.

FIGURE 2. Immunolocalisation of Kir2.2 channel protein in CHO cells, transiently transfected with Kir2.2 cDNA. Nuclei (N) were stained purple with Hoechst 33342.

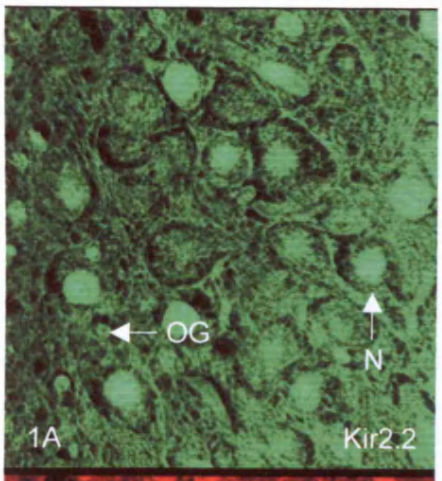
OG
N
1A
Kir2.2

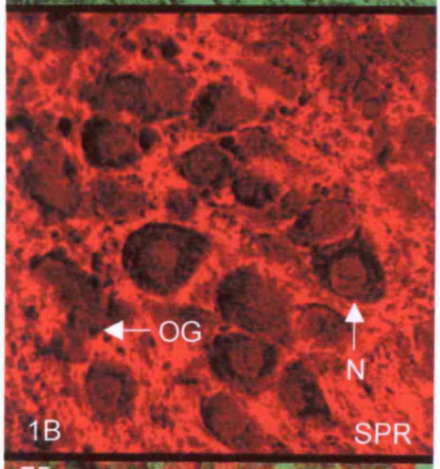
OG
N
1B
SPR

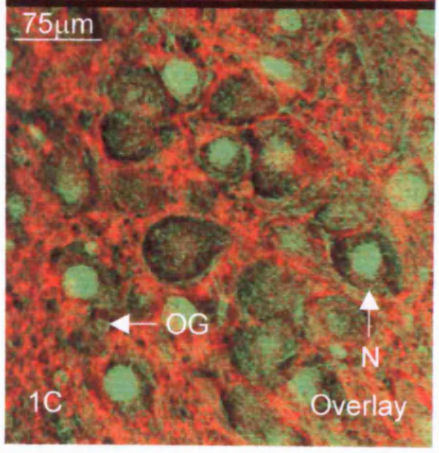
75µm
OG
N
1C
Overlay

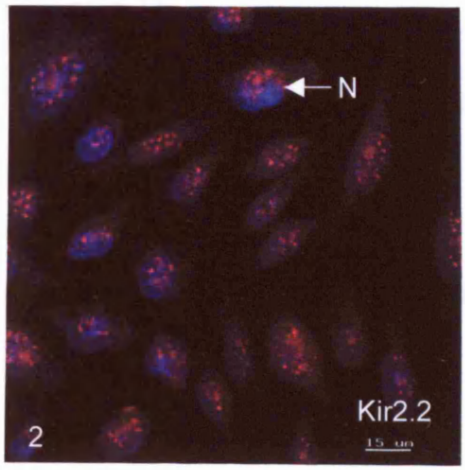
N
2
Kir2.2

In Press with: Histochemistry and Cell Biology

Anthony H. Stonehouse · J. Howard Pringle · Robert I. Norman · Peter R. Stanfield · Edward C. Conley · William J. Brammar

Characterisation of Kir2.0 proteins in the rat cerebellum and hippocampus by polyclonal antibodies

A. H. Stonehouse (✉) and W.J. Brammar

Department of Biochemistry, Adrian Building, University of Leicester, Leicester, LE1 7RH, UK. Tel: +44-(0)116-252-5586; Fax: +44-(0)116-252-5616

J. H. Pringle

Department of Pathology, Robert Kilpatrick Building, University of Leicester, Leicester, LE2 7LX, UK

R. I. Norman

Department of Medicine, Robert Kilpatrick Building, University of Leicester, Leicester, LE2 7LX, UK

P. R. Stanfield

Department of Cell Physiology and Pharmacology, Maurice Shock Building, University of Leicester, Leicester, LE1 9HN, UK

E. C. Conley

Department of Pathology c/o The Centre for Mechanisms of Human Toxicity, Hodgkin Building, Lancaster Road, Leicester, LE1 9HN, UK

Abstract Rabbit polyclonal antibodies were raised to rat Kir2.0 (Kir2.1, Kir2.2 and Kir2.3) inwardly rectifying potassium ion channel proteins. The antibody specificities were confirmed by immunoprecipitation of [^{35}S]-Methionine-labelled in vitro translated channel proteins and Western blotting. Immunohistochemistry revealed a different

patterns of expression of Kir2.0 subfamily proteins in the rat hind-brain (cerebellum and medulla) and fore-brain (hippocampus). Notably, (i) only Kir2.2 protein was detected in the cerebellum and medulla, (ii) Kir2.1, Kir2.2 and Kir2.3 proteins were expressed in the hippocampus, (iii) immunostaining was not limited to neuronal cell types. Anti-Kir2.1 (fore-brain only) and Anti-Kir2.2 (fore- and hind-brain) antibodies showed positive staining in macroglia, endothelia, ependyma and vascular smooth muscle cells. In contrast, Anti-Kir2.3 (fore-brain only) immunostaining was limited to neurons, macroglia and vascular smooth muscle. These results indicate that specific regions within the rat fore- and hind-brain have differential distributions of inwardly rectifying potassium ion channel proteins.

Introduction

Inwardly rectifying potassium (Kir) channels are expressed in a wide range of excitable and non-excitable cells, where they set the resting membrane potential (Hille 1992). Because Kir channels are open in the range of the resting potential, their modulation is important in the regulation of cellular excitability (Hille 1992). Electrophysiological investigation of the electrical excitability of several nuclei of the central nervous system has implicated unidentified Kirs in the control of neuronal excitation e.g., noradrenergic neurons of the locus coeruleus (Koyano et al. 1993; Shen and North 1992) and cholinergic neurons of nucleus basalis of Meynert (Stanfield et al. 1985; Yamaguchi et al. 1990).

Sites of expression of Kir channels within the rat and mouse central nervous system have been characterised by in situ hybridisation using radiolabelled oligonucleotides and cRNA probes (Horio et al. 1996; Karschin et al. 1994 and 1996; Kobayashi et al. 1995). These studies indicated that Kir2.0 and Kir3.0 subfamily isoforms have discrete

but often overlapping sites of expression. However, no previous study has addressed the issue of Kir expression at the protein level. Here we present data from rat fore- (hippocampus) and hind- (cerebellum and medulla) brain using anti-Kir2.1, anti-Kir2.2 and anti-Kir2.3 polyclonal antibodies raised and characterised in our laboratory. The fore-brain area was expected to have strong expression of Kir2.1, Kir2.2 and Kir2.3 channel proteins on the basis of the earlier in situ hybridisation studies (Horio et al. 1996; Karschin et al. 1994 and 1996; Kobayashi et al. 1995). In contrast, the hind-brain area was predicted to express only the Kir2.2 isoform. Our study of channel protein expression supports the earlier in situ hybridisation studies, but extends the information on expression of the Kir2.0 subfamily proteins in a wide variety of cell types, including neurons, macroglia, endothelia, ependyma and vascular smooth muscle cells.